The Dissertation Committee for Farith Adilson Díaz Arriaga Certifies that this is the approved version of the following Dissertation:

Influence of the Composition and Character of Dissolved Organic Matter (DOM) on the Removal of Mercury from Surface Water in Metal Based-Coagulation Systems

Committee:

Desmond F. Lawler, Supervisor

Lynn E. Katz, Co-Supervisor

Howard M. Liljestrand

Charles J. Werth

David J. Eaton

Influence of the Composition and Character of Dissolved Organic Matter (DOM) on the Removal of Mercury from Surface Water in Metal Based-Coagulation Systems

by

Farith Adilson Díaz Arriaga

Dissertation

Presented to the Faculty of the Graduate School of

The University of Texas at Austin

in Partial Fulfillment

of the Requirements

for the Degree of

Doctor of Philosophy

The University of Texas at Austin

December 2018

Dedication

To my family, especially to my grandmother, Rosa María, a humble, hardworking, and kind-hearted woman, whom with limited education was able to create her own business and raise an entire generation of educators.

Acknowledgements

I would like to express my deepest appreciation and gratitude to my advisors Dr. Lynn E. Katz and Dr. Desmond F. Lawler for their friendly guidance and mentorship and for believing in this work which focuses on a critical environmental issue in developing countries. Without their expertise and supervision, this dissertation would not have been possible. Working with Dr. Katz and Dr. Lawler helped me to become a better professor and researcher. I would also like to thank my committee members (Dr. Howard M. Liljestrand, Dr. Charles J. Werth, and David J. Eaton) for their helpful insights and valuable comments that improved the content of this work.

Special thanks to Fulbright Colombia, Colciencias, Colfuturo, and The University of Texas at Austin for giving me the opportunity to pursue doctoral studies. Thanks to the International Office's Global Research Fellowship program which allowed me to conduct field studies in Colombia during the summer of 2017. To Pamela Dahl, Amanda Golden, and Rebecca Silverblatt (coordinators of the General Engineering program at UT-Austin) thanks for the opportunity to work as a Graduate Teaching Assistant which has become one of the most memorable experience during my time at The University of Texas at Austin.

Special thanks are due to current and former member from Katz's group: Celina Dozier, Justin David, Sungmin Youn, Tongren Zhu, James Grundy, Aurore Mercelat, Joonkyung Han, Cameron Oden, Riki Lugo, Matt Landsman, and Sam Brodfuehrer. Special thanks as well to Lawler's group: Soyoon Kum, Ki Yeo, Stetson Rowles, and Anne Mikelonis. Thanks to EWRE students (past and present): Sedat Yalcinkaya, Alexandre Martinez, Gustavo Ochoa, Felipe Gutierrez, Bryant Chambers, Reinaldo

Alcalde, Indu Venu, Erin Berns, Ibrahim Kahraman, Gonzalo Espinoza, and Aida Tabakovic. Special thanks to Marisol Najera for working with me in the lab and help me to run a couple of experiments. I would also like to express my sincere appreciation to all my friends here in Austin: Silvia Higuera, Adriana Guerrero, Jaime Plazas, Carlos Galdeano, Maria Fernanda De La Fuente, Yenibel Ruiz, Andrea Tosi, Nicolás Gonzáles, Nathalia Sandoval, Santiago Tellez, Lucía Ramirez, and Damarys Acevedo.

I am pleased to acknowledge the support of all my family. First and foremost, thanks to my parents Ibeth and Alfonso for their sacrifice rising six children and giving us education, my brother and sisters for their continuous encouragement and love, and to other members of my family for their unconditional support.

Finally, I owe a great deal to all Afro-Colombians that paved the way for us, the future generation, to enjoy opportunities unthinkable to them.

Abstract

Influence of the Composition and Character of Dissolved Organic Matter (DOM) on the Removal of Mercury from Surface Water in Metal Based-Coagulation Systems

Farith Adilson Díaz, Ph.D.

The University of Texas at Austin, 2018

Supervisor: Desmond F. Lawler

Co-supervisor: Lynn E. Katz

According to The United Nations Environment Programme (UNEP), mercury pollution still represents a major threat to human health and the environment, mainly in regions where metallic mercury (Hg^0) is used to extract gold or where coal burning increases the emissions of mercury in the atmosphere. In the particular case of the metallic mercury used in artisanal and small-scale gold mining (ASGM), there is substantial evidence about the direct impact of mercury on human health, mainly due to the inhalation of vapor mercury and the intake of fish with high levels of methylmercury (MeHg). Once metallic mercury is dumped into rivers and soils, this pollutant can react with sulfur reduced ligands in sediments or can be converted to Hg(II) and it will interact with dissolved organic matter (DOM) in aquatic environments. Such interaction will control the fate of this pollutant in water, as well as its toxicity and mobility downstream rivers. Accordingly, these Hg-DOM interactions will also control the ability to remove this pollutant during water treatment.

This research shows that out, of the different functional groups present in

dissolved organic matter, reduced sulfur ligands (S_{red}) play a key role in removing mercury from waters with low Hg/DOM ratio. This trend is particularly evident in waters with low in aromatic content (which translate to low DOC removal) and high concentrations of S_{red} ligands. At much higher mercury concentrations, once the S_{red} ligands are saturated with mercury, the carboxylic ligands control the removal of mercury from solution. Under these conditions, the removal of mercury is a function of the removal of carbon (~1:1 ratio) as all the Hg(II) ions are bound to the all the functional groups available for Hg(II) complexation, even binding weak ligands such as carboxylic acids. In all cases, it is necessary to provide optimal coagulation conditions (pH and coagulant dose) to effectively remove dissolved organic matter, and therefore associated mercury, from solution.

Table of Contents

List of Tables xiii
List of Figures xvi

CHAPTER 1. INTRODUCTION 1

1.1 Background 1

1.2 Problem Statement and Research Objectives 3

1.3 Research Approach 5

CHAPTER 2. LITERATURE REVIEW 8

2.1 Natural organic matter in aquatic ecosystems 8

2.2 Hg-DOM interactions in aquatic environments 12

2.3 Mercury levels in surface water in regions impacted by ASGM 14

2.4 Mercury in Colombian rivers 16

2.5 Mercury treatment technologies and efficiency 23

CHAPTER 3. REMOVAL OF DISSOLVED ORGANIC CARBON (DOC) BY ALUM COAGULATION AS A FUNCTION OF THE AROMATIC CARBON CONTENT IN NATURAL ORGANIC MATTER (NOM) FROM DIFFERENT SOURCES 26

3.1 Introduction 26

3.2 Research Approach 29

3.2.1 Selection of NOM samples and preparation of DOM solutions 29

3.2.2 Characterization of DOM solutions 31

3.2.3 Simulating drinking water treatment at bench-scale jar tests 34

3.2.4 Analysis of aqueous samples 36

3.3 Results and Discussion 36

3.3.1 Characterization of DOM samples before treatment 36

3.3.2 Bench-scale jar tests results 39

3.4 Conclusions 48

CHAPTER 4. INFLUENCE OF THE COMPOSITION AND CHARACTER OF DISSOLVED ORGANIC MATTER (DOM) ON THE REMOVAL OF HG IN METAL-BASED COAGULATION SYSTEMS 50

4.1 Introduction 50

4.2 Research approach 52

4.2.1 Selection of NOM samples and preparation of DOM solutions 52

4.2.2 Hg removal as a function of the DOM character and composition in alum coagulation systems 54

4.2.3 Analysis of aqueous samples 56

4.2.4 Analysis of precipitates 57

4.3 Results and Discussion 58

4.3.1 Characterization of DOM samples 58

4.3.2 Removal of Dissolved Organic Carbon 59

4.3.3 Changes in $SUVA_{254}$ values 61

4.3.4 Hg removal at low Hg/DOC ratio 64

4.3.5 Hg removal at high Hg/DOC ratio 70

4.3.6 Surface characterization of the precipitates 73

4.4 Conclusions 81

CHAPTER 5. ANALYSIS OF THE INTERACTIONS BETWEEN MERCURY AND NATURAL ORGANIC MATTER (NOM) THROUGH STATISTICAL ANALYSIS, EQUILIBRIUM DIALYSIS LIGAND EXCHANGE (EDLE), FLUORESCENCE SPECTROSCOPY AN BENCH-SCALE JAR TESTS WITH AND WITHOUT AN ESTERIFIED NOM 83

5.1 Introduction 83

5.2 Research Approach 87

5.2.1 Natural Organic Matter (NOM) selection and characterization 87

5.2.2 Esterification of Natural Organic Matter (NOM) 88

5.2.3 Equilibrium Dialysis Ligand Exchange (EDLE) Experiments 89

5.2.4 Fluorescence spectroscopy of Hg-DOM interactions 92

5.2.5 Bench scale jar tests 94

5.3 Results and Discussion 94

5.3.1 $SUVA_{254}$ values of DOM samples 94

5.3.2 Esterification of Natural Organic Matter (NOM) 95

5.3.3 Jar tests with and without esterified DOM 97

5.3.4 Jar tests at extremely high Hg(II) concentrations 101

5.3.5 Equilibrium Dialysis Ligand Exchange (EDLE) Results 109

5.3.6 Fluorescence spectroscopy 113

5.3.7 Variables influencing the removal of Hg from surface water in alum-based coagulation systems 117

5.4 Conclusions 126

CHAPTER 6. FROM THE ILLEGAL TRADE OF MERCURY TO THE FORMALIZATION OF ILLEGAL MINERS: THE CHALLENGES TO REDUCE THE USE OF MERCURY IN ASGM IN THE LIGHT OF THE MINAMATA CONVENTION 128

6.1 Introduction 129

6.2 Mercury from ASGM as a source of environmental pollution 130

6.3 Mercury pollution in Colombia: A legacy that will last for decades 134

6.4 Fate of metallic mercury in rivers and aquatic ecosystems 137

6.5 Main challenges to reduce the use of mercury in ASGM regions: Study of the Colombian case 139

6.5.1 The presence of illegal armed groups and organized crime in ASGM regions and its involvement in the gold production 140

6.5.2 The illegal trade of metallic mercury in the light of the Minamata Convention 143

6.5.3 The arduous task to formalize and legalize illegal/informal miners 145

6.5.4 The lack of funding for environmental protection in the face of more urgent needs 148

6.6 A Needed task: The evaluation of the impact of ASGM in natural ecosystems and the degree of impairment associated with mercury pollution 150

6.7 Concluding remarks 156

CHAPTER 7. CONCLUSIONS 158

7.1 Removal of dissolved organic carbon (DOC) by alum coagulation as a function of the aromatic content 158

7.2 Influence of the character and composition of dissolved organic matter (DOM) on the removal of Hg(II) in metal-based coagulation systems at optimal coagulation conditions of pH and coagulant dose 159

7.3 Analysis of the interactions between Hg(II) and reactive functional groups in dissolved organic matter through statistical analysis, equilibrium dialysis ligand exchange (EDLE), fluorescence spectroscopy, and jar test with and without a modified NOM 161

7.4 Challenges to reduce metallic mercury in ASGM in the light of the Minamata Convention 163

7.5 Future Work 163

REFERENCES 165

VITA 179

LIST OF TABLES

Table 2-1. Acidic functional groups in NOMs selected for experimentation..... 13

Table 2-2. Mercury levels in water samples from Colombian rivers..... 19

Table 2-3. Mercury concentration discharged to Colombian rivers as measured by the IDEAM (2014)..... 23

Table 2-4. Comparison of the removal efficiency of Hg among different absorbent types 25

Table 3-1. Carbon distribution and acidic functional groups of selected NOMs 30

Table 3-2. Guidelines on the character of NOM and expected DOC removals 32

Table 3-3. Initial experimental conditions for jar test for selected NOMs..... 34

Table 3-4. Analytical techniques used to analyze aqueous samples..... 36

Table 3-5. $SUVA_{254}$, spectral slopes values, and notations for selected NOMs..... 37

Table 4-1. Conditional distribution coefficients between Hg and DOM as a function of the Hg/DOM ratio in different aquatic environments. Source: Haitzer et al. (2002)..... 51

Table 4-2. Carbon distribution and acidic functional groups of selected NOMs 53

Table 4-3. Initial experimental conditions for jar test experiments with selected NOMs..... 56

Table 4-4. Analytical techniques used to achieve the goals of this research..... 57

Table 4-5. Experimental conditions for surface characterization of precipitates. 58

Table 4-6. Characterization of DOM solutions used for experimentation..... 58

Table 4-7. Pairwise comparison of (Hg/DOC) removal ratios across categories of DOM at low Hg/DOC ratio 66

Table 4-8. Summary of the initial and final experimental conditions at low Hg/DOC ratio 67

Table 4-9. Pairwise comparison of (Hg/DOC) removed ratios across categories of DOM at high Hg/DOC ratio 71
Table 4-10. Summary of the initial and final experimental conditions at high Hg/DOC ratio 72
Table 4-11. Jar tests conditions for the surface characterization of the precipitate 74
Table 4-12. Percentage atomic concentration of the elements at the surface of the floc at different initial DOM concentrations 76
Table 5-1. $SUVA_{254}$, aromaticity, and notations for selected NOMs 95
Table 5-2. ^{13}C-NMR estimates carbon distribution comparison between SRFA and the esterified-SRFA 97
Table 5-3. Jar test initial experimental conditions at high Hg(II) concentrations 101
Table 5-4. Acidic functional groups per mole of mercury (mol/mol) for PLFA, SRFA, and SR-NOM samples at an initial mercury concentration of 10 µg/L. 106
Table 5-5. Summary of the removal efficiencies for Hg(II) and DOC at high mercury concentrations in the presence of PLFA, SRFA, and SR-NOM. The initial concentration of DOC was set at 5.0 mg/L. 109
Table 5-6. Summary of the parameters measured before and after equilibration 110
Table 5-7. Summary of the reaction of interested for the calculation of $K_{DOM'}$. Source Haitzer et. al [37] 111
Table 5-8. Summary of measured conditional stability constants (Log K_{HgL} and K_{HgL2}) reported in the literature for DOM of different origins (Adapted from [74], [150] 112
Table 5-9. Complexation parameters for PLFA and NAHA samples based on the modified Stern–Volmer model 117
Table 5-10. Characteristics of the DOM tested as shown in Chapter 4 118

Table 5-11. Experimental description of the jar tests performed at low Hg/DOM ratios 118
Table 5-12. Results of the regression analysis at low Hg/DOM ratio 118
Table 5-13. Excluded variables by the stepwise regression approach at low Hg/DOM ratios 119
Table 5-14. Experimental description of the jar tests performed at high Hg/DOM ratio 121
Table 5-15. Results of the regression analysis at high Hg/DOM ratio 121
Table 5-16. Excluded variables by the stepwise regression approach at high Hg/DOM ratio 121
Table 5-17. Experimental description of the jar tests performed at a much higher Hg/DOM ratio 123
Table 5-18. Results of the regression analysis at much higher Hg/DOM ratios 124
Table 5-19. Excluded variables by the stepwise regression approach at much higher Hg/DOM ratios 124
Table 6-1. Estimated Mercury Input to the Environment Due to Gold and Silver Mining 132
Table 6-2. Reference standards and guidelines for ambient levels of mercury in different countries 153

LIST OF FIGURES

Figure 2-1 Classification of natural organic matter (NOM) as usually found in aquatic ecosystems. Adapted from Pagano, Bida, and Kenny (2014). 9

Figure 2-2. Estimated composition of DOM in aquatic environments. Adapted from Ravichandran (2004) 10

Figure 2-3. Hypothetical structure of humic substances as expected in natural environments showing the portion rich in aromatic carbon (a) and the portion rich in aliphatic carbons (b) as well as the main functional groups for metal complexation. Adapted from: Wandruska (2000) and Leita et al. (2009). 11

Figure 2-4. Classification of natural organic matter (NOM) based on its polarity and acid-based character. Adapted from Bond et al. (2012) 12

Figure 2-5. Map of the estimated discharge of metallic mercury in soil and water during gold extraction in Colombia showing dissolved THg concentrations in nearby water sources. Map source: Instituto de Hidrología, Meteorología y Estudios Ambientales-IDEAM, Estudio Nacional del Agua 2014 (map version: 1.0, 03-Feb-2018). 21

Figure 3-1. $SUVA_{254}$ as a function of the percent aromatic determined by ^{13}C-NMR for NOM samples from different environments. Adapted from Weishaar et al. (2003), Hur and Schlautman (2003), and Korak et al, (2014). 28

Figure 3-2. Schematic of the steps to prepare DOM solutions for jar test experiments ... 31

Figure 3-3. Schematic of the jar test procedure used for experimentation. 35

Figure 3-4. Absorption spectra for the selected NOMs 38

Figure 3-5. $SUVA_{254}$ as a function of the aromatic content of NOM for the samples used in this work. 39

Figure 3-6. Residual Al(III) concentration at optimal coagulation conditions (pH = 6.7, Alum dose = 30 mg/L) for NOM from different environments. Error bars represent standard error from the replicates. 41
Figure 3-7. Amount of DOC removed for selected NOMs in alum-coagulation treatment at pH 6.7, 0.01M $NaNO_3$ ionic strength, and 30 mg/L alum dose. For each NOM, the initial DOC concentration was set at 5.0 mg/L. Error bars represent the standard deviation from the replicates. 42
Figure 3-8. Changes in spectral slopes values after alum coagulation at pH 6.7, 0.01M NaNO3 ionic strength, and 30 mg/L alum dose. For each NOM, the initial DOC concentration was set at 5.0 mg/L..... 43
Figure 3-9. Changes in $SUVA_{254}$ values after alum coagulation at pH 6.7, 0.01M $NaNO_3$ ionic strength, and 30 mg/L alum dose. For each NOM, the initial DOC concentration was set at 5.0 mg/L..... 44
Figure 3-10. DOC percent removal as a function of the $SUVA_{254}$ based on the guidelines provided by Edzwald and Tobiason (1999). 46
Figure 3-11. Residual $SUVA_{254}$ values and residual DOC concentrations after alum-coagulation treatment at pH 6.7, 0.01M $NaNO_3$ ionic strength, and 30 mg/L alum dose. For each NOM, the initial DOC concentration was set at 5.0 mg/L..... 47
Figure 4-1. Schematic of the jar test procedure used for experimentation..... 55
Figure 4-2. (a) Mercury species at pH 6.7 simulated by visual MINTEQ software (ver. 3.1) (I.S.=0.01M $NaNO_3$, T = 23ºC) (b) Hg removal in the absence of natural organic matter at different pH in alum-coagulation systems. 55

Figure 4-3. Residual Al(III) concentration at pH 6 and alum dose 30mg/L for NOM from different environments. Error bars represent standard error from the replicates. 60
Figure 4-4. DOC removed during bench-scale jar tests for NOMs from different sources. Error bars represent the standard deviation from the replicates (n). The initial DOC concentration in each sample was 5 mg/L. 61
Figure 4-5. Changes in $SUVA_{254}$ values for selected NOM after jar test experiments. Error bars represent standard error from the replicates (n). 62
Figure 4-6. Final $SUVA_{254}$ and DOC residual after alum coagulation for selected NOMs. The initial DOC concentration in each sample was 5 mg/L. 64
Figure 4-7. Hg removal at low Hg/DOC ratio for NOM samples from different environments: a) Hg removal percentage, b) Hg removed/DOC removed (µg/mg). The initial DOC concentration was 5 mg/L and the initial Hg concentration was 0.5 µg/L. 65
Figure 4-8. Comparison between changes in $SUVA_{254}$ values, removal of Hg(II), and S_{red} concentration in NOM from different sources in jar test at low Hg/DOM ratios. 69
Figure 4-9. Hg removal at high Hg/DOC ratio for NOM samples from different environments: a) Hg removal percentage, b) Hg removed/DOC removed (µg/mg). The initial DOC concentration was 5 mg/L and the initial Hg concentration was 10 µg/L. 70
Figure 4-10. Comparison between changes in $SUVA_{254}$ values, removal of Hg(II), and S_{red} concentration in NOM from different sources in jar test at high Hg/DOM ratios. 73

Figure 4-11. DOC and Hg removal percentages for experiments to evaluate the incorporation of mercury on alum flocs. 75
Figure 4-12. XPS spectra for jar test precipitates at different DOM concentrations after flocculation with alum: (a) Hg4f and Si2p (b) Al2p (c) C1s, and (d) O1s core-level XPS spectra. 78
Figure 4-13. Elemental maps of total ions, Hg, Al-O, and carbon on the surface of the floc after alum coagulation treatment by ToF-SIMS. Note: the bright lines on the lower-left side of the Hg-map are associated with the filter and are not related to the presence of Hg in that particular area of the floc..... 80
Figure 5-1. Schematic of the esterification of carboxylic acids with alcohols using EEDQ. Adapted from Zacharie et al., 1995. 85
Figure 5-2. Steps followed for the esterification of carboxyl groups in natural organic matter samples with EEDQ and excess alcohol..... 89
Figure 5-3. Representation of the experimental setup to determine the equilibrium constant between free Hg and DOM at low Hg/DOM ratio..... 90
Figure 5-4. (a) Liquid phase ^{13}C-NMR for SRFA sample, (b) Liquid phase ^{13}C-NMR for the esterified-SRFA. 96
Figure 5-5. Jar tests results with SRFA and esterified SRFA: (a) Hg residual at 0.5 µg/L (b) Hg residual at 5.0 µg/L (c) DOC residual after jar tests at 0.5 and 5.0 µg/L (d) Hg removed/total carbon added..... 98
Figure 5-6. Jar test results with and without SRHA and esterified SRHA: (a) Hg residual at 0.5 µg/L (b) Hg residual at 10 µg/L (c) DOC residual (d) Hg removed/total carbon added..... 100

Figure 5-7. Residual Al(III) concentration at pH 6 and alum dose 30 mg/L for NOMs from different environments. Error bars represent standard error from the replicates (n=3). 102
Figure 5-8. DOC removed during bench-scale jar tests for NOMs from different sources. Error bars represent the standard deviation from the replicates (5). The initial DOC concentration in each sample was 5 mg/L as C..... 103
Figure 5-9. Percentage mercury removal at different initial mercury concentrations for PLFA, SRFA, and SR-NOM samples. The initial DOC concentration was 5 mg/L. Error bars represent the standard deviation from the replicates (n=3). 104
Figure 5-10.Hg(II) removed/DOC removed (μg/mg) for PLFA, SRFA, and SR-NOM. The initial NOM concentration was 5 mg/L and the initial Hg(II) concentration range between 10-50 μg/L. Error bars represent the standard deviation from the replicates (n=3)..... 105
Figure 5-11. Acidic functional groups/Hg molar ratios (mol/mol) in jar tests at high mercury concentrations suing PLFA, SRFA, and SR-NOM samples. The initial DOC concentration was 5.0 mg/L..... 107
Figure 5-12. Partitioning of Hg(II) spiked in the outer containers in the presence of DOM. Experiments were performed at THg = 1.0 μg/L, pH = 6.7, with Spectra/Por® Biotech CE Tubing (MWCO 500-1000 D) as a dialysis membrane 110
Figure 5-13. Changes in fluorescence emission spectra of different samples with increasing concentrations of Hg(II) excited at 340 nm: (a) 0.01 M $NaNO_3$ solution, pH = 6.7, (b) EEDQ, (c) NAHA, and (d) (PLFA).

EEDQ and DOM solutions were prepared at 5 mg/L DOC, pH = 6.7, and 0.01 M $NaNO_3$. 115
Figure 5-14. (a) Fluorescence emission quenching at of at λ_{ex} =340 nm NAHA and PLFA with Hg(II), (b) Modified Stern–Volmer plot for NAHA and PLFA samples. DOM solutions were prepared at 5 mg/L DOC, pH = 6.7, and 0.01 M $NaNO_3$. 116
Figure 5-15. Regression describing the relationship between the observed Hg removal and the predicted Hg removal at low Hg/DOM ratios. 119
Figure 5-16. Regression describing the relationship between the observed Hg removal and the predicted Hg removal at high Hg/DOM ratios. 122
Figure 5-17. Regression describing the relationship between the observed Hg removal and the predicted Hg removal at low and high Hg/DOM ratios. 123
Figure 5-18. Regression describing the relationship between the observed Hg removal and the predicted Hg removal at much higher Hg/DOM ratios..... 125
Figure 6-1. 2017 Top 20 gold production and mean mercury released in ASGM among the top 20 gold mining countries in the world. Data sources: [27], [165] 133
Figure 6-2. (a) Annual gold production in Colombia in the last 10-years and (b) Gold production by state during the same period of time. Data from Unidad de Planeación Minero Energética [174]..... 135
Figure 6-3. (a) Gold production in Colombia and (b) Mercury contamination as a result of ASGM. Map source for Figure 6-3a: Subdirección de Minería-UPME (Agencia Nacional de Minería-ANM, Sep-2018) [174]. Map source for Figure 6-3b: Instituto de Hidrología, Meteorología y Estudios Ambientales-IDEAM, (map version: 1.0, 03-Feb-2018) [24]..... 136

Figure 6-4. The destruction of natural ecosystems is one of the main consequences of illegal mining in Colombia: a) Illegal dredging operation in Quito River (Chocó) spotted in June 2017, b) Illegal mining in Quito River has changed the course of the river and affected fishing and agriculture activities, c) Similar consequences can be seen in many states of Colombia as it is the case of El Bagre (Antioquia), d) Water intake for the water treatment plant in Ayapel (Córdoba). Mercury concentrations higher than 400 ng/L were detected in the Ayapel Swamp during this study. 137

Figure 6-5. Colombian National Security Forces fighting illegal mining activities around the country: a) Dredges destroyed in Rio Quito (Chocó), b) Illegal miners caught by the Colombia National Police in Cordoba, c) The confiscation of mining equipment and machinery is done along the country, d) Colombian Air Force supports military operations against illegal mining. Source: Websites from Policía Nacional De Colombia[189] and Fuerzas Militares de Colombia[190]..... 142

Figure 6-6. Framework for the legalization process of a Mining Production Unit in Colombia that lacks of mining rights. Source: Ministerio de Minas y Energía de Colombia [203] 147

Figure 6-7. (a) Actual and expected estimated expenditures of the EPA Superfund's program and (b) number of sites added to the Superfund's list by type. Adapted from: Probst, Superfund 2017 Cleanup Accomplishments and the Challenges Ahead [207] 149

Figure 6-8. General framework of the mechanism needed to identify, list, and restore soils and water bodies affected by ASGM activities following the

guidelines provided in section 303(d) of the Clean Water Act (U.S.) and the protocols designed by the Global Mercury Project (GMP). 155

CHAPTER 1. INTRODUCTION

1.1 Background

Mercury (Hg) contamination can enter water bodies from several natural and anthropogenic sources. Of the total Hg emissions to the atmosphere, 30% comes from anthropogenic sources, 10% from natural geological sources, and 60% are re-emissions from soil and oceans [1]. In surface water, besides atmospheric deposition from biomass burning [2]–[4], fossil fuel combustion [5], [6], deforestation [5], [7]–[9], forest fires [10], and volcanism phenomena [11], other important sources of mercury include soil weathering of mercury-bearing minerals [12], [13], soil erosion (most significant during rainy season) [7], [11], [13], and artisanal and small-scale gold mining (ASGM) [3], [7], [10], [14]–[17]. One of the main contributors to mercury pollution in surface waters in developing countries is from the Hg used illegally to extract gold [5], [18]–[22].

Gold mining pollution is particularly critical in Colombia, where it was reported that more than 80% of the gold production comes from illegal mining [23]. This activity has affected natural ecosystems in 17 of the 32 Colombian states including more than 80 municipalities [21]. A 2014 governmental study indicated that a least 20 rivers are polluted with mercury [24], although a newer publication claims that more than 80 rivers are impacted by this contaminant [25]. Similar Hg pollution problems can also be found in countries like China, Peru, Ecuador, Brazil, Indonesia, The Philippines, Tanzania, and Ghana, where tons of metallic mercury have being released to the environment as a result of ASGM [26], [27].

While the exposure to Hg(0) vapor at ASGM sites and ingestion of fish contaminated with methylmercury (MeHg) are the primary threats to human health in communities affected by ASGM, the continuous consumption of food with low levels of Hg(II) may also contribute to the total burden that impacts human health [5], [18], [28]–[32]. As conventional water treatment processes (i.e., coagulation, filtration, and

sedimentation) are typically employed in developing countries, it is important to evaluate their potential for reducing Hg from drinking water sources. In these processes, adsorption and co-precipitation are the primary removal mechanisms for heavy metals like Hg.

In 2006, the World Health Organization (WHO) changed the guideline value for mercury in drinking water from 1.0 μg/L of total mercury (THg) to 6.0 μg/L of inorganic mercury (IHg) based on the effect of the inorganic mercury on the renal system in rats [33]. This decision was also supported by the fact that organic mercury concentrations in drinking water are expected to be negligible, and that the information available at that time indicated that Hg contamination as a result of ingestion of drinking water was unlikely. To date, no guidelines for organic mercury in drinking water exist, despite the fact that the previous guideline was based on the toxicity of methylmercury [34]. A decade later, with new information about the impact of low-level Hg exposure on human health [29]–[32], and new techniques available to quantify Hg traces in water, it may be necessary to review the mercury guidelines in drinking water [34], particularly in countries where Hg pollution is already an environmental and public health concern.

Mercury removal is essential in water treatment plants serving communities in which the only drinking water sources are rivers or lakes that are contaminated. Certainly, this condition applies to many communities around the world, primarily those affected by ASGM, an activity that poses a risk to the public health and to natural ecosystems. In such communities, cost-effective and low maintenance treatment technologies such as chemical coagulation are desired. Therefore, optimization of water treatment processes for Hg(II) removal is necessary.

1.2 Problem Statement and Research Objectives

The fate of Hg in a given ecosystem is highly dependent on the numerous biogeochemical reactions that control Hg speciation in natural waters. Of particular interest with respect to drinking water sources and water treatment are the reactions between Hg and dissolved organic matter (DOM). Although the interactions between Hg and DOM in aquatic environments have been studied by different authors [10], [35]–[42], the effects of such interactions in water treatment processes have not been extensively evaluated. Considering that the character, composition, and concentration of DOM in water sources may differ from one ecosystem to another depending on the biochemical processes that take place in the ecosystem [43]–[45]; the behavior of Hg in the presence of DOM appears to follow a similar pattern: Hg(II) is strongly reactive with the humic fraction of the DOM. The humic fraction of DOM, which comprises humic and fulvic acids, is richer in aromatic and aliphatic carbon compared to the non-humic fraction which includes proteins, amino acids, and carbohydrates [35], [43], [46]–[49]. The humic substances are the most hydrophobic fraction of the DOM, have a higher $SUVA_{254}$ (defined as UV_{254}/DOC (mg/L)) and are more amenable to removal through conventional coagulation with metal salts [47], [48], [50]–[53].

In natural environments, it has been found that metal ions like Ni(II), Cu(II), Pb(II), and Hg(II) have a preferential affinity for the hydrophobic fraction of soil or DOM [35], [52], [54]–[57]. Metal ions in water form complexes with acidic functional groups in DOM like carboxylic acids, phenols, ammonia, alcohol, and thiols [35], but little information is known about the distribution of these functional groups in the structure of DOM. In soil humic substances, the molar ration between oxygen ligands and reduced sulfur ligands was determined to be ~200:1 [58], while in aquatic environments, carboxylic acids and phenols account for up to 90% of the acidic functional groups in DOM [59].

In aquatic environments, it was determined that the hydrophobic fraction of DOM is more effective in releasing Hg(II) ions from cinnabar (red HgS, $K_{sp} = 10^{-36.8}$), compared to the hydrophilic fraction [35], [60]. Previous studies shown that the dissolution of cinnabar by DOM is possible due to the complexation of mercury with reduced sulfur functional groups in DOM [35]. These reduced sulfur ligands are then strong enough to compete with inorganic sulfide in equilibration reactions [35]. However, the interaction between Hg and DOM also depends on the Hg/DOM ratio [35]–[37]. It was found that at low Hg/DOM ratios (<< 1.0 μg Hg/mg DOM) Hg bound reduced sulfur ligands in DOM, while at high ratios (e.g., ≥ 1.0 μg Hg/mg DOM), Hg also bound oxygen functional groups like carboxylic acids, which is more abundant than the sulfur ligands [35], [37], [61].

Both the concentration of Hg and the composition of the DOM play an important role in determining the mobility of Hg(II) in aquatic environments and these factors might also influence the potential for removal of mercury in water treatment. It is not clear, however, how the functional groups in the DOM influence the removal of this pollutant from water. Consequently, the hypothesis of this work is that the removal of Hg(II) from drinking water treatment with metal-based coagulants depends on the interactions between Hg(II) ions and those functional groups located in the fraction of DOM more reactive to metal coagulants rather than merely to the hydrophobicity of the DOM. To test this hypothesis, an experimental plan has been developed to:

1. Evaluate the removal of dissolved organic carbon (DOC) by alum coagulation as a function of the aromatic carbon content in natural organic matter (NOM) from different sources.
2. Evaluate the influence of the composition and character of dissolved organic matter (DOM) on the removal of Hg(II) in metal-based coagulation systems at optimal coagulation conditions of pH and coagulant dose.

3. Analyze the interactions between Hg(II) and reactive functional groups in dissolved organic matter (DOM) through statistical analysis, equilibrium dialysis ligand exchange (EDLE), fluorescence spectroscopy, and jar tests with and without a modified DOM.

1.3 Research Approach

The objectives described in section 1.2 were achieved through bench scale experiments; measurements of Hg(II), Al(III), DOC concentratios, $SUVA_{254}$ values, and fluorescence spectra; DOM and floc characterization; and statistical analysis. The description of each objective is presented next:

Objective 1: Evaluate the removal of dissolved organic carbon (DOC) by alum coagulation as a function of the carbon aromaticity in natural organic matters (NOM) from different sources

The first goal of this research was to evaluate the relationship between the aromatic content of natural organic matter (NOM) and the DOC removal efficiencies in simulated drinking water treatment. Dissolved organic matter (DOM) solutions were prepared from NOM with marked differences in carbon distribution and acidic functional groups. In this research, the term NOM also includes extracted humic substances such as humic acids and fulvic acids. The NOMs used for experimentation were obtained from the International Humic Substances Society (IHSS) who extracted them from the Suwannee River in the Okefenokee National Wildlife Refuge (ONWR) in southeastern Georgia; Pony Lake – an eutrophic saline coastal pond in the Antarctica- rich in NOM of microbial origin (no presence of terrestrial plants nearby); Upper Mississippi River in Minneapolis; and from the Lake Hellrudmyra, a small tarn located in Oslo (Norway)

[62]. DOM solutions were characterized based on their specific ultraviolet absorbance at 254 nm ($SUVA_{254}$), spectral slope (S_e), and carbon content. The spectral slope is another optical parameter used as a proxy for the aromatic content of water samples. A correlation between $SUVA_{254}$ and the aromatic content of the different DOM samples will be analyzed, as well as the relationship between $SUVA_{254}$ and the DOC removal efficiencies based on the guidelines provided by Edzwald and Tobiason (1999). The analysis of changes in $SUVA_{254}$ after alum-coagulation will provide some insight into the character of the DOM removed from solution. The analysis of the residual $SUVA_{254}$ values can also provide valuable information on the most likely composition of the residual carbon and the potential interactions between Hg(II) and functional groups available for mercury complexation in the DOM.

Objective 2: Evaluate the influence of the character and composition of dissolved organic matter (DOM) on the removal of Hg(II) in metal-based coagulation systems at optimal coagulation conditions of pH and coagulant dose

Natural organic matter (NOM) from different sources were also used for this purpose. Jar test experiments were conducted at different mercury concentrations, ionic strength of 0.01 M, pH 6.7, and 30 mg/L of alum dose (2.6 mg/L as Al(III)) to ensure the formation of amorphous $Al(OH)_3(s)$ precipitates. Although these NOMs were collected from different sources, the amount of carbon is practically the same regardless of the source of the NOM. Nevertheless, based on the source of the NOM, remarkable differences are expected in the percentage of aromatic and aliphatic carbon present in the NOM structure, as well as in the specific ultraviolet absorbance ($SUVA_{254}$) values, an indicator of the hydrophobicity of the sample. The removal of DOC and the removal of Hg(II) will be compared based on the $SUVA_{254}$ values of the different NOMs tested. Experiments at low Hg/DOM ratios help to evaluate the influence of S_{red} ligands on the

removal of Hg from solution, and experiments at high Hg/DOM ratios help to evaluate the role of both S_{red} and carboxylic acid on the removal of Hg. Analysis of the precipitates by X-ray photoelectron spectroscopy (XPS) will provide visual evidence of the incorporation of Hg-DOM complexes onto alum flocs.

Objective 3. **Analyze the interactions between Hg(II) and reactive functional groups in dissolved organic matter (DOM) through statistical analysis, equilibrium dialysis ligand exchange (EDLE), fluorescence spectroscopy, and jar tests with and without a modified DOM**

An esterification process will be performed aiming to modify the properties of selected DOMs by converting the carboxylic acids into esters. Jar test will be performed with and without a modified DOM to analyze the effectiveness of the esterification process and the removal of mercury in the absence of carboxylic functional groups. An equilibrium dialysis ligand exchange (EDLE) experiment will be performed to analyze the interactions between Hg(II) and DOM at low Hg/DOM ratios and fluorescence spectroscopy will be used to analyze the quenching of the emission spectra of different DOMs at high Hg/DOM ratio.

CHAPTER 2. LITERATURE REVIEW

2.1 Natural organic matter in aquatic ecosystems

Natural organic matter (NOM) in the environment is said to originate from allochthonous and autochtonous inputs [45], [63], [64]. **Pedogenic organic matter (allochthonous)** is produced by the incomplete decomposition of higher order plants and animals by bacteria and fungi in terrestrial sources. The resultant products of this decomposition are later leached to water sources by rainwater. **Aquogenic organic matter (autochthonous)** is directly produced in water bodies through the process of photosynthesis and decompositions of detritus (plankton, aquatic bacteria, and animal bodies).

NOM has also been classified with respect to its solubility in water as dissolved organic matter (DOM) and undissolved organic matter (UOM) [45]. It has been estimated that typically about 50% of the DOM is comprised of carbon [35], [43], [65], [66]. The main elements found in NOM, from high to low proportion, are C, O, H, N, S, and P. The amount of carbon found in organic compounds is often referred as total organic carbon (TOC). TOC includes both the dissolved organic carbon (DOC) – for organic compounds passing through a 0.45 μm filter- and the particulate organic carbon (POC) –for the particles retained on a 0.45 μm filter-. A comprehensive classification of natural organic matter is shown in Figure 2-1.

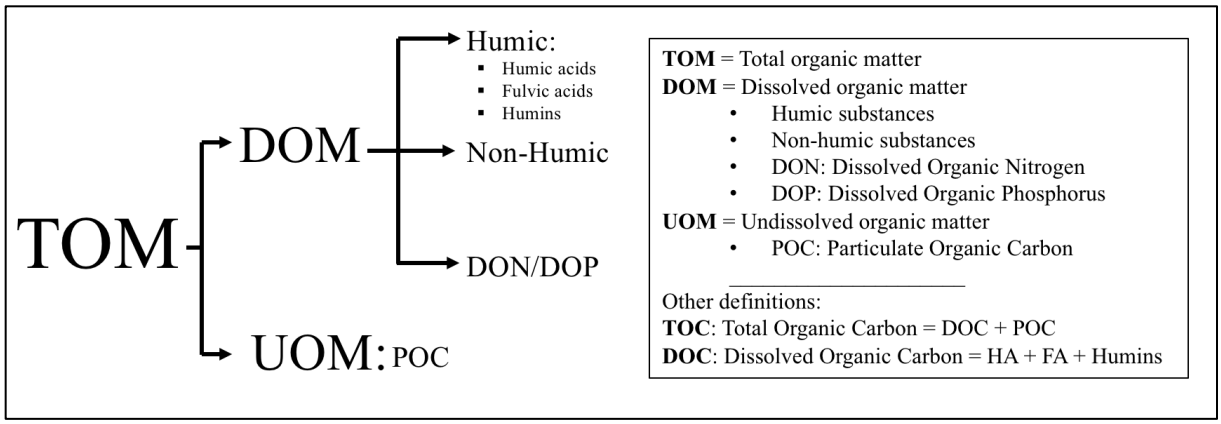

Figure 2-1 Classification of natural organic matter (NOM) as usually found in aquatic ecosystems. Adapted from Pagano, Bida, and Kenny (2014).

Regarding its chemical composition, dissolved organic matter (DOM) is usually defined as a complex mixture of aromatic and aliphatic compounds containing functional groups of different nature [67]. In aquatic environments, DOM consists mainly of fulvic and humic acids (~80% by weight) and a mixture of other compounds such as carbohydrates, amino acids, and hydrocarbons (~20%) [35] as can be seen in Figure 2-2 . Hydrophobic and hydrophilic acids are estimated to be the main components of humic substances.

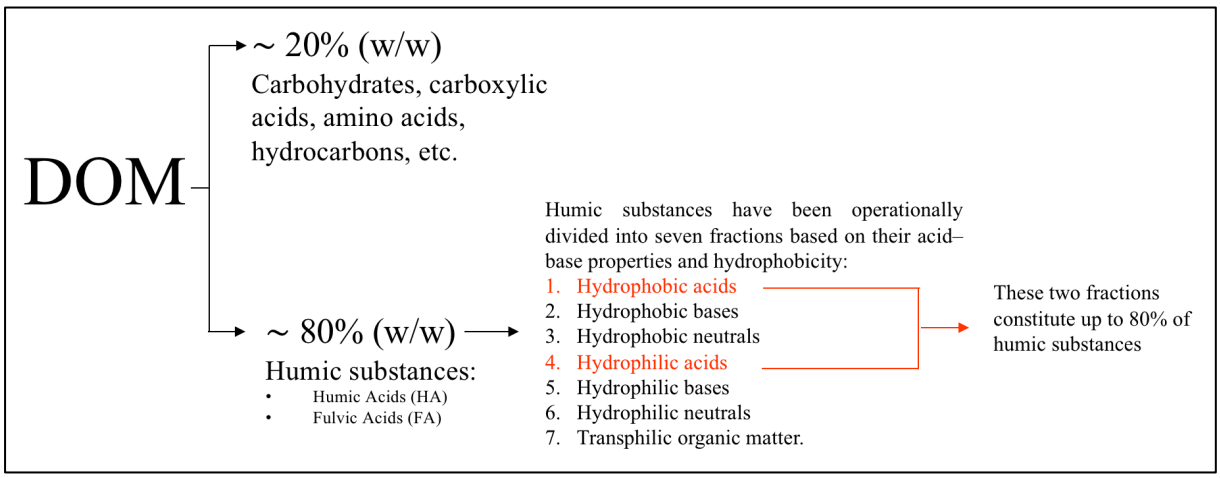

Figure 2-2. Estimated composition of DOM in aquatic environments. Adapted from Ravichandran (2004)

Hypothetical structures of humic substances are shown in Figure 2-3. This model includes both the hydrophobic and hydrophilic regions and shows the abundant functional groups present in this particular portion of the DOM. Functional groups present in NOM include carboxylic acids, enolic hydrogens, phenolic hydrogens, quinones, alcoholic hydroxyls, ethers, ketones, aldehydes, esters, lactones, amide, amine [35], [45], [68], [69], and sulfur [35], [37].

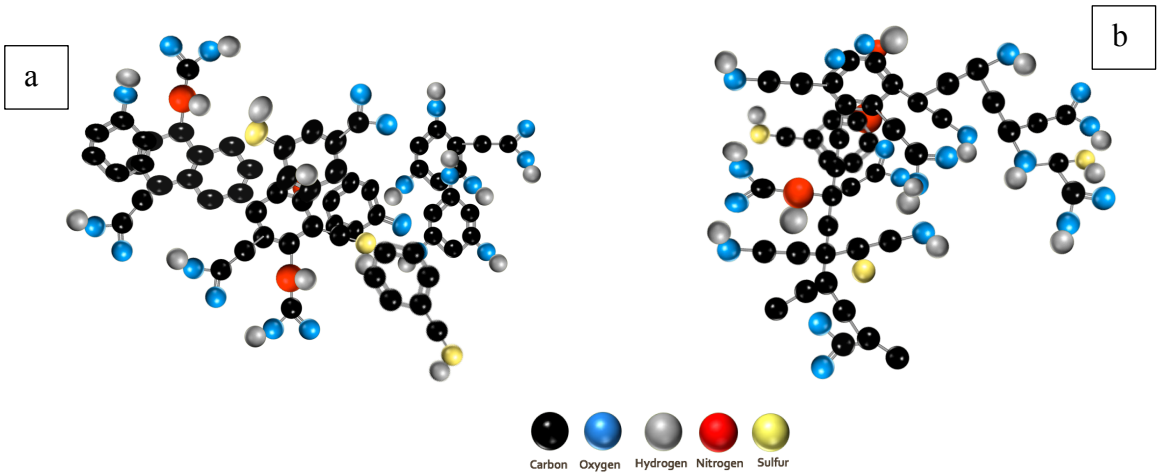

Figure 2-3. Hypothetical structure of humic substances as expected in natural environments showing the portion rich in aromatic carbon (a) and the portion rich in aliphatic carbons (b) as well as the main functional groups for metal complexation. Adapted from: Wandruska (2000) and Leita et al. (2009).

Of particular note is that the fulvic and humic fractions, the most hydrophobic portion of NOM, are more likely to be removed in water treatment and are more reactive to heavy metals in aquatic ecosystems. As a result, DOM is often classified based on the characteristics of the hydrophobic and hydrophilic fractions including their polarity and acid-base character as can be seen in Figure 2-4.

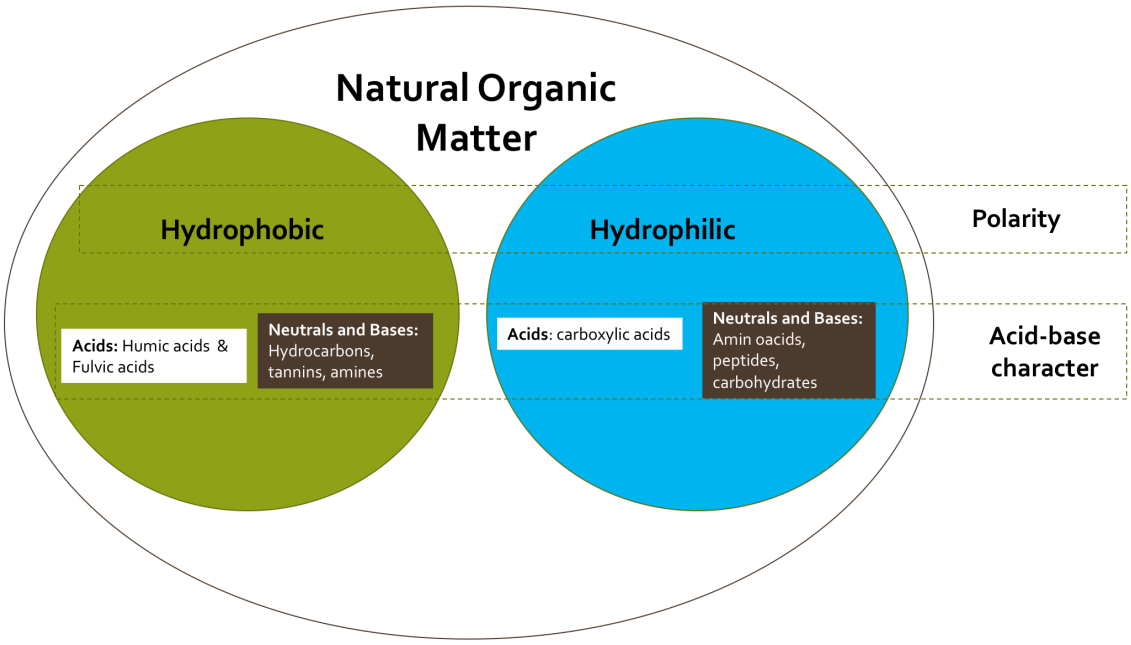

Figure 2-4. Classification of natural organic matter (NOM) based on its polarity and acid-based character. Adapted from Bond et al. (2012)

The nature and concentration of DOM in surface water varies according to the origin of the water, the hydrological cycles of the surroundings environment, and the season [43], [44], [50]. The concentration of DOC in surface waters can be as low as 0.5 mg/L or as high as 50 mg/L, depending on the environmental conditions and the biogeochemical characteristics of the water sources [70]. DOC concentrations can be particularly high after rainfall events, snowmelt runoff, or floods; reaching water sources used for drinking water purposes [43], [71].

2.2 Hg-DOM interactions in aquatic environments

The complexity of the structure of DOM and its ubiquity in aquatic environments make this substance an important sorbent for dissolved metals in water. Hg in water is expected to bind to the acid sites in the DOM, specifically to acidic functional groups such as carboxylic acids, phenols, ammonia, alcohols, and thiols [35]. Although

carboxylic acids and phenols comprise up to 90% of the acidic functional groups, dissolved Hg and MeHg (CH_3Hg^+) are expected to form the strongest complexes with reduced sulfur ligands (S_{red}), such as thiols [35], [37], [58], [61], [72]–[74]. However, when the ratio Hg/DOM is high, the number of sulfur ligands may be insufficient to complex a significant amount of Hg [35], [72]. In fact, in unpolluted ecosystems, where the Hg/DOM ratio is expected to be low (<< 1.0 µg THg/mg DOM), Hg(II) and MeHg will be strongly bound to sulfur reduced ligands in the DOM [35], [37], [74]. Conversely, at high Hg/DOM ratios (e.g., > 1.0 µg THg/mg DOM), as could be the case in polluted ecosystems such as those impacted by ASGM, Hg(II) and MeHg may also be bound to other functional groups such as carboxylic and phenolic ligands [37], [61].

Carboxyl and phenol content in DOM can be quantified by titration [37], and sulfur species can be identified and quantified using X-ray absorption near-edge structure (XANES) spectroscopy[35], [58], [75]–[81]. Table 2-1 shows the most relevant acidic functional groups in selected NOMs, where carboxylic groups are the most abundant ligands for Hg complexation.

Table 2-1. Acidic functional groups in NOMs selected for experimentation

NOM Description	% S_{red}[a] (S_{red}/S_{total})	S_{red} (mg/g C)	S_{red} (meq/g C)	Phenolic[b] (meq/g C)	Carboxyl[b] (meq/g C)
Suwannee River Fulvic Acid	53.5	4.70	0.294	2.8	11.2
Suwannee River Humic Acid	63.9	6.56	0.410	3.7	9.1
Nordic Aquatic Humic Acid	71.8	7.81	0.488	3.2	9.1
Pony Lake Fulvic Acid	68.2	39.4	2.461	1.8	7.1

[a]Manceau and Nagy (2012), Sred = Heterocyclic S + Exocyclic S. [b] IHSS (http://humic-substances.org/)

In humic substances, the four major sulfur oxidation groups are sulfate ester, sulfonate, sulfoxide, and thiol-sulfide [77]. Thiol-sulfide was lumped into a single functional group because the Gaussian peaks resulting from the curve-fitting analysis for thiol and sulfide groups from XANES spectroscopy were indistinguishable from each other [77]. Nevertheless, total sulfur is a minor component of DOM. In general, it was

determined that the total sulfur content in dissolved organic matter ranges from 0.5 to 2.0% (w/w), where reduced sulfur can make up to 70% of the total sulfur [35], [75]. Oxygen-functional groups are present at higher concentration than the S_{red} ligands in DOM (Table 2-1); therefore, it is possible that these oxygen-ligands also play a role in complexing and mobilizing Hg from polluted ecosystems.

2.3 Mercury levels in surface water in regions impacted by ASGM

Approximately 800 tons of mercury are released annually to surface water through the weathering of Hg-bearing minerals in igneous rocks [13]. Additionally, it was estimated that 260 tons of this element were released to rivers in 2010 through extensive erosion caused by deforestation [5], [13]. However, higher risk to water pollution persists in countries affected by ASGM because the amount of mercury discharged during this activity may easily surpass the environmental Hg released in such locations. ASGM alone accounts for one-third of the anthropogenic Hg emissions globally [19], [82]. It is clear that the combination of the legacy contamination associated with the tons of metallic mercury historically discharged in soils, rivers, and streams, and the mercury currently discharged by ASGM [9] represents a potentially large source of mercury pollution to the communities in ASGM regions.

Mercury from ASGM can reach soil and water bodies in many ways: during the amalgamation process and amalgam burning or purification, when it is spilled during dredging operations, and when it is leached from inadequate tailings ponds. The latter is possible when gold is extracted from soil and rocks [83]–[85]. Various forms of mercury are released during ASGM operations. During the amalgamation process, the burning of the Hg-Au complex releases several different species of mercury to the atmosphere: Hg^o (Hg vapor), Hg(II), and particulate Hg(II) (i.e., HgO(s)) [8].

In the case of metallic mercury (Hg^0), once this pollutant reaches aquatic ecosystems, its transformation to dissolved mercury (Hg(II)) is a function of the physical, chemical, and biogeochemical processes taking place primarily in bottom sediments [10], [86]–[89]. Partitioning to sediments is a dominant process in the distribution of Hg species into the particulate, colloidal, and dissolved phase [90]. In acidic environments, mercury will be present as Hg(II) and therefore can be taken up by aquatic microorganisms. At higher pH, functional groups in DOM, such as -OH and -COOH, deprotonate allowing the complexation of Hg(II) with DOM. As a result, the bioavailability of free metal ions and mercury's toxicity to aquatic organisms can be reduced considerably, but the now formed Hg-DOM complexes will travel downstream and thereby pollute water sources with mercury. Regardless of the mercury concentrations in sediments, dissolved mercury levels are expected to be very low in the water column, even during storms and wet seasons [91]. This fact suggests that, under natural conditions (wet/dry season), the amount of dissolved mercury in the water column is independent of the mercury concentration in bottom sediments [91], [92]. However, a different situation might occur if dredging operations, mining activities, or any other anthropogenic activity enhances physical erosion, because it will increase the suspended sediments load and consequently the presence of mercury in the water column [93], [94].

Appendix A includes a literature review of some of the most relevant mercury concentrations found in aquatic systems around the world located near gold mining districts. Three clarifications are necessary regarding the information collected in Appendix A. First, these concentrations were detected at specific times and locations, and might change temporally as a function of the mining operations, the hydrologic season, or any other physical or environmental factor. Second, with a few exceptions, for instance in Colombia, the Philippines, Brazil, and Tanzania, it is not specified if the water bodies listed in Appendix A are being used for drinking water intake, or any other purpose. However, because ASGM takes place in regions where poverty is the common

denominator, it is not surprising that miners, along with riverine villagers living around these ecosystems, use the surface water for recreation, agriculture, fishing, and domestic consumption. And finally, most samples were taken at depths not greater than 30 cm. As a result, mercury concentrations at deeper levels, where intake systems are usually located, are unknown.

Regarding ASGM, under specific circumstances, total mercury concentrations in water have been reported as high as 5.0 μg/L in Colombia [95], 6.78 μg/L in Tanzania [84], 7.0 μg/L in the Philippines [96], and approximately 10 μg/L in the Brazilian Amazon [14]. In the case of Colombia, legislation establishes a maximum mercury value of 2.0 μg/L for water bodies intended to be used as domestic water supplies [21]. Within the United States, relatively high dissolved mercury concentrations have been reported in areas of California (i.e., Mugu Lagoon, which is listed as impaired for mercury, and the San Francisco Bay which is an important case of estuarine mercury contamination), Nevada (the Carson River), Wisconsin, Minnesota, and the Northeastern United States; these high mercury concentrations are thought to be a consequence of anthropogenic sources (i.e., agricultural, industrial, military, and urban runoff) [52], [97]–[100].

2.4 Mercury in Colombian rivers

In the particular case of Colombia, most gold production comes from informal and illegal mining [23], [101]. According to the Colombian government, 86% of the 58 tons of gold annually produced by the country comes from illegal mining, and 232 out of the 1,150 rivers of the country cross heavily mercury polluted ecosystems [23]. In June 2017, water samples were retrieved from five different rivers, one swamp, and one creek in Colombia, to determine the levels of mercury downstream of different gold mining districts. The water bodies selected were the Magdalena River (Bolivar), the Nechí River (Antioquia), the Atrato River (Chocó), the Quito river (Chocó), the Tutunendo River

(Chocó), the Ayapel Swamp (Córdoba), and the Villa Creek (Antioquia). Stream water samples were collected at locations near water intake structures and other sites of interests for dissolved total mercury (THgd) analysis following the "clean hands, dirty hands" technique (US EPA Method 1669). The sites were selected considering the information provided by the Colombian government related to historic discharges of metallic mercury in gold mining [24]. These locations were also selected considering accessibility and security concerns due to the presence of armed groups that control an important part of the gold mining industry in the country.

Samples for THgd analysis were collected in acid-precleaned 250-mL Teflon® bottles and filtered using a polyethersulfone (PES) filter (0.45-µm) prior to preservation with BrCl. Samples for DOC and UV absorbance were collected in 50-mL polypropylene tubes and were filtered using cellulose acetate membrane filters (0.45-µm) prior to preservation with HCl analytical grade (only for DOC determination). According to the Standard Methods for measurement of UV absorbance, samples should not be acidified to pH values below 4. All samples were stored in coolers with ice packs and express-mailed to The University of Texas at Austin (Austin, TX) for THgd and DOC analysis and stored in a dark cold room at 4ºC.

Water samples were analyzed for THgd using cold-vapor atomic fluorescence spectrometry (CVAFS) (Tekran 2600; Tekran, Toronto, ON) following US EPA method 1631, revision E (US EPA, 2002). QA procedures for THgd analysis were maintained through blanks (field and method blanks). DOC was determined on a TOC $L_{CPH/CPN}$ analyzer (Shimadzu) using high-temperature (680 °C) catalytic oxidation. UV absorbance was measured at the Universidad de Medellín (Antioquia, Colombia) using a Spectroquant® Pharo 300 (Merck). Physicochemical parameters in the water column such as pH, total dissolved solids (TDS), and temperature were recorded *in situ* with a multiparameter probe (HANNA® HI 9813-6).

During the sampling period, an unusual rainy season was present across the country. Therefore, the areas around most of the sampled water bodies were flooded, especially on the Magdalena River, the Nechí River, and the Ayapel Swamp. Table 2-2 includes the results for THgd at each location, together with parameters such as DOC, pH, and TDS. The Tutunendo River (Chocó) was used as a reference site because this river is used for tourism, and no gold-mining activity has been reported around its watershed. Levels of THg in Table 2-2 correspond to grab samples, i.e., they reflect the Hg pollution in the water sources at a given time and at a specific location.

Table 2-2. Mercury levels in water samples from Colombian rivers

Municipality (State)	Description	Location	T (ºC)	pH	TDS (mg/L)	DOC (mg/L)	Hg (ng/L)
Magangué (Bolívar)	WTP Water Intake Magdalena River	9º 13' 30.7082" N 74º 44' 43.272" W	30.2	7.0	103	1.38	54.5±3.3
Ayapel (Córdoba)	WTP Water Intake	8º 17' 59.43" N 75º 8' 45.75" W	32.8	8.6	71	1.74	85.0±3.5
	Boca de Caño Barro entering to the Ayapel Swamp	8º 18' 47.688" N 75º 7' 7.75" W	32.2	7.5	80	2.47	473.5±16.9
Quibdó (Chocó)	Tutunendo River (Site Reference- No mining activity)	5º 44' 31.6" N 76º 32' 0.29" W	25.3	7.6	18	-	< 0.80
	~300 m u/s Hospital water intake on the Atrato River	5º 41' 42.968" N 76º 39' 42.887" W	25.4	6.3	14	-	147.0±9.9
	Quito River, ~200 m d/s dredging operation	5º 31' 46.782" N 76º 45' 2.328" W	26.9	5.2	52	2.05	208.0±17.2
El Bagre (Antioquia)	WTP Water intake (Quebrada Villa)	7º 35' 27.522" N 74º 47' 11.592" W	27.9	6.3	19	1.03	40.2±3.2
	Nechí River	7° 36' 5.378" N 74° 48' 51.516" W	28.5	6.4	39	1.58	485.0±45.2

Values of Hg from Table 2-2 are also included in Figure 2-5, which shows the estimated discharge of metallic mercury (Ton/yr) in soil and water during gold extraction. As Figure 2-5 shows, Hg pollution is widely extended across the country, particularly in the states of Antioquia, Chocó, Bolívar, Cauca, Córdoba, Sucre, and Nariño. Relatively high mercury concentrations were detected in water sources from these states, particularly in regions heavily polluted with metallic mercury. Some of these samples were taken in municipalities located more than 10 miles away from known mining districts. Although many other municipalities are located closer to the mining district, it was not possible to visit them for security reasons. Nevertheless, Figure 2-5 clearly indicates that mercury used in gold mining is the most likely cause of these atypical mercury concentrations in surface water.

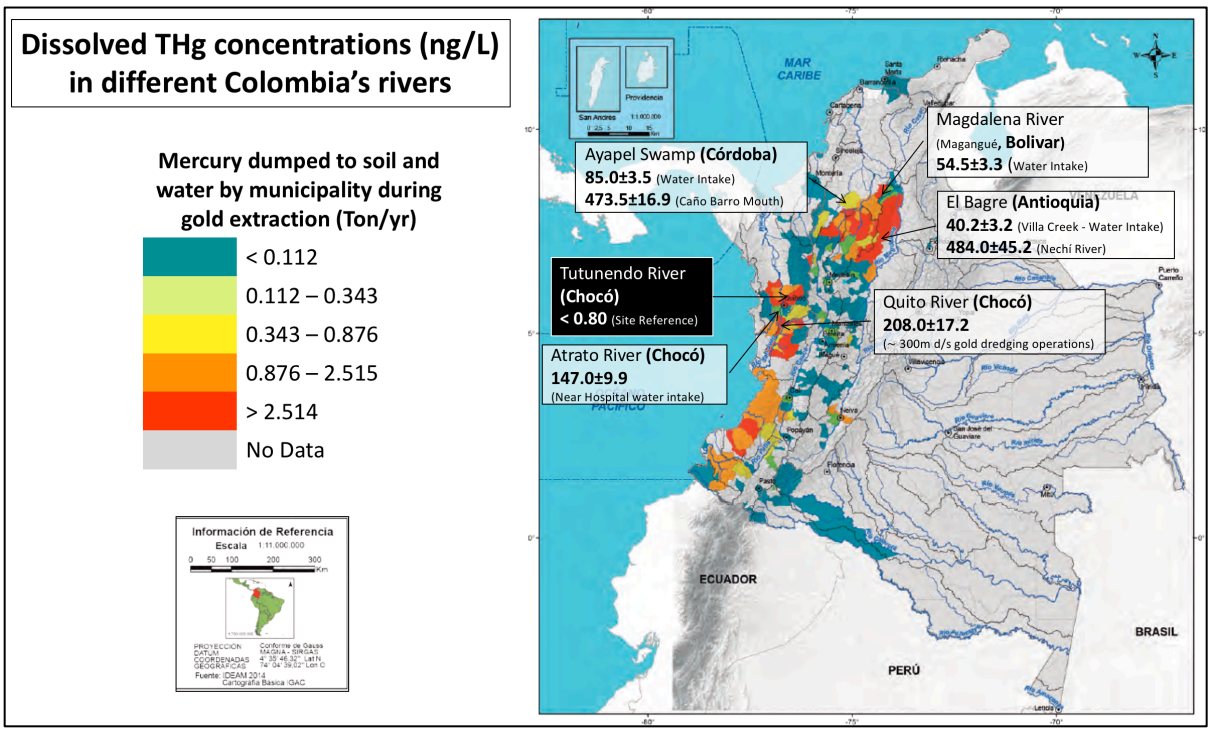

Figure 2-5. Map of the estimated discharge of metallic mercury in soil and water during gold extraction in Colombia showing dissolved THg concentrations in nearby water sources. Map source: Instituto de Hidrología, Meteorología y Estudios Ambientales-IDEAM, Estudio Nacional del Agua 2014 (map version: 1.0, 03-Feb-2018).

Dissolved mercury concentrations reported in Table 2-2, although atypical, are much lower than the total Hg levels measured in different mining sites by the Institute of Hydrology, Meteorology and Environmental Studies (abbreviated IDEAM in Spanish), a government agency, as part of an extensive study (Water National Study-2014) to evaluate the state and dynamics of the water resources in the country (see Table 2-3) [24]. Such results correspond to samples retrieved from different mining sites and at different times, but they are a consequence of the use of metallic Hg in ASGM. The use of metallic Hg in ASGM pollute water sources near to the mining sites where this activity is practiced. For instance, extremely high total Hg concentrations were detected at the Marmato stream's mouth (11.20 µg/L) in the state of Caldas and at the Magdalena River (6.35 µg/L) in the state of Bolivar, which will affect aquatic life and inhabitants living nearby these mining districts. ASGM is

the main reason that high mercury concentrations are found in many aquatic ecosystems [22] These high levels of mercury in water should raise some concern because they are above the concentrations expected to be found in unpolluted environments where the range of Hg has been measured between 0.2-15 ng/L[102] or 0.2-100 ng/L,[1] as is the case of the Tutunendo River (<0.80 ng/L).

Table 2-3. Mercury concentration discharged to Colombian rivers as measured by the IDEAM (2014)

State	Municipality	Stream/River	Longitude	Latitude	Total Hg (ng/L)
Caldas	Marmato	Marmato	-75.58027778	5.461666667	11,180
Bolivar	Regidor	Magdalena	-73.82080556	8.666333333	6,350
Tolima	Venadillo	Totare	-74.81802778	4.612027778	1,383
Santander	Puerto Wilches	Sogamoso	-73.91583333	7.211111111	1,020
Cundinamarca	Guaduas	Magdalena	-74.70911111	5.200722222	1,000
Magdalena	El Banco	Cesar	-73.97877778	8.985722222	982
Bolivar	Magangue	San Jorge	-74.73527778	9.150833333	973
Cundinamarca	Nariño	Magdalena	-74.83816667	4.387861111	923
Huila	Villavieja	Cabrera	-75.12075000	3.433611111	888
Tolima	Ambalema	Recio	-74.77255556	4.773416667	865
Tolima	Venadillo	Magdalena	-74.80844444	4.559638889	829
Cundinamarca	Girardot	Bogota	-74.83333333	4.300000000	827
Bolivar	Cordoba	Magdalena	-74.81538889	9.493583333	814
Tolima	Prado	Prado	-74.93625000	3.804638889	766
Tolima	Saldaña	Saldaña	-74.89105556	3.994555556	722
Caldas	La Dorada	La Miel	-74.66497222	5.772194444	715
Tolima	Melgar	Sumapaz	-74.74444444	4.248055556	710
Santander	Puerto Parra	Carare	-74.10333333	6.778055556	675
Antioquia	Pto Nare (Lamagdalena)	Nare	-74.58611111	6.206944444	670
Tolima	Purificacion	Magdalena	-74.93573333	3.849450000	659
Tolima	Coello	Coello	-74.89402778	4.288527778	636
Cundinamarca	Puerto Salgar	Rio Negro	-74.65130556	5.740916667	628
Cesar	Aguachica	Lebrija	-73.77305556	8.131111111	612
Bolivar	Magangue	Magdalena (Loba)	-74.60563889	9.016527778	583
Risaralda	La Virginia	Risaralda	-75.87416667	4.892611111	576
Cundinamarca	Puerto Salgar	Magdalena	-74.66191667	5.469222222	546

Source: Mesa N. A., Grupo Laboratorio de Calidad Ambiental (IDEAM) (personal communication, September 28, 2017)

2.5 Mercury treatment technologies and efficiency

In 2007, the U.S. Environmental Protection Agency (EPA) published a report called Treatment Technologies For Mercury in Soil, Waste, and Water in part to "help managers at sites with mercury-contaminated media and generators of mercury-contaminated waste and wastewater to identify proven and effective mercury treatment technologies" [103]. This report established that processes to reduce mercury concentrations to less than 2.0 μg/L from water include a combination of precipitation/coprecipitation, adsorption, and membrane filtration processes (Microfiltration, Ultrafiltration, Nanofiltration, Reverse osmosis).

Research focused on new technologies to remove mercury from water includes "modified nanometer sized adsorbents, ion exchangers or systems that can also be of interest for bio-applications."[104] Some of the materials that have been investigated are "carbon nanotubes, inorganic nanoparticles, zeolites, biopolymers and dendrimers." [104]. However, as reported, "most of the published work deals with relatively high and environmentally unrealistic mercury concentrations (≥20 mg/L) considering that mercury is very toxic to aquatic organisms in trace levels." [104].

Table 2-4 compares the removal efficiency of Hg from different water sources using adsorption processes [105]. With the exception of metal-based coagulant used as an absorbent, the concentration range examined in these studies is above the values expected in surface waters. Of equal importance is that this summary does not provide information regarding the presence of organic matter in the waters tested. Thus, there is a dearth of information regarding water treatment for mercury contamination at realistic concentrations.

Nevertheless, the removal efficiencies reported in Table 2-4 indicate that low mercury concentrations are possible in finished water when using adsorbents like 1,3-Benzendiamidoethanethiol, iron sulfide nanoparticles, DNA-condensation, chitosan-based ceramic, or modified magnetic iron oxide nanoparticles (M-MIONPs). However, the cost of these technologies would hinder their implementation in developing regions, where the most common water treatment is conventional coagulation with metal-based salts. A recent paper evaluated the use of metal-based coagulants to remove inorganic mercury (IHg) and MeHg from natural waters [52]. Researchers were able to remove up to 97% of IHg and 80% of MeHg from surface water through coagulation; in that study the initial THg concentration was 2.06 ng/L, and the DOC concentration was 2.61 mmol/L (~63 mg/L DOM) [28]. As can be noticed, this water had a very low Hg/DOM molar ratio of approximately 3.3×10^{-5} μg Hg/mg DOM which can explain the high mercury removal efficiencies achieved.

Table 2-4. Comparison of the removal efficiency of Hg among different absorbent types

Adsorbent type	Conc. range examined	Contact time (min)	Removal efficiency (%)
2-Mercaptobenzimidazole-clay	25-100 mg/L	480	>99
Polyacrylamide-iron(III) oxide	50-200 mg/L	240	95
1,3-Benzendiamidoethanethiol	65-188 µg/L	15	99.99
Sulfuric acid treated rice husk	200 mg/L	≥1000	>95
Metal-based coagulants	0.002 µg/L	60	97
Silica coated magnetite	50 µg/L	1200	74
Polyaniline/humic acid	50 mg/L	200	95
TiO2 nanoparticles	100 mg/L	30	65
Papain immobilized-alginate	10 mg/L	8	99
DNA condensation	0.02–100 mg/L	15	95
Dithiocarbamate-anchored	50 mg/L	60	40
O-benzenedithiol on cellulose	2 mg/L	10	100
Charcoal-immobilized papain	20 mg/L	2	99
Camel bone charcoal	10 mg/L	30	71
Aminated chelating fiber	1 mg/L	1440	99.9
Chitosan based ceramic	500 µg/L	120	99.9
Silver nanoparticle-adsorbent M-MIONPs	1 mg/L	1440	68
M-MIONPs	5-200 µg/L	4	92-99.0

Note: The information about metal-based coagulants is actually extracted from a paper about Hg immobilization on iron sulfide nanoparticles [105]. Source: Parham et al. (2012)

From the perspective of water treatment, a practical approach for the removal of Hg(II) from polluted sources is to consider the interactions between Hg(II) and the fraction of DOM amenable to coagulation with metal-based salts. Previous experiments determined that, in natural ecosystems, Hg(II) is more reactive to the aromatic fraction of DOM (the fraction with high molar mass and high hydrophobicity) [36], [52] and has a strong positive correlation with the hydrophobic acid fraction of DOM [66]. This approach would be valuable in drinking water treatment since *in situ* optical measurements such UV_{254} and fluorescence can provide reliable information about the character and composition of the DOM. Furthermore, UV_{254} measurements could eventually be used as a surrogate for predicting mercury concentrations in natural ecosystems [66]. Likewise, DOM measurements and Hg/DOM ratios could provide useful information to estimate Hg removal efficiencies from drinking water treatment.

CHAPTER 3. REMOVAL OF DISSOLVED ORGANIC CARBON (DOC) BY ALUM COAGULATION AS A FUNCTION OF THE AROMATIC CARBON CONTENT IN NATURAL ORGANIC MATTER (NOM) FROM DIFFERENT SOURCES

3.1 Introduction

The removal of natural organic matter (NOM) in alum coagulation treatment has been studied for decades due to concern regarding its role in the formation of disinfection by-products, and more recently due to either synergistic or antagonistic impacts on removal of fluoride, metals and other contaminants via adsorption and co-precipitation processes. This latter phenomenon is central to the objectives of this dissertation; namely, the impact of NOM on the removal of Hg(II) during alum coagulation. Thus, the focus of this chapter is to select a set of natural organic matter sources that provide a range of expected behavior during alum coagulation and a range of potential for Hg-NOM complexation. The results of these studies will be used to verify trends in removal of the selected NOMs during alum coagulation and to provide an analysis of the NOM remaining in solution after coagulation. With respect to the goals of this dissertation, the results will provide an assessment of the potential competition between Hg(II) complexation with the aluminum-NOM precipitates and the NOM remaining in solution after alum coagulation.

Natural organic matter (NOM) is a complex mixture of carbon structures and functionalities that changes in composition both temporally and spatially in a given watershed [35], [43], [45], [67], [68]. NOM is the main constituent of natural water that is responsible for the transportation of pathogenic microorganisms, for giving color to water sources, for the formation of trihalomethanes (THM) and other disinfection by-products (DBP) in drinking water treatment, and for carrying heavy metals such as iron, copper, chromium, lead, and mercury in natural ecosystems [68], [106]. Depending on its origin,

NOM can be rich in aromatic carbon when proceeding from terrestrial vegetation rich in lignin degradation by-products, or low in aromatic content as a result of the decay of vegetation and microbial activity in aquatic environments [45], [64], [68], [107]. The concentration and character of NOM in drinking water sources play a key role in the ability to remove this pollutant during water treatment. Relevant to this research, the negatively charged compounds in the NOM will react with the positively charged species provided by metal-based coagulants such as aluminum sulfate (alum), ferric sulfate, and polyaluminum chloride, among others.

$SUVA_{254}$, defined as the UV absorbance at 254 nm of a water sample divided by the concentration of dissolved organic carbon (DOC) [48], [53], [107], has been extensively used to predict the amount of DOC that can be removed in metal-based water treatment [47], [48]. Additionally, a strong positive correlation between the aromatic carbon content of NOM, determined by the ratio of the area of the aromatic carbon region (110-165 ppm) to the total area of ^{13}C-NMR spectra, and $SUVA_{254}$ values was found when analyzing organic isolates from different environments [53]. The strong correlation (R^2=0.91) between $SUVA_{254}$ and aromatic carbon content, shown in Figure 3-1, was obtained from a large and diverse pool of isolated NOM samples from soil and aquatic environments [53], [108], [109].

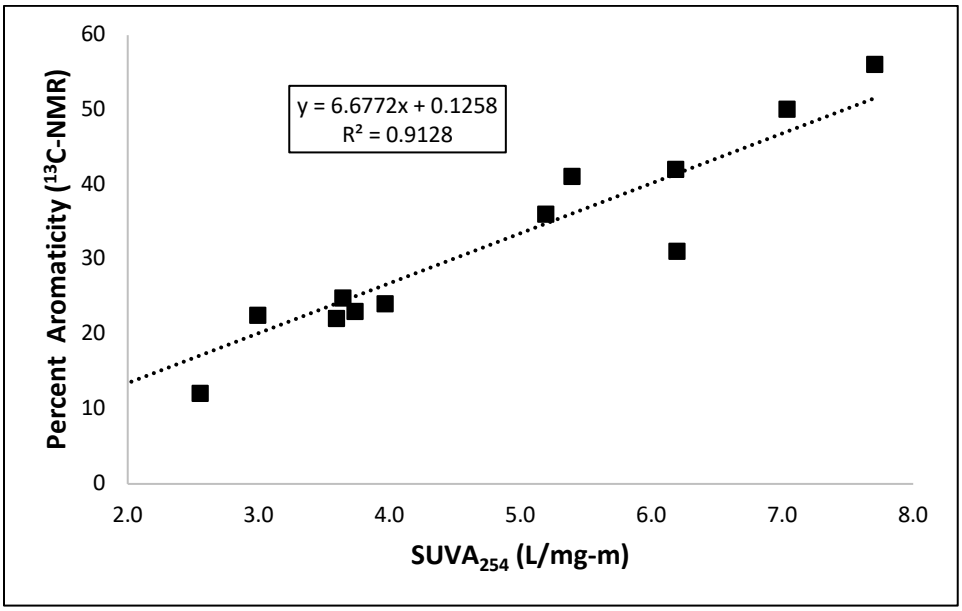

Figure 3-1. $SUVA_{254}$ as a function of the percent aromatic determined by ^{13}C-NMR for NOM samples from different environments. Adapted from Weishaar et al. (2003), Hur and Schlautman (2003), and Korak et al, (2014).

While such correlations appear to provide a relatively simplistic representation of the complexity of the structure and composition of the NOM, more detailed analyses of the interaction between free metals in aquatic ecosystems and the character of the NOM itself is quite difficult. Some approaches require sophisticated measurement tools that are not readily available in small-scale water treatment systems. One option to study such interaction would be from the perspective of the aromatic content of the NOM; that is, to study how free metal ions react with the fraction of NOM removed in water treatment. Another alternative to study free metals-NOM interactions would be from the perspective of the specific functional groups present in the NOM; this approach requires knowledge of which fraction of the NOM contains metal binding sites available for complexation, how strong are these sites, and what is the relative abundance of each.

In water treatment, changes in SUVA values can provide relevant information about the character of the NOM removed from the solution [45], [47], [50], [52], [53], [110], and accordingly, residual SUVA values could also offer some insight regarding the most likely

composition of the NOM remaining after the treatment process. Although it is unknown how the functional groups that are reactive to metal ions are distributed in the structure of the NOM, evidence of the high affinity of metal ions for the aromatic fraction of NOM has been reported for Ni(II), Cu(II) Pb(II), As(II), and Hg(II) [35], [52], [54]–[57], [111].

Consequently, the goal of this research was to evaluate how the aromaticity of the natural organic matter influences the removal of DOC in alum-based water treatment. $SUVA_{254}$ values will be used as a proxy for aromaticity and changes in $SUVA_{254}$ as indicator of the removal of the aromatic portion of NOM.

3.2 Research Approach

3.2.1 Selection of NOM samples and preparation of DOM solutions

The NOMs used in this work were obtained from the International Humic Substances Society (IHSS) and were selected based on the differences in aromatic carbon, reduced sulfur content, acidic functional groups concentration, geographical location, and commercial availability. A particular interest to the goals of this dissertation was to identify NOMs that cover a range of sulfur and aromatic carbon content. With these considerations, the NOMs selected were the Suwanee River NOM (unfractionated sample), as well as its humic and fulvic fractions; the Pony Lake Fulvic Acid, a microbially derived NOM with hydrophilic character [68], rich in reduced sulfur concentration and low in oxygen-functional groups; the Nordic Aquatic Humic Acid, rich in aromatic content and low in aliphatic carbon; and the Upper Mississippi River NOM (unfractionated sample), which has a low aromatic content compared to the other NOMs. A summary of the NOMs selected is presented in Table 3-1. Despite the differences already mentioned, total carbon constitutes approximately 50% of the natural organic matter in all cases.

Table 3-1. Carbon distribution and acidic functional groups of selected NOMs

[a]Catalog Number	NOM Description	% C	% Aromatic 165-110 ppm	% Aliphatic 60-0 ppm	Acidic functional groups (meq/g C)		
					[b]S_{red}	[a]Phenolic	[a]Carboxyl
1R109F	Pony Lake Fulvic Acid	52.47	12	61	2.46	1.75	7.09
2S101F	Suwannee River Fulvic Acid	52.34	22	35	0.294	2.84	11.17
2S101H	Suwannee River Humic Acid	52.63	31	29	0.410	3.72	9.13
1R105H	Nordic Aquatic Humic Acid	53.33	38	15	0.488	3.23	9.06
2R101N	Suwannee River NOM	50.70	N.A.	N.A.	N.A.	2.47	11.21
1R110N	Upper Mississippi River NOM	49.98	19	37	N.A.	0.830	12.43

[a]Source: International Humic Substances (http://www.humicsubstances.org/)
[b]Sred data extracted from Manceau and Nagy (2012)

Humic substances are estimated to account for up to 80% percent (w/w) of the composition of dissolved organic matter (DOM) in aquatic environments [35], [112]; the rest is a mixture of other compounds, mainly carbohydrates, carboxylic ligands, amino acids, and hydrocarbons [35]. Therefore, jar test experiments with unfractionated NOM and its two humic fractions (humic acids and fulvic acids) could provide useful information about the differences in removing specific fractions of NOM from water. Although both humic and fulvic acids are rich in aromatic components; in natural waters, fulvic acids have a lower molecular weight (between 600 and 1000 Da) than humic acids (between 1500 and 5000 Da) [45]. Another difference between these humic substances is the type of functional groups present in their structure. Previous research indicated that fulvic acids contains more carboxylic groups and are rich in oxygen atoms, while humic acids contains more phenolic and aromatic groups and have longer aliphatic chains [45]. As shown in Table 3-1, the carboxyl concentration in the fulvic fraction of the Suwannee River is 11.17 meq/g C, compared to 9.13 meq/ g C for its humic fraction. Similar differences were reported for samples of NOM extracted from Nordic Lake (Norway): 11.16 meq/g C (fulvic fraction) and 9.06 (humic fraction); and Pahokee Peat (a soil organic matter): 15.24 meq/g C (fulvic fraction) and 8.87 meq/g C (humic fraction) [62].

To prepare stock solutions of DOM for each NOM (i.e., the soluble fraction of the NOM), a determined amount of solid NOM sample was dissolved in ultrapure water (18 MΩ cm). The solution was mixed for 1-hr and sonicated for 30 min to break up big particles. pH was increased to 8.5 with NaOH to achieve complete dissolution of the NOM. Humic acids tend to precipitate at low pH (< 2) and fulvic acids are soluble at all pH values. After complete dissolution, solutions were filtered using a 0.45 µm cellulose nitrate membrane filter and stored in amber glass bottles in a dark cold room at 4ºC. A summary of the preparation process of the DOM solutions is shown in Figure 3-2.

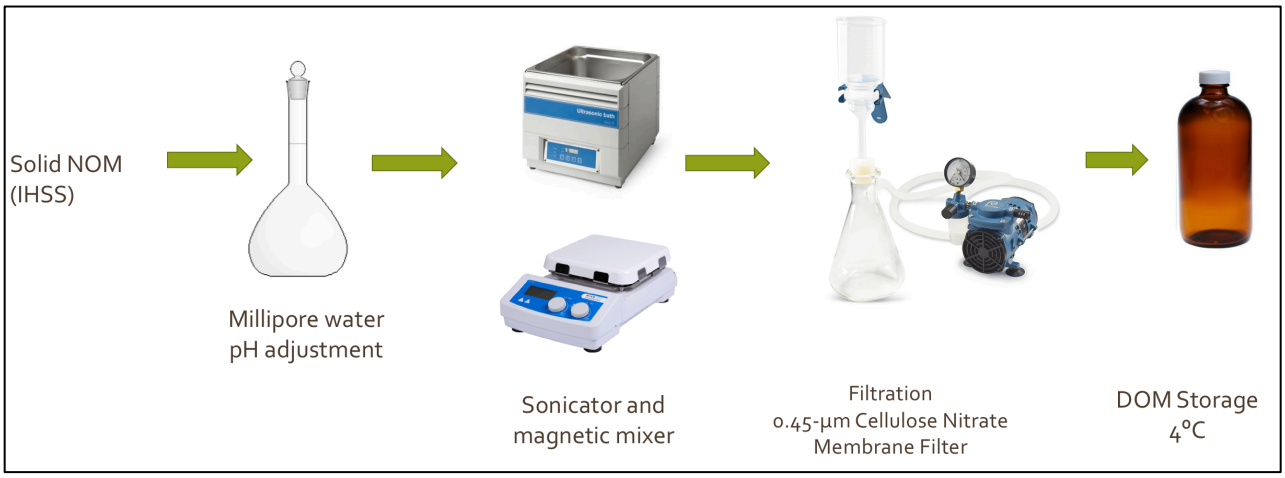

Figure 3-2. Schematic of the steps to prepare DOM solutions for jar test experiments

3.2.2 Characterization of DOM solutions

Concentrated DOM stock solutions were characterized by measuring the concentration of dissolved organic carbon (DOC), pH, total mercury (THg), the specific ultraviolet absorbance ($SUVA_{254}$), and the spectral slope (Se). $SUVA_{254}$ values (L/mg C•m) are calculated by dividing the UV absorbance at 254 nm by the DOC concentration. The $SUVA_{254}$ parameter is widely used in water treatment as an indicator of the aromaticity of DOM samples [47], [53]. A previous research determined that $SUVA_{254}$ values are strongly

correlated to the percentage of the aromatic carbon measured in the organic matter samples from aquatic ecosystems [53]. Table 3-2 shows how the magnitude of $SUVA_{254}$ controls the coagulation process. Samples with high aromatic content, and therefore high $SUVA_{254}$ values, are more easily treated with metal coagulant salts than samples with $SUVA_{254}$ values lower than 2.0.

Table 3-2. Guidelines on the character of NOM and expected DOC removals

$SUVA_{254}$	**Composition**	**Coagulation**	**DOC removals**
≥ 4.0	Mostly aquatic humics; high hydrophobicity, high molecular weight	NOM controls; Good DOC removals	>50% for alum; Potentially higher removals for ferric
2.0 – 4.0	Mixture of aquatic humics and other NOM; mixture of hydrophobic and hydrophilic NOM; mixture of molecular weights	NOM influences; DOC removals should be fair to good for these categories	25–50% for alum; Potentially higher removals for ferric >50%
< 2.0	Mostly nonhumics; low hydrophobicity, low molecular weight	NOM has little influence; Poor DOC removals	<25% for alum; Potentially higher removals for ferric

Source: Edzwald and Tobiason (1999).

Another useful parameter to characterize water samples is the spectral slope (Se). Se is also used as a proxy for aromaticity and changes in the composition of DOM (i.e., the ratio of humic acids to fulvic acids in the DOM) [113]. It was determined that chromophoric (colored) dissolved organic matter (CDOM) absorbs ultraviolet and visible light [44], [113], [114]. The optical properties of the CDOM fractions allow one to determine the nature of the DOM –aliphatic vs. aromatic- and consequently, its amenability for removal during the coagulation process. A simple model to describe light absorption by CDOM as a function of the wavelength was described by Twardowski et al. [113], and consists of an exponentially decreasing function as shown in equations 1 and 2.

$$a_g(\lambda) = Ae^{-S_e\lambda} \qquad \text{Equation 1}$$

$$a_g(\lambda) = \frac{2.303\ Abs(\lambda)}{L}$$ Equation 2

a_g = CDOM absorption coefficient (m^{-1})

A = Amplitude – a proxy for concentration.

S_e = Spectral slope parameter (nm^{-1}) – a proxy for changes in the composition of CDOM, the ratio of humic acids to fulvic acids, and DOM molecular weight.

λ = Reference wavelength (nm)

Abs (λ) = Absorbance measured at a given wavelength

L = Cell path-length (cm)

Spectral slope values can be calculated by using non-linear regression analysis over the range 280–350 nm [113]–[115]. Although reported spectra results values are sometimes contradictory [113], it is expected that samples with steep spectral slope values (close to 0.020 nm^{-1}) have a lower molecular weight DOM fractions, indicating that the sample is rich in aliphatic compounds, and consequently more hydrophilic. On the other hand, samples with shallow spectral slopes (close to 0.010 nm^{-1}) would be rich in aromatic carbon, and therefore, more hydrophobic and more amenable to removal during water treatment [52], [116].

Due to the strong correlation between $SUVA_{254}$ and carbon aromaticity, two different phenomenological equations were developed in previous research [115]. These equations show a linear correlation between the aromaticity of DOM, either with SUVA values at 254 nm (equation 3) or with the molar absorptivity $\in$ (L/mol-cm) at 280 nm (equation 4). The molar absorptivity is calculated by dividing the absorbance by the product of the cell length and DOC concentrations as show in equation 5.

$$Arom(\%) = 5.27\ x\ SUVA_{254} + 2.8$$ Equation 3

$$Arom(\%) = 0.057\ x\ \in_{280} + 3.0$$ Equation 4

$$\in = \frac{Absorbance\ @280\ nm}{Cell\ Length * [DOC]}$$ Equation 5

3.2.3 Simulating drinking water treatment at bench-scale jar tests

To evaluate the changes in $SUVA_{254}$ and the influence of the character of the NOM on the removal of DOC in alum-coagulation treatment, a set of jar test experiments were designed at constant DOC concentration, alum dose, pH, and ionic strength as shown in Table 3-3. To minimize mercury losses in subsequent experiments, jar tests were performed on magnetic stir plates using acid-cleaned Teflon® jars and Teflon® stirs bars

Table 3-3. Initial experimental conditions for jar test for selected NOMs

NOM	DOC (mg/L)	Alum Dose (mg/L)	pH	Ionic Strength (M)
All	5.0	30 (2.6 mg/L as Al(III))	6.7	0.01

To assure the removal of NOM through enhanced coagulation, a constant concentration of 30 mg/L alum (2.6 mg/L Al(III)) and a pH=6.7 were selected for these experiments. These coagulation conditions maximize the performance of the coagulant and minimize its residual concentration[48], [117], [118]. The selected pH is above the pH of minimum solubility of aluminum hydroxide which is 6.3 (at 25ºC) [119]. A schematic of this procedure is presented in Figure 3-3. Experiments were conducted with a N_2(g) blanket to avoid CO_2 interferences, thereby keeping the pH constant at 6.7.

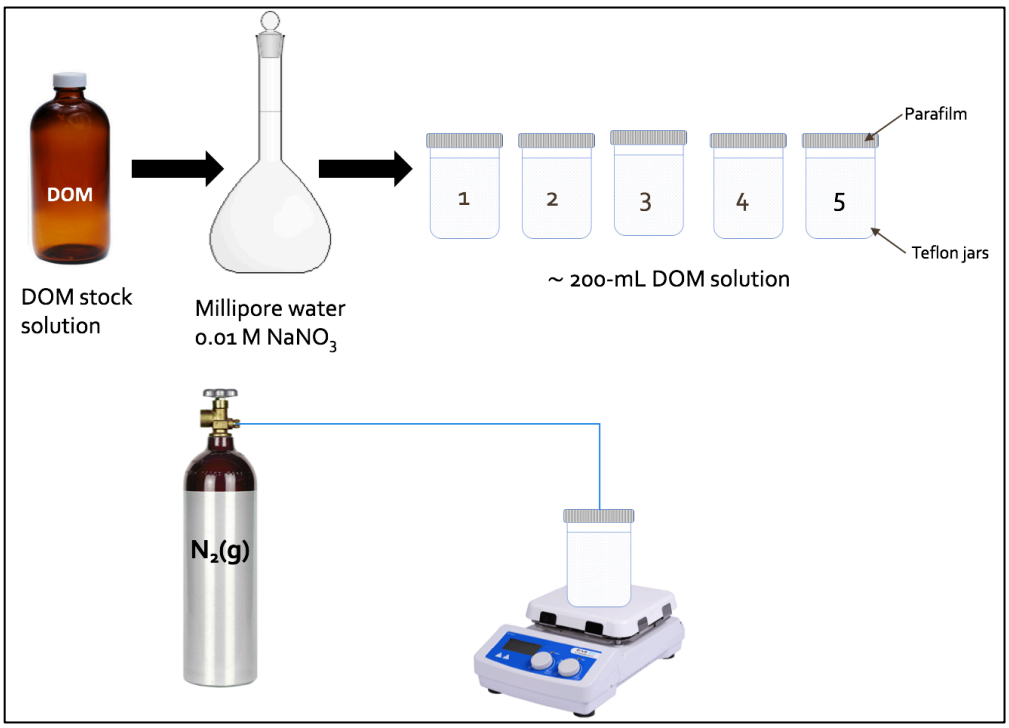

Figure 3-3. Schematic of the jar test procedure used for experimentation.

After settling, the supernatant was transferred to Teflon® vials for centrifugation. Once centrifuged, samples were taken for UV_{254}, DOC, and total Al(III) analysis. Reaction times (rapid mixing, slow mixing, and settling) of less than one hour ensure the formation of amorphous $Al(OH)_3$ precipitates [47], [120], [121]. A DOM-free control determined the amount of alum involved in the precipitation process. Previous research within our laboratories has shown that pH 6.7 provides optimal Al(III) removal for the alum used in this work. A summary of the procedure is listed below:

1. pH adjustment to 6.7 (HNO_3 or NaOH)
2. Rapid mix for 2 minutes to add coagulant
3. pH adjustment to 6.7
4. Slow mixing for 20 min
5. Settling for 30 min
6. Centrifugation for 30 min @ 665 x g

3.2.4 Analysis of aqueous samples

After each jar test, the supernatant was acidified with 80-µL concentrated H_2SO_4 per 40-mL sample and analyzed for DOC concentration in a TOC LCPH/CPN analyzer (Shimadzu) using high-temperature (680 °C) catalytic oxidation. Samples for aluminum determination were preserved with 385-µL concentrated HNO_3 per 5-mL sample and were analyzed using inductively coupled plasma spectroscopy (ICP) (Agilent Varian 710-ES, CA) at 309.271 nm and 396.152 nm wavelengths. UV_{254} was measured by spectrophotometry (Agilent 8453, CA) using either 1-cm or 5-cm quartz cells. $SUVA_{254}$ was determined from the UV_{254} reading and the DOC concentration of the sample. Samples were placed in a 4ºC storage room if not analyzed immediately. A summary of the analytical techniques used to achieve the goals of this research are outlined in Table 3-4.

Table 3-4. Analytical techniques used to analyze aqueous samples

Analysis	Technique	Method
DOC/TOC	TOC analyzer (Shimadzu)	USEPA 415.3
UV_{254}	UV spectroscopy	USEPA 415.3
[Al(III)]	Inductively Coupled Plasma Optical Emission Spectroscopy (ICP-OES) (Agilent Varian 710-ES, CA)	USEPA 6010D
Specific ultraviolet absorbance ($SUVA_{254} = UV_{254}/[DOC]$)	UV spectroscopy and TOC analyzer	USEPA 415.3
Spectral slope S_e (nm^{-1})	UV spectroscopy	----

3.3 Results and Discussion

3.3.1 Characterization of DOM samples before treatment

DOM solutions were characterized by measuring the concentration of dissolved organic carbon (DOC), pH, total mercury (THg), the specific ultraviolet absorbance ($SUVA_{254}$), and the spectral slope (S_e). The concentration of DOC for each DOM solution

was 5.01±0.14 mg/L. This concentration falls within the range of reported dissolved organic carbon in surfaces water, which can be as low as 0.5 mg/L or as high as 50 mg/L depending on the geology and activities associated with the watershed. To facilitate the comparison between the different NOMs used in this research, a short notation was given to each NOM as shown in Table 3-5. Table 3-5 also includes the $SUVA_{254}$ and S_e values measured for each DOM solution.

Table 3-5. $SUVA_{254}$, spectral slopes values, and notations for selected NOMs

NOM	NOTATION	% Aromatic 165-110 ppm[a]	$SUVA_{254}$ (L/mg C-m)	Se (nm^{-1})
Pony Lake Fulvic Acid	PLFA	12	2.53±0.13	0.015
Suwannee River Fulvic Acid	SRFA	22	4.51±0.20	0.015
Suwannee River Humic Acid	SRHA	31	5.94±0.13	0.011
Nordic Aquatic Humic Acid	NAHA	38	6.49±0.03	0.011
Suwannee River NOM	SR-NOM	N.A.	3.80±0.03	0.014
Upper Mississippi River NOM	MR-NOM	19	3.35±0.03	0.016

[a]Source: International Humic Substances (http://www.humicsubstances.org/)

The spectral slope values were calculated by non-linear regression analysis over the range 280–350 nm, using equations 1 and 2 as shown in Section 3.2.2. Figure 3-4 shows the spectral slope (as the exponential coefficient) for the different types of NOM used in this work. Even though a small difference is observed when comparing spectral slopes between samples, the relative steepness of the spectrum (Se) indicates the character of the NOM [113]. Samples low in aromatic content reported high spectral slopes (0.015-0.016), while samples high in aromatic carbon reported lower spectral slopes value (0.011).

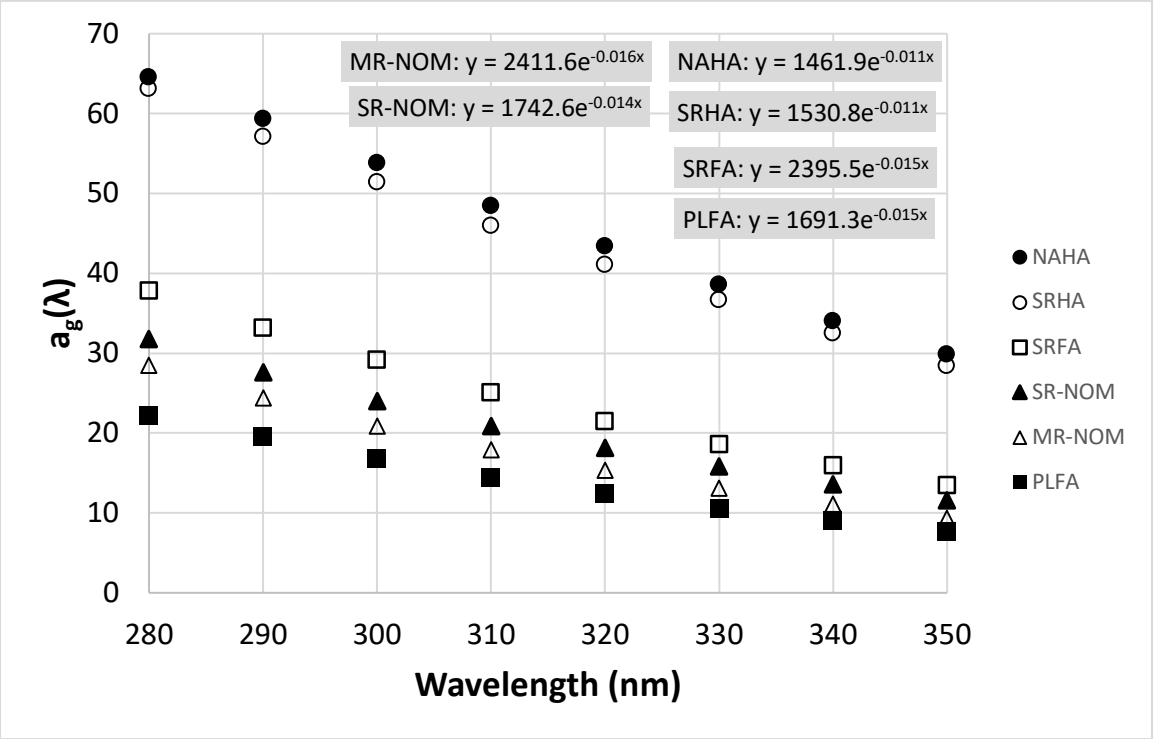

Figure 3-4. Absorption spectra for the selected NOMs

$SUVA_{254}$ values from Table 3-5 were also plotted in Figure 3-5 (slope = 5.83), together with the results shown in Figure 3-1 (slope= 6.68). As was expected, $SUVA_{254}$ values increase as the aromaticity of the NOM increases. Differences between these two lines can be attributed to fact that this work used exclusively NOMs extracted from freshwater ecosystems, while the data points for Figure 3-1 correspond to samples extracted from multiple environments such as marine water, dark water rivers, and soil. The data points that overlap correspond to referenced samples obtained from the same provider (i.e., IHSS) such as PLFA ($SUVA_{254}$ = 2.53 L/mg-C), SR-NOM ($SUVA_{254}$ = 3.80 L/mg-C), and SRHA ($SUVA_{254}$=6.2 L/mg-C).

The aromaticity of the SR-NOM used for experimentation (2nd batch with reference: 2R101N) was calculated using the phenomenological equations 3 and 4 to get 22.8% and 22.4%, respectively. IHSS reported a 23% aromaticity for the 1st batch collected of the same NOM (Reference: 1R101N). It is expected that the carbon composition of a reference NOM

sample does not change dramatically between batches when taken under similar conditions. The percentage of aliphatic carbon (0-60 ppm ^{13}C-NMR region) for the Suwanee River NOM (Ref: 1R101N) was 27%.

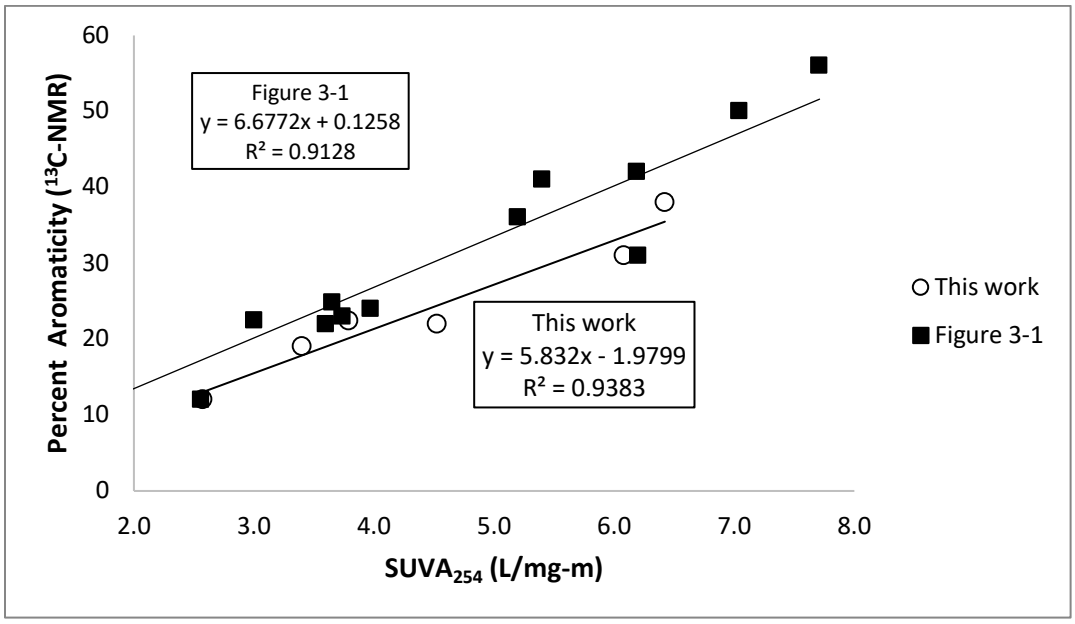

Figure 3-5. $SUVA_{254}$ as a function of the aromatic content of NOM for the samples used in this work.

The strong correlation ($R^2 = 0.94$) between aromaticity and $SUVA_{254}$ values of the prepared DOM samples corroborates the finding that, despite the differences in aquatic environments, $SUVA_{254}$ is a strong indicator of the composition of the NOM and can be used as a surrogate measurement for DOC aromaticity [45], [48], [53], [67].

3.3.2 Bench-scale jar tests results

A series of jar tests were performed for each of the NOMs selected to evaluate the removal efficiencies of $SUVA_{254}$ and DOC concentrations as a function of the character of the NOM in alum-based coagulation systems. Only the optimal coagulation conditions for the removal of NOM, fixed at pH=6.7 and alum dose of 30 mg/L were employed in this

research as the main objective for alum coagulation in developing countries is still turbidity removal. Coagulation at pH 6.7 favored the formation of an amorphous $Al(OH)_3$(am) precipitate. Under these conditions, it has been suggested that the mechanism for the removal of NOM is (a) the formation and precipitation of Al-NOM complexes (charge neutralization) and (b) the adsorption of NOM or Al-NOM complexes on the surface of the precipitate of $Al(OH)_3$(am) [106], [118], [120]–[124]. Previous research determined that humic substances absorbed onto the surface of alum flocs in the pH range from 5.0 to 7.0 [125]. Nevertheless, new studies suggest that the mechanism of interaction between humic substances and metal-based coagulant depends on the pH value [126]. Although previous research showed that no differences in carbon removal were found between coagulation at pH = 5 and pH = 7.0; charge neutralization was suggested as the main mechanism at pH = 5, while sweep coagulation was suggested as the control mechanisms at pH = 7, but at much higher alum doses than the one used at pH = 5 [127]. Thus, the dominant mechanism for the removal of NOM in our studies is in the range of sweep flocculation and therefore the removal of NOM is more likely due to the adsorption of NOM onto $Al(OH)_3$ precipitates.

The pH plays an important role in the removal of carbon through alum coagulation due to the protonation/deprotonation of the multiple functional groups present in NOM. At low pH, conjugated functional groups such as thiols, carboxyl, phenol, hydroxyl, and carbonyl, will remain protonated; at high pH, a complete deprotonation of these acidic functional groups is expected [111], [126], [128]–[130]. Nevertheless, carboxylic ligands are expected to be the main constituent responsible for the negative charge of the NOM, since these functional groups are ionized at pH above 6.0, while phenolic hydroxyls are expected to be nonionized below pH 8 [117]. In aquatic environments, trace metals like Hg(II) can be found bound to acidic functional groups such as carboxylic acids (pKa = 1- 5), phenols (pKa = 1-11), saturated thiols (R-SH, pKa = 8.5 – 12-5), aromatic thiols (ar-SH, pKa = 3 - 8), saturated alcohols (R-OH, pKa > 14), and ammonium ions (pKa= 2.6 – 12.5) [35], [131].

After jar tests, no significant differences were found in the residual aluminum concentrations among the NOMs tested (Figure 3-6). In all cases, the aluminum removal was approximately 92%. Therefore, the operational conditions for the jar test, pH 6.7 and alum dose of 30 mg/L, favored the removal of aluminum from solution.

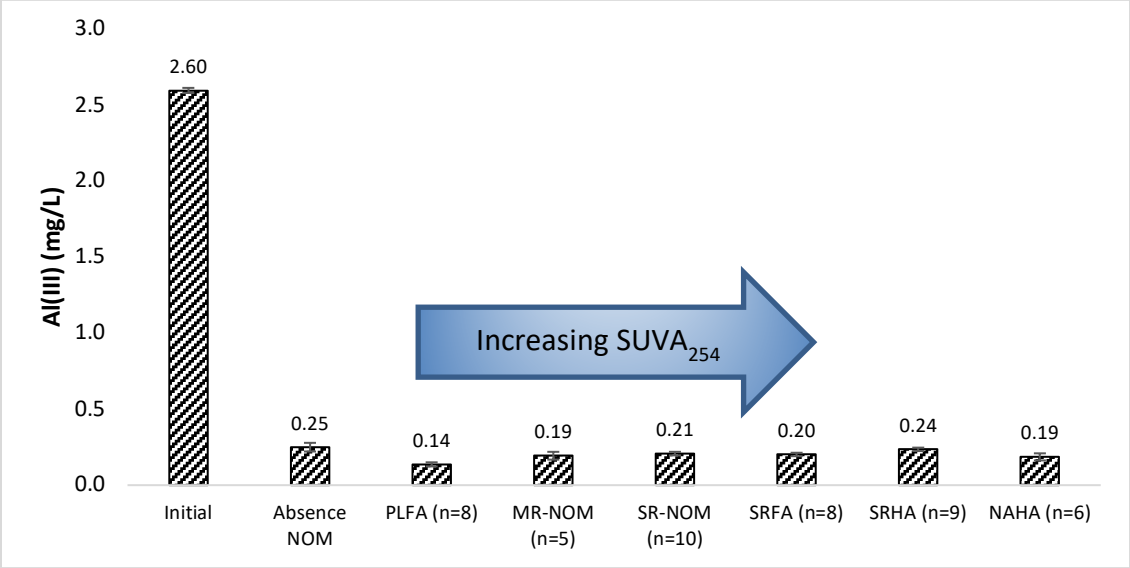

Figure 3-6. Residual Al(III) concentration at optimal coagulation conditions (pH = 6.7, Alum dose = 30 mg/L) for NOM from different environments. Error bars represent standard error from the replicates.

Regarding the removal of carbon, the largest amount of DOC was removed for the humic acids samples, SRHA and NAHA, with 4.4 and 4.1 mg/L, respectively (Figure 3-7). These two NOMs also had the highest aromatic content among the NOMs tested, 31% and 38%, respectively. PLFA (12% aromaticity) showed the lowest amount of DOC removed with 2.3 mg/L. The amount of carbon removed for the other fulvic acid tested, SRFA (22% aromaticity), was much higher than PLFA with a removal of 3.4 mg/L. Both, the unfractionated NOM samples, SR-NOM (~23% aromaticity) and MR-NOM (19% aromaticity), showed similar amount of carbon removed, with 3.2 and 2.9 mg/L, respectively.

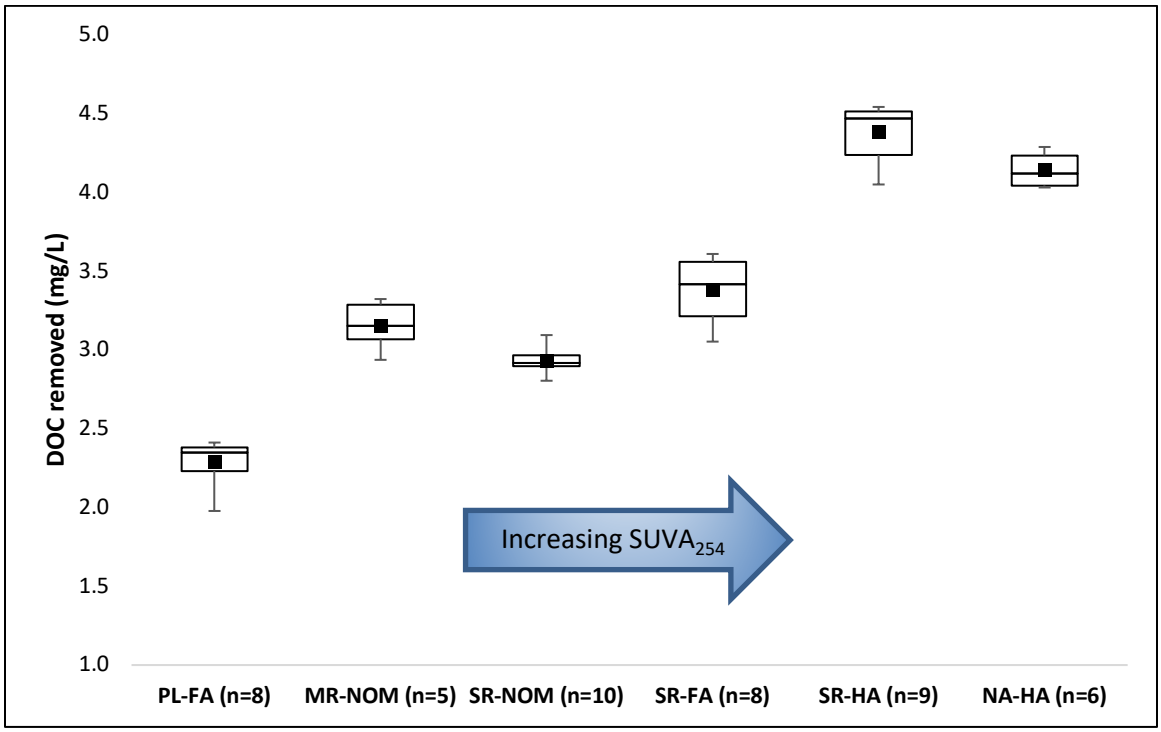

Figure 3-7. Amount of DOC removed for selected NOMs in alum-coagulation treatment at pH 6.7, 0.01M $NaNO_3$ ionic strength, and 30 mg/L alum dose. For each NOM, the initial DOC concentration was set at 5.0 mg/L. Error bars represent the standard deviation from the replicates.

A post-hoc analysis showed no statistical differences in mean DOC removed values between SRHA and NAHA (Anova with post-hoc Tukey HSD Test, $p > 0.05$), SRFA and MR-NOM ($p > 0.05$), or between MR-NOM and SR-NOM ($p > 0.05$).

The first indication of changes in the composition of the NOM remaining after jar tests is provided by the changes in spectral slope (Se). Figure 3-8 shows the Se values, before and after treatment for each of the NOM tested. In all cases, the Se (the exponential coefficient) increased compared to the initial value, reflecting a decrease in the aromaticity of the NOM after the treatment process. Higher changes were observed in the MR-NOM and SR-NOM, the unfractionated NOMs, where the Se value increased from 0.016 to 0.020 and 0.014 to 0.020, respectively. A high increase was also noticed in the NAHA sample, which changed from 0.011 to 0.015. The increases in Se values for the other three NOM samples were relatively small.

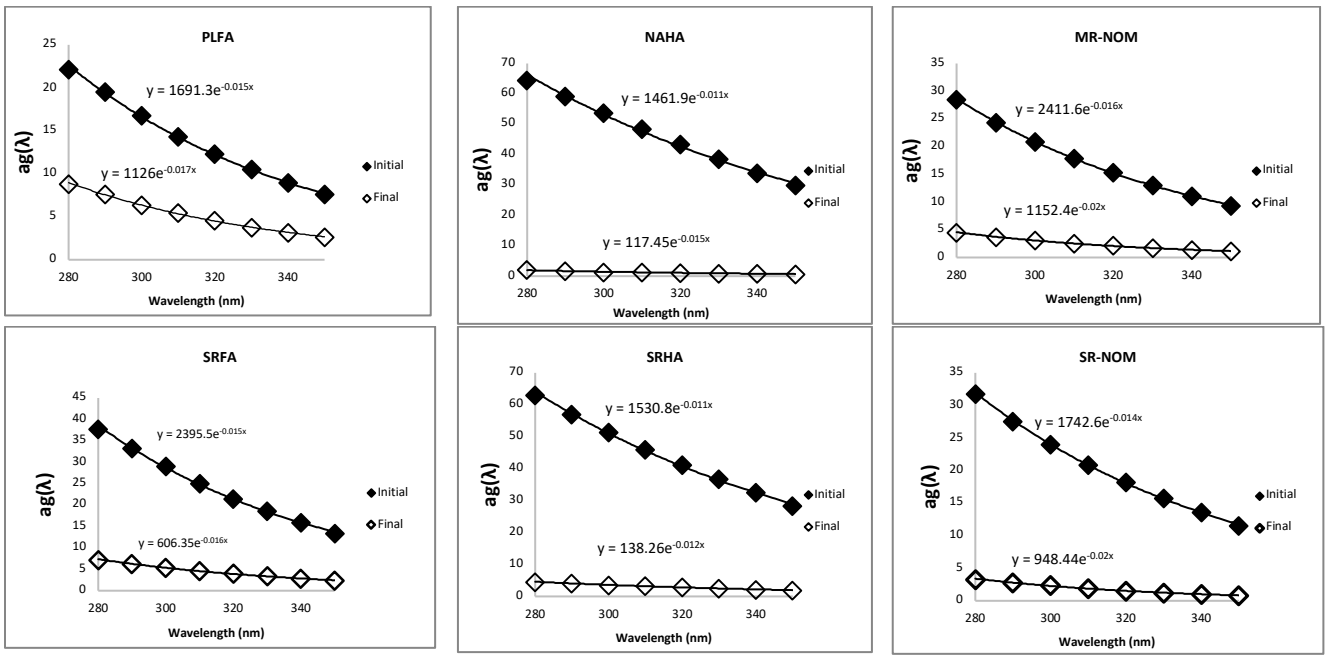

Figure 3-8. Changes in spectral slopes values after alum coagulation at pH 6.7, 0.01M NaNO3 ionic strength, and 30 mg/L alum dose. For each NOM, the initial DOC concentration was set at 5.0 mg/L.

High spectral slope values are usually associated with low aromaticity or the presence of lower molar mass compounds in NOM from aquatic environments [52], [132]; however, the most common parameter used in water treatment as a proxy for aromatic content is the $SUVA_{254}$ value. Changes in $SUVA_{254}$ values are shown in Figure 3-9. A drop in $SUVA_{254}$ values was observed in all the NOMs tested.

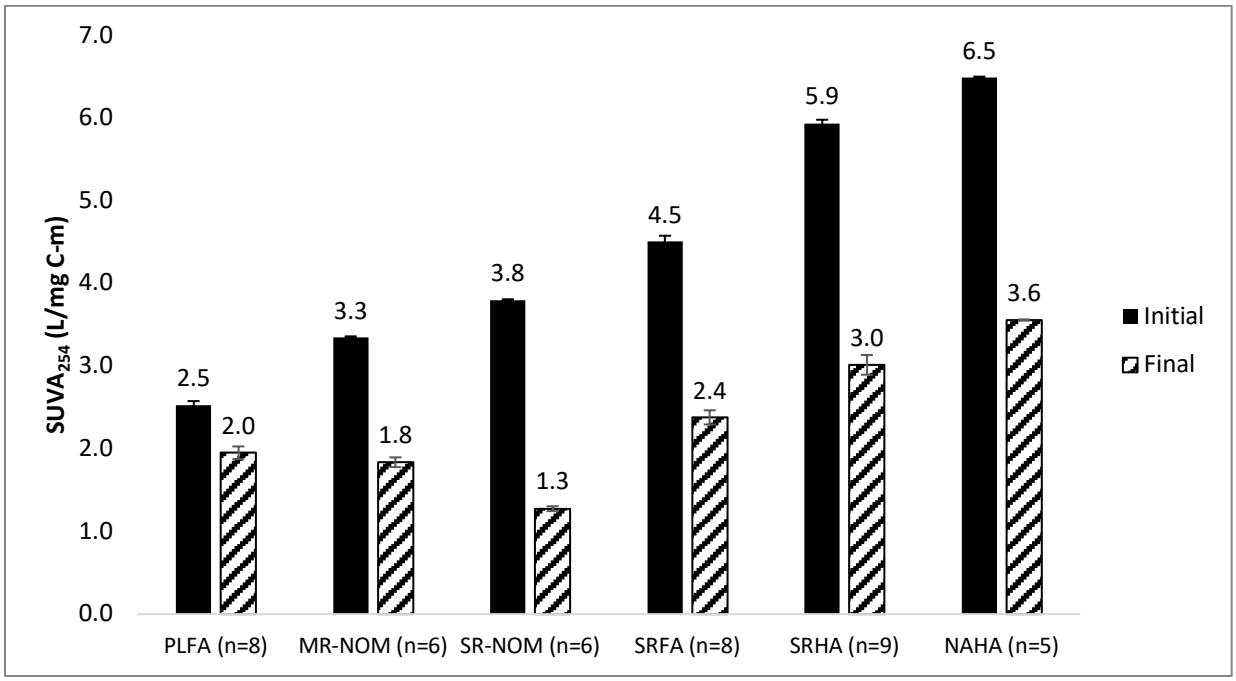

Figure 3-9. Changes in $SUVA_{254}$ values after alum coagulation at pH 6.7, 0.01M $NaNO_3$ ionic strength, and 30 mg/L alum dose. For each NOM, the initial DOC concentration was set at 5.0 mg/L.

NOM from samples high in $SUVA_{254}$ are found to be more reactive to metal-based coagulants than NOM from samples low in $SUVA_{254}$ [47], [48], [121]. This trend held true for the two unfractionated NOMs used in this study: SRNOM, with an initial $SUVA_{254}$ value of 3.8 L/mg C-m, dropped 66%, whereas MRNOM, with an initial $SUVA_{254}$ of 3.3 L/mg C-m, decreased by 45%. Likewise, out of the four fractionated NOMs, the three with the highest initial $SUVA_{254}$ values (SRFA, SRHA, and NAHA) all had decreases of $SUVA_{254}$ in the range of 45-49%, whereas PLFA, with the lowest $SUVA_{254}$ value of the six NOMs tested, had the lowest $SUVA_{254}$ decrease at 23%. Therefore, a larger drop in $SUVA_{254}$ after alum coagulation would indicate a preferential removal of the hydrophobic portion of the NOM, that is, the fraction with higher molar mass and abundant concentration of aromatic carbon [47], [48], [52], [133]. The data in Figure 3-9 suggest that a moderate aromaticity was still present in the finished water for SRHA ($SUVA_{254\ final}$ = 3.0), NAHA ($SUVA_{254\ final}$ = 3.6), and SRFA ($SUVA_{254\ final}$ = 2.4); while a preponderance of hydrophilic, low molecular weight

compounds were present in the finished water of PLFA ($SUVA_{254\ final}$ = 2.0), MR-NOM ($SUVA_{254\ final}$ = 1.8), and SR-NOM ($SUVA_{254\ final}$ = 1.3). The decreases in $SUVA_{254}$ values are reasonably consistent with the increases in the Se values reported above, inasmuch as the three samples with the greatest increases in Se values also showed high percentages of $SUVA_{254}$ decrease, and the PLFA sample showed small changes in both parameters.

As indicated in Table 3-2, the percent removal of DOC can be predicted based on the $SUVA_{254}$ value of the water sample [48]. Hence, the percent removal of the NOMs tested was plotted against their initial $SUVA_{254}$ values as can be seen in Figure 3-10. As predicted, DOC removal increases as $SUVA_{254}$ increases. Nevertheless, the fractionated NOMs are the samples that perfectly meet the guidelines in Table 3-2. For instance, the DOC removal of PLFA, with a $SUVA_{254}$ between 2.0 and 4.0 L/mg C-m, fell in the 25-50% removal box; while the DOC removal for SRFA, SRHA, and NAHA, with $SUVA_{254}$ values larger than 4.0 L/mg C-m, fell in the 50-90% removal box. The other two samples (MR-NOM and SR-NOM) had a greater DOC removal than the guidelines suggested, which is likely because the guidelines were developed for more complex real waters than the simplified solutions (without particles and limited other soluble constituents) used in this research.

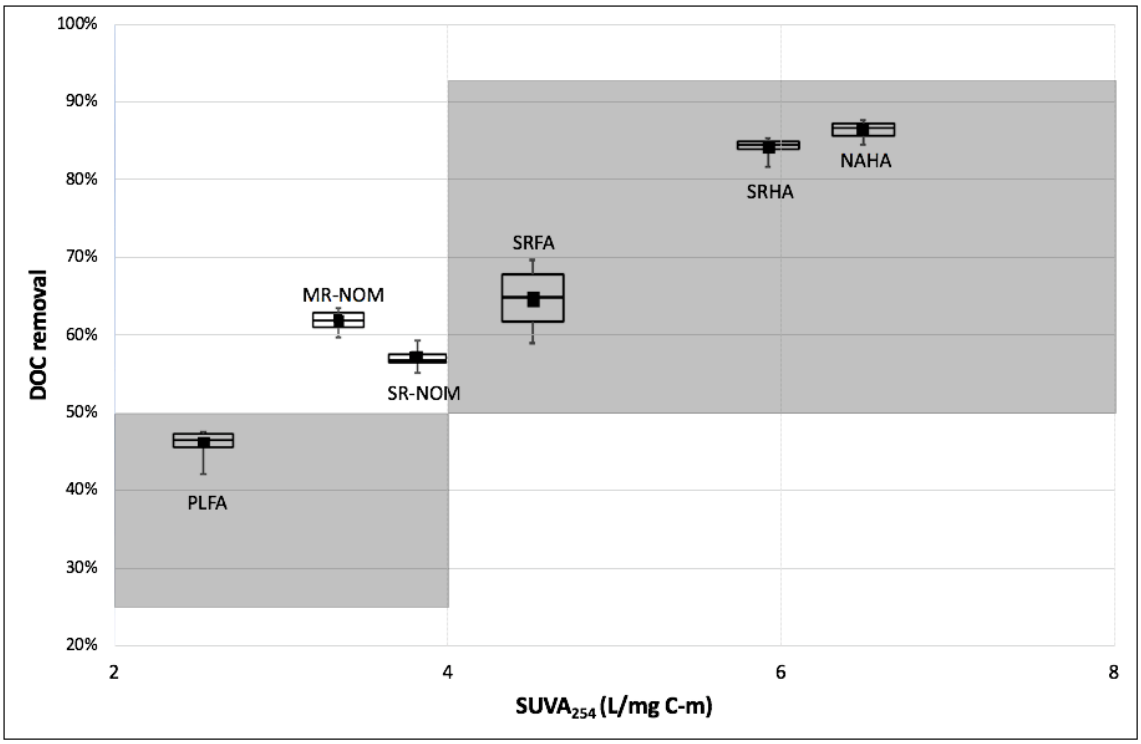

Figure 3-10. DOC percent removal as a function of the $SUVA_{254}$ based on the guidelines provided by Edzwald and Tobiason (1999).

An additional analysis is possible by comparing the residual DOC concentrations and their respective $SUVA_{254}$ values (Figure 3-11). NOMs high in aromatic carbon, SRHA and NAHA, not only allow larger DOC removal efficiencies (~85% removal in both cases), but their residual $SUVA_{254}$ values suggest that the carbon species that are not removed by alum treatment also have similar aromatic characteristics. On the other hand, the amount of residual DOC for PLFA samples is both high in concentration and more likely rich in hydrophilic compounds. High residual DOC concentrations represent an additional issue in drinking water treatment; not only because they will promote the formation of trihalomethanes (THM), but also because any reactive functional groups in the residual NOM will increase the concentration of undesired contaminants, such as heavy metals, in the finished water.

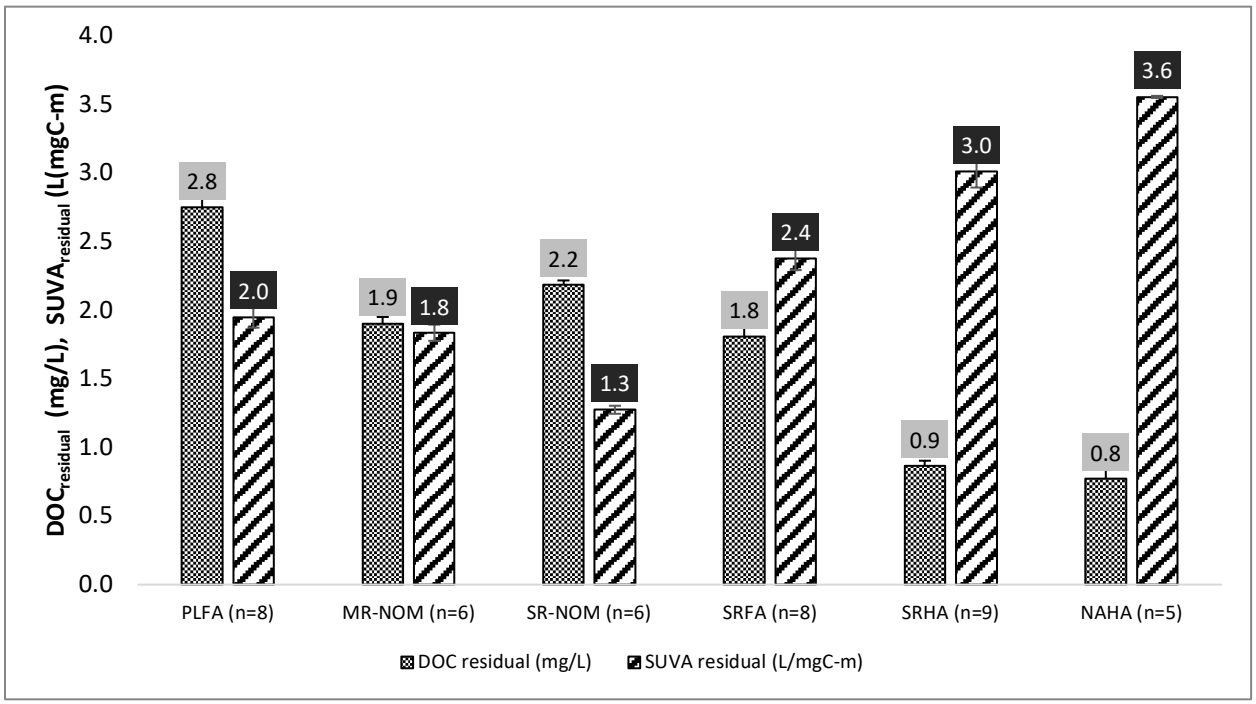

Figure 3-11. Residual $SUVA_{254}$ values and residual DOC concentrations after alum-coagulation treatment at pH 6.7, 0.01M $NaNO_3$ ionic strength, and 30 mg/L alum dose. For each NOM, the initial DOC concentration was set at 5.0 mg/L.

In conventional water treatment, it has been reported that the concentration of carboxylic functional groups in the treated water is much larger than in the untreated water [117]. Among the NOMs tested in this work, an increase of up to three-fold in the carboxyl content was also observed in the treated water. It has been reported that the low molar mass compounds from humic substances that remain in solution after treatment contain a greater proportion of carboxylic ligands than the fraction of humic substances that has been removed from solution [117]. That is, in humic substances, the concentration of carboxylic acids is inversely related to the molar mass [117]. As a consequence, the remaining compounds after alum treatment are expected to have a higher charge density than the original sample.

Accordingly, the results from this work indicate that, when comparing fulvic acids with humic acids, it is expected that PLFA or SRFA has a higher carboxylic content in the treated water compared to SRHA or NAHA. This expectation stems from the fact that, as

shown in section 3.2.1, fulvic acids have a higher carboxyl content than humic acids. As can be seen in Figure 3-11, fulvic acids are less likely to be removed from solution compared to humic acids. As a result, the portion of the fulvic acids that remain in solution after treatment is comprised of low molar mass compounds rich in carboxylic functional groups.

3.4 Conclusions

$SUVA_{254}$, a proxy for the aromaticity of natural organic matter (NOM), has been shown to be a good predictor of the removal of DOC in alum-coagulation. A strong correlation between $SUVA_{254}$ and the percentage aromaticity (measured by ^{13}C-NMR) was determined by preparing DOM solutions from NOMs extracted from different environments. Larger DOC removals (>80%) were possible for NOMs with $SUVA_{254}$ values larger than 5.0 L/mg C-m as was the case for SRHA (6.0 L/mg C-m) and NAHA (6.5 L/mg C-m). The lowest DOC removal was obtained for PLFA (46%), the NOM with the lowest $SUVA_{254}$ (2.5 L/mg C-m) and lowest aromaticity (12%). For most cases, the percentages in DOC removal meet the trend predicted for removal of NOM in metal-based coagulation systems as a function of their $SUVA_{254}$ values [48]. For $SUVA_{254}$ values larger than 4.0 L/mg C-m, more than 50% of the DOC can be removed, while for $SUVA_{254}$ values between 2.0 – 4.0 L/mg C-m, a removal of DOC between 25% - 50% is expected.

When comparing residual DOC concentrations with their respective $SUVA_{254}$, it was noticed that depending on the character of the DOM, it is possible to end up with finished water with low carbon concentration but high $SUVA_{254}$ (SRHA and NAHA) or finished water with high carbon concentration but low $SUVA_{254}$ (PLFA, MR-NOM, and SR-NOM). Consequently, the $SUVA_{254}$ value of the residual DOM solution can determine any additional treatment required to remove this pollutant from water and thus avoid the potential formation of disinfection by-products (DBPs), as well as the transportation of heavy metals and pathogenic microorganisms to other units of the treatment plant. Changes in $SUVA_{254}$ can

indicate changes in the composition of the DOM in alum-coagulation systems. In all cases, the $SUVA_{254}$ value decreased compared to the initial $SUVA_{254}$. Low $SUVA_{254}$ values are expected in DOM samples with low molecular weight and rich in nonhumic material. This trend was supported by the changes in spectral slope values. For all the DOMs tested, the spectral slope values increased after water treatment, which also suggests that the residual DOM is more hydrophilic in character and contains low molar mass compounds.

Given the high affinity of dissolved metals ions for the aromatic fraction of NOMs, residual $SUVA_{254}$ values can be used as indicator of the possible presence of heavy metals like Ni(II), Cu(II), Pb(II), As(II), and Hg(II) in the knowledge that carboxylic acids, a very reactive functional group, can remain in solution as part of the NOMs fraction not removed in the coagulation process. This recognition will be particularly useful when dealing with water sources heavily polluted with metals.

To conclude, $SUVA_{254}$ is a quick and inexpensive analysis to estimate the aromaticity of an aqueous samples. Nevertheless, changes in $SUVA_{254}$ could indicate the character of the NOM being removed from solution, while residual $SUVA_{254}$ values could indicate the presence of functional groups, like carboxylic ligands, in the finished water. The NOMs selected in this study vary in origin, aromatic/aliphatic content, reduced sulfur concentration, and oxygen functional groups such as phenols and carboxylic acids. Therefore, these ranges in properties and composition allow one to know the behavior of NOMs extracted from different water sources, as well as their eventual interaction with heavy metals, which are present in many aquatic ecosystems in developing countries.

CHAPTER 4. INFLUENCE OF THE COMPOSITION AND CHARACTER OF DISSOLVED ORGANIC MATTER (DOM) ON THE REMOVAL OF HG IN METAL-BASED COAGULATION SYSTEMS

4.1 Introduction

Mercury pollution is a critical problem in Africa, Asia, and South America, where metallic mercury is being used in artisanal and small-scale gold mining (ASGM) for the extraction of gold from ores and sediments [5]. In these regions, more than 10 million miners work in ASGM and it was estimated that around 1,400 tons of metallic mercury were used in this activity in 2011 [5]. Mercury contamination from ASGM is particularly relevant in countries like China, The Philippines, Indonesia, Tanzania, Ghana, Brazil, Peru, and Colombia.

Some insights into the Hg-Dissolved Organic Matter (DOM) interactions can be drawn from the previous research conducted in natural environments [10], [35]–[42]. Evidence of a strong positive correlation between dissolved total Hg with DOC concentration (r^2=0.87), UV_{254} absorbance (r^2=0.92), and the hydrophobic acid fraction of DOM (HPOA) (r^2=0.91) in forested watersheds in the northeastern USA was reported in 2009 [66]. In this geographical area, Hg pollution is mainly attributed to the atmospheric Hg deposition that has been occurring since the late 1800s [66]. It was also found that, in natural ecosystems where the Hg/DOM ratio is expected to be low (<< 1.0 µg Hg/mg DOM), Hg will be strongly bound to sulfur reduced ligands in the DOM [37]. Conversely, at high Hg/DOM ratios (e.g., ≥ 1.0 µg Hg/mg DOM), as could be the case in polluted ecosystems such as those impacted by ASGM, Hg will also be bound to carboxylic functional groups [37], [61].

To study Hg-DOM interactions in natural ecosystems, equilibrium dialysis ligand exchange (EDLE) and ion exchange techniques were used to determine the conditional stability constants for the binding of Hg(II) to DOM ($K_{Hg\text{-}DOM'}$) [37], [61], [74]. Table 4-1

shows that at low Hg/DOM ratios, the stability constant between Hg-DOM is similar to the stability constant between Hg and thiol groups ($K_{Hg\text{-}DOM'} \approx K_{Hg\text{-}Thiol} \approx 10^{23}$ L/Kg). At higher Hg/DOM ratios, $K_{Hg\text{-}DOM'}$ decreases until reaching a value near to 10^{11} L/Kg, which correspond to the stability constant for the interaction between Hg and oxygen functional groups (i.e., phenols and carboxylic ligands) [37], [61], [74].

Table 4-1. Conditional distribution coefficients between Hg and DOM as a function of the Hg/DOM ratio in different aquatic environments. Source: Haitzer et al. (2002)

Hg/DOM	**$K_{DOM'}$ (L/kg)**	**Note**
≤ 1.0	$\sim 10^{23.3\pm1}$	Strong interaction. Indicative of Hg-thiols bond
> 10	$\sim 10^{10.7\pm1}$	Consistent with Hg binding oxygen functional groups

On the other hand, the characteristics and composition of DOM in aquatic environments differ from one ecosystem to another based, among other things, on the biogeochemical processes that take place in the ecosystem [43]–[45], [51]. Variations in the concentration of DOM and changes in the aromatic carbon content are also possible in a natural ecosystems as a consequence of seasonal variability, anthropogenic activities occurring within the watershed, and climate change. In any case, previous research [51] has established a strong correlation between the specific ultraviolet absorbance ($SUVA_{254}$ with units of L/mg C-m and defined as the UV absorbance at 254 nm divided by the dissolved organic carbon (DOC) concentration) and the percentage aromaticity of dissolved organic matter (DOM) extracted from different environments. This correlation was verified for the NOMs in this research (Chapter 3). Thus, $SUVA_{254}$ is widely used as an indicator of the aromatic content of a water sample, as well as a predictor of the amount of DOC that can be removed in metal-based water treatment [48], [53], [107]. Since total dissolved Hg(II) is correlated to DOM concentrations and $SUVA_{254}$ is correlated to DOC removal in water

treatment processes, it is likely that $SUVA_{254}$ may be an effective surrogate for Hg(II) removal as well.

Until now, few researchers have studied the effect of Hg-DOM interactions in drinking water systems [52]; specifically, research studies are lacking in traditional systems such as metal-based coagulation, sedimentation, and filtration which is the most common drinking water treatment in developing countries. Consequently, the goal of this research was to evaluate how the composition and character of the DOM influence the removal of Hg in alum-coagulation systems. Mercury pollution represents a real threat to water sources affected by ASGM; therefore, assessment of the role of Hg-DOM interactions in metal-based coagulation treatment is needed.

4.2 Research approach

4.2.1 Selection of NOM samples and preparation of DOM solutions

Four organic matter isolates (referred as NOMs in this publication) were used in this study. These samples were obtained from the International Humic Substances Society (IHSS) and were collected from three different environments. From the Suwannee River (Georgia, U.S.) were obtained its humic fraction (SRHA, reference: 2S101H), and its fulvic fraction (SRFA, reference: 2S101F); from the Nordic Lake (Norway) was obtained its humic fraction (NAHA, reference: 1R105H), and from the Pony Lake (Antarctica) was obtained its fulvic fraction (PLFA, reference: 1R109F). A summary of the characteristics of the selected NOMs is presented in Table 4-2.

Table 4-2. Carbon distribution and acidic functional groups of selected NOMs

[a]Catalog Number	NOM Description	% C	% Aromatic 165-110 ppm	% Aliphatic 60-0 ppm	Acidic functional groups (meq/g C)		
					[b]S_{red}	[a]Phenolic	[a]Carboxyl
1R109F	Pony Lake Fulvic Acid	52.47	12	61	2.46	1.75	7.09
2S101F	Suwannee River Fulvic Acid	52.34	22	35	0.294	2.84	11.17
2S101H	Suwannee River Humic Acid	52.63	31	29	0.410	3.72	9.13
1R105H	Nordic Aquatic Humic Acid	53.33	38	15	0.488	3.23	9.06

[a]Source: International Humic Substances (http://www.humicsubstances.org/)
[b]Sred data extracted from Manceau and Nagy (2012)

As can be seen in Table 4-2, these four isolated samples vary in origin, aromatic and aliphatic content, and reduced sulfur and oxygen functional groups concentration. This diverse pool of samples might cover most of the variability in DOM composition expected in different aquatic environments, particularly for humic substances which are highly reactive to dissolved metals in solution [35], [54]–[57], [111]. Moreover, the selection of these four samples was based on the availability of data quantifying the reduced sulfur content. In all cases, the reduced sulfur content was measured using x-ray absorption spectroscopy which has the capability of distinguishing reduced S species from oxidized species.

DOM stock solutions were prepared by dissolving the NOM samples in ultrapure water (18 MΩ cm), mixing the solution for 1-hr and sonicating for 30 min. The pH of each DOM solution was increased to approximately 8.5 with NaOH reagent grade to achieve a complete dissolution of the NOM. Solutions were later filtered through a 0.45 μm cellulose nitrate membrane filter and stored in amber glass bottles in a dark cold room at 4ºC until using it for experiments. Solutions were characterized by measuring the concentration of DOC, pH, total Hg, and the specific ultraviolet absorbance ($SUVA_{254}$). Total Hg concentrations in DOM stock solutions were below the detection limit (0.5 ng/L) of the selected method (US EPA method 1631, revision E).

4.2.2 Hg removal as a function of the DOM character and composition in alum coagulation systems

To evaluate the influence of the character and composition of DOM on the removal of Hg through coagulation, a set of jar test experiments were designed at constant alum dose, pH, and ionic strength. To minimize mercury losses during the experimentation, jar tests were performed on magnetic stir plates using acid-cleaned Teflon® jars and Teflon® stir bars. An abbreviated procedure is listed below:

1. Spike DOM samples to desired Hg concentration by adding known amounts of $HgNO_3$ solution
2. pH adjustment to 6.7 (HNO_3 or NaOH)
3. Rapid mix for 2 minutes to add coagulant
4. pH adjustment to 6.7
5. Slow mixing for 20 min
6. Settling for 30 min
7. Centrifugation for 30 min @ 665 x g

Each solution was prepared at an ionic strength of 0.01M $NaNO_3$. The alum dose was set at 30 mg/L (0.05 mM Alum, 2.6 mg/L Al(III)). Experiments were conducted with a N_2(g) blanket to avoid CO_2 interferences, thereby keeping the pH constant at 6.7. A schematic of the jar test procedure is shown in Figure 4-1.

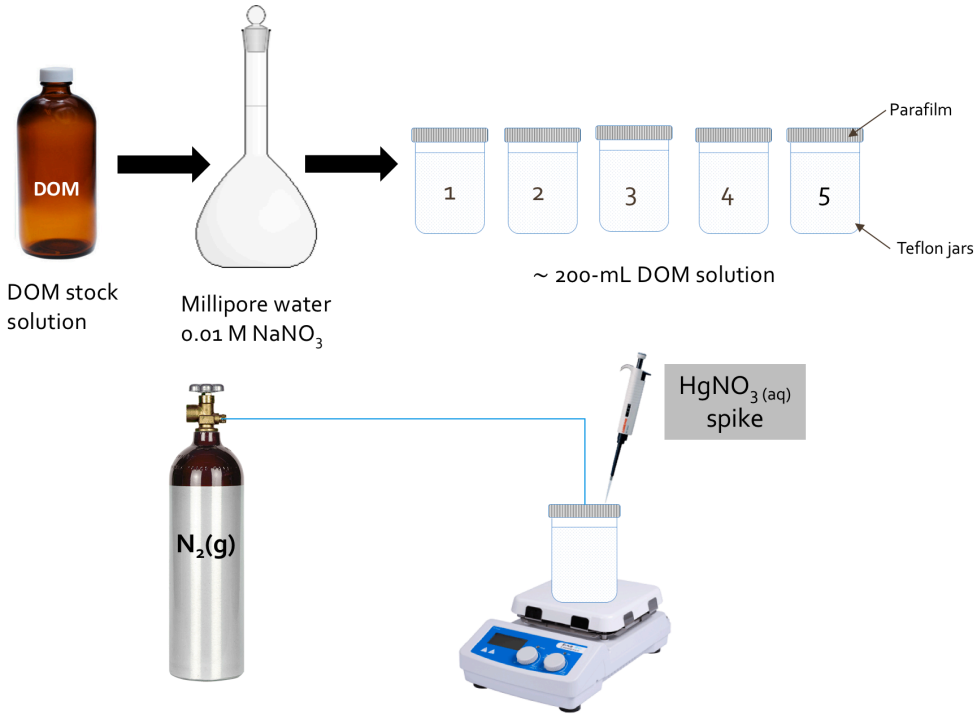

Figure 4-1. Schematic of the jar test procedure used for experimentation

At pH 6.7, the dominant Hg species in water is $Hg(OH)_2$ (Figure 4-2a). At this pH, and for an alum concentration of 0.05 mM the predominant aluminum species to be found in water is $Al(OH)_{3(amorphous)}$ [106], [122]. In the absence of NOM, mercury is poorly absorbed onto alum flocs as can be seen in Figure 4-2b.

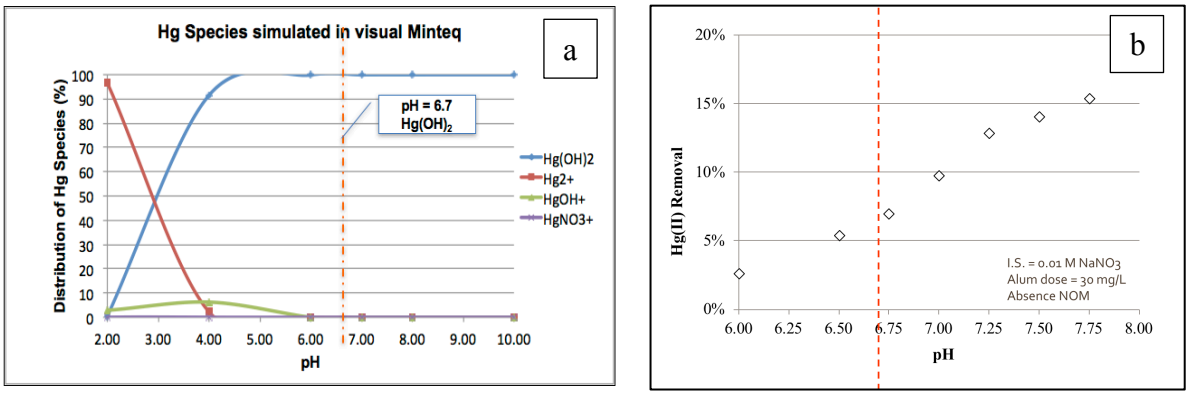

Figure 4-2. (a) Mercury species at pH 6.7 simulated by visual MINTEQ software (ver. 3.1) (I.S.=0.01M $NaNO_3$, T = 23ºC) (b) Hg removal in the absence of natural organic matter at different pH in alum-coagulation systems.

The different DOMs selected were tested at a constant DOC concentration of 5.0 mg/L and two different Hg concentrations as shown in Table 4-3. A Hg concentration of 0.5 µg/L allows study of the interaction between Hg and DOM at a low Hg/DOM ratio (0.05 µg Hg/mg DOM ≈ 0.1 µg Hg/mg DOC), allowing Hg ions to interact with the strongest ligands present in the solution. A Hg concentration of 10.0 µg/L allows study of the interaction between Hg and DOM at higher Hg/DOM ratios (≥1.0 Hg/mg DOM), where, after saturating the strongest ligands in solution, Hg is expected to bind to weaker, but more abundant, ligands in the DOM structure such as carboxylic functional groups. In some cases, experiments were also conducted at higher doses of up to 50 µg/L.

Table 4-3. Initial experimental conditions for jar test experiments with selected NOMs

NOM	DOC (mg/L)	Hg (µg/L)	Hg/DOC ratio (µg/mg)	Alum Dose (mg/L)	pH	I.S. (M)
Each NOM	5.0	0.5 10.0	0.10 2.00	30 (2.6 mg/L as Al(III))	6.7	0.01

4.2.3 Analysis of aqueous samples

After the jar tests were completed, an aliquot of the supernatant was taken for UV_{254}, DOC, total Al(III), and THg analyses. A TOC LCPH/CPN analyzer (Shimadzu) using high-temperature (680 °C) catalytic oxidation was used for TOC/DOC analysis. THg analysis was performed using cold-vapor atomic fluorescence spectrometry (CVAFS) (Tekran 2600; Tekran, Toronto, ON) following US EPA method 1631, revision E (US EPA, 2002). Samples for aluminum determination were preserved with 385-µL concentrated HNO_3 per 5-mL sample and were analyzed using inductively coupled plasma spectroscopy (ICP) (Agilent Varian 710-ES, CA) at 309.271 nm and 396.152 nm wavelengths. UV_{254} was measured by spectrophotometry (Agilent 8453, CA) using, either a 1-cm or 5-cm quartz cell. $SUVA_{254}$ was determined from the UV_{254} reading and the DOC concentration of the sample. Samples were placed in a 4ºC storage room if not analyzed immediately. A summary of the instruments used to analyze the precipitate and aqueous samples are outlined in Table 4-4.

Table 4-4. Analytical techniques used to achieve the goals of this research

Analysis	Technique	Method
DOC/TOC	TOC analyzer (Shimadzu)	USEPA 415.3
UV_{254}	UV spectroscopy	USEPA 415.3
[Al(III)]	Inductively Coupled Plasma Optical Emission Spectroscopy (ICP-OES) (Agilent Varian 710-ES, CA)	USEPA 6010D
Specific ultraviolet absorbance ($SUVA_{254} = UV_{254}/[DOC]$)	UV spectroscopy and TOC analyzer	USEPA 415.3
Total Hg	CVAFS Tekran 2600	USEPA 1631, Revision E

4.2.4 Analysis of precipitates

X-ray photoelectron spectroscopy (XPS) and Time of Flight Secondary Ion Mass Spectrometer (ToF-SIMS) were used for determining the composition of the precipitate and the distribution of the Hg, C, O, and Al atoms on the surface of the floc. The results from both techniques can also provide visual evidence for the incorporation of Hg-DOM complexes onto alum flocs. To analyze the precipitate, jar tests were conducted for the unfractionated Suwannee River NOM (SR-NOM, reference 2R101N) which contains both the humic and fulvic fractions used in this study. Experiments were performed at constant Hg concentration and different initial DOM concentrations than those specified in section 4.2.2. A Hg concentration of 1.0 mg/L was selected in order to assure that a representative amount of Hg adsorbed onto the flocs for a proper detection of this element with the techniques used. The solution remaining in the jars were filtered through a 0.45 μm cellulose nitrate filter to collect the precipitates. Solid samples were dried for approximately six hours under N_2 gas before XPS and ToF-SIMS analysis. A description of these experiments is provided in Table 4-5.

Table 4-5. Experimental conditions for surface characterization of precipitates.

NOM	Jar	DOM (mg/L)	Hg (µg/L)	Alum Dose (mg/L)	pH	I.S. (M)
SR-NOM (Ref: 2R101N)	**1**	1.0	1000	80	6.7	0.1
	2	5.0				
	3	10.0				

4.3 Results and Discussion

4.3.1 Characterization of DOM samples

Freshly prepared DOM samples were characterized before and after jar test experiments. Before jar tests, $SUVA_{254}$ values were determined (Table 4-6) at a DOC concentration of 5.0 mg/L, pH ~ 6.0, and ionic strength of 0.01 M as $NaNO_3$. A short notation was given to each DOM sample used for experimentation as shown in Table 4-6.

Table 4-6. Characterization of DOM solutions used for experimentation

DOM	NOTATION	% Aromatic carbon (^{13}C-NMR chemical shift)[a] 165-110 ppm	$SUVA_{254}$ (L/mg C-m)
Pony Lake Fulvic Acid	PLFA	**12**	2.57±0.09
Suwannee River Fulvic Acid	SRFA	**22**	4.53±0.30
Suwannee River Humic Acid	SRHA	**31**	6.08±0.16
Nordic Aquatic Humic Acid	NAHA	**38**	6.42±0.07

[a]Source: International Humic Substances (http://www.humicsubstances.org/)

The $SUVA_{254}$ values also indicate the character of the DOM sample [48]: $SUVA_{254}$ < 2.0 indicates a DOM sample with low hydrophobicity and low molecular weight species; values between 2.0 and 4.0 indicate a mixture of molecular weights and a mixture of hydrophilic and hydrophobic carbon compounds; and values > 4.0 correspond to DOM samples with high hydrophobicity and high molar mass carbon compounds.

As can be seen from Table 4-6, $SUVA_{254}$ values match the percentage of aromatic carbon for each of the DOM selected. The low $SUVA_{254}$ value for the PLFA (12% aromaticity) indicates that this sample is rich in hydrophilic compounds and, consequently, a poor removal of DOC should be expected. The intermediate $SUVA_{254}$ value for the SRFA (22% aromaticity) indicates a fair removal of DOC in this sample, while the large $SUVA_{254}$ for the SRHA (31% aromaticity) and NAHA (38% aromaticity) predict good removal of carbon for both DOM samples.

4.3.2 Removal of Dissolved Organic Carbon

At pH 6.7 and 30 mg/L alum dose, the performance of the coagulant is optimal which minimizes its residual concentration [117], [118]. The low Al(III) concentration present in solution after jar testing (Figure 4-3) points out the high reactivity between alum and DOM. Such reactivity has been attributed to the presence of negatively charged functional groups in the structure of DOM, particularly to those that contains oxygen such as carboxyl, phenolic, carbonyls, and hydroxyl [120], [126]. The average removal of Al(III) from solution was approximately 92%.

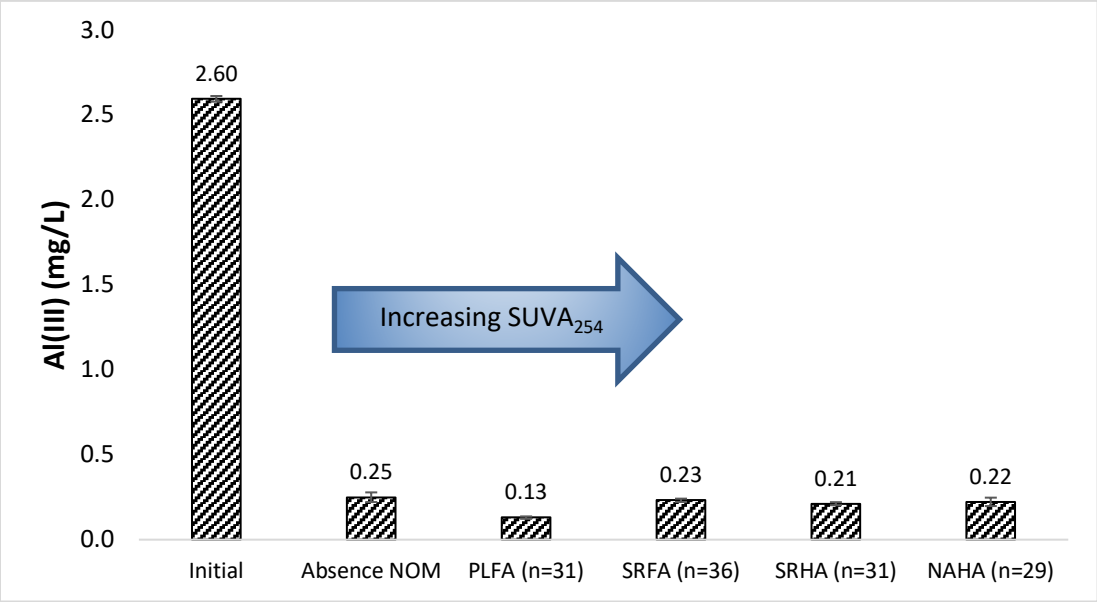

Figure 4-3. Residual Al(III) concentration at pH 6 and alum dose 30mg/L for NOM from different environments. Error bars represent standard error from the replicates.

Comparing the performance of each DOM selected under similar coagulation conditions, it is clear that the removal of carbon follows the trend predicted by the $SUVA_{254}$ values. As Figure 4-4 shows, low DOC removal is obtained when using PLFA (~2.3 mg/L of DOC removed), the DOM with the lowest $SUVA_{254}$ (2.6 L/mg C-m); while higher DOC removal was possible with SRHA (4.3 mg DOC/L) and NAHA (4.2 mg DOC/L), the DOMs rich in aromatic carbons and high $SUVA_{254}$ values, 6.1 and 6.4 L/mg C-m, respectively.

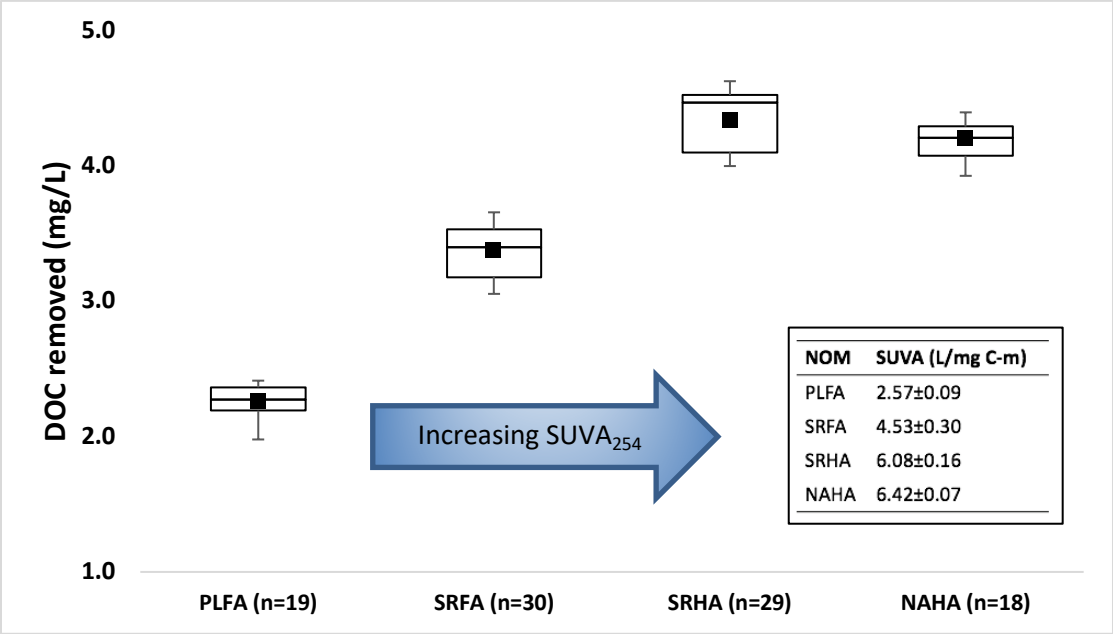

Figure 4-4. DOC removed during bench-scale jar tests for NOMs from different sources. Error bars represent the standard deviation from the replicates (n). The initial DOC concentration in each sample was 5 mg/L.

Kruskal–Wallis One Way Analysis of Variance on Ranks revealed no statistical difference in the mean DOC removed values between SRHA and NAHA ($p > 0.05$). Differences in mean DOC values were found between PLFA and SRFA ($p < 0.05$), PLFA and SRHA ($p < 0.05$), PLFA and NAHA ($p < 0.05$), SRFA and SRHA ($p < 0.05$), and SRFA and NAHA ($p < 0.05$). The statistical software IBM® SPSS® ver. 25 for Mac OS was used for this analysis. Thus, the selection of NOMs provided a range of samples with varying removal in alum coagulation systems.

4.3.3 Changes in $SUVA_{254}$ values

Differences in the composition of the DOM during the treatment process can be noticed by tracking the changes in $SUVA_{254}$ values of the different organic matter isolates evaluated. Figure 4-5 shows that a 23% decrease in $SUVA_{254}$ was observed for PLFA, the DOM with the lowest aromaticity, while approximately a 50% decrease in $SUVA_{254}$ was

observed for all the other DOMs: SRHA (22% aromaticity), SRHA (31% aromaticity), and NAHA (38% aromaticity). A decrease in $SUVA_{254}$ has been associated with the removal of the fraction of DOM high in molar mass and aromatic carbon [47], [48], [133].

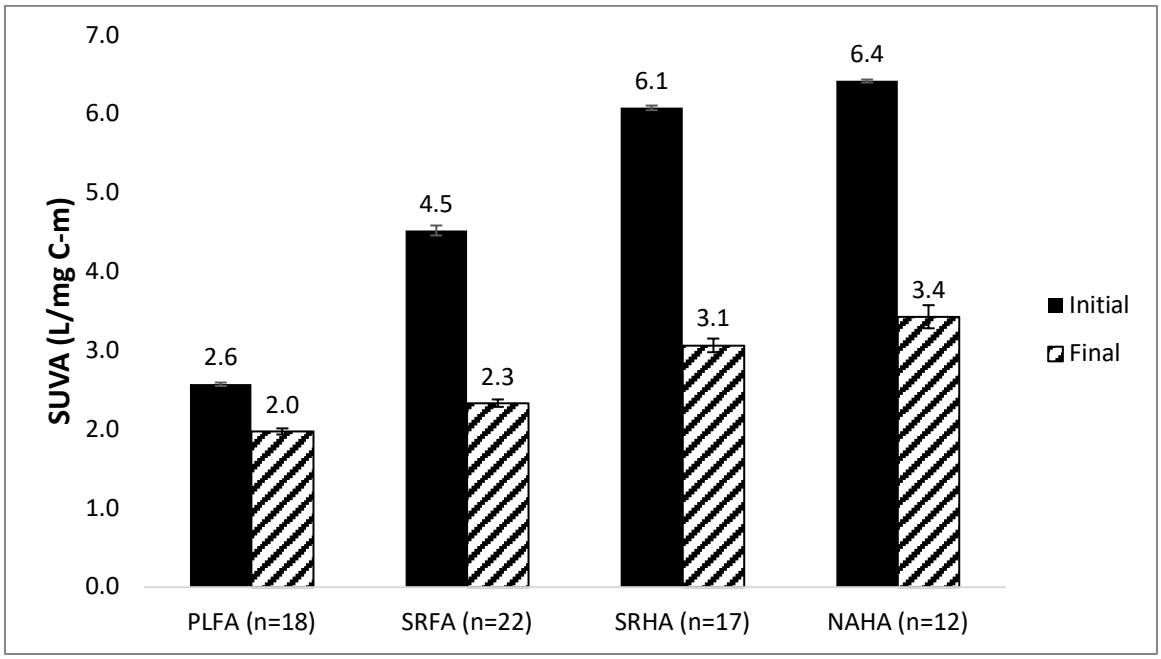

Figure 4-5. Changes in $SUVA_{254}$ values for selected NOM after jar test experiments. Error bars represent standard error from the replicates (n).

As mentioned before, changes in $SUVA_{254}$ values also provide useful information regarding the amount of aromatic carbon present in solution and the expected removal of carbon from water treatment. For instance, SRFA and SRHA have similar changes in $SUVA_{254}$ values (nearly a 50% decrease), which would indicate that similar proportions of aromatic carbon were removed from each solution; however, DOC removal was lower for SRFA (66%) compared to SRHA (88%) which is consistent with the trends in aromatic content; Table 4-6 indicates that SRHA contains 31% aromaticity and SRFA contains 22% aromaticity. For PLFA, a 23% decrease in $SUVA_{254}$ translates to 45% removal of DOC, which is also consistent with the low aromatic content of the PLFA sample (12% aromaticity).

When comparing the residual DOC concentrations with their corresponding $SUVA_{254}$ values (Figure 4-6), it was observed that samples with low residual DOC concentrations can contain a mixture of hydrophobic and hydrophilic compounds (based on the guidelines provided by Edzwald and Tobiason (1999), as it is the case for SRHA ($SUVA_{254\ final}$ = 3.1 L/mg C-m) and NAHA ($SUVA_{254\ final}$ = 3.4 L/mg C-m). Further removal of DOC is still possible for samples with $SUVA_{254}$ values larger than 2.0 L/mg C-m, such as SRHA and NAHA. In contrast, samples with high concentrations of DOC remaining in the residual solution after coagulation and settling, as is the case for PLFA (2.8 mg/L), and to some extent SRFA (1.8 mg/L), can be rich in low hydrophobic/low molecular weight compounds, and that makes any further removal of organic carbon in traditional drinking water systems difficult. Finished water low in $SUVA_{254}$ and high in DOC poses a potential threat to managers and users of drinking water plants due to the potential for formation of disinfection by-products (DBP) or the presence of pathogenic microorganisms or heavy metals which can be transported with the residual organic carbon.

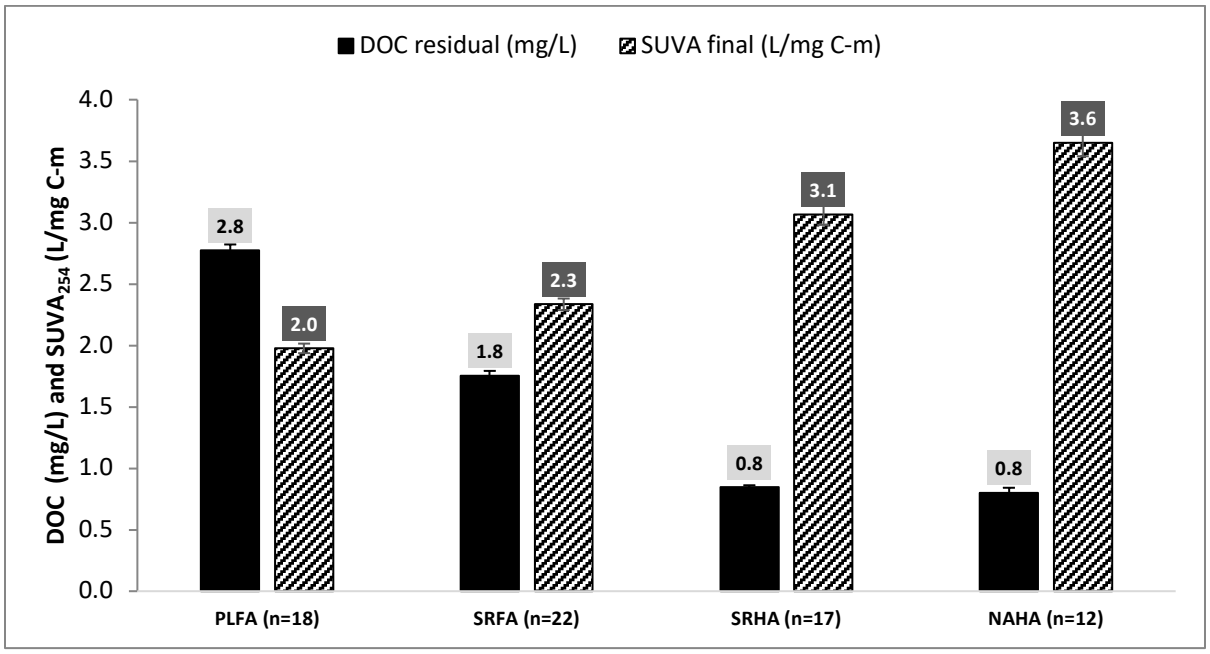

Figure 4-6. Final $SUVA_{254}$ and DOC residual after alum coagulation for selected NOMs. The initial DOC concentration in each sample was 5 mg/L.

4.3.4 Hg removal at low Hg/DOC ratio

Experiments at low Hg/DOM ratios were intended to produce conditions that isolate interactions between Hg(II) ions and sulfur reduced ligands, which are the strongest ligands for Hg complexation in DOM in aquatic ecosystems [35], [37], [61], [134]. Experiments were performed at an initial Hg concentration of 0.5 µg/L and DOC concentration of 5.0 mg/L. Under similar coagulations of pH, alum dose, and ionic strength, it was observed that the removal of Hg was above 80% for each of the DOMs used in this study, regardless of its character and composition (Figure 4-7). Figure 4-7a shows that much higher Hg removal efficiencies were possible when using PLFA, SRHA, and NAHA (~95% removal) compared to the lower removal obtained for SRFA (~84%). SRFA had the lowest reported S_{red} value in Table 4-2. When normalizing the amount of Hg removed to the amount of DOC removed, Figure 4-7b shows a higher value for PLFA (~0.20 µg Hg/mg DOC) compared to the lower

ratios obtained with SRFA (~0.13 µg Hg/mg DOC), SRHA (~0.11 µg Hg/mg DOC), and NAHA (~0.11 µg Hg/mg DOC).

A simultaneous analysis of Figure 4-7a and Figure 4-7b provides a more comprehensive understanding of the influence of the nature and composition of DOM in removing Hg in alum coagulation treatment. The data in Figure 4-7a suggest that, at low Hg concentrations, the DOMs with high aromaticity but low in S_{red} ligands (SRHA and NAHA) can remove as much Hg as the DOM low in aromatic content but high in concentration of S_{red} ligands (PLFA). Additionally, Figure 4-7b shows that PLFA is able to remove twice the amount of the Hg compared to either the SRHA or the NAHA, this despite the fact that a poor removal of DOC is obtained with PLFA (45%) compared to SRHA (84%) or NAHA (84%).

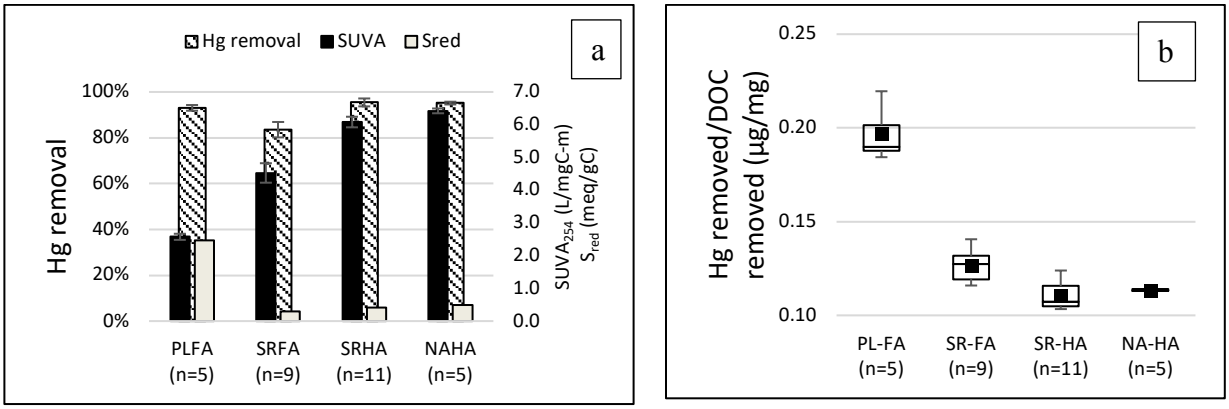

Figure 4-7. Hg removal at low Hg/DOC ratio for NOM samples from different environments: a) Hg removal percentage, b) Hg removed/DOC removed (µg/mg). The initial DOC concentration was 5 mg/L and the initial Hg concentration was 0.5 µg/L.

One-way Anova with post-hoc Tukey test showed statistical differences in the amount of Hg removed/DOC removed between PLFA and SRFA ($p < 0.05$), SRHA ($p < 0.05$), and NAHA ($p < 0.05$). Statistical differences were also observed between SRFA and SRHA ($p < 0.05$) and NAHA ($p < 0.05$). In contrast, no differences in the mean Hg

removed/DOC removed values were found between SRHA and NAHA ($p > 0.05$) as the pairwise comparison shows in Table 4-7.

In summary, similar amounts of Hg can be removed with either PLFA, SRHA, and NAHA even though less carbon was removed with the PLFA compared to SRHA and NAHA. These results highlight that removal of Hg is dependent on both the S_{red} content of the DOM and as the propensity for adsorption of DOM (which is related to its aromaticity and hydrophobicity) to the aluminum hydroxide flocs formed during coagulation. Thus, the lower percentage Hg removal for SRFA can be attributed to the fact that this DOM has a moderate aromatic content and the lowest concentration of S_{red} ligands among the NOM evaluated.

Table 4-7. Pairwise comparison of (Hg/DOC) removal ratios across categories of DOM at low Hg/DOC ratio

Sample 1	Sample 2	Std. Error	Sig.	95% Confidence Interval	
				Lower Bound	Upper Bound
PLFA	SRFA	0.00472	0.000	0.0573	0.0832
	SRHA	0.00456	0.000	0.0739	0.0989
	NAHA	0.00535	0.000	0.0687	0.098
SRFA	SRHA	0.0038	0.001	0.0057	0.0266
	NAHA	0.00472	0.047	0.0001	0.026
SRHA	NAHA	0.00456	0.908	-0.0156	0.0095

Each row tests the null hypothesis that the sample 1 and sample 2 distribution are the same.
Asymptotic significances (2-sided tests) are displayed. The significance level is 0.05.

A numerical description of the initial and final experimental conditions at low Hg/DOC ratios is summarized in Table 4-8. Besides the S_{red}/Hg molar ratio included in Table 4-8, an additional analysis needs to consider the fact that not all these S_{red} ligands might be available for Hg complexation. The term reduced sulfur includes many sulfur species detected in DOM samples (by XANES spectroscopy) such as thiols, sulfides, disulfides, cysteine, thiazine, and dothiepin, among others [75]. Some of these sulfur species involve the

presence of aromatic structures bridged by sulfur ions where the formation of Hg-S_{red} complexes seems unlikely [35]. The most likely complexation of Hg with DOM in aquatic environments will be with more simple S_{red} species like thiols (R-SH) [35], [61]. As shown in this study, the concentration of S_{red} in DOM may vary depending on the source of the DOM (e.g., PLFA, the sample with the highest S_{red} content, is a microbially derived DOM); therefore, the concentration of thiol ligands, may also differ depending on the origin of the DOM. Previous research estimated that approximately between 0.5 to 2.4% of the S_{red} in the Suwanee River humic acid (SRHA) form complexes with methylmercury[135]. As this is the only reference available, the ratio thiols/Hg included in Table 4-8 was calculated assuming that 2.0% of the S_{red} in DOM are thiols.

Table 4-8. Summary of the initial and final experimental conditions at low Hg/DOC ratio

	PLFA	**SRFA**	**SRHA**	**NAHA**
Hg initial (µg/L)		0.5		
DOC initial (mg/L)		5.0		
Hg/DOC (µg/mg)		0.10 (equivalent to 0.05 µg Hg/mg DOM)		
Aromatic content (%)[a]	12	22	31	38
S_{red} (meq/g C)[b]	2.46	0.294	0.410	0.488
Carboxyl (meq/g C)[a]	7.09	11.17	9.13	9.06
$(S_{red}/Hg)_{initial}$ (mol/mol)	2,467	295	411	489
$(Thiols/Hg)_{initial}$ (mol/mol)	49.3	5.9	8.2	9.8
$(Carboxyl/Hg)_{initial}$ (mol/mol)	14,222	22,406	18,314	18,173
$SUVA_{254\ initial}$ (L/mg C-m)	2.6±0.1	4.5±0.3	6.1±0.2	6.4±0.1
Decreased in $SUVA_{254}$	23%	48%	50%	47%
DOC removal (%)	46.8±1.2	64.5±3.9	83.4±2.3	85.2±1.2
Hg removal (%)	93.1±1.2	83.5±3.4	95.4±1.7	95.1±0.6
$(Hg/DOC)_{removed}$ (µg/mg)	0.20±0.014	0.13±0.008	0.11±0.007	0.11±0.002

[a]Source: International Humic Substances (http://www.humicsubstances.org/)
[b]Sred data extracted from Manceau and Nagy (2012)

As the data in Table 4-8 show, for the PLFA, the fraction of the DOM that was effectively removed from solution was able to remove 93% of the initial concentration of Hg. These results suggest that, at low Hg/DOC ratios, Hg is being removed from solution not just because this pollutant is bound to the S_{red} ligands available for Hg complexation, but because these S_{red} ligands might be located in the most aromatic/high molar mass fraction of the DOM, which is absorbed onto the alum flocs. While $SUVA_{254}$ is widely used as a proxy for aromaticity, a decrease in $SUVA_{254}$ indicates preferential removal of the most hydrophobic portion of DOM (i.e., carbon molecules with higher molar mass and high aromatic content) [53], [132]. As Figure 4-8 shows, PLFA, the sample with the lowest aromaticity (12%), only reported a 23% decrease in $SUVA_{254}$; while other samples like SRHA (31% aromaticity) and NAHA (38% aromaticity) reported up to 50% decrease in $SUVA_{254}$ each. SRFA (22% aromaticity) also had ~50% decrease in $SUVA_{254}$. Consequently, the few aromatic carbon molecules in PLFA, that are removed from solution most likely contain most of the S_{red} ligands binding Hg(II) ions and help to remove up to 93% of Hg(II) from solution through alum coagulation.

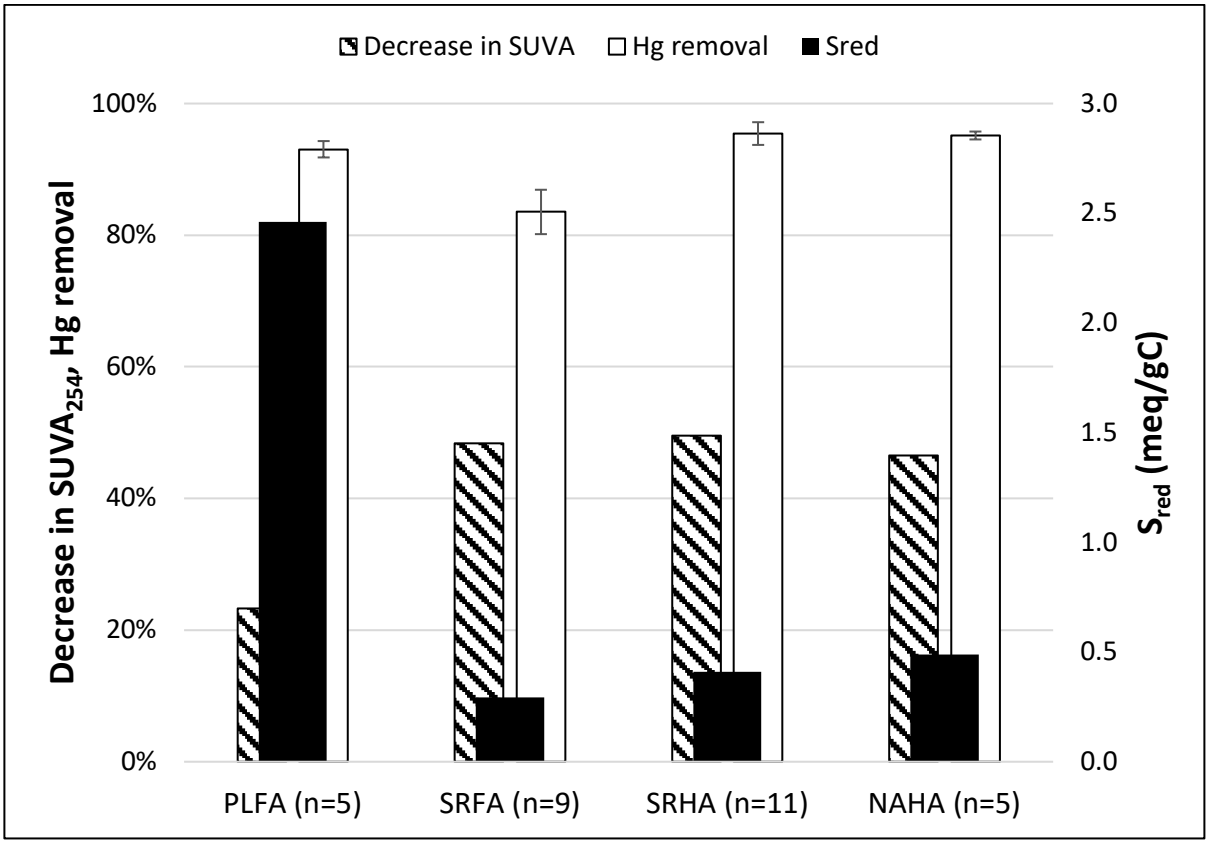

Figure 4-8. Comparison between changes in $SUVA_{254}$ values, removal of Hg(II), and S_{red} concentration in NOM from different sources in jar test at low Hg/DOM ratios.

Although it has been reported that fulvic acid isolates (such as PLFA and SRFA) contain more carboxylic ligands than its humic counterpart [45], these oxygen functional groups seem to be spread out across the DOM molecule based on hypothetical structures presented in previous research [69], [136]. Consequently, S_{red} ligands seem to control the removal of Hg from solution at low Hg/DOC ratios. Indeed, the high S_{red}/Hg molar ratio of nearly 2,500, for PLFA, suggests that there are abundant S_{red} ligands available to yield high Hg removal.

4.3.5 Hg removal at high Hg/DOC ratio

At higher mercury concentrations, Hg(II) ions will saturate the S_{red} ligands available for complexation in the DOM molecule and consequently will bind with other functional groups, particularly carboxylic ligands. Figure 4-9a shows that the mercury removal percentage varies between 54% for SRFA and 73% for PLFA. Compared to the results obtained at low Hg concentrations, the removal of Hg decreased considerably at high Hg/DOM ratios; however, the trends in removal for the various NOMs remained the same. Of particular note is the reduction of Hg removal for the PLFA; percentages decreased from 93% to 73%. The average removal for NAHA was similar, decreasing from 95% to 71%. When normalizing the mass of Hg removed to the amount of carbon removed, the resulting plot (Figure 4-9b) also follows the same pattern as that obtained at the low Hg/DOC ratio; a higher Hg removed/DOC removed ratio is obtained for PLFA (~3.30 µg Hg/mg DOC) in comparison to the values obtained with SRFA (~1.76 µg Hg/mg DOC), SRHA (~1.62 µg Hg/mg DOC), and NAHA (~1.82 µg Hg/mg DOC).

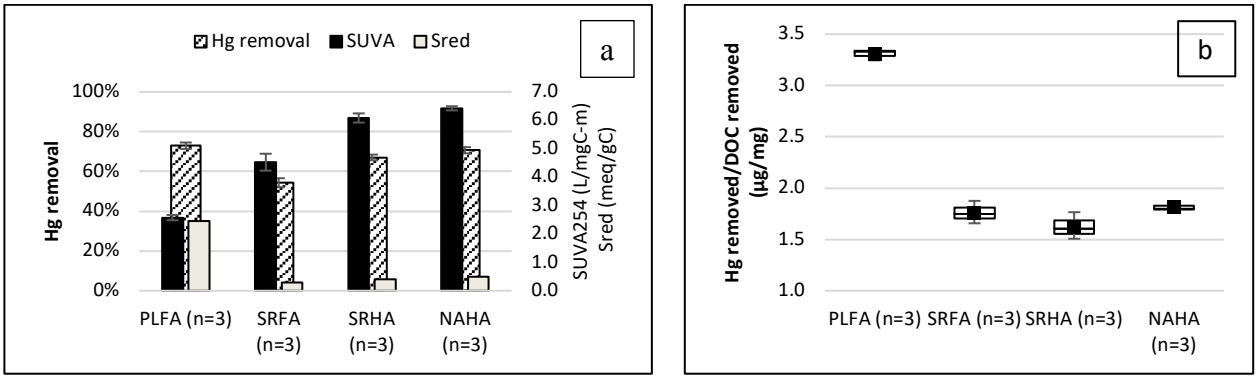

Figure 4-9. Hg removal at high Hg/DOC ratio for NOM samples from different environments: a) Hg removal percentage, b) Hg removed/DOC removed (µg/mg). The initial DOC concentration was 5 mg/L and the initial Hg concentration was 10 µg/L.

One-way Anova with post-hoc Tukey test revealed statistical differences in Hg removed/DOC removed values between PLFA and SRFA ($p < 0.05$), SRHA ($p < 0.05$), and

NAHA ($p < 0.05$). In contrast, no statistical differences in Hg removed/DOC removed ratios were observed between SRFA and SRHA ($p > 0.05$), neither between SRFA and NAHA ($p > 0.05$). Also, no statistical differences were observed between SRHA and NAHA ($p > 0.05$) as the pairwise comparison shows in Table 4-9.

Table 4-9. Pairwise comparison of (Hg/DOC) removed ratios across categories of DOM at high Hg/DOC ratio

Sample 1	Sample 2	Std. Error	Sig.	95% Confidence Interval	
				Lower Bound	Upper Bound
PLFA	SRFA	0.07506	0.000	1.2963	1.777
	SRHA	0.07506	0.000	1.433	1.9137
	NAHA	0.07506	0.000	1.243	1.7237
SRFA	SRHA	0.07506	0.331	-0.1037	0.377
	NAHA	0.07506	0.89	-0.2937	0.187
SRHA	NAHA	0.07506	0.129	-0.4304	0.0504

Each row tests the null hypothesis that the sample 1 and sample 2 distribution are the same.
Asymptotic significances (2-sided tests) are displayed. The significance level is 0.05.

A numerical description of the initial and final experimental conditions is summarized in Table 4-10. A simultaneous analysis of Figure 4-9a and Figure 4-9b, together with the additional information provided in Table 4-10, show that the NOMs that allow larger removal of carbon (SRHA and NAHA) are also the ones that provide higher removal of Hg; while less removal is obtained with the NOMs that provide less removal of DOC such as SRFA and PLFA.

Table 4-10. Summary of the initial and final experimental conditions at high Hg/DOC ratio

	PLFA	**SRFA**	**SRHA**	**NAHA**
Hg initial (µg/L)		10.0		
DOC initial (mg/L)		5.0		
Hg/DOC (µg/mg)		2.0 (1.0 µg Hg/mg DOM)		
Aromatic content (%)[a]	12	22	31	38
S_{red} (meq/g C)[b]	2.46	0.294	0.410	0.488
Carboxyl (meq/g C)[a]	7.09	11.17	9.13	9.06
$(S_{red}/Hg)_{initial}$ (mol/mol)	123	15	21	24
$Thiols/Hg)_{initial}$ (mol/mol)	2.5	0.30	0.41	0.49
$(Carboxyl/Hg)_{initial}$ (mol/mol)	711	1,120	916	909
$SUVA_{254\ initial}$ (L/mg C-m)	2.6±0.1	4.5±0.3	6.1±0.2	6.4±0.1
Decreased in $SUVA_{254}$	23%	48%	50%	47%
DOC removal (%)	45.8±1.9	64.2±1.4	82.6±0.6	84.4±0.8
Hg removal (%)	72.9±1.6	54.3±2.3	67.0±1.4	70.7±1.6
$(Hg/DOC)_{removed}$ (µg/mg)	3.30±0.05	1.76±0.11	1.62±0.13	1.82±0.04

[a]Source: International Humic Substances (http://www.humicsubstances.org/)
[b]Sred data extracted from Manceau and Nagy (2012)

An important observation comes from the results provided by the PLFA. The high concentration of S_{red} in the PLFA can explain the similarities in Hg removal percentage between PLFA (12% aromaticity) and SRHA (31% aromaticity) and NAHA (38% aromaticity), despite the fact that PLFA reported a much lower $SUVA_{254}$ removal than any other NOM (Figure 4-10). In this case, S_{red} ligands seem to play a significant role in removing Hg when using PLFA (45% DOC removal). SRHA and NAHA contain low concentrations of S_{red} ligands, but provide high removal of carbon (84%) which is abundant in carboxylic ligands as the DOM structure suggests [69], [136].

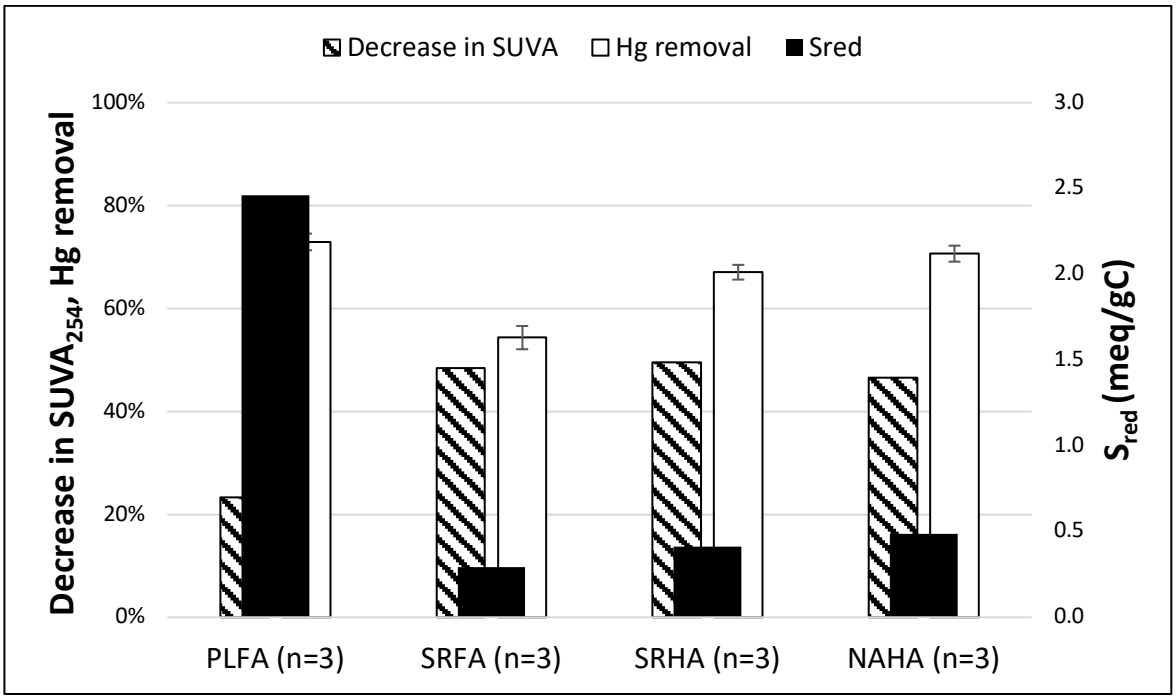

Figure 4-10. Comparison between changes in $SUVA_{254}$ values, removal of Hg(II), and S_{red} concentration in NOM from different sources in jar test at high Hg/DOM ratios.

4.3.6 Surface characterization of the precipitates

To evaluate the composition of the precipitates, it was necessary to produce enough sample to assure that a representative amount of Hg was adsorbed onto the flocs for a proper detection of Hg with the techniques used. Jar tests were performed at an alum dose of 30 mg/L, pH 6.7, ionic strength of 0.01 M as $NaNO_3$, initial Hg concentration of 1.0 mg/L, and different DOM concentrations, as shown in Table 4-11. After flocculation, precipitates were collected on a 0.45 µm cellulose nitrate filter, and samples were dried for approximately six hours under N_2 gas. X-ray photoelectron spectroscopy (XPS) and Time-of-Flight Secondary Ion Mass Spectrometry (ToF-SIMS) were used to determine the composition of the precipitate and the distribution of the Hg, C, O, and Al atoms on the surface of the floc. The

results from these techniques also provide visual evidence of the incorporation of Hg-DOM complexes onto alum flocs.

Table 4-11. Jar tests conditions for the surface characterization of the precipitate

Jar/Sample	DOM [mg/L]	Hg [µg/L]	Alum Dose [mg/L]	pH	I.S. [M]
1	1.0	1000	30	6.7	0.01
2	5.0	1000			
3	10.0	1000			

The NOM selected for this experiment was the unfractionated Suwannee River NOM (SR-NOM, reference 2R101N) which contains both the humic and fulvic fractions tested in this study. A DOM solution from this NOM was prepared following the procedure described in section 4.2.1. After centrifugation, aqueous samples from the supernatant were analyzed for THg, UV_{254}, and DOC. Results show that Hg removal increases with the removal of DOC as can be seen in Figure 4-11, as more Hg binding sites are provided with the addition of carbon at the optimal coagulation conditions selected for experimentation.

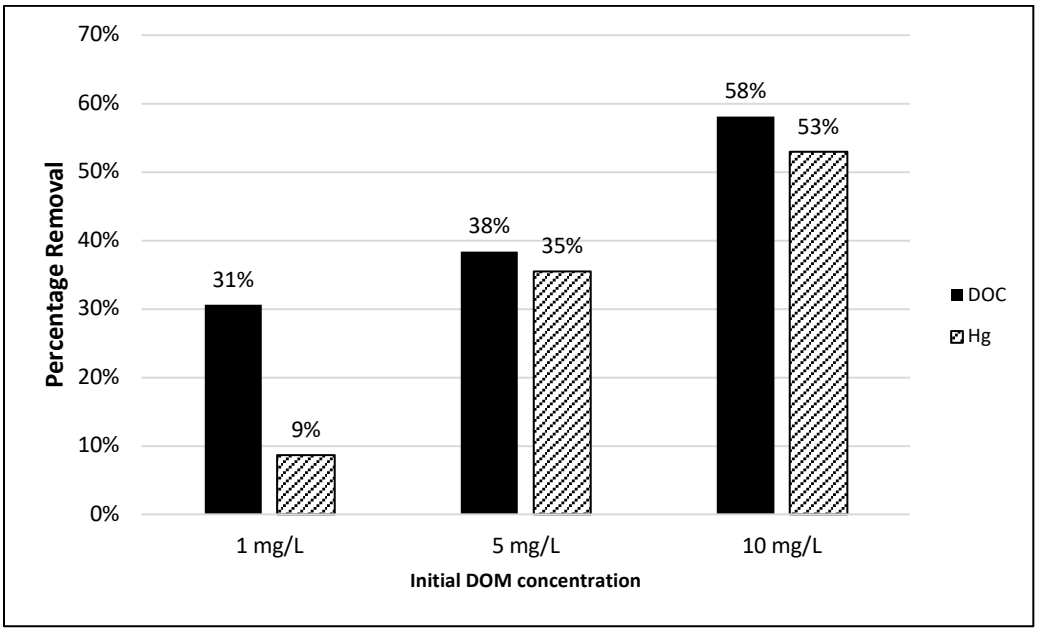

Figure 4-11. DOC and Hg removal percentages for experiments to evaluate the incorporation of mercury on alum flocs.

XPS measurements were performed on a Kratos X-ray Photoelectron Spectrometer – Axis Ultra DLD at the Texas Materials Institute (TMI) at the University of Texas in Austin. The equipment has a sensitivity between of 0.1 to 1.0 atomic percent and an AlKa source 1486.5 ev was used as the anode. High-resolution scans were recorded using a fixed pass energy of 20 eV. Binding energy (BE) of the adventitious C1s peak was used as an inner standard calibration at 284.8 eV. CASAXPS program (version 2.3.17PR1.1 Casa Software Ltd) was used as a fitting program to process the XPS data assuming a Lorentzian–Gaussian distribution of 20%, with a Shirley linear background in order to determine the binding energy of the elements. A typical XPS analysis can penetrate samples between 5 to 20 Å (0.5– 2.0 nm) below the surface of the floc [137].

The relative atomic concentration of the elements in the precipitate and the approximate composition of the surface are shown in Table 4-12. While the amount of carbon detected on the surface of the precipitate increases as DOM content increases (10 mg/L DOM ≈ 5.0 mg/L DOC), the percentage of aluminum decreases, indicating the buildup

of carbon onto alum flocs. The relative concentration of oxygen on samples also decreases, likely due to the uptake of carbon onto the flocs. Similarly, Hg uptake onto the flocs also increases as DOC content increases, although for tests at 1 and 5 mg/L DOM, the concentration of Hg is essentially the same.

Regarding the sulfur content in the DOM samples and its interaction with Hg(II) ions, it was previously determined that sulfur alone is a minor component in DOM. Sulfur concentration in DOM is estimated to be between 0.5 to 2% by weight of DOM [35], [40], [58]. The amount of S_{red} among the DOMs used in this work varies between 54 to 72% by weight of the total sulfur. Consequently, the atomic percentage of the S_{red} in the DOMs used for experimentation (numbers in parenthesis) were calculated based on the elemental composition provided by the International Humic Substances Society (IHSS): PLFA (0.53%), SRFA (0.07%), SRHA (0.011%), and NAHA (0.12%). These atomic percentages are similar to the elemental sensitivity of the techniques used for surface characterization of the precipitates; however, these concentrations are expected to decrease once the floc is formed due to the interactions between DOM with alum and Hg in solution. This would explain why no reduced sulfur (S_{red}) was detected by XPS or ToF-SIMS.

Table 4-12. Percentage atomic concentration of the elements at the surface of the floc at different initial DOM concentrations

Element	**%Atomic Concentration**		
	1 mg/L DOM	**5 mg/L DOM**	**10 mg/L DOM**
O 1s	37.9%	30.1%	24.7%
C 1s	37.5%	50.1%	60.6%
Al 2p	17.2%	11.5%	7.6%
Si 2p	4.4%	4.0%	2.6%
Hg 4f	2.9%	4.4%	4.5%
Total	**100.0%**	**100.0%**	**100.0%**
Surface Composition	$C_{12.8}Al_{5.9}O_{13}Hg$	$C_{11.5}Al_{2.6}O_{6.9}Hg$	$C_{13.4}Al_{1.7}O_{5.5}Hg$

The resultant surface compositions of precipitates were normalized by dividing by the atomic percentage of Hg (% atomic concentration) in each sample. These results indicate that, although the proportion of carbon are similar, the relative amount of Hg, O, and Al change depending on the initial DOM concentration used for experimentation. Precipitate from jar 3 (10 mg/L DOM), which have the highest initial concentration of DOM, contains higher amounts of mercury, and consequently the surface chemical composition of this precipitate will have a lower amount of Al and O, as Table 4-12 shows.

Figure 4-12 shows the XPS-spectra results for the most representative elements in the samples, that is, Hg, Al, C, and O. Both survey and high-resolution scans were used to determine the approximate composition of the surface and to quantify these key elements. As a result of the similarities in binding energies for Si_{2p} and Hg_{4f} (approximately 99 eV), it was expected that the spectra from these two elements would overlap between 99 - 104 eV[138], [139], as can be seen in Figure 4-12 (a). Hg4f doublet and its oxidized forms $Hg4f_{7/2}$ and $Hg4f_{5/2}$ can be observed in Figure 4-12(a). The binding energies for $Hg4f_{7/2}$ and $Hg4f_{5/2}$ peaks are centered around 100.9 eV and 104.4 eV, respectively. To quantify the amount of Hg on the surface of the precipitate, "the Si_{2p} core-level spectra [was] separated from Hg_{4f} spectra by using the area of the Si_{2s} core-level spectra and the intensity ratios of the two Si spectral lines," as was recommended by previous authors [138], [139]. Figure 4-12 (b) seems to indicate the uptake of carbon onto alum flocs in the presence of larger DOM concentrations. This situation is corroborated in Figure 4-12 (c) where carbon seems to be the dominant species on the first layer of the precipitate. The presence of oxygen in samples may be attributed to oxygen species such as HgO, $Hg(OH)_2$, $Al(OH)_3$, SiO_2, C=O and C-O bond, among other Hg-O and Al-O species. Therefore, the sample that contains the lowest amount of DOM (1 mg/L) will yield a higher proportion of oxygen in the precipitate, as Figure 4-12(d) shows.

To spot differences between samples, it is not recommended to compare peak areas directly, mainly because "not all the electrons emitted from the sample are recorded by the instrument."[140] The most accurate method is to compare the percentage atomic concentrations, as shown in Table 4-12, which represent "the ratio of the intensity to the total intensity of electrons in the measurement." [140]. Nevertheless, the spectra itself are useful to visualize the binding energy associated with an element and its chemical composition in a

given sample, as well as any chemical shift of binding energy, which provides information about the oxidation states and the chemical environment.

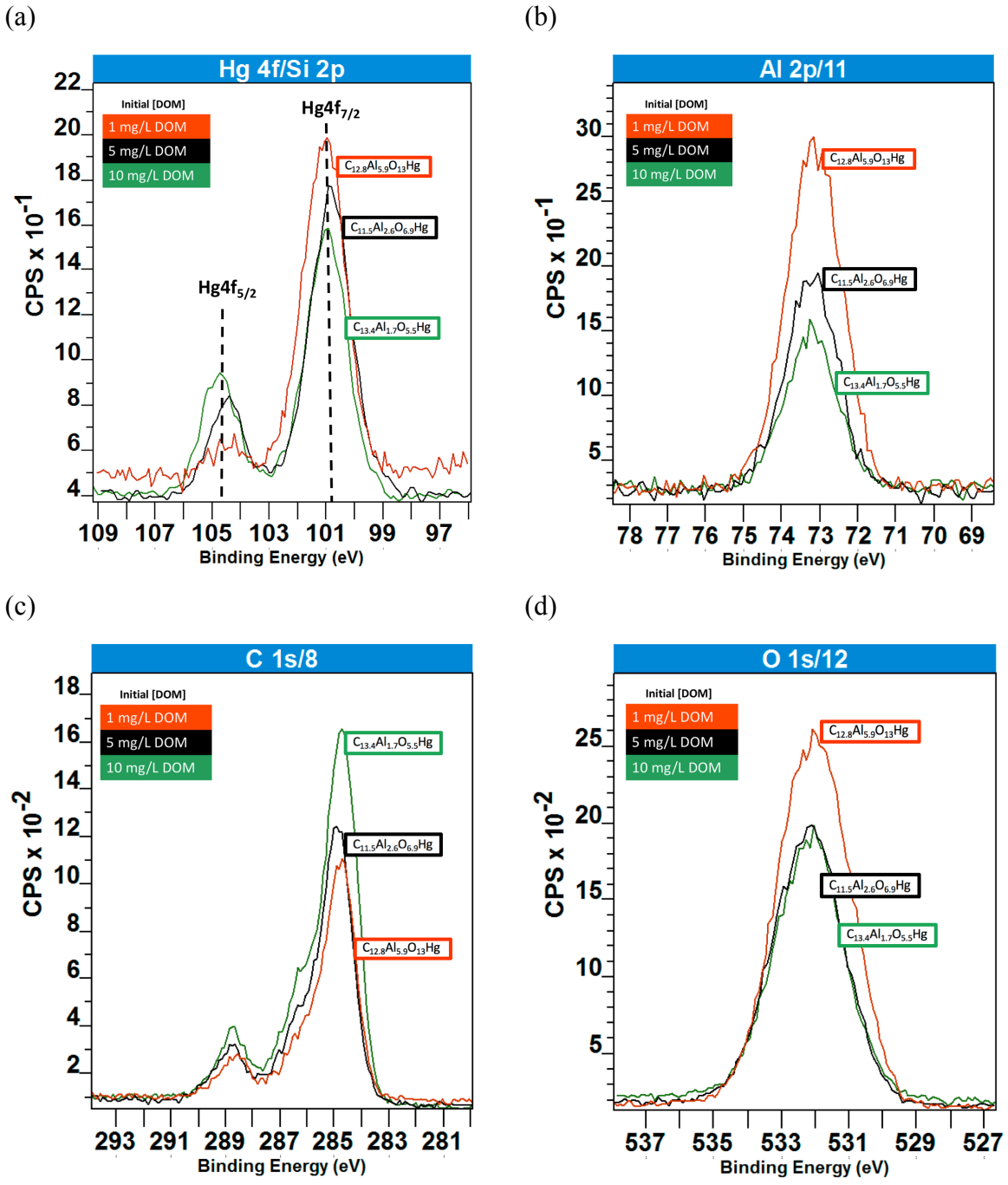

Figure 4-12. XPS spectra for jar test precipitates at different DOM concentrations after flocculation with alum: (a) Hg4f and Si2p (b) Al2p (c) C1s, and (d) O1s core-level XPS spectra.

An additional surface floc characterization was possible using Time-of-Flight Secondary Ion Mass Spectrometry (ToF-SIMS) which provides elemental information from the surfaces of the floc. Figure 4-13 shows the total positive ion image of the floc (upper left) as well as the ion images for Hg, C, and Al-O interactions. These images indicate that Hg, C, Al, and O ions are randomly distributed throughout the surface of floc, where the Al-O ions seem to be more concentrated on the right side of the sample. A more detailed analysis of the regions of interest (ROI) was conducted through further analysis of the Hg-DOM interactions. By looking at the ROI of the selected images, it appears that increases in intensity of Hg are coupled with increased C intensity. This trend would suggest that Hg (II) ions are chemically attracted to functional groups in carbon compounds in DOM samples.

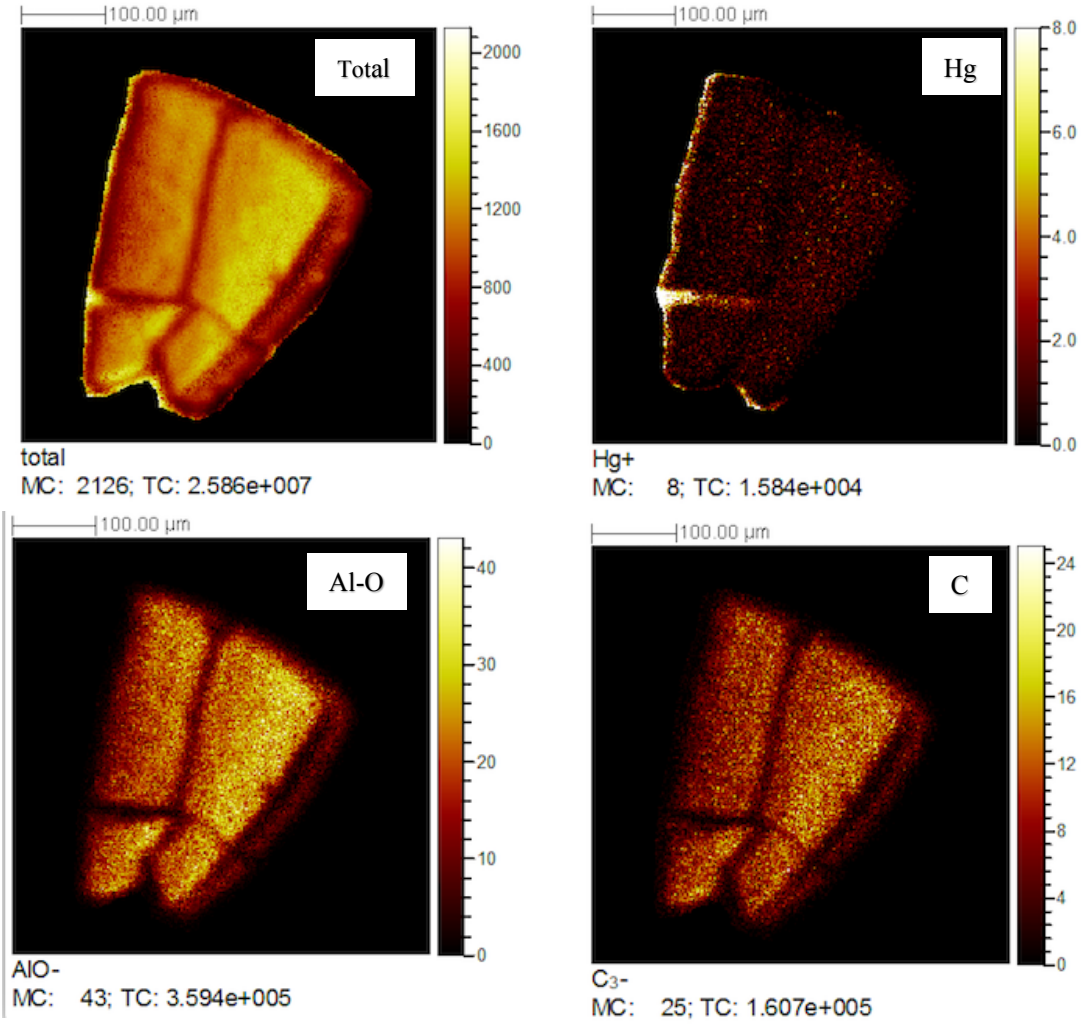

Figure 4-13. Elemental maps of total ions, Hg, Al-O, and carbon on the surface of the floc after alum coagulation treatment by ToF-SIMS. Note: the bright lines on the lower-left side of the Hg-map are associated with the filter and are not related to the presence of Hg in that particular area of the floc.

4.4 Conclusions

Experiments at low Hg/DOM ratio indicated that Hg is associated with the aromatic fraction of the DOM and the S_{red} species in the DOM sample. High Hg removal efficiencies seem to be possible regardless of the character of the DOM and the amount of carbon removed from solution under low Hg/DOM ratios. S_{red} species, the strongest ligand for Hg complexation, play a determinant role in removing Hg from solution during alum coagulation. Even for DOM samples with low aromaticity, such as PLFA, high Hg removal efficiencies were possible due the high concentration of reduced sulfur present in this particular natural organic isolate. The low aromaticity of this isolate provided poor removal of carbon compared to the other DOM samples, but the concentration of reduced sulfur in PLFA is on average six times that of the other DOM samples. Consequently, results suggest that the S_{red} ligands are mainly located in the aromatic fraction of the DOM, which allows the removal of Hg from solution in alum coagulation systems, even for highly hydrophilic DOM.

DOM structure and composition also affect the reactivity of this pollutant and its treatability with aluminum-based coagulants at high Hg/DOM ratios. Experiments at high Hg/DOM ratios provide a glimpse into the limitations for removing Hg from surface waters. While the S_{red} ligands seem to be concentrated in the fraction of DOM more attractive to aluminum hydroxide precipitates, other ligands such as carboxylic functional groups are more likely distributed throughout the structure of the DOM molecule. As a consequence, it seems that any Hg ion bound to the carboxylic ligand in the aromatic fraction of the DOM will be removed from solution, as was the case for the SRHA and NAHA, while those ions bound to the hydrophilic fraction of the DOM are more likely to stay in the supernatant, as the results for the PLFA indicate.

As reduced sulfur species in DOM are frequently defined differently depending on the study, it is important to recognize that not all S_{red} species are available for Hg complexation [35], [37], [75]. Thus, estimates of S_{red} alone may not be sufficient to quantify

the amount of Hg that can be removed via Hg-S_{red} complexes; it may be necessary to quantify the thiols and sulfide content. Nevertheless, the results from this work indicate that ratios of S_{red} to Hg(II) can be used as a guide for assessing the significance of these ligands for a particular water. At higher concentrations of mercury, both S_{red} and carboxylic ligands influence the removal of Hg in highly polluted ecosystems.

Finally, it is important to emphasize that the character of DOM will determine the extent of the removal of DOC from solution and the changes in $SUVA_{254}$ values in metal-based coagulation systems; however, the composition and distribution of Hg-reactive functional groups is equally important for determining the potential for Hg removal from solution.

CHAPTER 5. ANALYSIS OF THE INTERACTIONS BETWEEN MERCURY AND NATURAL ORGANIC MATTER (NOM) THROUGH STATISTICAL ANALYSIS, EQUILIBRIUM DIALYSIS LIGAND EXCHANGE (EDLE), FLUORESCENCE SPECTROSCOPY AN BENCH-SCALE JAR TESTS WITH AND WITHOUT AN ESTERIFIED NOM

5.1 Introduction

Carboxylic acids are one of the most abundant functional groups in dissolved organic matter (DOM) [69], [136]. However, their importance for Hg(II) complexation of DOM is often overlooked because mercury binding at low Hg(II) to DOM ratios is often dominated by reduced sulfur ligands. Depending on the concentration of mercury in aquatic ecosystems, Hg (II) ions can form strong complexes with sulfur reduced ligands (S_{red}) or bond to carboxylic acids in DOM [37], [61]. To study the interactions between Hg and DOM in the absence of carboxylic functional groups, two experiments were designed. The goal of the first experiment was to eliminate carboxylic ligands by transforming them into a different functional group with less affinity for Hg ions. In this research, the goal was to transform the carboxylic acids into esters. The second experiment was designed to prove that, at low Hg/DOM ratios, Hg binding is dominated by S_{red} ligands and, at high Hg/DOM ratios, they are dominated by carboxylic ligands. This experiment utilized two different approaches for measuring the Hg-DOM binding constants, Equilibrium dialysis ligand exchange (EDLE) and fluorescence quenching (FQ). The first method is the most common approach and values have been reported for numerous DOMs including some used in this work, and the method has the advantage that the Hg(II) binding can be studied at low Hg concentrations enabling measurement of Hg-S_{red} binding constants. In contrast, fluorescence quenching requires high concentrations of Hg, or rather, high Hg/DOM ratios; hence, the values obtained from FQ are consistent with Hg binding to weaker carboxylic ligands. Thus, representative DOMs were selected for analysis using each method to highlight the dominance of Hg-S_{red} binding at low

Hg to DOM ratios. Finally, a statistical analysis was performed using the data obtained in Chapter 4. Hence, the goal was to determine whether significant relationships existed between mercury removal percentages and independent variables such as reduced sulfur content (S_{red}), carboxylic acids content (COOH), aromatic carbon concentration ($DOC_{aromatic}$), and the amount of total carbon removed from solution ($DOC_{removed}$).

EEDQ Esterification

The esterification of carboxylic acids is an ancient process in organic chemistry where carboxylic acids are converted to esters in the presence of alcohol and an acid catalyst [141], [142]. After the discovery of the Fisher ester synthesis, efforts were made to design more environmentally and economically friendly processes, particularly at room temperature [142]. Hence, the conversion of carboxylic acids to esters using 2-Ethoxy-1-ethoxycarbonyl-1,2-dihydroquinoline (EEDQ) in excess alcohol, discovered by Zacharie et al. (1995) [141], was developed. EEDQ serves as a peptide coupling agent in this esterification process. This process has been applied to a variety of compounds containing carboxylic groups, works well under neutral conditions, and is suitable for natural products [141].

In summary, it is expected that by adding EEDQ, an active acid anhydride will be formed, together with quinoline and ethanol [141]. The active anhydride will react with the alcohol added in excess to form the corresponding esters in the DOM sample. The reactions involved in the esterification process are presented in Figure 5-1.

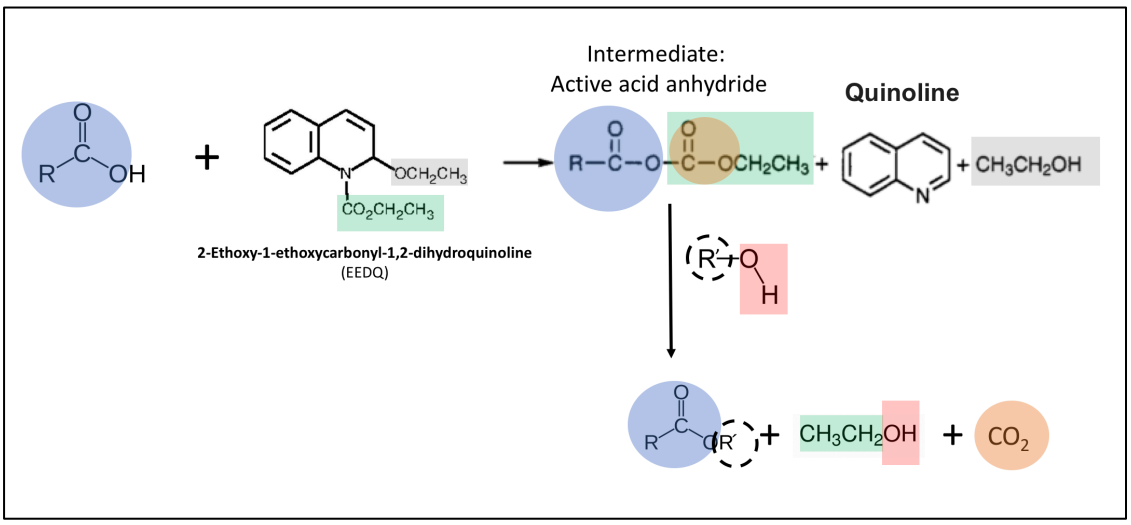

Figure 5-1. Schematic of the esterification of carboxylic acids with alcohols using EEDQ. Adapted from Zacharie et al., 1995.

Comparing jar test results between esterified and non-esterified DOMs can provide some insight into the role of carboxylic ligands for the removal of mercury in metal-based coagulation systems. Jar test experiments at extremely high Hg concentrations using a non-esterified DOM can also provide some information on the influence of carboxyl ligands after saturating the strongest Hg-binding ligands in DOM.

Equilibrium Dialysis Ligand Exchange (EDLE)

Due to the complex composition of the DOM and the different functional groups present in its structure, it is practical to estimate the strength of the Hg-DOM interactions by measuring the conditional stability constants of Hg-DOM complexes ($K_{Hg\text{-}DOM}$ or $K_{DOM'}$). The term conditional stability constant was developed to consider the acid-base reactions that occur simultaneously with complexation reactions [143]. This concept was introduced by Schwartzenbach (1956) [144] and, as its name implies, the magnitude of the K determined depends on the experimental conditions.

Different techniques have been used to determine $K_{DOM'}$. Values of the resultant $K_{DOM'}$ vary according to the experimental conditions and the technique used. Some of these

techniques are competitive ligand exchange (CLE), sorption equilibrium modeling (SE), equilibrium dialysis ligand exchange (EDLE), solvent-solvent extraction (SSE), ion exchange (IE), solid-phase extraction with competitive ligand exchange (CLE–SPE), and Reducible Hg. The technique used in this work was EDLE because it produces reliable data based on the work from previous authors and was specifically developed to measure metal ion-DOM interactions at nanomolar metal concentrations [37], [74].

Fluorescence Quenching (FQ)

Fluorescence spectroscopy is an established tool for measuring binding constants of compounds that form complexes with fluorophores in DOM. A fluorophore is a chromophore (a molecule that contains functional groups that absorb UV or visible light) that remits absorbed photons at a longer wavelength upon light excitation. DOM contains aromatic group fluorophores that make it ideal for employing fluorescence-based techniques. Thus, when organic matter is exposed to UV and visible light, electrons in atoms or molecules are excited by absorbing photons. Some of these molecules can also lose energy in the form of light (fluorescence) when the electrons fall to a lower energy level [145], [146]. In the presence of metal ions, it was observed that the intensity of spectra for DOM samples can either be enhanced or quenched as a function of the concentration of the metal, the fluorescence properties of the binding site, and the experimental conditions [130], [147]. Changes in the intensity of the spectra are assumed to be caused by protonation, deprotonation, or metal complexation of reactive functional groups in DOM [146], [148].

As an optical measurement, fluorescence spectroscopy has the advantages of speed and simplicity which allows both equilibrium and kinetic measurements. Comparisons between the fluorescence intensity of the product of a reaction such as Hg(II) + DOM ⇔ Hg-DOM with the reactant (DOM) can be determined within seconds. Addition of mercury reduces the fluorescence in this case. In fluorescence quenching titrations, the metal (e.g., Hg(II)) is titrated into a sample of DOM and the change in fluorescence is assumed to follow

the stoichiometry of the reaction. Thus, it is possible to determine Hg-DOM binding constants by analyzing the reduction in fluorescence with increasing Hg(II) addition to the system. A detailed description of the reaction chemistry and analysis approach is presented in the classic paper by Esteves da Silva et al. [9] Consequently, an additional goal of this work was to analyze the interactions between Hg ions and carboxylic ligands in DOM samples through fluorescence quenching titrations. Results from this research can provide further insight into the functionalities in the structure of the DOM that allow Hg ions either to be transported in aquatic ecosystems or to be removed from drinking water systems.

5.2 Research Approach

5.2.1 Natural Organic Matter (NOM) selection and characterization

Natural organic matter (NOM) samples for this experimental work were purchased from the International Humic Substances Society (IHSS) and were chosen based on their availability and concentration of acidic functional groups, especially the presence of reduced sulfur and carboxylic groups. NOM characterization was mostly obtained from the IHSS, which provided the carbon distribution of the NOMs by using Carbon-13 Nuclear Magnetic Resonance Spectrometry (^{13}C NMR), the elemental composition for C, H, O, N, S, and P in %(w/w) of dry samples, and the concentrations of acidic functional moieties such as phenolic and carboxyl groups as shown in Table 3-1. Reduced sulfur content data was obtained from Manceau and Nagy (2012), which used X-ray absorption near-edge structure (XANES) spectroscopy to quantify sulfur functionalities in NOM samples [75].

DOM stock solutions were prepared by adding a known amount of solid NOM to ultrapure water (18 MΩ cm). The solution was mixed for 1-hr and sonicated for 30 min to break up big particles. pH was increased to approximately 8.5 to achieve a complete dissolution of the NOM. Afterwards, the solution was filtered using a 0.45-µm cellulose nitrate membrane filter and stored in an amber glass bottle in a dark cold room at 4ºC.

Each NOM selected in this test was characterized by measuring their DOC concentration, UV_{254}, and $SUVA_{254}$ values. $SUVA_{254}$ is defined as the UV absorbance at 254 nm of a water sample divided by the concentration of dissolved organic carbon (DOC) [48], [53], [107]. This value can be used as proxy for aromatic content of the DOM samples in aquatic environments [47], [48].

5.2.2 Esterification of Natural Organic Matter (NOM)

The NOMs selected for esterification were the Suwannee River Fulvic Acid (2S101F) and the Suwannee River Humic Acid (2S101H). To esterify each NOM, approximately 200 mg of solid NOM was dissolved into 30-mL of ethanol for 30-min. Subsequently, EEDQ (1.41 mmol) was added to the DOM solution. The reaction was stirred for 12-h at room temperature. Afterwards, the solution was transferred to a filter flask and the solvent was evaporated under reduced pressure. Ethyl acetate (20-mL) was added to dissolve the residue, and the solution was sonicated for approximately 30-min. Later, the ethyl acetate was also removed under reduced pressure and the residue was dissolved in 120-mL of ultrapure water (18 MΩ cm). The esterified-SRFA was analyzed for ^{13}C-NMR (after concentration in a rotovapor), DOC, UV_{254}, and fluorescence spectroscopy. A schematic of the esterification process is presented in Figure 5-2.

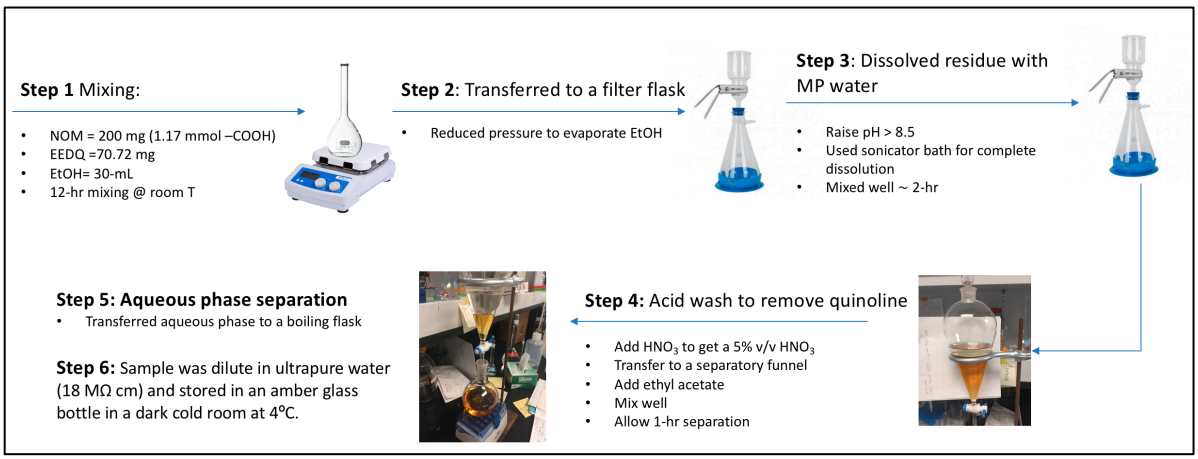

Figure 5-2. Steps followed for the esterification of carboxyl groups in natural organic matter samples with EEDQ and excess alcohol.

5.2.3 Equilibrium Dialysis Ligand Exchange (EDLE) Experiments

The EDLE technique was used to determine the conditional stability constants ($K_{DOM'}$) for the binding of Hg(II) to DOM, following the experimental procedures described by Haitzer et al. (2002, 2003). This technique has proven to be useful to separate bound and unbound Hg fractions at equilibrium using a dialysis membrane.

To avoid Hg losses from solution, the experimental setup included the use of acid-cleaned Teflon® jars and a Spectra/Por® Biotech CE Tubing (MWCO 500-1000 D) as a dialysis membrane. This membrane was chosen because it does not contain sulfur as a residue of the manufacturing process, and it minimizes the leakage of DOM through the membrane.

Experiments were conducted in triplicate using Teflon® jars containing 90-mL of solution placed on the outside of the dialysis tubing and 10-mL of DOM solution placed inside the tubing. The inner solution contained in the dialysis membrane was sealed with standard Spectra/Por® closures on both sides of the membrane. A KH_2PO_4/ K_2HPO_4 buffer solution was used in both compartments to keep the pH at 6.7 and the ionic strength of the solution was set to 0.1 M with $NaClO_4$, taking into account the ionic strength effects of

EDTA and the buffer. Only the inner solution contained 10 mg/L of DOM (Suwannee River NOM, Catalog # 2R101N). At the start of the experiment, 100-µL of a Hg(II) stock solution (1.0 mg/L in 10% HNO_3) was added to the solution in the outer compartment. A representation of the experimental setup is shown in Figure 5-3.

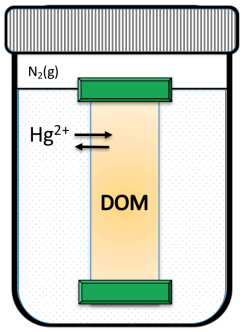

Inner compartment: Dialysis bag
10-mL, 10 mg/L DOM solution
I.S.= 0.1M $NaClO_4$
EDTA: 0.001M
pH = 6.7

Outer compartment (Teflon® jar)
90-mL
I.S.= 0.1M $NaClO_4$
EDTA: 0.001 M
pH = 6.7

Figure 5-3. Representation of the experimental setup to determine the equilibrium constant between free Hg and DOM at low Hg/DOM ratio.

Teflon® jars were sealed with parafilm. Samples were equilibrated in a reciprocating shaker for 5-days, although preliminary results indicated that equilibrium was reached after 3-days of reaction time at ~22ºC. After equilibration, aliquots were taken from the inside and outside compartments and analyzed for THg, DOC, and UV_{254}.

Following the procedure described by Haitzer et al., the conditional stability constant for Hg-DOM interactions ($K_{DOM'}$) assumes that the stoichiometry between Hg(II) and DOM is 1:1 [46], so the reaction between these two compounds is given by Hg + DOM → HgDOM as follows:

$$\mathrm{Hg} + \mathrm{DOM} \rightarrow \mathrm{HgDOM} \qquad \text{Equation 6}$$

From here $K_{DOM'}$ can be obtained as show below:

$$K_{DOM'} = \frac{[\mathrm{HgDOM}]}{[\mathrm{Hg}](\mathrm{DOM})} \qquad \text{Equation 7}$$

Where

$K_{DOM'}$ = Conditional distribution coefficient (L/kg)

(DOM) = Mass DOM concentration (kg/L)

[Hg] = Molar mercury concentration (mol/L)

[HgDOM] = Molar Hg-DOM concentration (mol/L)

Considering that it is expected that [Hg] << [DOM] and that there may be some leakage of DOM between the two compartments, Equation 7 can be transformed into Equation 8.

$$K_{DOM'} = \frac{\mathrm{Q}\alpha_{Hg}}{(DOM)_{in} - (DOM)_{out}(Q+1)} \qquad \text{Equation 8}$$

Where the distribution ratio (Q) can be calculated as follow:

$$Q = \frac{[Hg]_{in} - [Hg]_{out}}{[Hg]_{out}} \qquad \text{Equation 9}$$

EDTA is a typical auxiliary ligand (L) to allow detectable Hg levels at equilibrium [37]. The parameters $(DOM)_{in}$ and $(DOM)_{out}$ represent the concentrations of DOM (kg/L) in the inner and outer compartment, respectively. Q is a measure of the concentration of Hg in the inner and outer compartment as shown by Equation 9, and α_{Hg} is a measure of the complexation of Hg by the auxiliary ligand L and OH- as can be seen in Equation 10, assuming that $[Hg]_{total}$ << $[Ligand]_{total}$ [37].

$$\alpha_{Hg} = 1 + \sum_{i=1}^{n} \beta_i^L [L]^i + \sum_{k=1}^{o} \beta_k^{OH} [H]^{-k} = 1 + \sum_{i=1}^{n} \beta_i^L \left(\frac{[L]_{total}}{1 + \sum_{j=1}^{m} [H]^j \beta_j^H} \right) + \sum_{k=1}^{o} \beta_k^{OH} [H]^{-k}$$ Equation 10

β_i^L and β_j^H are the overall stability constants for the stepwise binding of L to Hg and H (protons) to L, respectively. β_k^{OH} is the overall hydrolysis constant referring to the formation of $Hg(OH)_k$ from Hg + kH_2O [37].

EDLE was employed in this research for a representative NOM to validate the high Hg-DOM constants that are obtained at low Hg:DOM ratios in which Hg-S_{red} binding is expected to dominate. This value is compared to literature values obtained for other DOMs used in this research as well as a wide range of DOMs. The results are used to support the hypothesis that at low Hg:DOM ratios, complexation to S_{red} ligands controls binding.

5.2.4 Fluorescence spectroscopy of Hg-DOM interactions

A series of fluorescence quenching titrations with increasing concentrations of $Hg(NO_3)_2$ were performed to obtain quantitative and qualitative information of the interaction between Hg and DOM (i.e., stability conditional constants and the percent of fluorophores that participates in the binding of Hg(II)). Each sample was prepared at a DOC concentration of 5.0 mg/L, pH 6.7, and ionic strength (0.01M $NaNO_3$). The intensities of the fluorescence emission spectra in the absence of mercury were also measured.

Fluorescence spectra were obtained in a 1 cm quartz fluorescence cell (3.5-mL volume, Starna® 3-Q-10) at room temperature (20ºC), using a Fluorimeter (Fluorolog®-3 model FL3-122) equipped with a Xenon arc lamp as the light source. Fluorescence emission spectra were obtained at wavelengths ranging from 350 to 650 nm with an excitation wavelength of 340 nm. A 5 nm bandpass for excitation and emission wavelengths and 0.25 s integration time were used.

For mercury titrations, a 3-mL aliquot of DOM sample was transferred to a 15-mL vial. A known amount of a $Hg(NO_3)_2$ solution (1.0 mg/L or 180 mg/L in 10% HNO_3) was added to the DOM. Samples were vortex-mixed thoroughly before measuring the spectra and fluorescence quenching was assumed to be proportional to the formation of 1:1 complexes [130]. Consequently, a modified Stern–Volmer equation could be used to quantify complexing parameters, according to the procedure described by Esteves da Silva et al. and Lu and Jaffe [130], [147]. Details of the analytical procedures are found in the referred articles. The modified Stern–Volmer equation allows calculation of the binding constant and the fraction of the initial fluorescence that corresponds to the binding fluorophores:

$$\frac{F_0}{\delta F} = \frac{1}{f K_{DOM'}[Hg]} + \frac{1}{f} \qquad \text{Equation 11}$$

F_0 = Fluorescence intensity of the sample with addition of Hg(II)

F = Fluorescence intensity of the sample without addition of Hg(II)

$\delta F = F_0 - F$

f = Fraction of the initial fluorescence that corresponds to the binding fluorophores

$K_{DOM'}$ = Conditional stability constants between Hg and DOM

According to Equation 11, plotting $F_0/\delta F$ vs. 1/[Hg], $K_{DOM'}$ and f can be determined using multiple linear regression analysis. Results, therefore, provide the conditional stability constant of the Hg-DOM interactions and the fraction of fluorescence binding sites (FBSs). Moreover, since these experiments are conducted at high Hg to DOM ratios, complexation with carboxylic groups is expected to dominate.

5.2.5 Bench scale jar tests

Jar test experiments with and without esterified NOMs were designed at a constant alum dose of 30 mg/L as alum, pH 6.7, and 0.01 M $NaNO_3$ ionic strength. To minimize mercury losses during experimentation, jar tests were performed on magnetic stir plates using acid-cleaned Teflon® jars and Teflon® stirs bars. The desired mercury concentration was spiked in to the DOM solution by adding $Hg(NO_3)_2$ and the pH was adjusted to 6.7 with HNO_3 or NaOH solutions. A two-minute rapid mix period was provided during the addition of coagulant. Twenty minutes were allowed for slow mixing and 30 minutes for settling. Samples were centrifuged for 30 min at 665 x g. Afterward, the supernatant was analyzed for DOC, THg, total Al(III). Similar procedure was followed for jar tests experiments at much higher mercury dose (10-50 μg/L) using a non-esterified NOM.

5.3 Results and Discussion

5.3.1 $SUVA_{254}$ values of DOM samples

The $SUVA_{254}$ values were calculated for each of the NOMs used for experimentation. As expected $SUVA_{254}$ values are correlated with the aromatic content of DOM samples (Table 5-1). PLFA, the sample with the lowest aromatic content (12%) has a $SUVA_{254}$ value of 2.5 L/mgC-m, while NAHA, the sample with the highest aromatic content, has a $SUVA_{254}$ value of 6.5 L/mgC-m).

Table 5-1. $SUVA_{254}$, aromaticity, and notations for selected NOMs

NOM	NOTATION	% Aromatic 165-110 ppm[a]	$SUVA_{254}$ (L/mg C-m)
Pony Lake Fulvic Acid	PLFA	12	2.53±0.13
Suwannee River Fulvic Acid	SRFA	22	4.51±0.20
Suwannee River Humic Acid	SRHA	31	5.94±0.13
Nordic Aquatic Humic Acid	NAHA	38	6.49±0.03
Suwannee River NOM	SR-NOM	23	3.80±0.03

[a]Source: International Humic Substances (http://www.humicsubstances.org/)

5.3.2 Esterification of Natural Organic Matter (NOM)

EEDQ was selected for the esterification of DOM in this study because its reaction is known to be specific to carboxylic groups. The esterification of SRFA was done as indicated in section 5.2.2. ^{13}C-NMR spectra for SRFA and the esterified-SRFA showed differences in the chemical structure between both samples. Signals in the chemical shift ranges δ_C=60-160 ppm are missing in the esterified sample as can be seen in Figure 5-4.

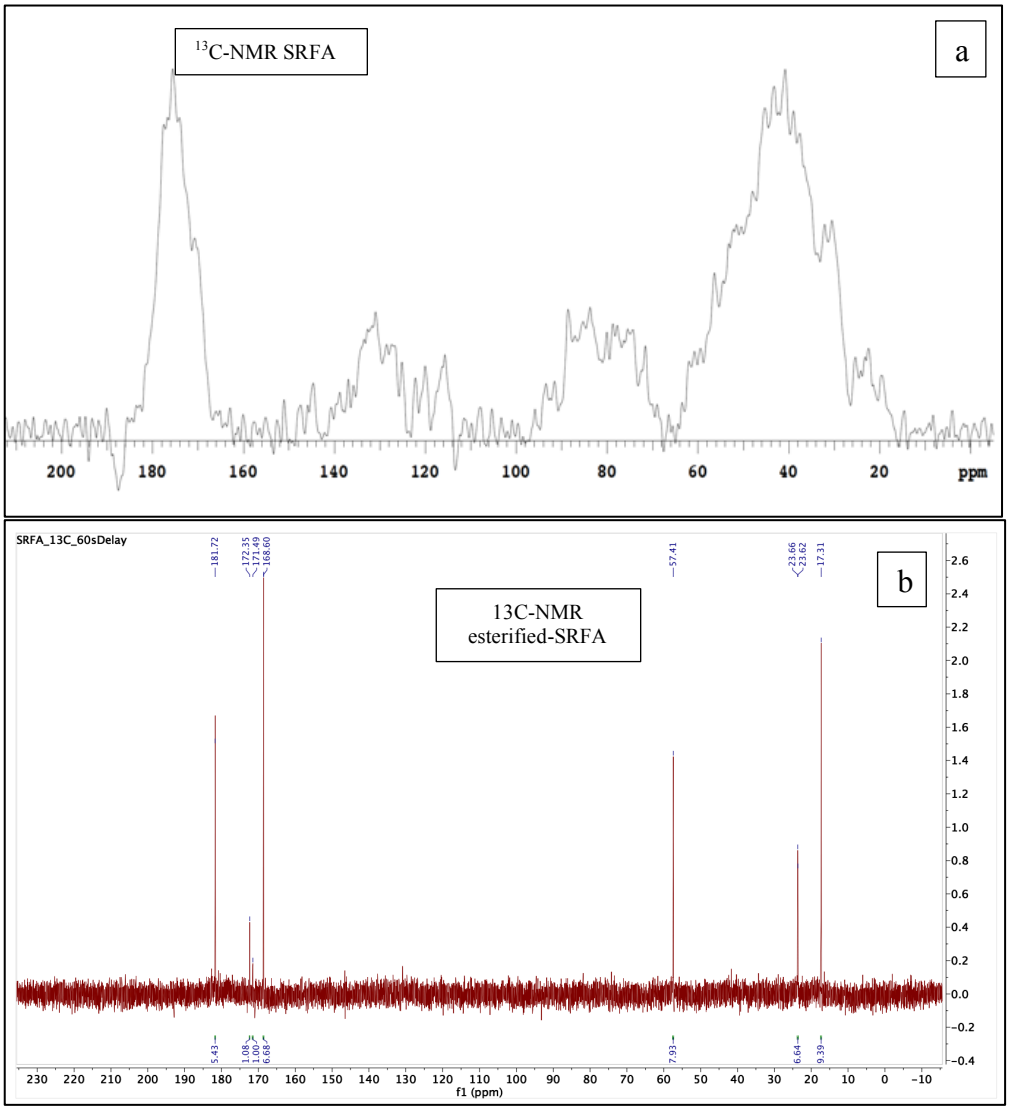

Figure 5-4. (a) Liquid phase ^{13}C-NMR for SRFA sample, (b) Liquid phase ^{13}C-NMR for the esterified-SRFA.

A closer look at the peaks observed in the esterified NOM allows identification and quantification of the different carbon species present in this NOM. Results are shown in Table 5-2.

Table 5-2. ^{13}C-NMR estimates carbon distribution comparison between SRFA and the esterified-SRFA

	ppm	SRFA (IHSS)	Esterified-SRFA
Aliphatic	60-0	35%	63%
Heteroaliphatic	90-60	16%	-
Acetal	110-90	6%	-
Aromatic	165-110	22%	-
Carboxyl, amides, esters	190-165	17%	37%
Carbonyl	220-190	5%	-

^{13}C-NMR results show that the carbon distribution changed dramatically after the esterification process. The esterified-SRFA now contains more carbon species in the chemical shift ranges δ_C=0-60, where alkanes, alcohols, and ethers can be dominant, as well as in the chemical shift ranges δ_C=165-190 where species like amides, esters, and carboxylic acids can be found. The increase in the carbon species in the δ_C=165-190 region might indicate that the esterification of the SRFA actually occurred. Nevertheless, additional analysis is needed to support this conclusion.

5.3.3 Jar tests with and without esterified DOM

Jar tests with the esterified and non-esterified SRFA sample are presented in Figure 5-5. In each case, the total concentration of organic carbon was 5 mg/L. However, in the case of the esterified NOM, only about 40% of the organic carbon came from SRFA and the rest came from the by-products of the esterification process. When a concentration of ~0.5 µg/L Hg(II) was added to the solution, a higher removal of mercury was obtained with the SRFA (~81%) compared to the percentage removed with the esterified sample (26%) (Figure 5-5a). At a mercury concentration of 5.0 µg/L, the removal of mercury decreased to 49% in the SRFA sample and to 14% with the esterified-SRFA (Figure 5-5b). In all cases, the removal

of carbon was approximately 67% for SRFA and 26% for the esterified-SRFA (Figure 5-5c). When normalizing the amount of Hg removed by the total amount of carbon added, it was evident that at both concentrations, 0.5 and 5.0 µg/L, the ratio Hg removed/total carbon was lower for the esterified samples (Figure 5-5d). This difference would suggest that the SRFA lost some of its capacity to remove Hg from solution once it was esterified.

It is important to mention that the $SUVA_{254}$ value measured for the esterified-SRFA was approximately 2.8 L/mgC-m, compared to 4.5 L/mgC-m obtained for the SRFA sample. The removal of aluminum during aluminum hydroxide precipitation was similar in both samples (92%).

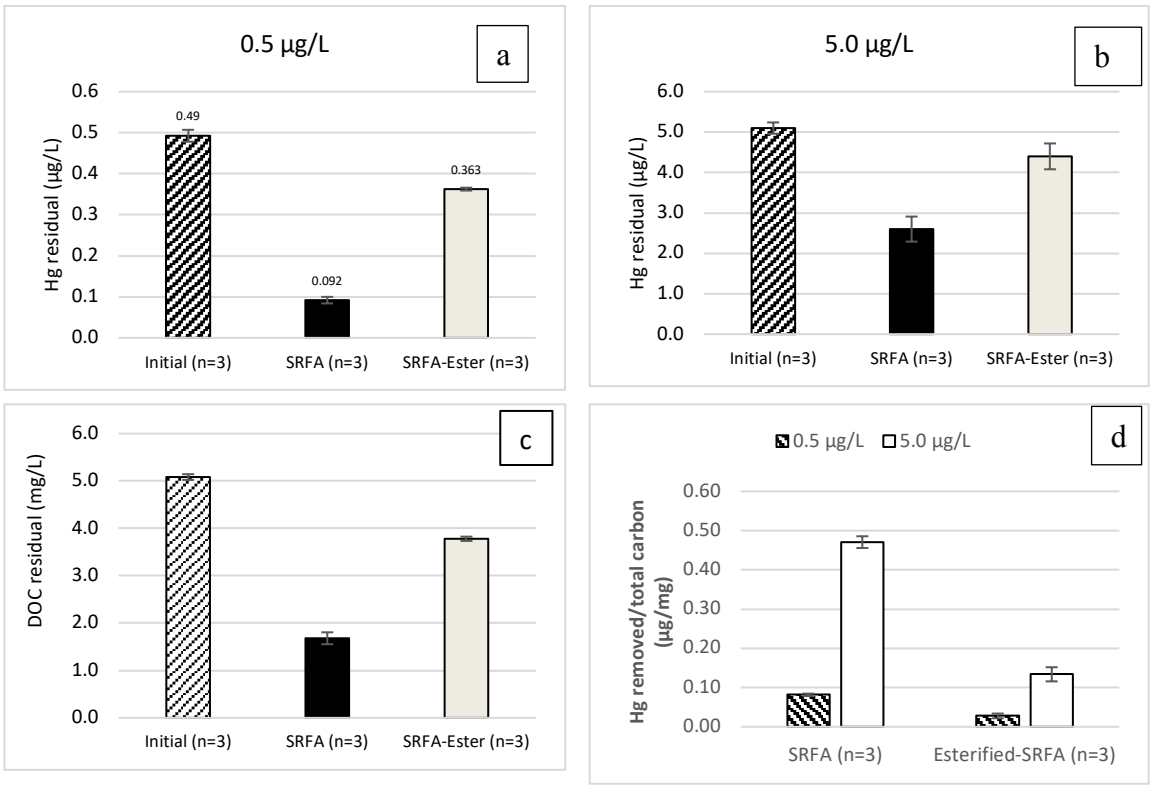

Figure 5-5. Jar tests results with SRFA and esterified SRFA: (a) Hg residual at 0.5 µg/L (b) Hg residual at 5.0 µg/L (c) DOC residual after jar tests at 0.5 and 5.0 µg/L (d) Hg removed/total carbon added.

A similar esterification process was done with the Suwannee River Humic Acid (SRHA), this time at 0.5 and 10.0 μg/L dose of Hg (Figure 5-6). Again, the percentage aluminum removal was approximately 93% regardless of the NOM used. Unlike Figure 5-5a, similar levels of mercury removal were possible at low Hg concentrations (Figure 5-6a). This may be due to the higher S_{red} content of the SRHA compared to the SRFA. At higher mercury concentrations, the performance of the SRHA was consistent with the SRFA; in both cases the non-esterified sample produced superior removal of Hg per mg of carbon compared to the esterified-SRHA (Figure 5-6d). In all cases, the removal of carbon was approximately 85% for the SRHA and 26% for the esterified-SRHA. The $SUVA_{254}$ value of the esterified samples also decreased dramatically to 2.1 L/mgC-m, compared to a value for the SRHA ~6.0 L/mgC-m.

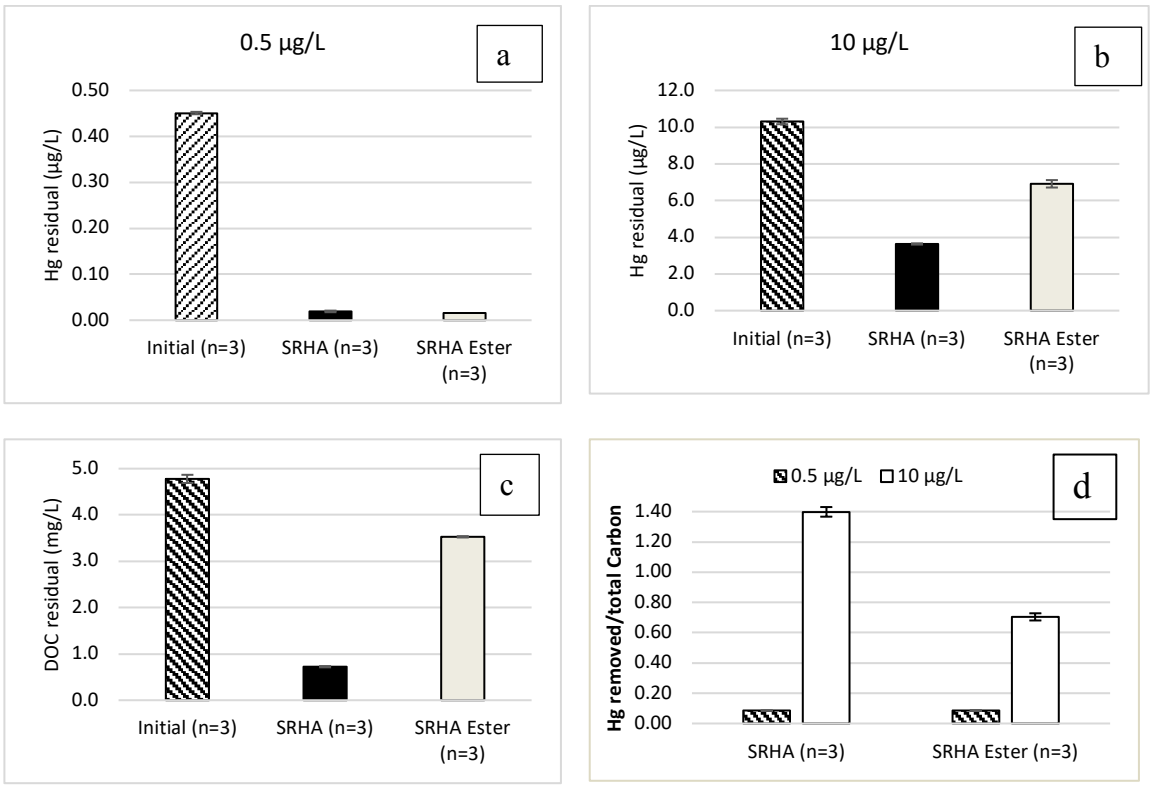

Figure 5-6. Jar test results with and without SRHA and esterified SRHA: (a) Hg residual at 0.5 µg/L (b) Hg residual at 10 µg/L (c) DOC residual (d) Hg removed/total carbon added.

The NMR results suggest that major changes occurred in the structure of the NOM after carrying the esterification process. However, in the absence of an esterified-NOM reference to compare with, it is not possible to elucidate the extent of the changes. The esterification process may affect humic substances in different ways, as the results from Figure 5-5 and Figure 5-6 suggest. Humic acids are richer in aromatic molecules with high molar mass while fulvic acids, which contains more aliphatic chains and a higher concentration of carboxylic ligands, may have undergone a greater transformation than its humic counterpart. Nevertheless, the results suggest that the loss of carboxylic functional groups does impact Hg binding to DOM in SRHA samples.

5.3.4 Jar tests at extremely high Hg(II) concentrations

A comparison in the removal of mercury was conducted between PLFA and SRFA, the two fulvic acids samples, and SR-NOM, the unfractionated NOM. This comparison was done for mercury concentrations between 10 and 50 μg/L, which are atypical of concentrations in natural aquatic environments. While these values are higher than expected in aquatic environments or even in locations downstream of mining operations, Hg(II) values in this range have been observed in amalgamation tailing ponds in gold mining regions [149]. Nevertheless, jar tests under these extreme conditions allow study of the interaction between Hg(II) and carboxylic ligands for conditions that are expected to saturate the sulfur reduced functional groups in DOM. A summary of coagulation conditions for these NOMs is presented in Table 5-3.

Table 5-3. Jar test initial experimental conditions at high Hg(II) concentrations

NOM	DOC (mg/L)	Hg (μg/L)	Coagulant dose (mg/L)	pH
SR-NOM SRFA PLFA	5.0	10-50	30	6.7

Experimental results indicated that the removal of alum was similar among the NOMs tested (92.3%). These results demonstrate that optimal coagulation conditions were provided for NOM removal for all samples as is shown in Figure 5-7.

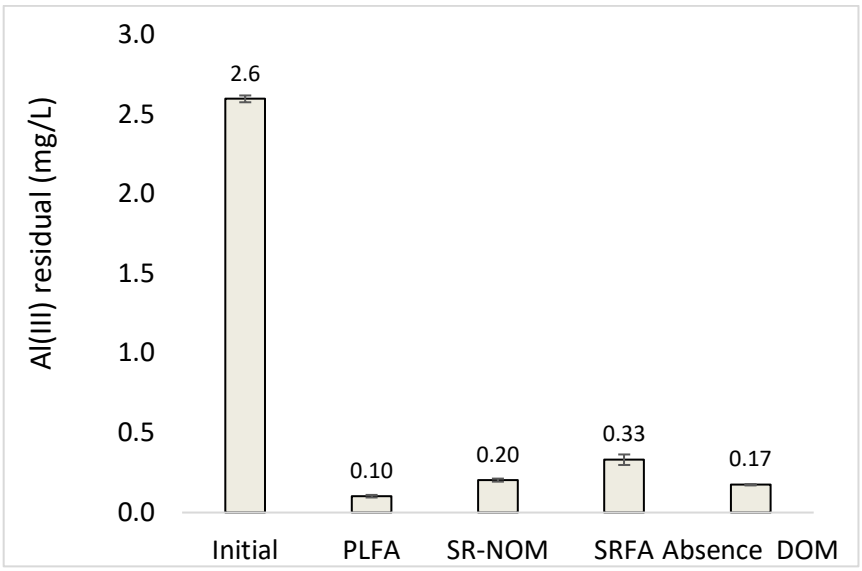

Figure 5-7. Residual Al(III) concentration at pH 6 and alum dose 30 mg/L for NOMs from different environments. Error bars represent standard error from the replicates (n=3).

As expected, the removal of carbon is correlated with $SUVA_{254}$ content as can be seen in Figure 5-8. A higher carbon removal was observed with the SRFA sample, which contains the higher $SUVA_{254}$. A lower carbon removal was observed when using the PLFA, the sample with lowest aromatic carbon, and consequently lowest $SUVA_{254}$ value.

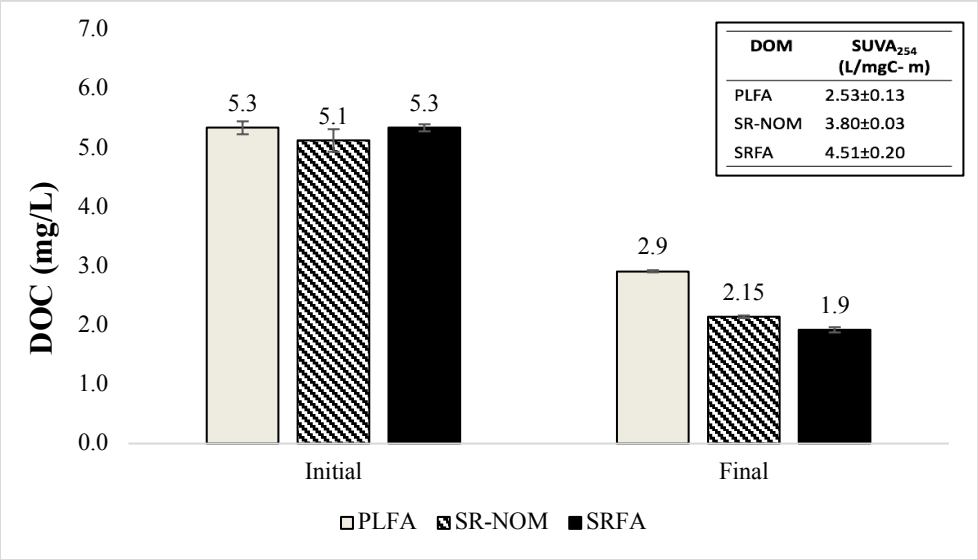

Figure 5-8. DOC removed during bench-scale jar tests for NOMs from different sources. Error bars represent the standard deviation from the replicates (5). The initial DOC concentration in each sample was 5 mg/L as C.

The removal of Hg was relatively constant as the concentration of Hg increased, regardless of the NOM tested, as shown in Figure 5-9. Because this test was done at constant DOC concentration and increasing Hg(II) dose, the lack of variability in the percentage removal of mercury is likely related to the fact that carboxylic ligands are the dominant functional groups under this new condition. Similar Hg(II) removal percentages were obtained using either SR-NOM or SR-FA, while a higher removal of mercury was possible with the PLFA.

The fact that the percentage removal of Hg(II) remains invariable while the amount of Hg(II) removed from solution increases, suggests that a dynamic equilibrium exists between those Hg(II) ions bound to the fraction of carbon that adsorbs onto aluminum hydroxide flocs and those Hg(II) ions bound to the fraction of carbon that remains in the aqueous phase.

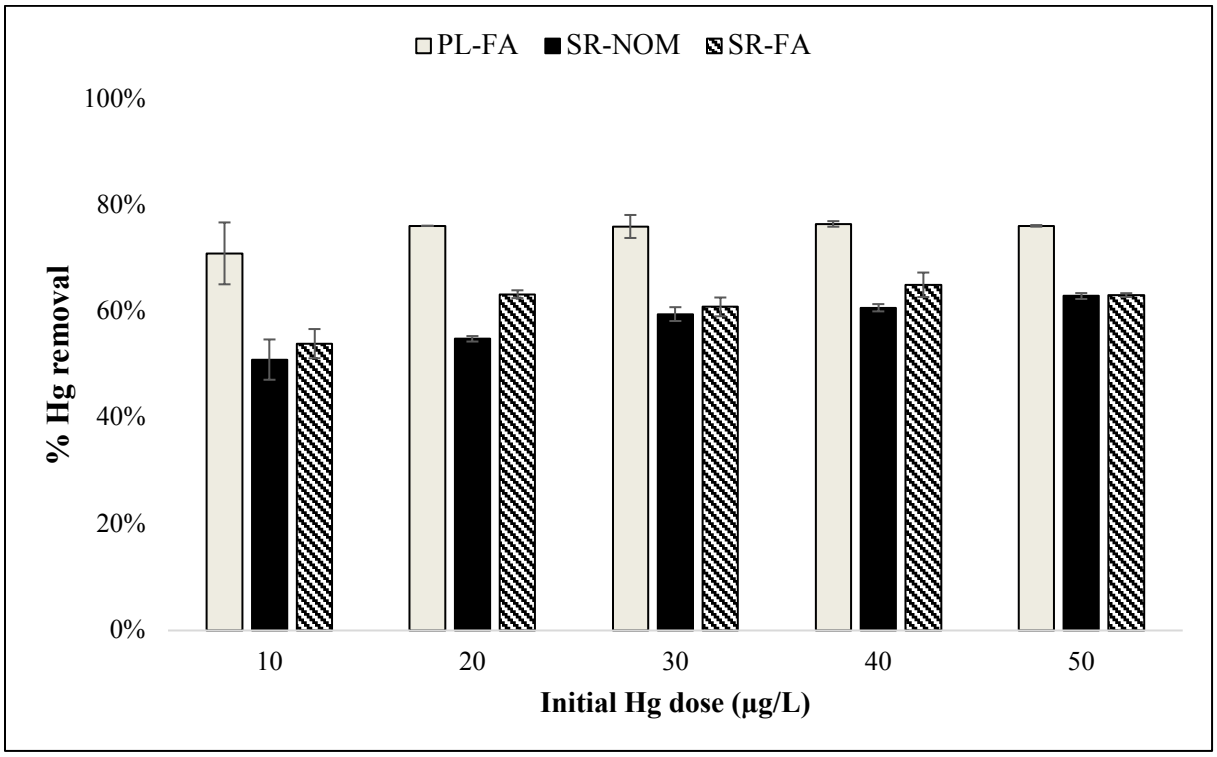

Figure 5-9. Percentage mercury removal at different initial mercury concentrations for PLFA, SRFA, and SR-NOM samples. The initial DOC concentration was 5 mg/L. Error bars represent the standard deviation from the replicates (n=3).

Figure 5-10 shows the amount of Hg(II) removed from solution normalized by the amount of carbon removed. Lower Hg/DOC ratios are obtained at low Hg(II) concentrations, but this ratio increases as the dose of mercury increases. PLFA, the sample with the lowest aromaticity (12%) and highest S_{red} content (2.46 meq/g C), also reported the highest Hg removed/DOC removed ratio.

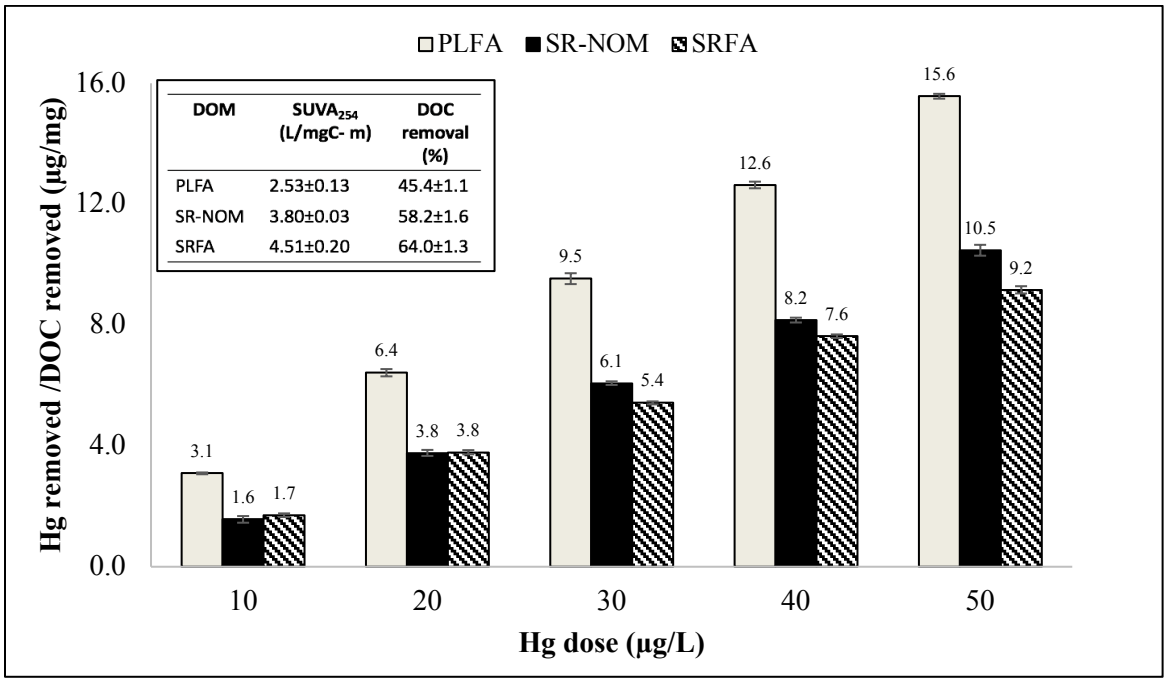

Figure 5-10.Hg(II) removed/DOC removed (µg/mg) for PLFA, SRFA, and SR-NOM. The initial NOM concentration was 5 mg/L and the initial Hg(II) concentration range between 10-50 µg/L. Error bars represent the standard deviation from the replicates (n=3).

As mentioned before, as the concentration of mercury increases, the availability of acidic functional groups decreases. Table 5-4 shows the results after calculating the acidic functional groups normalized by the amount of Hg(II) added (mol/mol) for the three NOM samples selected for this experiment. The concentration of S_{red} in the SR-NOM was estimated as the average of the S_{red} concentration between SRFA and SRHA (see Table 3-1), which are the humic substances extracted from the same water source.

Table 5-4. Acidic functional groups per mole of mercury (mol/mol) for PLFA, SRFA, and SR-NOM samples at an initial mercury concentration of 10 µg/L.

	PLFA	**SRFA**	**SR-NOM**
Hg added (µg/L)	10		
Hg added (mol/L)	4.99E-08		
DOC initial (g/L)	5.E-03		
S_{red} (meq/g C)	2.46	0.294	0.352
Carboxyl (meq/g C)	7.09	11.17	11.21
S_{red}/Hg (mol/mol)	123	15	18
Thiols/Hg (mol/mol)	2.47	0.29	0.35
Carboxyl/Hg (mol/mol)	711	1120	1124

All of the S_{red} are not readily available for Hg(II) complexation [35], [37]. The thiols/Hg molar ratio was calculated assuming that ~2.0% of the thiol ligands form 1:1 complexes with Hg(II) ions in solution [135]. The analysis shown in Table 5-4 was repeated for mercury concentrations between 20 and 50 µg/L. The results of this analysis are plotted in Figure 5-11. As can be seen, the thiol/Hg molar ratio for the PLFA, the DOM with highest aromatic content, decreases from 2.47 to 0.82 when 30 µg/L of mercury are added to the DOM solution. At this concentration, all the thiols ligands would be theoretically saturated with Hg(II) ions.

Regarding the SRFA and SR-NOM, the thiol/Hg molar ratio is < 1.0 across the experiment. In contrast to the magnitude of the ratio between thiols and Hg(II), the molar ratio between carboxylic acids and Hg(II) was always above 100, even at highest mercury concentration of 50 µg/L.

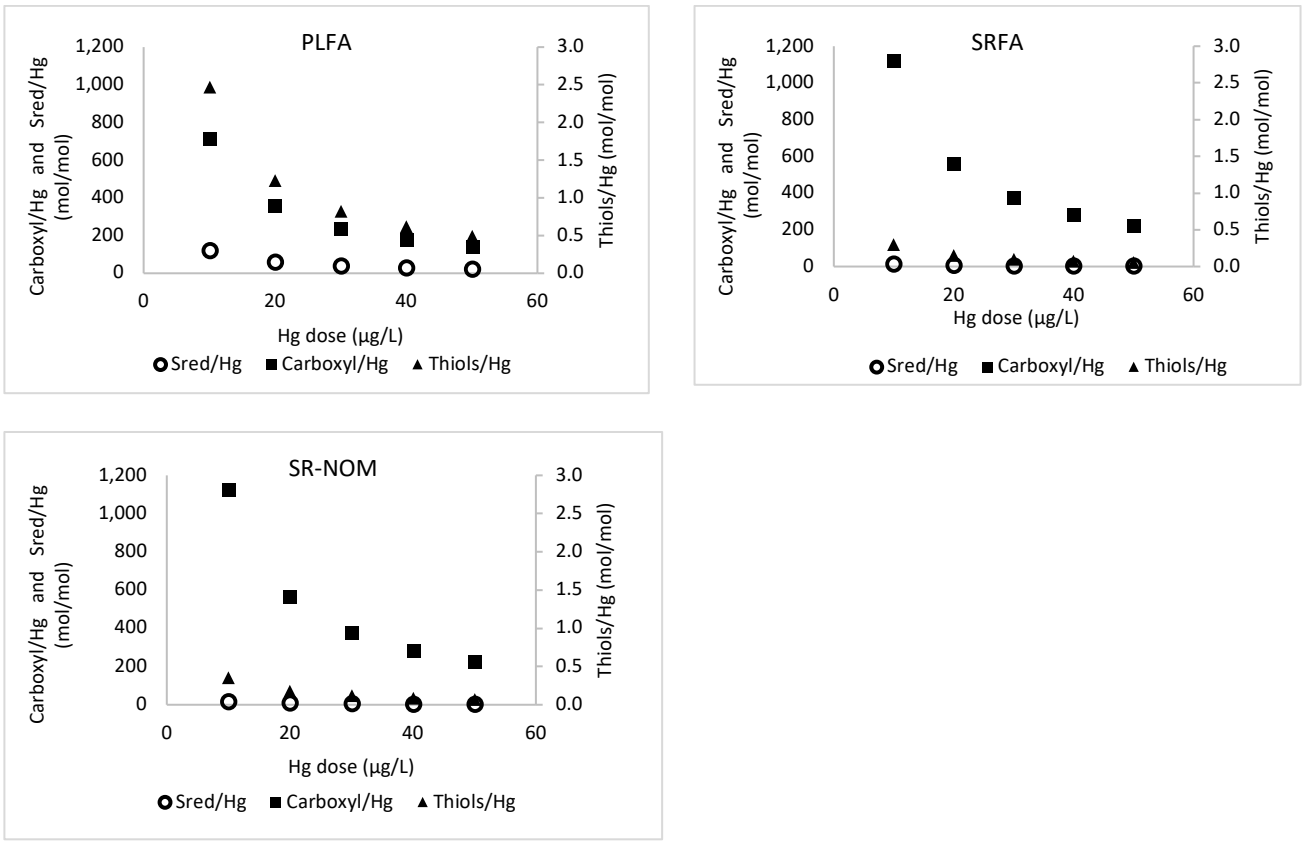

Figure 5-11. Acidic functional groups/Hg molar ratios (mol/mol) in jar tests at high mercury concentrations suing PLFA, SRFA, and SR-NOM samples. The initial DOC concentration was 5.0 mg/L.

As a consequence, the abundant concentration of carboxyl acids, would indicate that once Hg(II) is added to the solution, all of the Hg(II) ions will find a functional group to bind with, even at concentrations as high as 50 µg/L total Hg(II). Furthermore, the concentration of carboxylic ligands is more likely to increase after jar testing. A potentiometric titration of the humic substances used in this study showed that the concentration of carboxyl acids was approximately 3-fold greater in the treated water compared to the untreated water. Similar results has been observed in full scale drinking water treatment [117].

A deeper insight into the results observed in Figure 5-9 allows the following analysis. At equilibrium, the any amount of mercury added to the jar test will be present either as aqueous mercury ($[Hg(OH)_2]_{aq}$), as mercury bound to DOM that remains in solution

($[HgDOM]_{aq}$), or as mercury bound to DOM that absorbs onto alum flocs ($[HgDOM]_{surface}$), therefore, the total mercury concentration at equilibrium can be expressed as shown in Equation 12.

$$TOT_{Hg(II)added} = [Hg(OH)_2]_{aq} + [HgDOM]_{aq} + [HgDOM]_{surface} \qquad \text{Equation 12}$$

Additionally, the total concentration of Hg(II) in the supernatant will depend on the aqueous $Hg(OH)_2$ in solution (if any) and the HgDOM complexes in aqueous phase (Equation 13).

$$TOT_{Hg(II)aq} = [Hg(OH)_2]_{aq} + [HgDOM]_{aq} \qquad \text{Equation 13}$$

In both equations the $[Hg(OH)_2]aq$ is expected to be negligible, and the amount of mercury removed from solution ($[Hg\text{-}DOM]_{surface}$), will be the difference between equation 12 and equation 13. As a result, the percentage removal efficiency of mercury can be written as followed:

$$\%Hg\ removal = \frac{TOT_{Hg(II)added} - TOT_{Hg(II)aq}}{TOT_{Hg(II)added}} \qquad \text{Equation 14}$$

This is, as the dose of Hg(II) increases, the [HgDOM]aq also increases, particularly due to the presence of carboxylic ligands. Such interaction will keep the removal efficiency of mercury approximately constant and proportional to the removal of the DOC that adsorbed onto aluminum hydroxide flocs. Table 5-5 summarizes the results obtained from the jar tests and highlights that the percent removal of DOC and Hg(II) are similar for the two DOMs with lower S_{red}. In contrast, the percent removal of Hg(II) for PLFA is higher than the DOC removal suggesting that even though the thiols are fully saturated, these and other reduced sulfur ligands are contributing to a greater extent to the removal of mercury from solution.

Indeed, previous studies have suggested that S_{red} dominates in the hydrophobic portion of NOM [35], [42], the same portion that is more readily adsorbed to aluminum hydroxides [48], [117].

Table 5-5. Summary of the removal efficiencies for Hg(II) and DOC at high mercury concentrations in the presence of PLFA, SRFA, and SR-NOM. The initial concentration of DOC was set at 5.0 mg/L.

DOM	S_{red} (meq/gC)	Carboxyl + Phenols (meq/gC)	$SUVA_{254}$ (L/mgC-m)	% Hg(II) removal at 50 µg/L	DOC removal (%)
PLFA	2.46	8.84	2.53±0.13	76.3±0.2	45.4±1.1
SRFA	0.294	14.01	4.51±0.20	63.1±0.36	64.0±1.3
SR-NOM	0.352	13.68	3.80±0.03	63.0±0.56	58.2±1.6

5.3.5 Equilibrium Dialysis Ligand Exchange (EDLE) Results

The EDLE technique was used to quantify the Hg-DOM conditional stability constant $K_{DOM'}$ using natural organic matter extracted from the Suwannee River (SR-NOM). A previous test was designed to estimate the equilibration time for the formation of Hg-DOM complexes. This equilibration time depends on different variables, such as the molecular weight cutoff (MWCO) of the membrane and the diffusion rate of the molecules in solution. Previous research indicated that between 2- and 3-days reaction time was sufficient to reach equilibrium, which is consistent with the equilibration time found in this work as shown in Figure 5-12.

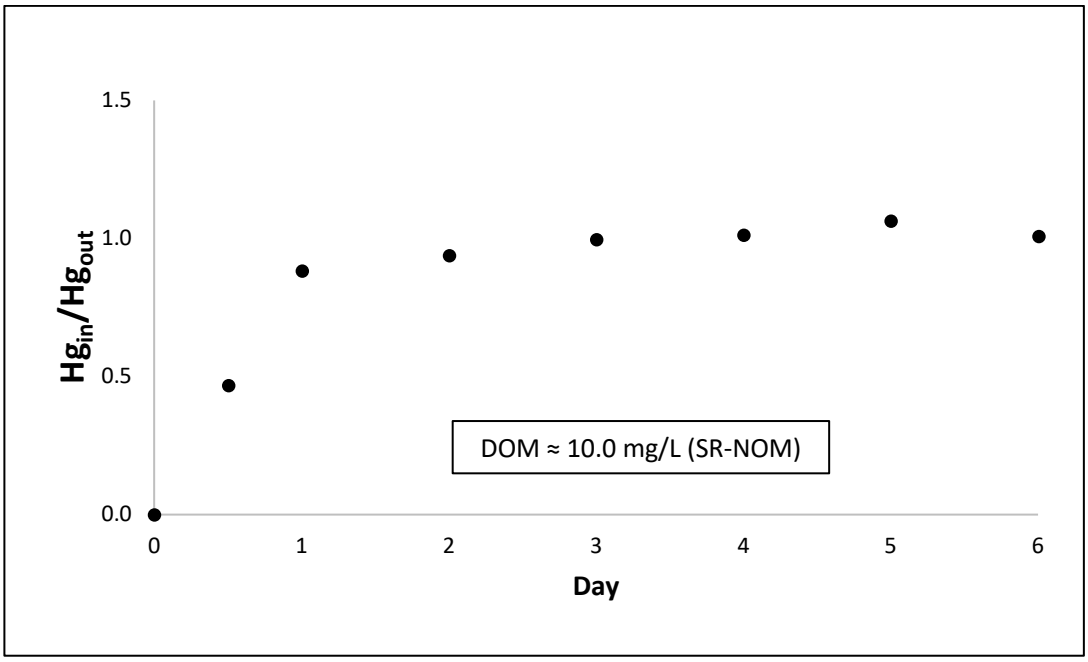

Figure 5-12. Partitioning of Hg(II) spiked in the outer containers in the presence of DOM. Experiments were performed at THg = 1.0 µg/L, pH = 6.7, with Spectra/Por® Biotech CE Tubing (MWCO 500-1000 D) as a dialysis membrane

Once the optimal reaction time was determined, the experiment was performed as described in section 5.2.3. The experimental conditions before and after equilibrium are presented in Table 5-6. Using Equation 9 (section 5.2.3), it was found the distribution ratio Q = 0.637.

Table 5-6. Summary of the parameters measured before and after equilibration

	Day 0		**Day 5**	
	Inner	**Outer**	**Inner**	**Outer**
Total Hg (µg/L)	1.011	< DL	1.520	0.9284
DOM (mg/L)	9.936	-	8.30	0.300
DOM (kg/L)	-	-	$8.3x10^{-6}$	$3.0x10^{-7}$

The most relevant reactions expected during the equilibration process are between Hg(II) with EDTA and hydroxyl ions. The binding constants for these reactions are summarized in Table 5-7 as presented by Haitzer et. al (2002) for the calculation of $K_{DOM'}$ under similar experimental conditions.

Table 5-7. Summary of the reaction of interested for the calculation of $K_{DOM'}$. Source Haitzer et. al [37]

Reaction	β
$Hg^{2+} + EDTA^{4-} \Rightarrow HgEDTA^{2-}$	6.3E+21
$HgEDTA^{2-} + H^{+} \Rightarrow HgEDTAH^{-}$	1.3E+03
$EDTA^{4-} + H^{+} \Rightarrow EDTAH^{3-}$	1.6E+10
$EDTA^{4-} + 2H^{+} \Rightarrow EDTAH_2^{2-}$	2.5E+16
$EDTA^{4-} + 3H^{+} \Rightarrow EDTAH_3^{-}$	1.3E+19
$EDTA^{4-} + 4H^{+} \Rightarrow EDTAH_4$	1.3E+21
$Hg^{2+} + OH^{-} \Rightarrow HgOH^{+}$	1.6E+10
$Hg^{2+} + 2OH^{-} \Rightarrow Hg(OH)2$	1.6E+21

Equation 8 was used to calculate $K_{DOM'}$ from where the average of duplicate measurements was determined as Log $K_{DOM'}$ = 21.8 ± 0.2. Reported values of log $K_{DOM'}$ for different DOM isolates are consistent with the results obtained in this work. Moreover, a summary of conditional stability constants for Hg-DOM interaction, reported by different authors, is presented in Table 5-8. As can be seen, values of Log $K_{DOM'}$ range from 10 to 40. The variability in the range of log $K_{DOM'}$ values depends on the method, the experimental conditions, or the binding model used [74]; as well as all the problems associated when Hg(II) is used for experimental analysis, i.e., sorption and partitioning to materials used in the experiments [150]. The high values of these binding constants and the low Hg(II) to DOM ratios used (<< 1.0 µg Hg/mg DOM) suggest that the binding constants are dominated by binding to thiol and other reduced sulfur groups. Indeed, the binding constants of Hg-thiol have been reported in this range [35], [37], [134].

Table 5-8. Summary of measured conditional stability constants (Log K_{HgL} and K_{HgL2}) reported in the literature for DOM of different origins (Adapted from [74], [150])

DOM sample	Source	Log K_{HgL} (M^{-1})	Log K_{HgL2} (M^{-1})	Technique	pH	I.S. (M)	Reference
Organic Matter isolated from Florida Everglades		10.6 - 11.8	-		6.0	0.04	Benoit et al. (2001)
Surface water	-Wastewater, an eutrophic lake, a creek located d/s of an abandoned Hg mine, and Model water containing SRHA	21.2 - 30.2	-	CLE-SPE	7.0	N/A	Hsu and Sedlak (2003
F1 HPoA	Hydrophobic acid isolated from the Everglades (Florida)	26 - 30	-	CLE-SPE	7.0	0.1	Gasper (2007)
F1 TPiA	Transphilic acid isolated from the Everglades (Florida)	25 - 30	-	CLE-SPE	7.0	0.1	Gasper (2007)
2BS HPoA	DOM isolate from a relatively pristine sawgrass (Cladium jamicense)-dominated environment (Florida)	26 - 31	-	CLE-SPE	7.0	0.1	Gasper (2007)
F1 HPoA		25.5	-	EDLE	7.0	0.1	Haitzer et al. (2002)
		19.8	-	Octanol-water partitioning	6.0	0.01	Benoit et al. (2001)
F1 Peat DOC		23.2	-	Peat sorption isotherms	6.0	0.01	Drexel et al. (2002)
Aquatic humic substance	Isolates from the Florida Everglades	18.4 - 19.8	-		6.0	0	
		25.5	-		7.0	0.1	
EFPC-HBA	Aquatic hidrophobic (HBA), and hydrophilic (HLA) DOM from a contaminated East Fork Poplar Creek (EFPC) site (TN)	22.7	30.8	IE	8.0	0.1	Dong (2011)
EFPC-HLA		21.9	30.1	IE	8.0	0.1	Dong (2011)
IFRC-HA	Soil Humic Acid (HA) and Fulvic Acid (FA) - from the Integrated Field Research Challenge (IFRC) site in Oak Ridge (TN)	23.6	31.6	IE	8.0	0.1	Dong (2011)
IFRC-FA		22.5	30.7	IE	8.0	0.1	Dong (2011)
SRHA, SRFA	Black water river draining the Okeefenokee Swamp; Sampled at Fargo, GA; Vegetation types: Southern Flood plain Forest (Quercus, Nyassa, Taxodium); International Humic Substances Society Standard Humic and Fulvic Acids.	22.5-23.0	-	EDLE	4-7	0.1	Haitzer et al. (2003)
DOM	Artic Lakes (Alaska), Spring Lake (Minnesota), Connecticut River (CT), Pawcatuck River (RI)	21-24	-	Reducible Hg	7.5	N/A	Lamborg et al. (2003)
HBA, HLA	Florida Everglades surface waters: - Hydrophobic fraction of DOM from a eutrophic, sulfidic site (F1-HPoA) and- Hydrophilic fraction from an oligotrophic, low-sulfide site (2BS-HPiA)	21.4 - 23.8	-	CLE-SSE	4-6	0.06	Benoit et al. (2001)
HBA		28.5	28.7	EDLE	7.0	0.1	Haitzer et al. (2002, 2003)
DOM		29.9 - 33.5	-	CLE-SPE	7.4-7.8	N/A	Black et al. (2007)
HA and Peat	Pahokee peat humic acid (1R101H-2) from IHSS Surface soil from wetland in Grand Rapids MN	-	38.2 - 40.4	CLE-SE	3-5	0.5	Khwaja et al. (2006)

5.3.6 Fluorescence spectroscopy

To determine binding constants at higher Hg(II) to DOM ratios, fluorescence emission spectra were obtained at an excitation wavelength of 340 nm for increasing concentrations of $Hg(NO_3)_2$ solution added to ultrapure water, PLFA, and NAHA samples, all with ionic strength of 0.01M $NaNO_3$. $Hg(NO_3)_2$ was also added to a 2-Ethoxy-1-ethoxycarbonyl-1,2-dihydroquinoline (EEDQ) solution, 0,01M $NaNO_3$, to analyze the effect of Hg(II) ions in the presence of aromatic compounds with condensed aromatic rings in their structure.

The resultant fluorescence spectra represent the interaction between Hg(II) and all the Hg(II)-reactive fluorophores in the sample. Some of the relevant functionalities in the structure of DOM are aromatic, phenolics, carboxylic, and hydroxyl functional groups [151], as well as sulfur ligands which are abundant in PLFA.

Figure 5-13 shows the four uncorrected fluorescence emission spectra at increasing Hg(II) concentrations. As can be seen, the emission spectrum of ultra-pure water (0.01 M $NaNO_3$) remains unaltered as the concentration of Hg(II) increases (Figure 5-13a). The shoulder that appears between 360-400 nm is due to the Raman band for water. For the DOM samples, NAHA and PLFA, Figure 5-13c and Figure 5-13d show that the fluorescence intensities of these samples decrease as the Hg(II) doses increases.

Quenching of fluorescence spectra can be caused by changes in the electronic polarization of the metal ion and the fluorophore in the DOM molecule, which results in a decrease or increase in the intensity of the emission spectra [54]. Quenching fluorescence can also be explained by the aggregation of humic substances induced by the metal ions [56], or by a combination of mechanisms such as static quenching (when a complex is formed) or dynamic (collisional) quenching, which is caused by collisions between the fluorophore and the quenching molecule [56], [147].

In contrast to the fluorescence quenching of DOM spectra, the fluorescence emission spectrum of the 2-Ethoxy-1-ethoxycarbonyl-1,2-dihydroquinoline (EEDQ) solution is enhanced in the presence of Hg(II). It was suggested that under the experimental conditions used in this test, (i.e., pH = 6.7 and ambient temperature) EEDQ hydrolyzed to ethanol and quinoline [152]. Quinoline is a well-known fluorophore and can be used as a chemosensor to detected low mercury concentrations (>100 µg/L) in aquatic environments[153]. The enhancement mechanisms observed in EEDQ could be explained then by the formation of complexes between Hg(II) ions and the N atom of the quinoline molecule. Such interaction will enhance the fluorescence intensity of the spectra [153] according to the chelation-enhanced quenching mechanism [154]. Regardless, these results suggest that residual EEDQ remaining in the esterified DOM samples can interfere with the fluorescence quenching determination of DOM binding constants. Thus, it was not possible to obtain binding constants for the esterified DOMs.

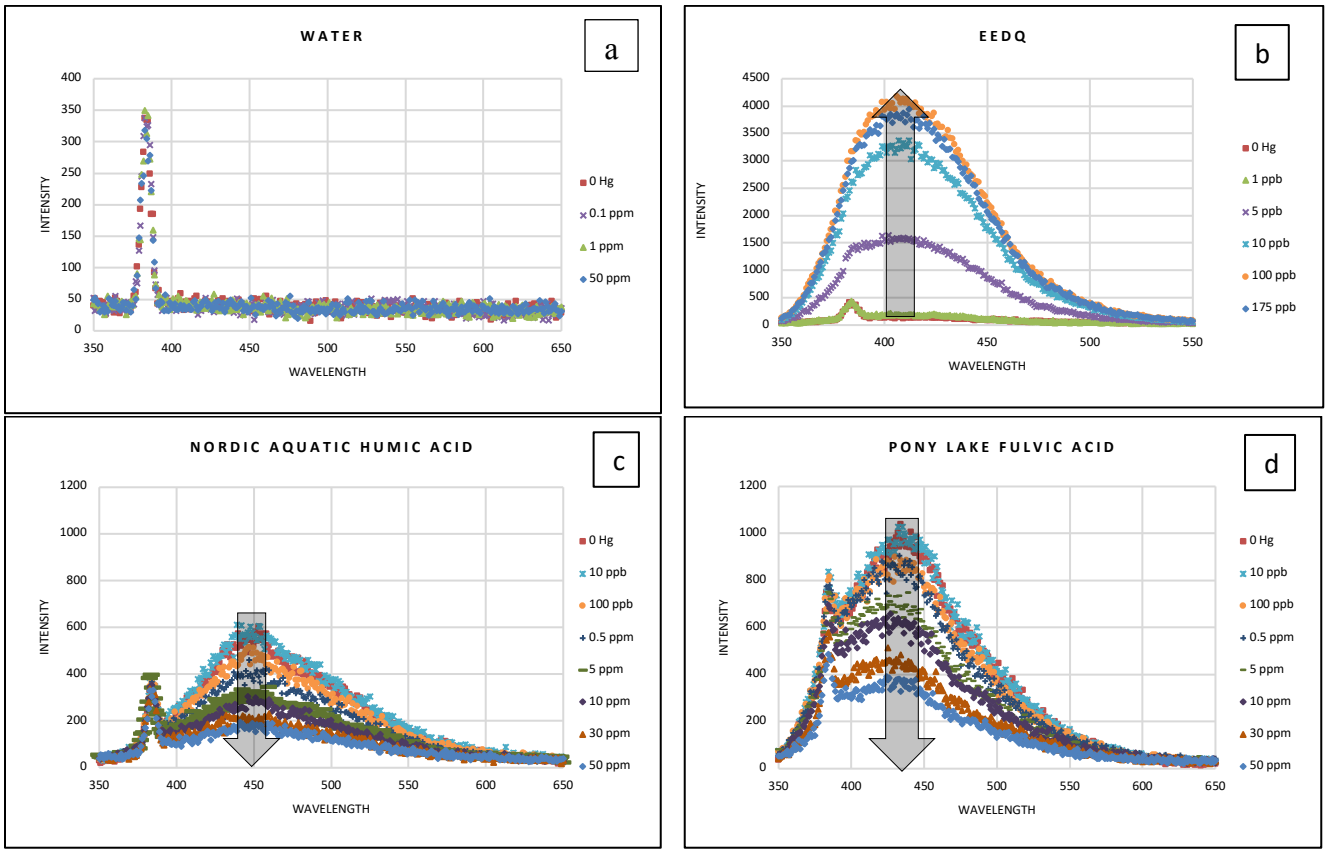

Figure 5-13. Changes in fluorescence emission spectra of different samples with increasing concentrations of Hg(II) excited at 340 nm: (a) 0.01 M $NaNO_3$ solution, pH = 6.7, (b) EEDQ, (c) NAHA, and (d) (PLFA). EEDQ and DOM solutions were prepared at 5 mg/L DOC, pH = 6.7, and 0.01 M $NaNO_3$.

Additional information about the Hg-DOM interaction can be obtained by using the modified Stern–Volmer equation to estimate the complexing parameters K_{DOM}, and *f*, the conditional stability constant and the binding fraction of the initial fluorophores, respectively [130]. Figure 5-14a shows that fluorescence intensities (F/F_0) of NAHA and PLFA samples decreases at different proportions. Results suggest that the complexing capacity of the NAHA is slightly higher than PLFA. This difference indicates that NAHA has more Hg(II)-binding ligands than PLFA; nevertheless no specific information about the amount and composition of the Hg(II)-binding ligands can be determined from Figure 5-14. The concentration of DOC in the samples titrated was 5.0 mg/L (equivalent to ~10

mg/L DOM). The final concentration of Hg(II) in solution range between 1 µg/L to 50 mg/L. As a consequence, the maximum Hg/DOM ratio was approximately 5,000 µg Hg/mg DOM.

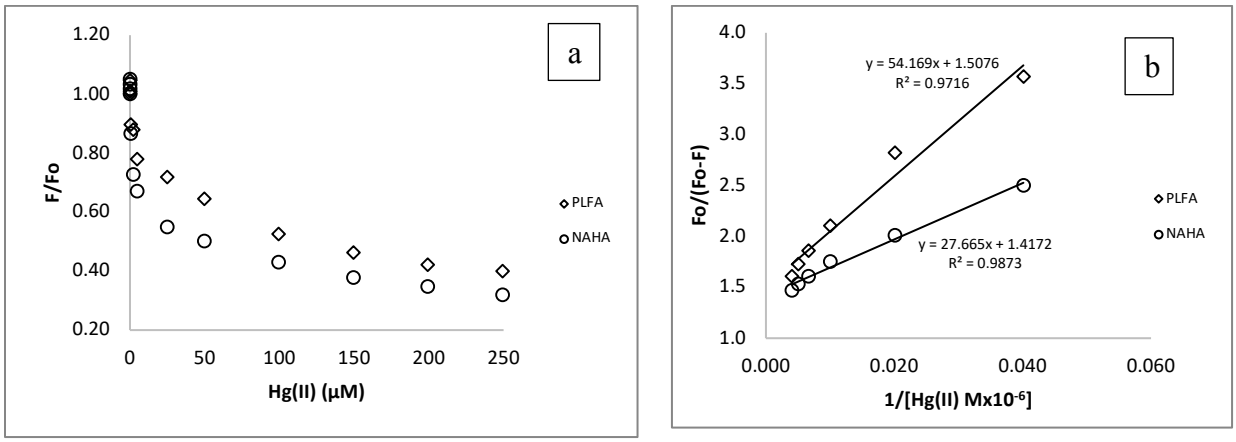

Figure 5-14. (a) Fluorescence emission quenching at of at λ_{ex} =340 nm NAHA and PLFA with Hg(II), (b) Modified Stern–Volmer plot for NAHA and PLFA samples. DOM solutions were prepared at 5 mg/L DOC, pH = 6.7, and 0.01 M $NaNO_3$.

Additionally, the slopes from Figure 5-14b ($1/f\,K_{DOM'}$) and the intercepts ($1/f$) provide the complexing parameters, $K_{DOM'}$ and f, which values are summarized in Table 5-9. $K_{DOM'}$ values represent the average conditional stability constants which account for all the weak and strong ligands available for Hg(II) complexation in DOM. These $K_{DOM'}$ values reported in Table 5-9 are much lower than the conditional stability constants reported by previous authors [37], [134]. Such differences can be attributed to the differences in the methods used to estimate $K_{DOM'}$ and the characteristics of the DOM sample used for experimentation, among other factors. More importantly, since the S_{red} ligands were likely saturated under the conditions of the test, these complexation constants are representative of the weaker binding constants within the DOM. Comparison between PLFA and NAHA, the two DOM samples that were tested under these conditions indicate that although similar, NAHA has a slightly larger percentage

of fluorescence binding sites (FBSs) complexing Hg(II) ions compared to PLFA as indicated by the value of *f* (see Table 5-9), but the "average" binding constant of these sites is lower.

Table 5-9. Complexation parameters for PLFA and NAHA samples based on the modified Stern–Volmer model

DOM	DOC (mg/L)	pH	Log $K_{DOM'}$	*f*	R^2
PLFA	5.0	6.7	4.44	0.66	0.972
NAHA			4.73	0.71	0.987

$K_{DOM'}$ = the conditional stability constant; *f* = binding fraction of initial fluorophores.

Other studies have evaluated log $K_{DOM'}$ values of Hg(II) and NOMs between 4 to 5 from surface water samples in the Florida Everglades [130], streams in Ontario [155] as well as SRFA [151]. Thus, these results for PLFA and NAHA are consistent with these.

5.3.7 Variables influencing the removal of Hg from surface water in alum-based coagulation systems

A stepwise regression approach, performed at a 95% confidence level, was used to determine whether significant relationships existed between mercury removal percentages and independent variables such as reduced sulfur content (S_{red}), carboxylic acids content (COOH), aromatic carbon concentration ($DOC_{aromatic}$), and the amount of total carbon removed from solution ($DOC_{removed}$), for the data obtained in Chapter 4. The analysis was performed at low and high Hg/DOM ratios and all variables were expressed in mmol/L. The program IBM® SPSS® Statistic was used to determine the outcomes of all the possible models. $SUVA_{254}$ values, aromatic content, and acidic functional groups of the DOMs tested are presented in Table 5-10.

Table 5-10. Characteristics of the DOM tested as shown in Chapter 4

DOM	NOTATION	$SUVA_{254}$ (L/mg C-m)	% Aromaticity[a]	Sred (meq/gC)[b]	Carboxyl (meq/g C)[c]
Pony Lake Fulvic Acid	PLFA	2.57±0.09	12	2.46	7.09
Suwannee River Fulvic Acid	SRFA	4.53±0.30	22	0.294	11.17
Suwannee River Humic Acid	SRHA	6.08±0.16	31	0.410	9.13
Nordic Aquatic Humic Acid	NAHA	6.42±0.07	38	0.488	9.06

[a,c]Source: International Humic Substances (http://www.humicsubstances.org/). The aromatic carbon content of DOM is determined by the ratio of the area of the aromatic carbon region (110-165 ppm) to the total area of 13C-NMR spectra
[b]Sred data extracted from Manceau and Nagy (2012)

The results of the models tested are presented next.

I. Regression Analysis at low Hg/DOM ratios

Table 5-11. Experimental description of the jar tests performed at low Hg/DOM ratios

NOM	DOM (mg/L)	Hg (µg/L)	Hg/DOM (µg/mg)	Alum dose (mg/L)	pH
PLFA SRFA SRHA NAHA	10.0	0.5	0.05	30	6.7

Table 5-12. Results of the regression analysis at low Hg/DOM ratio

	Coefficient	t	p-value	Predictor Importance	r^2	Adjusted r^2	Significance F
Constant	1.03	30.36	2.1E-22				
COOH (mmol)	-5.83	-9.48	4.4E-10	0.678	0.802	0.788	54.764
$DOC_{removed}$ (mmol)	0.526	6.53	5.3E-07	0.322			

Best model:

Predicted Hg removal (%) = 1.03 – 5.83*(COOH) + 0.526*($DOC_{removed}$)

The column for predictor importance included in Table 5-12 was added to indicate the relative importance of each predictor in estimating the model. Although this indicator

does not predict the accuracy of the model, it shows the influence of each variable when making a prediction. The sum of the values for all predictors is equal to one.

Table 5-13. Excluded variables by the stepwise regression approach at low Hg/DOM ratios

	Beta In	t	p-value	Partial correlation	Collinearity Statistics Tolerance
S_{red} (mmol)	0.211	0.817	0.421	0.158	0.111
$DOC_{aromatic}$ (mmol)	0.039	0.137	0.892	0.027	0.096

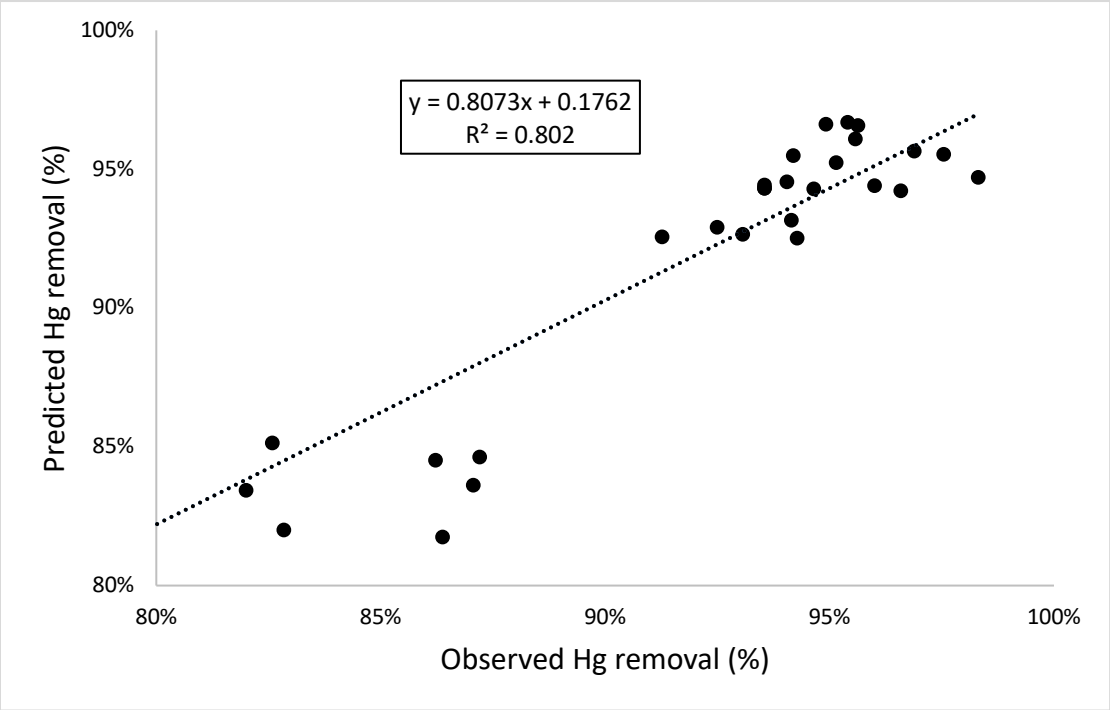

Figure 5-15. Regression describing the relationship between the observed Hg removal and the predicted Hg removal at low Hg/DOM ratios.

Analysis of results at low Hg/DOM ratio

Experimental results indicated that at low Hg/DOM ratios, Hg(II) ions will bind to sulfur reduced ligands (S_{red}) in DOM (conditional stability constants $K_{Hg\text{-}DOM} \approx K_{Hg\text{-}Thiols}$). High mercury removal efficiencies obtained at low Hg/DOM ratios suggest that most of the Hg-S_{red} complexes are removed from solution. Therefore, the concentration of

reactive S_{red} ligands in the DOM sample would determine the minimum amount of mercury that can be effectively removed from solution in alum-based coagulation systems. Additionally, experimental results from the jar tests indicated that the fraction of DOM removed from solution is the most aromatic portion of the DOM (changes in $SUVA_{254}$ values and DOC removal percentages were larger for the DOM samples rich in aromatic carbon). As a consequence, it seems that the independent variables S_{red}, $DOC_{removed}$, and $DOC_{aromatic}$ are likely correlated to each other. This is, S_{red} seems to be mainly located in the aromatic fraction of DOM, and this fraction is more amenable to removal through alum coagulation. As can be seen in Table 5-13, two out of the three collinear variables (i.e., S_{red}, $DOC_{removed}$, and $DOC_{aromatic}$) were removed from the model during the stepwise regression approach.

The best model for the mercury removal percentage shows that the coefficient for COOH is negative and for $DOC_{removed}$ is positive. Jar test experimental results suggested that COOH is indeed an ambiguous variable. This variable can be considered positive if Hg-COOH complexes are in the fraction of DOC that absorbed onto alum flocs, or it can be considered negative if Hg-COOH complexes are in the fraction of DOC that remains in solution. Therefore, the negative sign for the COOH predictor might indicate that, in contrast to the Hg-S_{red} complexes that mostly will precipitate together with the carbon removed, Hg(II) ions bound to carboxylic acids are more likely to remain in solution. Nevertheless, the effect of the negative sign in COOH would be minimum in DOM samples rich in aromatic content, because most of the carbon in these samples is expected to precipitate at optimal coagulation conditions. Regarding the $DOC_{removed}$ variable, this predictor has a positive sign because the removal of mercury is directly proportional to the removal of carbon, either if Hg is bound to S_{red} ligands, carboxylic acids, or any other functional groups reactive to Hg(II).

II. Regression Analysis at high Hg/DOM ratios

Table 5-14. Experimental description of the jar tests performed at high Hg/DOM ratio

NOM	DOM (mg/L)	Hg (µg/L)	Hg/DOM (µg/mg)	Alum dose (mg/L)	pH
PLFA SRFA SRHA NAHA	10.0	10	1.0	30	6.7

Table 5-15. Results of the regression analysis at high Hg/DOM ratio

	Coefficient	t Stat	p-value	Predictor Importance	r^2	Adjusted r^2	Significance F
Constant	1.02	21.489	4.8E-09				
COOH (mmol)	-9.00	-8.614	1.2E-5	0.910	0.892	0.868	37.11
$DOC_{aromatic}$ (mmol)	0.554	2.717	0.0237	0.090			

Best model:

Predicted Hg removal (%) = 1.017 – 9.00*(COOH) + 0.554*($DOC_{aromatic}$)

Table 5-16. Excluded variables by the stepwise regression approach at high Hg/DOM ratio

	Beta In	t	p-value	Partial correlation	Collinearity Statistics Tolerance
S_{red} (mmol)	0.993	3.679	6.2E-3	0.793	0.069
$DOC_{removed}$ (mmol)	-0.419	-0.858	0.416	-0.29	0.052

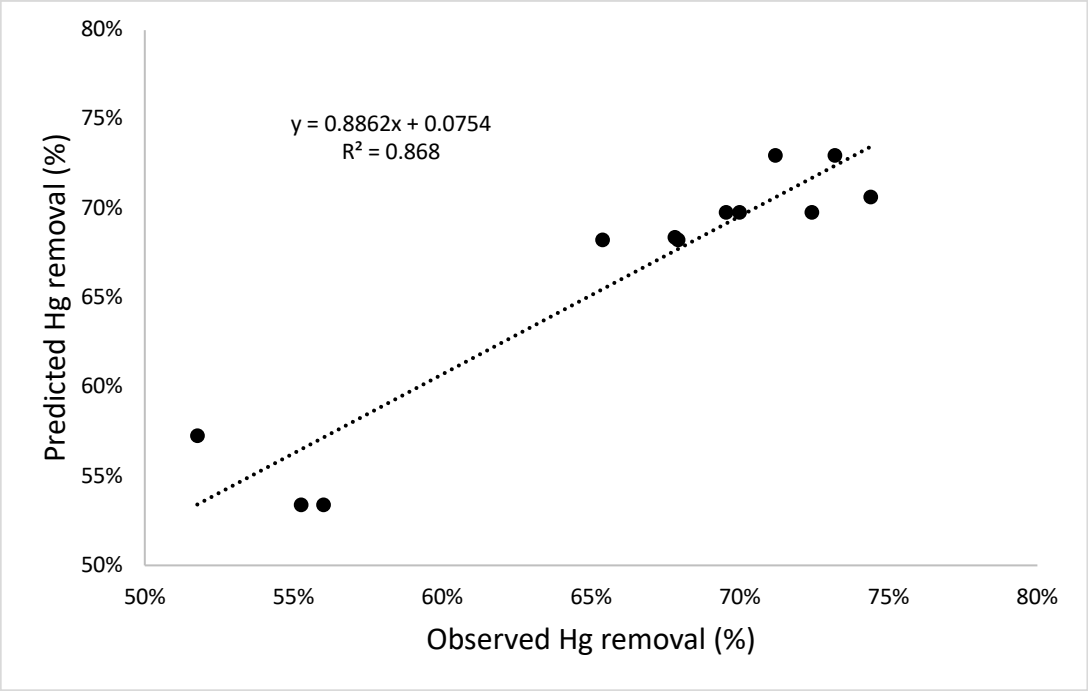

Figure 5-16. Regression describing the relationship between the observed Hg removal and the predicted Hg removal at high Hg/DOM ratios.

Analysis of results at high Hg/DOM ratio

Similar to the analysis at low Hg/DOM ratio, the most relevant Hg removal predictors were COOH and one of the three collinear variables (S_{red}, $DOC_{removed}$, and $DOC_{aromatic}$). This time, the $DOC_{aromatic}$ variable proved to be a better predictor than $DOC_{removed}$ (as shown in Table 5-15, S_{red} and $DOC_{removed}$, the other two collinear predictors were excluded from the model). Although $DOC_{removed}$ seems to be a more robust predictor of the removal of mercury compared to $DOC_{aromatic}$; when testing COOH and $DOC_{removed}$ as the only variables in the model, it turns out that $DOC_{removed}$ was not a significant predictor as expected ($p > 0.05$) compared to $DOC_{aromatic}$ ($p < 0.05$). The reasons behind this behavior are unclear considering that $DOC_{removed}$ is highly correlated to $DOC_{aromatic}$. Similarly, when modeling COOH and S_{red} as the only variables in the model, COOH proved to be a significant predictor of the removal of Hg ($p < 0.05$), in contrast to S_{red} ($p > 0.05$).

A plot showing the regression analysis at low and high Hg/DOM ratios in presented next.

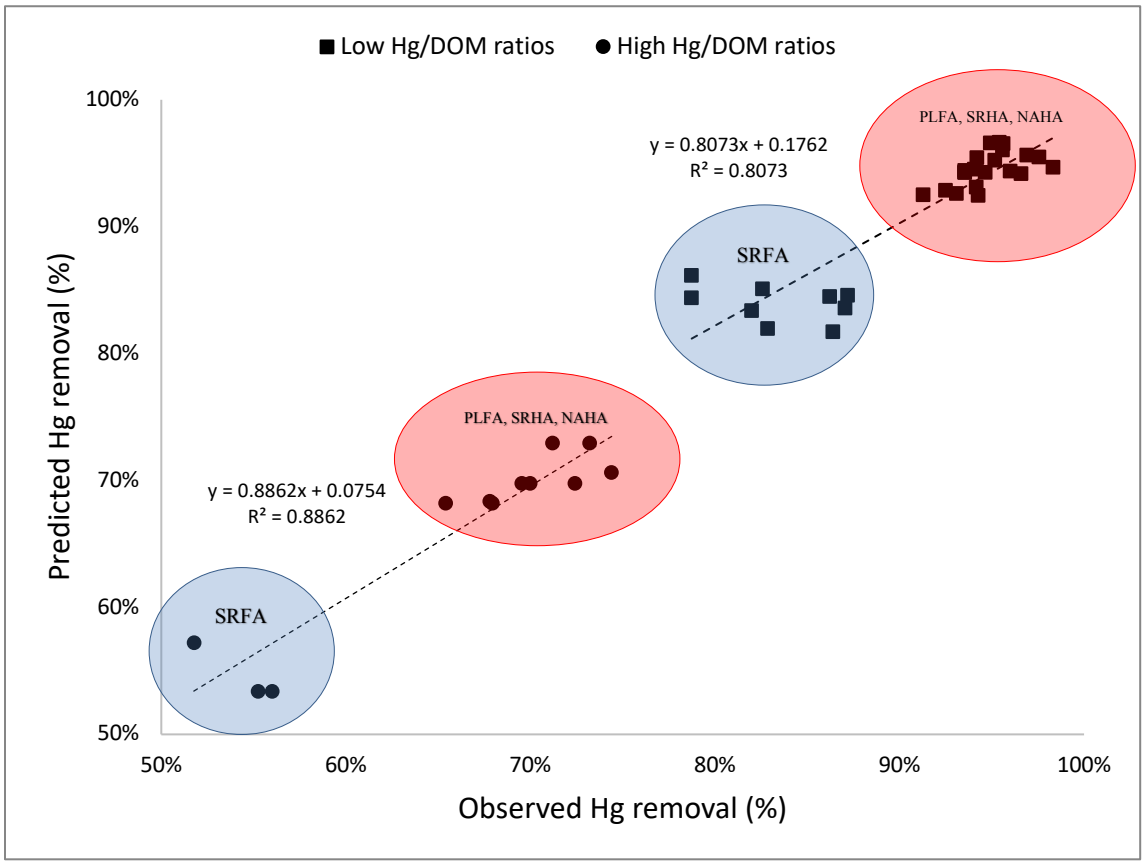

Figure 5-17. Regression describing the relationship between the observed Hg removal and the predicted Hg removal at low and high Hg/DOM ratios.

III. Regression Analysis at much higher Hg/DOM ratios

Table 5-17. Experimental description of the jar tests performed at a much higher Hg/DOM ratio

NOM	DOM (mg/L)	Hg (µg/L)	Hg/DOM (µg/mg)	Alum dose (mg/L)	pH
PLFA SRFA	10.0	10-50	1.0-5.0	30	6.7

Table 5-18. Results of the regression analysis at much higher Hg/DOM ratios

	Coefficient	t Stat	p-value	Predictor Importance	r^2	Adjusted r^2	Significance F
Constant	0.589	42.10	7.28E-27		0.636	0.623	49.01
S_{red} (mmol)	21.05	7.00	1.30E-07	1.0			

Best model:

Predicted Hg removal (%) = 0.589 + 21.05*(S_{red})

Table 5-19. Excluded variables by the stepwise regression approach at much higher Hg/DOM ratios

	Beta In	t	p-value	Partial correlation	Collinearity Statistics Tolerance
Hg dose (mmol)	0.166	1.492	0.147	0.276	1.00
COOH (mmol)	0.938	1.085	0.288	0.204	0.0172
$DOC_{aromatic}$ (mmol)	2.05	1.628	0.115	0.299	7.74E-03
$DOC_{removed}$ (mmol)	0.577	1.678	0.105	0.307	0.103

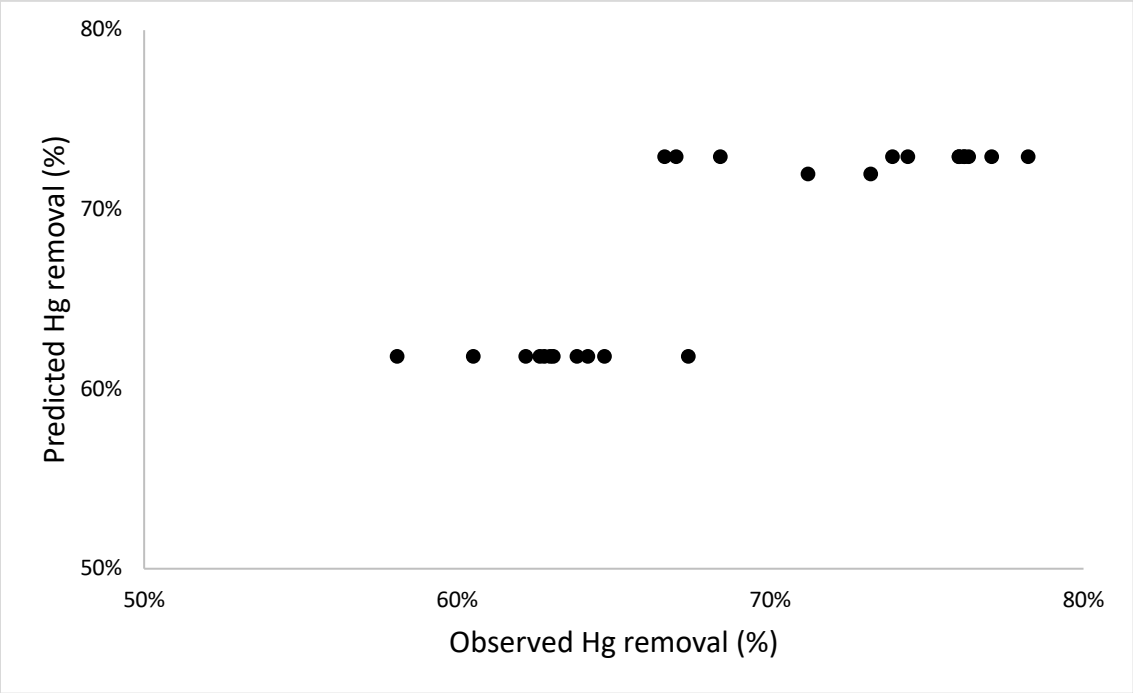

Figure 5-18. Regression describing the relationship between the observed Hg removal and the predicted Hg removal at much higher Hg/DOM ratios.

Analysis of results at much higher Hg/DOM ratio

The predicted model does not fit the observed Hg removal percentage data. The experimental results showed that, at extremely high mercury concentrations, the removal of mercury tends to reach a plateau because the amount of Hg removed from solution is correlated to the amount of Hg that remain in the supernatant. In this new scenario, the removal of mercury will mainly depend on the adsorption of DOM onto alum flocs. That is, at high doses of mercury, both the strong adsorption sites (e.g., with S_{red}) and the weaker adsorption sites (e.g., with COOH) are being used to a great extent; the latter are divided into those that are adsorbed onto $Al(OH)_3$ solids and those that are not. Mercury is present both in the precipitated solids and in the supernatant and so the preferential behavior for adsorption onto the aluminum hydroxide seen at lower Hg doses is obscured.

5.4 Conclusions

^{13}C-NMR spectra suggest that the carbon distribution of NOM is altered during the esterification process. Although the exact composition of the esterified-NOM is unknown, the performance of this esterified-NOM in jar test experiments suggest that the number of carboxylic ligands decreases, as well as the aromaticity of the sample.

Jar test experiments at extremely high mercury concentrations demonstrate the limitations for removing this pollutant from water in alum coagulation systems where S_{red} ligands control the removal of Hg(II) at low Hg(II) concentrations. Results of this study support the hypothesis that S_{red} ligands are more likely to be located in the fraction of carbon that adsorbed onto aluminum hydroxide flocs as high mercury removal efficiencies were obtained with PLFA, the sample with the lowest amount of carbon removed. In scenarios where the S_{red} ligands are saturated, the carboxylic acids control the amount of mercury removed from solution through a dynamic equilibrium between the carbon that absorbs onto aluminum hydroxide flocs and the fraction that remains in the supernatant. Once the carboxylic ligands control the efficiency of the process, it was shown that the amount of mercury removed from solution is proportional to the amount of carbon removed.

The Hg-DOM equilibrium constant ($K_{DOM'}$) estimated with the modified Stern–Volmer model provided much lower values compared to the ones obtained with the EDLE method. The EDLE method used to estimate $K_{DOM'}$ allowed determination of $K_{DOM'}$ at very low Hg(II) concentrations, while significantly higher amounts of Hg(II) were needed when using fluorescence quenching in conjunction with the modified Stern–Volmer model. These high Hg(II) concentrations explain the low values obtained for $K_{DOM'}$, since the strongest ligands for Hg(II) complexation would be saturated. Thus, the low values obtained for fluorescence quenching of NAHA and PLFA demonstrate that, at high Hg(II) to DOM ratios, binding is dominated by the weaker binding sites. In contrast, the enhancement in the fluorescence spectra of EEDQ demonstrated that Hg(II) ions also

interact with compounds such as EEDQ, which may have been present as a residual of the esterification process and then hydrolyzed and converted to quinoline, a well-known fluorophore.

CHAPTER 6. FROM THE ILLEGAL TRADE OF MERCURY TO THE FORMALIZATION OF ILLEGAL MINERS: THE CHALLENGES TO REDUCE THE USE OF MERCURY IN ASGM IN THE LIGHT OF THE MINAMATA CONVENTION

Abstract:

Since the start of the gold rush period in the XVI century, tons of metallic mercury has been deposited in natural ecosystems around the world. It has been estimated that more than 200,000 metric tons of mercury were released in South America, and some tons more were discharged in many other countries, mostly in Central America, Africa, and Asia. Remarkably, annual discharge quantities of this pollutant due to artisanal and small-scale gold mining (ASGM) are still on the order of tons, according to data from the United Nations Environment Programme (UNEP). Metallic mercury, once deposited in rivers and streams, concentrates in soil and bottom sediments and transforms into more hazardous species such as methylmercury. Mercury compounds often travel long distances due to its association with dissolved and particulate organic matter. Along the way, this metal pollutes water bodies used for fishing, drinking, agriculture, and recreation. Focused on Colombia, where 17 out of the 32 states are affected by illegal gold mining, this paper discusses the impact of ASGM in natural environments and the challenges for governments and communities to reduce the use of mercury in this activity. The solution to this problem are hindered by a number of challenges: the involvement of illegal armed groups in gold mining, the illegal trade of Hg(II) in ASGM regions, the need to formalize and legalize illegal/informal miners, and the lack of funding for environmental protection. The discussion provided here is presented in the light of the Minamata Convention on Mercury, which entered into full-force on August 2017.

6.1 Introduction

The term artisanal miners "[encompasses] all small, medium, large, informal and illegal miners who use rudimentary processes to extract gold from secondary and primary ores."[82] According to the United Nations Environment Programme (UNEP), artisanal and small-scale gold mining (ASGM), an activity extensively practiced in developing countries, releases approximately 650 to 1350 tons of mercury per year to the environment [5]. This amount of mercury accounts for one-third of the global anthropogenic mercury emissions [19], [82]. ASGM is intensively practiced in countries from Africa, Asia, and South America. This activity poses an environmental problem for soils, fauna, aquatic organisms, freshwater sources, and communities around and downstream gold mining districts because miners often dump high amounts of metallic mercury into rivers and soils, without legal consequences due to the absence of active government and environmental authorities.

Despite being a hazardous and illegal practice in many countries, the use of mercury for gold amalgamation is still the most common technique used in ASGM because mercury is highly efficient, easy-to-use, readily available, and relatively inexpensive [82]. Nevertheless, the United Nations and other international organizations have made remarkable efforts to minimize the use of mercury in ASGM in developing countries. One of these efforts was the Global Mercury Project (GMP), an initiative created in 2002 to "help demonstrate ways of overcoming barriers to the adoption of best practices, waste minimization strategies, and pollution prevention measures that limit contamination of the international waters."[82] The latest effort to control the use of mercury is the Minamata Convention on Mercury, entered into full-force on August 2017, which is a global treaty to protect the human health and the environment from the adverse effects of mercury.

Although the continued use of mercury in ASGM is a concern, the greater cause of mercury contamination stems from this long term of mercury use for gold mining, leading to a substantial legacy of mercury in riverbeds and sediments. Communities located in regions affected by ASGM use rivers and streams for multiple purposes, and even build water intake structures to produce potable water. Despite the effort of multilateral organizations and local governments to reduce the use of mercury in ASGM, new challenges continue to emerge while seeking to regulate an ancestral practice in many developing countries, including Colombia, the focus of this paper.

After more than 50 years of an internal armed conflict and a recent peace agreement signed between the government and left-wing Revolutionary Armed Forces of Colombia (Farc) rebels, it seems that no other country will face a more difficult challenges to reduce or eliminate the use of mercury in ASGM than Colombia. The involvement of organized crime and illegal armed groups (right-wing paramilitarism and leftist-guerilla) in the gold mining industry, the remote geographical regions where some illegal miners operate, the increasing inequality of the country (after Honduras, Colombia is the country with the 2nd most unequal distribution of wealth in Latin America and 7th in the world [156]), the lack of territorial control by local authorities, the illegal trade of mercury, the already extensive damage caused by ASGM, and the number of illegal and informal miners for which ASGM is the primary source of income for their families, poses serious challenges to a problem that has existed for centuries and likely will continue for a few more decades.

6.2 Mercury from ASGM as a source of environmental pollution

In their attempt to quantify the amount of mercury released from anthropogenic sources to the aquatic environment, the UNEP considered five different categories: (a) point sources -from industrial and domestic atmospheric emissions (~185 Tons/yr), (b)

diffuse sources-such as mercury remobilization from contaminated sites (~8.3–33.5 Tons/yr), (c) mercury-containing pesticides and fungicides used in agriculture (data not available), (d) deforestation (~269 Tons/yr), and (e) ASGM (~800 Tons/yr) [18]. Regarding ASGM in the Americas, mercury has been used for more than 450 years in gold mining to separate gold particles during the amalgamation process [157]. Table 6-1 shows the estimated amount of mercury historically discharged to the environment due to gold and silver mining in some countries around the world. As part of the process, the gold-mercury mix is separated using retorts where metallic mercury is vaporized as a result of applying heat [10], [12], [22], [158], [159]. Part of the metallic mercury is lost into rivers and soils during the amalgamation process and another fraction is lost to the atmosphere during the amalgam burning and gold purification *in situ* or in gold-dealer's shops [91]. Previous studies estimated that for each kilogram of gold produced in ASGM, 1.32 kg of mercury are released to the environment, from which 45% (0.60 Kg) goes to aquatic systems and 55% (0.72 Kg) to the atmosphere[160], [161]. This value was later updated to 1.0 kg of mercury per kg of gold produced [91].

Several previous researchers have noted that mercury emissions from gold mining activities represent an environmental problem in developing countries, mostly in Asia, Africa, and Latin America, with Brazil being the country where most research has been done about the impact of mercury pollution from ASGM [3], [7], [10], [14]–[17], [91], [162], [163].

Table 6-1. Estimated Mercury Input to the Environment Due to Gold and Silver Mining

	Period	Total Input (Tons)	Annual Input (Tons/yr)
Spanish Colonial America	1554-1880	196,000	600
All North America	1840-1900	60,000	1,000
Colonial Brazil	1800-1880	400	5
Brazilian Amazon	1979-1994	2,300	150
Venezuela	1988-1997	360	40
Colombia	1987-1997	240	30
Bolivia (Pando Department)	1979-1997	300	20
Philippines	1985-1997	200	26
Tanzania	1991-1997	24	6
China	1992-1997	480	120

Source: Malm [157]

One report from the United Nations Environment Programme (UNEP), entitled Mercury: Time to Act [5], includes some important data that helps to visualize the global magnitude of ASGM:

- More than 10 million people work in ASGM in Africa, Asia, and South America.
- Mercury from ASGM moves long distances downstream in rivers and remains in the environment for decades even after mining activities cease.
- New technologies that do not involve the use of mercury are available, but socio-economic barriers limit their implementation.

In Brazil, the mercury already present in the Amazon region is being cycled and remobilized from its temporary sinks such that the mercury contamination in this region will persist for many years [5], [91]. This fact suggest that the biggest threat to water pollution with mercury is not the mercury recently discharged during mining activities but what is already present in soils and bottom sediments from previous years.

Figure 6-1 compares gold production and estimated mercury released in ASGM among the top 20 gold mining countries in the world. The data used in the development of Figure 6-1 indicate that 17 of these countries use mercury in gold production [27]. Additionally, one of the most revealing aspects of this chart is that mercury pollution seems to be particularly critical in countries like China, Peru, Indonesia, Ghana, Brazil,

and Colombia. These countries, together with the Philippines, Democratic Republic of Congo, and Bolivia are usually listed as the main mercury polluters in the world [26], [27]. Previous publications indicate that China is the world's largest mercury polluter, with an annual mercury emission from ASGM between 240 to 650 tons, followed by Indonesia with between 130 to 160 tons per year, and Colombia, in third place, with 50 to100 tons per year [26], [164].

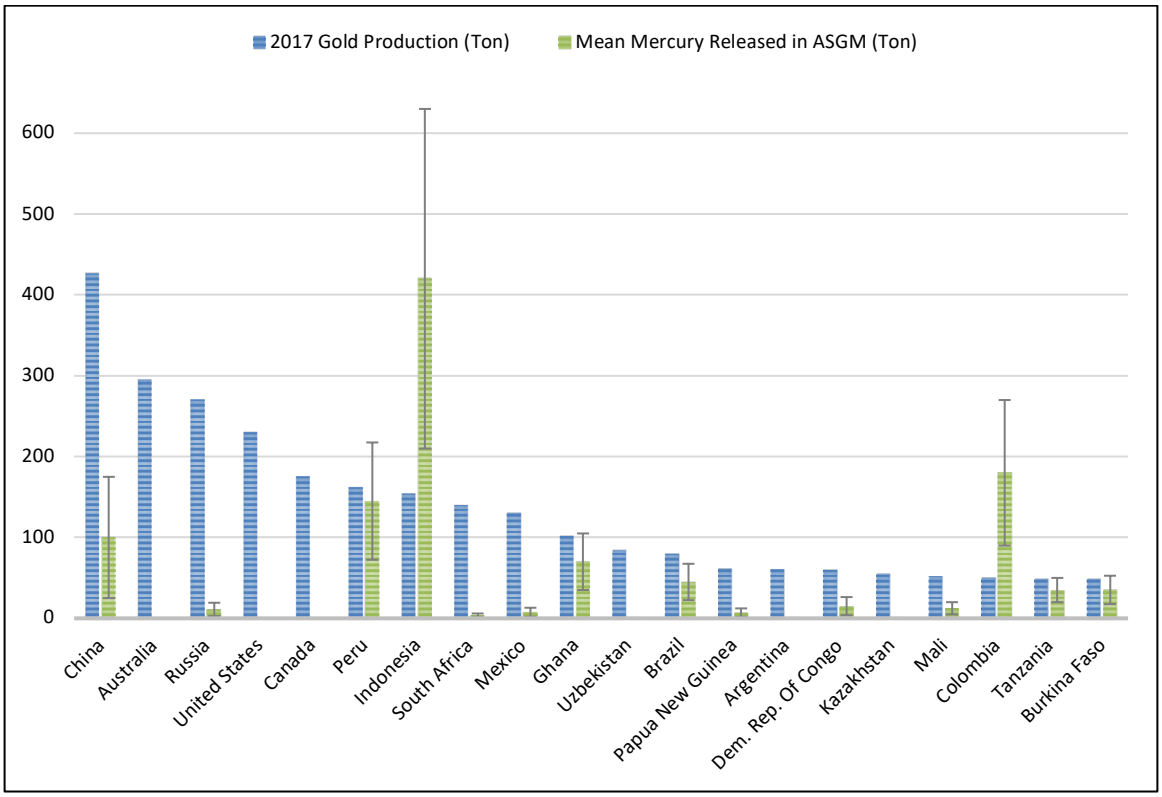

Figure 6-1. 2017 Top 20 gold production and mean mercury released in ASGM among the top 20 gold mining countries in the world. Data sources: [27], [165]

A recent report estimated the percent of gold produced from illegal mining in Latin America: Venezuela (80-90%), Colombia (80%), Ecuador (77%), Bolivia (31%), Peru (28%), Nicaragua (13%), Brazil (10%), and Mexico (9%) [166], [167]. As Figure 6-1 shows, it is clear that a good portion of the global gold production relies on the use of metallic mercury for this purpose.

Figure 6-1 shows that in Indonesia, the average amount of mercury used in ASGM is almost triple the amount of the gold produced by the country in 2017. In Colombia, the average amount of mercury used in gold mining is almost four times the annual gold production. An additional detail is that Indonesia is ranked seventh in global gold production, while Colombia is ranked 18th. The negative impact of ASGM in the environment and human health are evident in these two countries as was already reported by different authors [85], [164], [168]–[170].

6.3 Mercury pollution in Colombia: A legacy that will last for decades

Until 1937, Colombia was the largest gold producer in the Americas [101]. Today, Colombia is the 4th largest gold producer in South America, behind Peru, Brazil, and Argentina [165]. More than 80% of the gold produced in Colombia comes from illegal mining [23], [101], [171], and it is mainly extracted from six out of the 32 states of the country. As Figure 6-2a shows, despite a drop in 2017, the production of gold in Colombia during the last 10-years (2008-2017) has been relatively consistent. Most of the gold produced in the country comes from the states of Antioquia (45.3%), Chocó (29.3%), Bolivar (7.1%), Nariño (6.0%), Cauca (5.3%), and Caldas (3.3%) (Figure 6-2b), and it is mostly extracted from alluvial deposits, mainly in the states of Chocó, Antioquia, and Nariño [172]. It was estimated that alluvial gold exploitation has affected approximately 80,000 hectares of land [173] and that 79% of these lands are located in the states of Antioquia and Chocó. Some of the lands degraded by mining activities are inhabited by Afro-Colombian and indigenous communities, who also own the land and, in many cases, allow its use for gold exploitation.

As expected, many tons of mercury are also dumped in those states where gold mining is particularly intensive. Previous studies reported that the states with the highest

use of mercury in Colombia are Bolivar, Chocó, and Antioquia, with 304, 195, and 170 tons per year, respectively [24], [172].

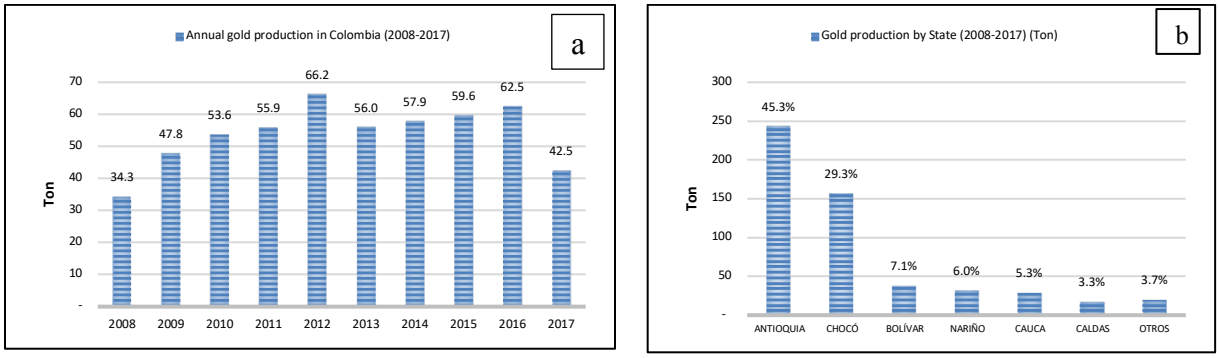

Figure 6-2. (a) Annual gold production in Colombia in the last 10-years and (b) Gold production by state during the same period of time. Data from Unidad de Planeación Minero Energética [174].

Colombia provides a clear example of the devastating and long-lasting effects of employing mercury in ASGM. More than 200 rivers, 17 out of 32 states of the country, and more than 300 municipalities are impacted by ASGM [21], [25], [175]–[178]. Colombia is also considered the world's highest per capita mercury polluter [164] and as Figure 6-1 shows, the amount of mercury released from ASGM surpasses the annual gold production.

In 2004, a governmental study determined that 193 tons of mercury per year were used in the gold mining industry in Colombia, from this, 105 tons were used in legal mining and 88 tons in illegal mining [179], [180]. The negative impacts of both legal and illegal gold mining are evident along the Colombian territory. Figure 6-3a show the regions of Colombia where legal and illegal gold mining is taking place. Gold production in Colombia is concentrated along the Pacific Region and some areas of the Andean Region of the country. Figure 6-3b shows that the same regions from where gold is extracted are also the regions where most of the metallic mercury is dumped. According to the Institute of Hydrology, Meteorology and Environmental Studies (abbreviated

IDEAM in Spanish), a Colombian government agency, 205 tons of mercury were discharged to the environment in 2012 in 179 municipalities of the country [24]. 27.5% of the total mercury was dumped during the extraction of silver and 72.5% during the extraction of gold [24].

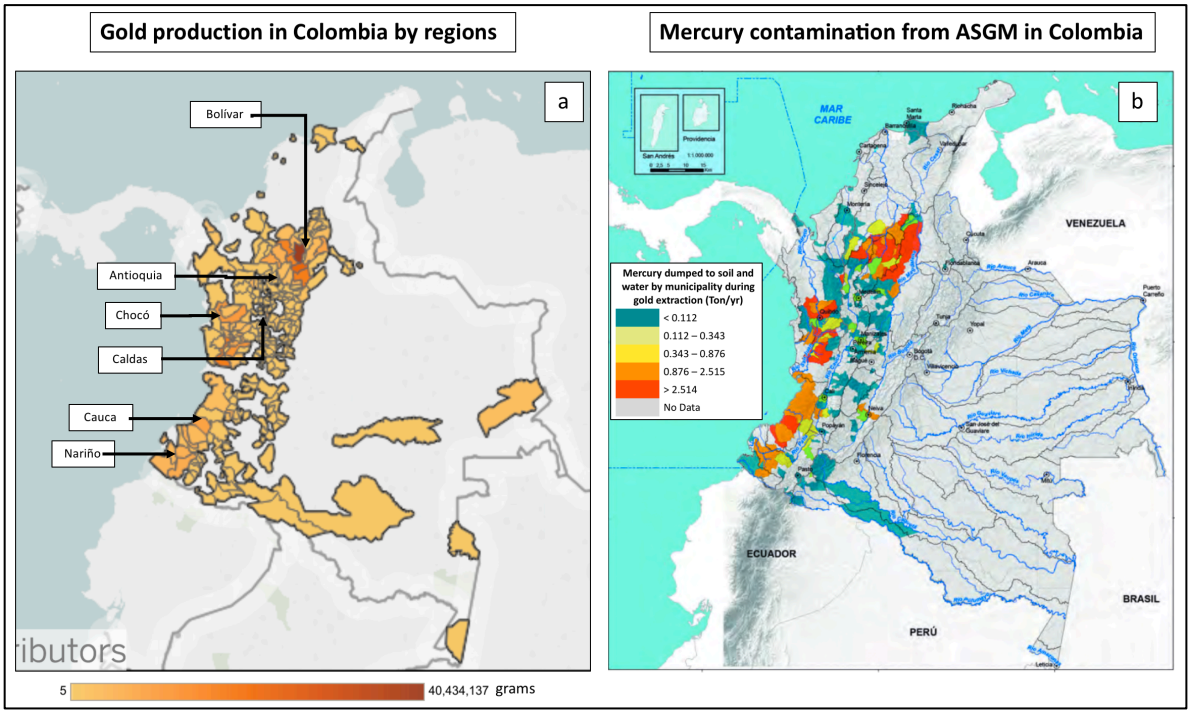

Figure 6-3. (a) Gold production in Colombia and (b) Mercury contamination as a result of ASGM. Map source for Figure 6-3a: Subdirección de Minería-UPME (Agencia Nacional de Minería-ANM, Sep-2018) [174]. Map source for Figure 6-3b: Instituto de Hidrología, Meteorología y Estudios Ambientales-IDEAM, (map version: 1.0, 03-Feb-2018) [24].

The huge disproportion between the amount of gold produced by the country and the amount of metallic mercury used to produce it reflect the poor management practices associated with metallic mercury used in ASGM by the miners, the lack of control by the environmental authorities, and the difficulties in enforcing the laws and regulations by the police authorities to control the use of this pollutant. Figure 6-4 shows the destruction of natural ecosystems in the states of Chocó and Antioquia (Figure 6-4a, 4b, and 4c), and a

water intake structure in the Ayapel Swamp (Córdoba) (Figure 6-4d), where high mercury concentrations have been detected [95].

Figure 6-4. The destruction of natural ecosystems is one of the main consequences of illegal mining in Colombia: a) Illegal dredging operation in Quito River (Chocó) spotted in June 2017, b) Illegal mining in Quito River has changed the course of the river and affected fishing and agriculture activities, c) Similar consequences can be seen in many states of Colombia as it is the case of El Bagre (Antioquia), d) Water intake for the water treatment plant in Ayapel (Córdoba). Mercury concentrations higher than 400 ng/L were detected in the Ayapel Swamp during this study.

6.4 Fate of metallic mercury in rivers and aquatic ecosystems

The fate of mercury in aquatic ecosystems is influenced by the chemical form in which this metal is released, by the biochemical processes that it undergoes, and by the limnological conditions of the water body [5], [8], [10]. In aquatic ecosystems, the distribution and speciation of mercury is controlled by physical, chemical, biological, and

geological processes, which can be enhanced by anthropogenic activities [93]. Due to its high density, metallic mercury goes directly to riverbeds where downstream transport is minimal in this oxidation state [82], [83]. In riverbeds, it is possible to find mercury in its metallic form or as a gold-mercury amalgam, like in the case of sediment samples taken from the Madeira River in Brazil [181]. When mercury is oxidized, it tends to adsorb to soil and sediment particles and moves with the streams and run-off waters. Further, in aquatic systems, metallic mercury is not very stable in the presence of organic rich sediments, rapidly forming soluble mercury-organic complexes that allow it to get transported downstream in rivers and streams [2], [82].

Inorganic mercury can be transformed into methyl- or ethyl mercury, elemental mercury, or particulate-bound mercury in anoxic environments [94]. When metallic mercury is at equilibrium in a simple aquatic system, undissociated mercury $Hg^{o}(aq)$ is the predominant species in solution but it is practically insoluble unless there is dissolved organic matter (DOM) present [10]. In fact, organic matter-mercury complexes are the most stable species found in natural ecosystems[182]. Mercury is also eventually removed from both freshwater and saltwater by natural processes such as deep burial in sediments, and photochemical reduction followed by re-emission to the atmosphere[18].

The fact that mercury in its oxidized form (Hg(II)) is more soluble and reactive than other mercury species implies that metallic mercury needs to be oxidized to form organic species such as methyl- and ethyl-mercury [82]. The most abundant complexes formed by mercuric mercury (Hg(II)) in aquatic environments are hydroxo-complexes in freshwater ecosystems, and chloro-complexes in marine ecosystems. Regarding inorganic ligands in natural organic matter (NOM), the hydroxyl group (OH-) is usually the dominant one; and for organic ligands, the thiol groups (–SH) are perhaps the most important species to be accounted for, especially in reducing environments [183]. When cyanide is used in gold extraction, the formation of cyanide-mercury complexes is another species to be found in water[184].

In Zimbabwe, in an area where mining districts are located far away from river or stream beds, the presence of metal sorbing iron and aluminum laterites in soils and sediments, as well as the presence of metal-complexing organic matter, prevent the dispersion of mercury in soils and streams [185]. Nevertheless, mercury-bound particles can still reach rivers and water bodies through run-off during the rainy season. Once metallic mercury enters the environment, most of this mercury will remain in the place where it was discharged. It will accumulate in soil and sediments around the mining district [186]. Metallic mercury will also be lost to the atmosphere largely through evaporation in metallic, inorganic, or organic form in processes promoted by high temperatures, the presence of organic matter, and different nutrients already present in the ecosystem [186].

Total mercury concentration in rivers may fluctuate with the suspended solids concentration in it. Based on the fact that mercury in aquatic ecosystems is strongly bound to dissolved and particulate organic matter [97], [187] the concentration of mercury in aquatic systems is then a function of the flow, the activities occurring in the riverbed, and the nature and concentration of the dissolved organic matter (DOM). In general, in ASGM regions, sediments are the main source of mercury pollution in the water column [22], [188]. Consequently, the amount of mercury already present in bottom sediments in many mercury hotspots around the world poses a threat to the quality of water sources that are used for multiple purposes in ASGM regions [22].

6.5 Main challenges to reduce the use of mercury in ASGM regions: Study of the Colombian case

The singularities observed in the gold mining industry in Colombia make this country a good case scenario to analyze some of the barriers to reduce or eliminate the use of mercury in gold mining and to avoid the degradation on natural ecosystems as a

consequence of mining activities. The long tradition of illegal and informal mining, the increasing number of miners whose livelihood depend on this activity, the large number of municipalities and states where illegal mining is practiced, the illegal trade of mercury, the remote location of many mining sites, the difficulties to legalize this practice, and the involvement of illegal armed groups are some of the challenges faced by the Colombian government to control the use of mercury in ASGM.

6.5.1 The presence of illegal armed groups and organized crime in ASGM regions and its involvement in the gold production

Despite the efforts made by former Colombian president, Juan Manuel Santos, to reduce the epidemic violence that has been engulfing the country during the last 50 years, the involvement of mafia and illegal armed groups in the already illegal extraction of gold has hampered the attempts of the Colombian government to control illegal and informal mining activities. Nevertheless, This activity places Colombia in the top 20 gold producing countries in the world.

A major complication in the effort to control illegal or informal activities in Colombia, such as gold mining or even coca crops, is that, for several decades, the country has been in the grip of a devastating internal armed conflict that exceeded the response capacity of the State. During this time, the Colombian state was not able to protect their own citizens, particularly in rural areas dominated by illegal armed groups, let alone control the Colombian territory. Besides fighting against leftist rebels, the Colombian armed conflict grew as more actors entered the scene including right-wing paramilitary groups, drug cartels, and corrupt governmental and military officials. Years of conflicts left extensive areas of the Colombian territory unattended by the State. Even

today, many areas are under the control of mafias and illegal armed groups, which are also expanding toward territories once occupied by the Farc rebels.

Nevertheless, in the last years, the Colombian army and the national police have carried out important military operations against illegal gold miners in remote areas of the country. The Colombian air force also supports the fight against illegal mining activities either by using drones or though military overflights in conflictive ASGM regions. Figure 6-5 shows some of the actions taken by the military and national police force to fight illegal miners in Colombia.

Figure 6-5. Colombian National Security Forces fighting illegal mining activities around the country: a) Dredges destroyed in Rio Quito (Chocó), b) Illegal miners caught by the Colombia National Police in Cordoba, c) The confiscation of mining equipment and machinery is done along the country, d) Colombian Air Force supports military operations against illegal mining. Source: Websites from Policía Nacional De Colombia[189] and Fuerzas Militares de Colombia[190].

The military operations carried out by the Colombia Military Forces has exposed the presence of foreigners involved in illegal activities in the country. Citizens from Peru, Venezuela, and Brazil have been seized in illegal gold mining districts by the Colombia authorities. The porous border between Colombia and neighbor countries makes it easy for illegal migrants to cross the border, and for mafias to smuggle arms, machinery, illicit drugs, and metallic mercury. Small-scale miners can also be victims of human trafficking and often are seen as criminals, rather than as the victims they are [166].

In 2017, Colombia's ranking fell two positions (from 16 to 18) in the top 20 Gold Mining Rank. Colombian gold output fell 11.4% in 2017 [165]; and based on data from the Unidad de Planeación Minero Energética (Figure 6-2), the country's gold production

fell from 62.5 tons (2016) to 42.5 tons (2017), which represents a 32% decrease in the annual gold production [174]. The reasons for this drop could be explained by two factors. First, coca crops in Colombia, particularly in conflictive areas and/or ASGM regions, increased dramatically in the past year, reaching a historic record of 71,000 ha, a 17% increase compared to 2016 [191]. Second, the continuous blows to illegal gold mining activities and the destruction of machinery and seizure of illegal mines seem to play a role in the reduction of the gold production [165].

The increase in coca crops suggests that inhabitants from rural areas switched from traditional productive crops and illegal gold mining to coca crops despite the more than $10 billion spent in the last two decades to fight illegal drugs in the country [192]. This increase in coca production has been attributed to multiple factors[193]: the reestablishment of drug mafias in areas formerly controlled by the Farc, the leftist-guerilla group that negotiated a peace agreement with the Colombian government in 2016; the low levels of eradication of illegal crops, the increasing seizure of cocaine by the Colombian authorities, and the failures in programs intended to replace illegal crops.

6.5.2 The illegal trade of metallic mercury in the light of the Minamata Convention

The Minamata Convention on Mercury, a legally-binding treaty aiming to protect human health and the environment, became effective on August 16, 2017. So far, 128 of the 193 United Nations member countries have signed this initiative. This agreement requires that participating countries take a number of measurements to reduce or eliminate the use and release of mercury from ASGM, to control air mercury emissions in industrial activities, to reduce the use of elemental mercury in mass consumption goods such as batteries, cosmetics, and lights; as well in manufacturing processes such as chlor-alkali production, to address the supply and trade of mercury, and to develop strategies to

remediate mercury-contaminated sites [194]. After signed it, this convention has been ratified by 101 of the 128 participant countries, including several where ASGM is practiced such as Brazil, China, Ecuador, Ghana, Peru, Bolivia, and Colombia.

Today, many mercury-free techniques for gold mining which are safer for miners and for the environment are available. Gravimetric concentration methods such as panning, sluicing, shaking tables, spiral concentrators, vortex concentrators, and centrifuges, have shown to be an alternative for miners in ASGM regions [195]. Nevertheless, the socio-economic conditions, the need for easy money, the easy accessibility to metallic mercury, and the lower efficiencies compared to Hg based processes seems to be the main barriers for miners to adopt better practices [5], [82]. Some of the countries impacted by ASGM created new regulations to control the use of metallic mercury in industrial activities. In Brazil, the decree 97.507 prohibits the use of mercury and cyanide in ASGM, except when its use is authorized by a competent environmental organization. In Colombia, Law1658/2013 was issued to control the use and merchandising of mercury in industrial and mining activities. This law will be fully implemented by 2018 for the mining sector. In Ecuador, the mining laws prohibit the use of mercury in ASGM (Ley de Minería) and restrict the use and distribution of metallic mercury in the country (environmental regulation N. 003, Official Registry No. 909, March, 21th, 2013). And, in Peru, a multisectoral action plan was approved to implement the Minamata Convention on Mercury (decree No. 010-2016-MINAM).

Despite these governmental efforts to reduce the use of mercury in ASGM, the historical use of mercury in illegal mining is expected to continue due to the creation of a black market that will supply the mercury needed in illegal mining, at least for a few decades until local governments take full control of the chain supply of this metal. Bypassing the mercury controls has proven to be easy in Latin America. For instance, in Ecuador, artisanal miners still use mercury despite its prohibition. Most of them use this metal in their own houses to evade the control of the authorities. Local miners use a

secret network to buy mercury from smugglers [196]. In Colombia, the smuggling of mercury is expected to increase, as well as its cost. Approximately, 272 kg of mercury, valued at more than $70,000, were seized by the local police in Antioquia in May 2018 [197]. Some of the mercury smuggled to the country enters across the Colombia-Ecuador border. The amount of mercury smuggled may surpass 50 ton per year [198]. In Brazil, it was reported that 99.3% of artisanal miners use mercury and cyanide without legal authorization [199]. Illegal mercury trade has also been reported in West Africa, the Philippines, Malaysia, and Indonesia [27].

The main strategies for the illegal and undocumented mercury trade seem to involve hiding mercury among other goods, mislabeling the containers that transport mercury, and shipping high quality mercury as cheap product, among others [27]. This illegal trade of mercury is one of the main challenges faced by developing countries affected by illegal mining activities in the implementation of the Minamata Convention [27].

6.5.3 The arduous task to formalize and legalize illegal/informal miners

In 2017, the annual gold production decreased globally, mainly in countries with a long tradition of ASGM such as China (6.0% drop), Peru (3.7%), Indonesia (11.8%), Brazil (4.9%), and Colombia (11.4%) [165]. The reasons for these drops are believed to be the tightening of environmental regulations and the pressure of local governments on illegal gold mining. Although the definition of ASGM includes both informal and illegal miners, a legal differentiation is necessary to avoid the criminalization of informal miners. Informal or artisanal gold mining has been a sustainable activity practiced by many communities worldwide. In those communities, villagers use ancestral traditions to

extract gold from rivers, streams, and soils manually, using pans, trays, or nonmechanical equipment.

An informal miner is one who is working outside of the law but has the option to become legal through appropriate mechanisms to formalize his/her practice [200]. In contrast, an illegal miner is one whose mining practice is impossible to legalize either because it is associated with criminal groups or operates in prohibited areas [200]. Consequently, informal mining operates without mining rights and environmental licenses. Under this scenario, miners lack social protection and occupational health and safety training [172]. In contrast, formal mining, besides meeting mining, environmental, and labor regulations, pays royalty revenues and taxes [172].

Data from 2013 estimated that 10 to 15 million miners work in ASGM in Africa, Asia, and South America [5]. A report from 2016 estimated the numbers of miners working in illegal mining in some countries from Latin America [167]: Peru (~100,000 miners), Brazil (~75,000 in the Brazilian Amazon basin), Colombia (~50,000), Ecuador (~10,000), Bolivia (~45,000), and Venezuela (~4,000 in the border with Colombia and Brazil).

In Colombia, the term 'mining production unit' (abbreviate UPM in Spanish) refers to "a set of tasks, with facilities, operations and/or equipment, that make up an economic and administrative infrastructure, aimed to the exploitation of minerals."[201] Out of the 14,357 mining production units identified by the government during the 2010-2011 census, it was found that only 37% own a mining right (or mining title)[202]. Out of the 4,133 mining production units dedicated to gold exploitation in 16 states of the country, only 550 (13.3%) own a mining title and 899 (21.8%) pay royalty revenues [202].

The Colombian government has tried multiple times, without success, to legalize informal and illegal miners. Some of the laws created to accomplish these goals are Law 141/1994 (decree 2636), Law 685/2001, Law 1382/2010, Law 1685/2013, and Law

1753/2015. Such laws allow mechanisms to apply for a mining title, to get concession rights contract, to delineate areas for mining operation, and to request the legalization of mining production units (UPMs), among others. The framework for the legalization process for the worst-case scenario, a UPM without mining rights, is described in Figure 6-6. The process starts with a dialogue between the government and informal miners and ends with either the legalization of UPMs, or miners moving to a different industrial activity, or with the closure of the UPMs.

Among the benefits to regulate informal miners are the reduction of the environmental impacts on natural ecosystems, the protection of water sources used for drinking water, recreation, fishing or agricultural purposes, the reduction of deforested areas, the protection of the biodiversity, the minimization of the mercury used, and the control of the criminal activities surrounding this practice.

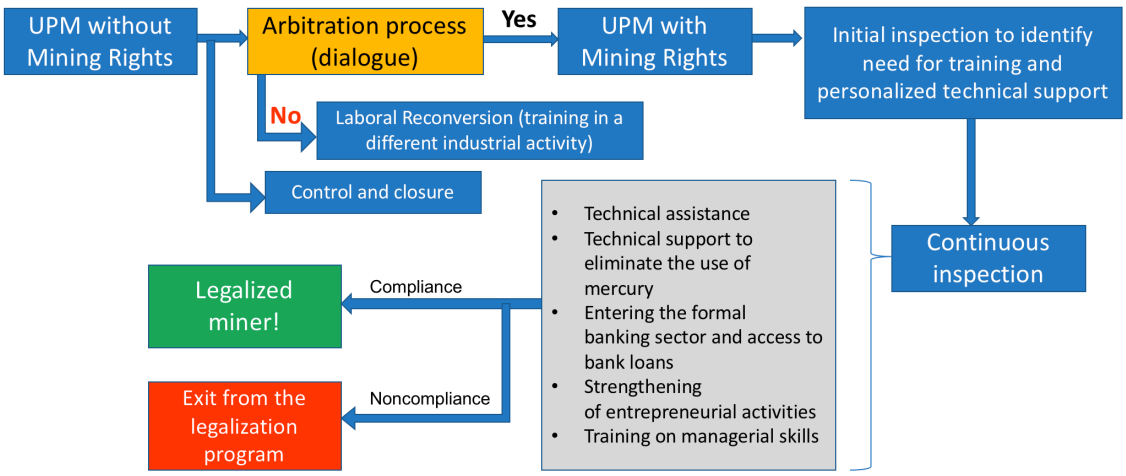

Figure 6-6. Framework for the legalization process of a Mining Production Unit in Colombia that lacks of mining rights. Source: Ministerio de Minas y Energía de Colombia [203]

According to the Colombian National Miners Confederation (abbreviated Conmineros in Spanish), which brought together around 250,000 miners from different activities and 18 states, the main barriers faced by miners to formalize their practice are

the excessive bureaucracy, the lack of information, the absence of sufficient economical, technical, and legal support provided by the government, and the preferential treatment to multinationals and large-mining companies, which compete for the mining lands and which benefit from legislation that allow them to get mining rights in a short period of time.

ASGM is the main source of anthropogenic mercury emissions to the environment [5]. To comply with the Minamata Convention, governments need to implement National Action Plans (NAPs) to reduce or eliminate the use of mercury in their territories. The implementation of this plan seems to be a daunting challenge in ASGM regions given the many external factors surrounding the production of gold in those regions, such as the involvement of illegal armed groups, the geographical locations where illegal miners operates, and the illegal trade of mercury. However, the most important challenge comes from the recognition that between 10 and 15 millions miners worldwide are employed by this activity and around 100 million people depend on it [5], [204].

6.5.4 The lack of funding for environmental protection in the face of more urgent needs

The protection of human health, wildlife, and natural environments demands a large amount of financial, technological, and human resources that are only affordable to developed countries. In the U.S., the Comprehensive Environmental Response, Compensation, and Liability Act (CERCLA), commonly known as Superfund, was created for "cleaning up abandoned or uncontrolled contaminated sites that affect human health and the environment."[205] This program is managed by the U.S. Environmental Protection Agency (EPA) which actual and estimated budget is shown in Figure 6-7a. By 2013, 1,158 contaminated sites were identified and listed in the U.S., and it was estimated that approximately 39 million people (13% of the U.S. population) live within 3 miles of

some of the listed sites [206]. Despite the interest of the U.S. government to identify and remediate polluted sites, in the last decades, the annual appropriations to EPA's Superfund program have been reduced from ~$2 billion to $1.1 billion [206]. The number of contaminated sites included in the Superfund's program decreased as well [207], as can be seen in Figure 6-7b.

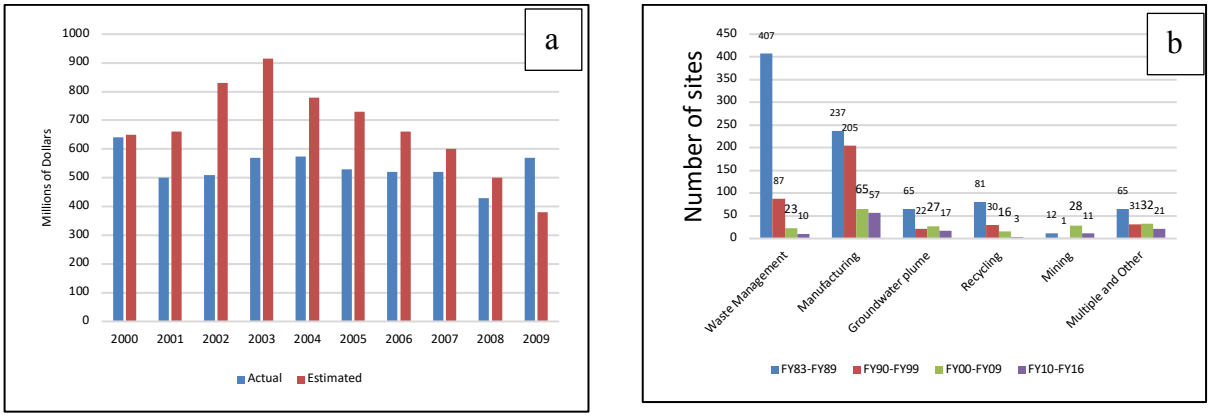

Figure 6-7. (a) Actual and expected estimated expenditures of the EPA Superfund's program and (b) number of sites added to the Superfund's list by type. Adapted from: Probst, Superfund 2017 Cleanup Accomplishments and the Challenges Ahead [207]

In Canada, a Federal Contaminated Sites Action Plan (FCSAP) was created to help provinces manage contaminated sites under their jurisdiction. This action plan started in 2005 and will run until 2020. It was estimated that, as March of 2013, the remaining environmental liability associated with federal contaminated sites was approximately $10.6 billion [208]. A total of 24,990 contaminated sites were listed at that time, which include open, closed, and deleted sites [208].

Both the U.S. and Canada apply the polluter pays principle to force corporations, private companies, and individuals to provide financial compensation for environmental damage. The polluter pays principle is more difficult to apply in ASGM regions. Polluters are usually poor families or communities that use illegal gold mining as their primary source of income. In other cases, the polluters are criminal organizations whose leaders

are not easy to identify and are much less interested in paying compensation for destroying the environment.

In Colombia, the lack of funding to protect the environment and to enforce regulations on the use of mercury in ASGM is critical. After the peace agreement between the government and the Revolutionary Armed Forces of Colombia (Farc), it was determined that Colombia needed approximately $31 billion to finance post-conflict programs during a 10-year period [209]. Such programs are designed to finance projects related to rural development, agrarian jurisdiction, local governance, and rural property registration. No major emphasis was done to restore the damage caused to the environment by the over 50-years of armed conflict that include terrorist attacks that caused oil-spills, deforestation, illegal mining, and fauna trafficking, among others. Consequently, appropriation of funds to protect the environment, to enforce regulations aimed to prevent the use of metallic mercury in illegal mining, and to remediate ecosystems affected by ASGM seems unlikely in the short term.

6.6 A Needed task: The evaluation of the impact of ASGM in natural ecosystems and the degree of impairment associated with mercury pollution

Mercury from ASGM can reach soil and water bodies in many ways: during the amalgamation process and amalgam burning or purification, when mercury is spilled during mining operations, and when it is leached from inadequate tailings ponds. The latter is possible when gold is extracted from soil and rocks [83]–[85]. About 800 tons of mercury are released annually to surface water through the “weathering of mercury-bearing minerals in igneous rocks”[13] and nearly two hundred and sixty tons of this element were released to rivers in 2010 through extensive erosion caused by deforestation [5]. Additionally, it was estimated that rivers transport approximately 2,800 tons of

mercury every year from which about 380 tons reach offshore;[18] therefore, considering these figures, a higher risk of water pollution is more likely in countries where the amount of mercury discharged by ASGM surpasses the amount released by natural sources.

Despite the extended mercury pollution affecting natural ecosystems in developing countries, most of the mercury regulations in water are intended to protect human health, which is expected, but less effort seems to be done to protect aquatic organisms and wildlife. For instance, in Colombia, the maximum contaminant level (MCL) for mercury in water sources intended to be used as drinking water supplies was set at 2.0 µg/L while the MCL to preserve flora and fauna was set at 10 µg/L. Additionally, despite the critical situation caused by the use of metallic mercury in illegal gold mining, no major actions have been taken to amend environmental legislation and to assess the impact of ASGM on the environment and human health. The creation of a mechanism to identify polluted water bodies when they fail one or more water quality standards is needed. Similar situations occur in other countries such as Bolivia, Brazil, and Peru. Table 6-2 shows mercury regulations form different countries based on the type of water and its intended use. Peru created standards for mercury in water used in fish farming, and the U.S. and Canada set low mercury standards to protect aquatic life in both fresh water and marine ecosystems.

Most countries set their MCL for mercury in drinking water based on the recommendations of the World Health Organization (WHO). In the past, the WHO set the MCL for mercury at 1.0 µg/L as total mercury (inorganic + organic). However, in 2006 the WHO changed this guideline to 6.0 µg/L as inorganic mercury [28] because the presence of organic mercury species (i.e., methyl- and ethyl-mercury) is unlikely in drinking water compared to inorganic mercury, which is the most common form of mercury found in drinking-water [28], [34].

In countries affected by ASGM, a mechanism is needed to identify polluted waters, impaired water bodies that fail water quality standards, or pristine waters that need protection. Water bodies such as lakes, rivers, streams, and wetlands polluted with mercury or any other contaminant may not be suitable for drinking water, recreation, fishing, or agricultural purposes, nor to be used in fish or mollusks farming

Table 6-2. Reference standards and guidelines for ambient levels of mercury in different countries

	Drinking Water (µg/L)	Water bodies used for drinking water treatment (µg/L)	Livestock uses (µg/L)	Fish Farming (µg/L)	Surface Water (µg/L)	Irrigation (µg/L)	Aquatic Life freshwater (µg/L)	Aquatic Life marine (µg/L)	Ref.
Bolivia	1.0	-	-	-	< 0.005	2.0	-	-	[210]
Brazil	1.0	-	10.0	-	1.0 (Recreation)	2.0	-	-	[210]
Colombia	1.0	2.0	10.0		-	-	10.0	10.0	[210] Dec. 1584/94
Peru	1.0	1.0 – 2.0	10.0	0.10 – 1.8	1.0 (Recreation) 0.10 (Swamps, Lakes, Rivers, and Marine water)	1.0	-	-	[211]
WHO	6.0 as IHg								[212]
European Union (EU)	1.0	0.5 – 1.0	-	-	-	2.0 (Germany)			[210]
U.S.	2.0	-	-	-	0.19 (freshwater) 0.14 (Marine water)		1.4 (acute) 0.77 (chronic)	1.8 (acute) 0.94 (chronic)	[213]
Canada	1.0		3.0			-	0.026 (Inorganic) 0.004 (Organic)	0.016 (Inorganic)	[214]

The mechanism to identify, listing, and restoring impaired water bodies can follow similar guidelines to the one included in the 1972 U.S. Clean Water Act (CWA), section 303(d) [215], managed by the U.S. EPA, together with the Protocols for Environmental and Health Assessment of Mercury Released by Artisanal and Small-Scale Gold Miners, designed by the Global Mercury Project (GMP)[82]. In this protocol, *mining hotspots* were defined as sites with high concentrations of metallic mercury, while *environmental hotspots* were defined as sites where mercury is already present as a toxic species, such as MeHg [82]. A framework for the mechanisms of identification and listing of impaired water bodies is presented in Figure 6-8.

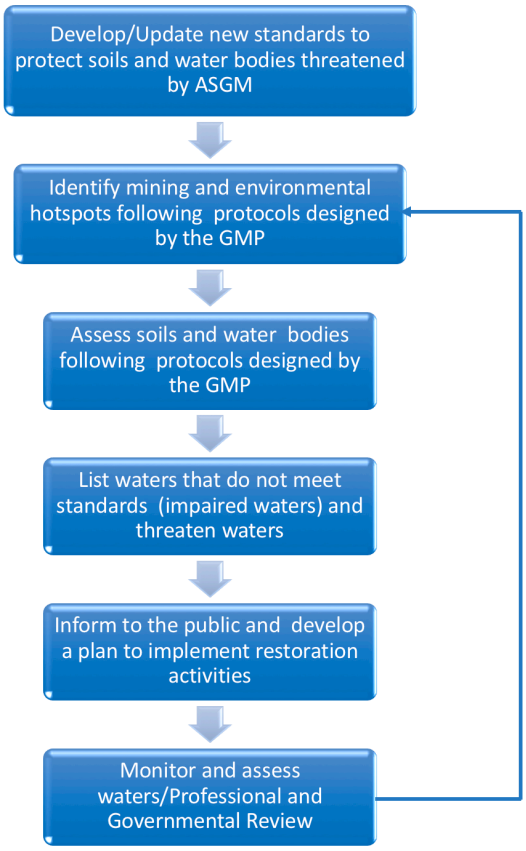

Figure 6-8. General framework of the mechanism needed to identify, list, and restore soils and water bodies affected by ASGM activities following the guidelines provided in section 303(d) of the Clean Water Act (U.S.) and the protocols designed by the Global Mercury Project (GMP).

6.7 Concluding remarks

The consequences of the gold rush in previous centuries, and the lack of control and environmental responsibility regarding the use of mercury in the gold mining industry, have created mercury hotspots around the world, mainly in soils and rivers in developing countries. The enrichment of mercury in soils and water bodies from the continuous release of mercury during gold mining has also created environmental and public health issues due to the use of these now contaminated lands for agriculture and livestock, and the pollution of water bodies used for fishing, consumption, and recreation.

In the light of the Minamata Convention on Mercury, participant countries can reduce risks by implementing National Actions Plans (NAPs) to minimize or eliminate the use of mercury in their territories. The Minamata Convention does not ban the use of mercury in ASGM but aims to reduce or eliminate its use. Consequently, participant governments are the ones called to create new legislation to prohibit mercury in mining activities and to enforce the law. For instance, the Colombian government published an ambitious plan in 2014 (Plan Nacional Nacional de Mercurio), aiming to reduce/eliminate the use of mercury in the mining sector by 2018 and in other industrial activities by 2023. This plan includes four programs to address the issue of mercury from different perspectives: (1) program for institutional strengthening, (2) program for social, technological, and environmental management, (3) educational and communication program, and a (4) research program on environmental, health, and technological innovations.

Nevertheless, implementing these NAPs in ASGM regions is challenging. The remote locations of many illegal mines, the illegal trade of mercury, the involvement of mafias and illegal armed groups in the gold industry, the difficulties in the legalization of illegal miners, and the lack of funding to enforce environmental regulations are the main barriers for a successful reduction of metallic mercury in ASGM. All the same, any

successful plan needs to count on the commitment of miners to use free-mercury alternatives and eliminate the use of mercury from their mining practice.

Mitigation and remediation techniques are available to treat mercury pollution in soil, wastes, and sediments (i.e., capping and dredging, immobilization, electro-remediation, thermal desorption, phyto/bioremediation, solidification/stabilization, soil washing and acid extraction, etc.) and technologies to remove low levels of mercury in drinking water systems already exist (i.e., membrane filtration, ion exchange, adsorption treatments, precipitation/coprecipitation, etc.).

However, the main goal should be to eliminate the use of mercury in mining activities. This will require nations to implement the strategies developed by the United Nations Environment Programme (UNEP) as well as other tailored strategies based on the individual needs of each country. The effects of mercury pollution in the environment are estimated to last for decades. Governments may need decades to create and consolidate programs that eliminate the use of this pollutant from mining activities. Educating future generations in ASGM regions and providing them with alternatives to make a living can prevent the pollution of their territory.

CHAPTER 7. CONCLUSIONS

The goals of this study were (1) to evaluate the removal of dissolved organic carbon (DOC) by alum coagulation as a function of the aromatic carbon content in natural organic matters (NOMs) from different sources containing a range of reduced sulfur content, (2) evaluate the influence of the composition and character of dissolved organic matter (DOM) on the removal of mercury in metal-based coagulation systems at optimal coagulation conditions of pH and coagulant dose, at low and high mercury/DOM ratios, and (3) analyze the interactions between mercury and reactive functional groups in dissolved organic matter through statistical analysis, equilibrium dialysis ligand exchange (EDLE), fluorescence spectroscopy and jar tests with and without a modified NOM.

7.1 Removal of dissolved organic carbon (DOC) by alum coagulation as a function of the aromatic content

The overall goal of this research was to assess the removal of Hg(II) during alum coagulation. Data suggest that the removal of Hg(II) onto aluminum hydroxide solids formed during alum coagulation is minimal in the absence of DOM. Complexation of Hg(II) to the DOM followed by adsorption of DOM is the primary mechanism for Hg(II) removal during alum coagulation. Thus, the study of Hg(II) removal during alum coagulation will be dependent on the extent of Hg(II) binding as well as the extent of DOM adsorption to the aluminum hydroxide precipitates. The aromaticity of dissolved organic matter (DOM) plays a major role in the removal of carbon from drinking water treatment as was verified in this study with the use of DOM isolates selected for this research. However, binding of Hg(II) is typically expected to be dominated by reduced sulfur ligands present in the hydrophobic portion of DOM. Therefore, the selection of DOMs for this research relied heavily on the availability of DOMs with measured reduced sulfur content as well as measured aromaticity. The first set of studies conducted

in this research were aimed at verifying that typical trends in removal of DOM were applicable to the selected NOMs.

While $SUVA_{254}$ (defined as the UV absorbance at 254 nm of a water sample divided by the concentration of dissolved organic carbon) is a good predictor of the aromaticity of DOM samples in untreated water, changes in $SUVA_{254}$ values would also have the potential to predict the most likely fraction of DOM removed from solution, as well as the most likely carbon composition remaining in the treated water. DOM isolates rich in aromatic content like Suwannee River Humic Acids (SRHA) and Nordic Aquatic Humic Acids (NAHA) with $SUVA_{254}$ values of 6.0 L/mgC-m and 6.5 L/mgC-m, respectively, were the samples that provided the greatest removal of carbon from solution (~84% in both cases), but are also the samples with the highest residual $SUVA_{254}$ in solution. Pony Lake Fulvic Acid, the organic isolate with the least aromatic carbon and a $SUVA_{254}$ value of 2.46 L/mgC-m, provided the lowest removal of carbon (46%) among the NOMs tested, and its residual $SUVA_{254}$ suggests that a good portion of hydrophilic carbon still remains in solution after alum coagulation. The trends for removal of NOM were indeed consistent with previous research and the NOMs selected for further study provided a range of reduced sulfur content.

7.2 Influence of the character and composition of dissolved organic matter (DOM) on the removal of Hg(II) in metal-based coagulation systems at optimal coagulation conditions of pH and coagulant dose

The goal of this study was to analyze the removal of mercury from solution under two relevant conditions for the interactions between Hg(II) and DOM in aquatic environments. First, experiments were conducted at low Hg(II) concentrations (relative to the amount of DOM added to the system), where Hg(II) ions are expected to bind to reduced sulfur functional groups (i.e., thiols), the strongest ligands for Hg(II)

complexation. Second, experiments were conducted under conditions which both sulfur and carboxylic acids were responsible for Hg(II) complexation; the carboxylic ligands are weaker but more abundant than the reduced sulfur ligands. While Hg(II) binding ligands in DOM play an important role in the distribution, toxicity, and fate of mercury in aquatic environments, their role in the removal of Hg(II) during alum coagulation systems is dependent on the ability of the fraction of DOM containing these ligands to adsorb to the aluminum hydroxide flocs. Thus, the aromaticity of the DOM and the presence of Hg(II)-binding ligands in the fraction of carbon that adsorbs to aluminum hydroxide flocs are the key variables that control removal.

As was determined in this research, at low Hg/DOM ratios, high Hg(II) removal (>90%) can be achieved by alum coagulation in two circumstances: (1) when the DOM is low in reduced sulfur ligands but rich in aromatic content (as was the case for SRHA and NAHA) and (2) when the DOM is rich in S_{red} ligands (i.e., when S_{red}/Hg(II) >> 1) and low in aromatic content (as was true for PLFA). In both cases, the adsorption of the aromatic carbon onto alum flocs is responsible for the removal of mercury from solution because essentially all of the Hg(II) in the water is complexed to DOM. The interaction of high levels of mercury with organic isolates with low reduced sulfur content DOM and intermediate aromaticity will yield poorer removal of mercury, as was the case for the SRFA sample. At high Hg/DOM ratios, good mercury removal (60-70%) are also possible under the two circumstances stated above

In summary, not only does the character of DOM determine the extent of the removal of carbon, it also determines the minimum removal of Hg(II) in alum-based coagulation systems. This is, the removal of mercury is controlled by the removal of carbon because Hg(II) ions will form complexes with the reactive Hg-binding ligands (i.e., S_{red} and COOH) present in the portion of DOM that is removed from solution. Additionally, S_{red} controls Hg(II) removal in water treatment only when the ratio S_{red}/Hg(II) >> 1 regardless the aromaticity.

It is worth mentioning that the chemical structure of the S_{red} ligands in DOM suggests that not all of the reduced sulfur species are suitable for Hg(II) complexation. Previous research indicated thiols (-SH) are the most likely ligands readily available for Hg(II) complexation in DOM samples [35], [37].

Evidence of the incorporation of Hg-DOM complexes onto the surface of alum flocs was observed using X-ray photoelectron spectroscopy (XPS) and Time of Flight Secondary Ion Mass Spectrometer (ToF-SIMS). Although the goal was to visualize the interactions between Hg(II) and S_{red} ligands using these techniques, reduced sulfur represented only a tiny fraction of the total composition of DOM, and high mercury doses would be required to detect this metal with the techniques used.

7.3 Analysis of the interactions between Hg(II) and reactive functional groups in dissolved organic matter through statistical analysis, equilibrium dialysis ligand exchange (EDLE), fluorescence spectroscopy, and jar test with and without a modified NOM

An alternative analysis for the interactions between Hg(II) and natural organic matter (NOM) seemed possible by using NOM samples without carboxylic ligands in their structure. A method to produce this type of NOM was an esterification process in which the carboxylic ligands are converted to esters in the presence of alcohol and EEDQ, a peptide coupling agent. This process, discovered by Zacharie et al. [141], was carried out in this work, and the modified-NOM was employed in alum coagulation jar tests. The results were compared to the results with the non-esterified NOMs.

Results from the esterification of the Suwanee River Fulvic Acid (SRFA) showed that the carbon distribution of this organic isolate changed dramatically after the process. For instance, ^{13}C-NMR results show that the signal for carbon structures in the chemical shift ranges δ_C=60-160 ppm are missing in the esterified sample. The $SUVA_{254}$ of the

esterified-SRFA was much lower (2.8 L/mgC-m) compared to the SUVA of the non-esterified SRFA (4.5 L/mgC-m). An additional NOM sample was also esterified (SRHA) and a similar decrease in SUVA value was observed with the esterified-SRHA NOM (from 6.0 L/mgC-m to 2.1 L/mgC-m).

Jar test experiments performed to compare the removal efficiency of mercury with and without esterified-NOMs indicated that both of the esterified NOMs lost some of its capacity to remove Hg(II) from solution, as suggested by the reduction of the Hg(II) removed/carbon-added ratio. The lower $SUVA_{254}$ values of the esterified NOMs are the reason why lower removal of carbon was obtained during jar tests. As a consequence, the comparison between esterified and non-esterified NOMs is hindered by the fact that the removal of Hg depends on the removal of carbon as well on its interaction with reactive ligands in the DOM portion that adsorbs onto alum flocs. In summary, the esterification process altered the capacity of the DOM to remove Hg, but the extent of the esterification was not quantifiable.

Experiments at extremely high mercury concentration aiming to analyze the role of carboxylic ligands in DOM suggest that all Hg(II) ions in solution bind to carboxylic ligands, either in the fraction of DOM that adsorbed onto $Al(OH)_3$ precipitates or in the fraction of DOM that remains in solution. As a consequence, the removal efficiency of mercury tends to remain constant regardless of the dose of Hg(II) added as it is solely dependent on the removal of carbon from solution.

Finally, when comparing Hg-DOM equilibrium constants ($K_{DOM'}$) estimated with the modified Stern–Volmer model versus the ones obtained with the EDLE method, it is possible to ¨isolate¨ the effect of S_{red} ligands and focus on carboxylic ligand binding. This difference may be seen as a limitation of this technique but was helpful for this work. The low $K_{DOM'}$ values obtained with the modified Stern–Volmer model provide insight into the binding strength of the NOMs after saturation of the reduced sulfur ligands and suggest that Hg(II) is bound to weak functional groups (carboxylic acids) under high

Hg(II) concentration conditions. These results support the hypothesis that, even at these high Hg(II) to DOM ratios, Hg(II) complexes within DOM still dominate Hg(II) speciation.

7.4 Challenges to reduce metallic mercury in ASGM in the light of the Minamata Convention

An additional chapter presented in this dissertation discussed the challenges to eliminate or reduce the use of metallic mercury in countries affected by illegal mining. Despite the implementation of the Minamata Convention in 2017 and the fact that the use of metallic mercury in ASGM was already prohibited in many countries, a decrease in the use of mercury seems unlikely in the long term, mainly because (1) criminal groups are profiting from gold mining activities; (2) illegal trade of mercury is already taking place in many ASGM countries like Colombia, Brazil, Perú, The Philippines, and Indonesia; (3) the colossal task required to formalize/legalize illegal miners and persuade them to use a more environmentally friendly alternatives; and finally (4) the lack of interest or capacity of governments to control the use of mercury in the gold mining industry, an activity that in the long term benefits the economy of the country, as more gold is produced and exported regardless of its origin. In any case, the negative impacts of ASGM on the environment and the people living in ASGM regions will continue for years. Consequently, governments may need decades to consolidate programs that eliminate the use of this pollutant from ASGM.

7.5 Future Work

Future work should focus initially on employing EXAFS and other sensitive surface techniques that identify the Hg-S interaction and the Hg(II) distribution between aluminum hydroxide flocs and water. Despite the many advantages provided by

fluorescence spectroscopy techniques for studying NOM from different environments, the ability to identify the interactions between Hg(II) and NOM at very low Hg/DOM ratios, a common situation in aquatic environments, is still limited. A more sensitive response for this technique will allow determination of Hg(II)-binding constants faster and more reliably compared to the existing techniques.

Although the results obtained with the esterified NOMs suggested a loss of its complexing capacity, a detailed characterization of this modified NOM is needed to determine what major changes affected the NOM structure beyond simply reducing the carboxylic content and the effects of adding or producing other aromatic compounds.

REFERENCES

[1] M. S. Bank, *Mercury in the environment: pattern and process*, 1st ed. Univ of California Press, 2012.

[2] J. Meech, M. Veiga, and D. Tromans, "Emission and stability of mercury in the Amazon," *Can Metall Q*, vol. 36, no. 4, pp. 231–239, Oct. 1997.

[3] N. Veiga, M. M., Meech, J. A., & Oñate, "Mercury pollution from deforestation," *Nature*, vol. 368, no. 6474, pp. 816–817, 1994.

[4] M. Roulet, M., Lucotte, M., Farella, N., Serique, G., Coelho, H., Passos, C. S., ... & Amorim, "Effects of recent human colonization on the presence of mercury in Amazonian ecosystems," *Water Air Soil Pollut*, vol. 112, no. 3–4, pp. 297–313, 1999.

[5] G. Kirby, A., Rucevska, I., Yemelin, V., Cooke, C., Simonett, O., Novikov, V. & Hughes, "Mercury–Time to Act," Aug. 2013.

[6] AMAP/UNEP, "Technical Background Report for the Global Mercury Assessment 2013," Oslo, Norway, 2013.

[7] M. Roulet, M., Lucotte, M., Canuel, R., Rheault, I., Tran, S., De Freitos Gog, Y. G., ... & Amorim, "Distribution and partition of total mercury in waters of the Tapajós River Basin, Brazilian Amazon," *Sci Total Environ*, vol. 213, no. 1, pp. 203–211, 1998.

[8] E. Diaz, "Mercury Pollution at Gold Mining Sites in the Amazon Environment," *Princ Environ Toxicol*, no. November, 2000.

[9] a H. Fostier, M. C. Forti, J. R. Guimarães, a J. Melfi, R. Boulet, C. M. Espirito Santo, and F. J. Krug, "Mercury fluxes in a natural forested Amazonian catchment (Serra do Navio, Amapá State, Brazil)," *Sci Total Environ*, vol. 260, no. 1–3, pp. 201–11, Oct. 2000.

[10] D. Meech, J. A., Veiga, M. M., & Tromans, "Reactivity of mercury from gold mining activities in darkwater ecosystems," *Ambio*, vol. 27, no. 2, pp. 92–98, 1998.

[11] L. Maurice-Bourgoin, I. Quiroga, J. Chincheros, and P. Courau, "Mercury distribution in waters and fishes of the upper Madeira rivers and mercury exposure in riparian Amazonian populations.," *Sci Total Environ*, vol. 260, no. 1–3, pp. 73–86, Oct. 2000.

[12] C. H. Gammons, D. G. Slotton, B. Gerbrandt, W. Weight, C. a Young, R. L. McNearny, E. Cámac, R. Calderón, and H. Tapia, "Mercury concentrations of fish, river water, and sediment in the Río Ramis-Lake Titicaca watershed, Peru.," *Sci Total Environ*, vol. 368, no. 2–3, pp. 637–48, Sep. 2006.

[13] M. J. Mangal, "Assessing mercury contamination in the Amazon Basin," 2001.

[14] R. Malm, O., Pfeiffer, W. C., Souza, C. M., & Reuther, "Mercury pollution due to gold mining in the Madeira River basin, Brazil.," *Ambio*, vol. 19, no. 1, pp. 11–15, 1990.

[15] W. R. Pfeiffer, W. C., Malm, O., Souza, C. M. M., Drude de Lacerda, L., Silveira, E. G., & Bastos, "Mercury in the Madeira river ecosystem, Rondonia, Brazil," *For Ecol Manage*, vol. 38, no. 3, pp. 239–245, 1991.

[16] J. A. Veiga, M. M., & Meech, "Gold mining activities in the Amazon: clean-up

techniques and remedial procedures for mercury pollution," *Ambio*, vol. 24, no. 6, pp. 371–375, 1995.
[17] W. De Lacerda, L. D., & Salomons, *Mercury from Gold and Silver Mining. A Chemical Time Bomb?* Springer, 1998.
[18] UNEP, "Global Mercury Assessment 2013: Sources, Emissions, Releases, and Environmental Transport," *UNEP Chem Brand*, vol. Geneva, Sw.
[19] UNEP CHEMICALS, "– Assessment Report – Excess Mercury Supply in Latin America and the Caribbean, 2010-2050," 2009.
[20] S. J. Spiegel and M. M. Veiga, "International guidelines on mercury management in small-scale gold mining," *J Clean Prod*, vol. 18, no. 4, pp. 375–385, Mar. 2010.
[21] F. Diaz-Arriaga, "Mercurio en la minería del oro: impacto en las fuentes hídricas destinadas para consumo humano," *Rev Salud Pública*, vol. 16, no. 6, pp. 947–957, 2014.
[22] K. Telmer, M. Costa, R. Simões Angélica, E. S. Araujo, and Y. Maurice, "The source and fate of sediment and mercury in the Tapajós River, Pará, Brazilian Amazon: Ground- and space-based evidence.," *J Environ Manage*, vol. 81, no. 2, pp. 101–13, Oct. 2006.
[23] U. Investigativa, "Así entra al país el mercurio que envenena pueblos y ríos," *El Tiempo*, Bogotá D.C., 09-Apr-2017.
[24] IDEAM, "Estudio nacional del agua 2014," Bogotá D.C., 2015.
[25] J. C. Henao and A. C. Gonzalez Espinosa, Eds., *Minería y Desarrollo. Tomo 2: Medio Ambiente y Desarrollo Sostenible*. Bogotá: U. Externado de Colombia, 2016.
[26] Artisanal Gold Council, "Mercurywatch: Mercury released from ASGM," 2009. [Online]. Available: http://www.mercurywatch.org/.
[27] U. United Nations Environment Programme, "UN Environment, 2017. Global mercury supply, trade and demand. United Nations Environment Programme, Chemicals and Health Branch," Geneva, Switzerland, 2017.
[28] World Health Organization, "Mercury in Drinking-water. Background document for development of WHO guidelines for Drinking Water Quality," Geneva, 2005.
[29] P. Holmes, K. a F. James, and L. S. Levy, "Is low-level environmental mercury exposure of concern to human health?," *Sci Total Environ*, vol. 408, no. 2, pp. 171–82, Dec. 2009.
[30] M. R. Karagas, A. L. Choi, E. Oken, M. Horvat, R. Schoeny, M. Karagas, A. L. Choi, E. Oken, M. Horvat, R. Schoeny, E. Kamai, W. Cowell, P. Grandjean, and S. Korrick, "Evidence on the Human Health Effects of Low-Level Methylmercury Exposure Elizabeth Kamai , Whitney Cowell , Philippe Grandjean and Susan Korrick Published by : The National Institute of Environmental Health Sciences Stable URL : http://www.jstor.org/stabl," vol. 120, no. 6, pp. 799–806, 2017.
[31] T. Yorifuji, T. Tsuda, S. Takao, E. Suzuki, and M. Harada, "Total mercury content in hair and neurologic signs: historic data from Minamata.," *Epidemiology*, vol. 20, no. 2, pp. 188–93, 2009.
[32] F. B. Teixeira, A. C. A. de Oliveira, L. K. R. Leão, N. C. F. Fagundes, R. M. Fernandes, L. M. P. Fernandes, M. C. F. da Silva, L. L. Amado, F. E. S. Sagica, E. H. C. de Oliveira, M. E. Crespo-Lopez, C. S. F. Maia, and R. R. Lima, "Exposure to Inorganic Mercury Causes Oxidative Stress, Cell Death, and Functional Deficits

in the Motor Cortex," *Front Mol Neurosci*, vol. 11, no. May, pp. 1–11, 2018.
[33] B. Gordon, P. Callan, and C. Vickers, "WHO guidelines for drinking-water quality.," *WHO Chron*, vol. 38, no. 3, p. 564, 2008.
[34] S. H. Frisbie, E. J. Mitchell, and B. Sarkar, "Urgent need to reevaluate the latest World Health Organization guidelines for toxic inorganic substances in drinking water," *Environ Heal*, vol. 14, no. 1, p. 63, Aug. 2015.
[35] M. Ravichandran, "Interactions between mercury and dissolved organic matter--a review.," *Chemosphere*, vol. 55, no. 3, pp. 319–31, Apr. 2004.
[36] G. Aiken, M. Haitzer, J. N. Ryan, and K. Nagy, "Interactions between dissolved organic matter and mercury in the Florida Everglades," *Journal De Physique Iv*, vol. 107. pp. 29–32, 2003.
[37] M. Haitzer, G. R. Aiken, and J. N. Ryan, "Binding of mercury(II) to dissolved organic matter: The role of the mercury-to-DOM concentration ratio," *Environ Sci Technol*, vol. 36, no. 16, pp. 3564–3570, 2002.
[38] K. H. Telmer and M. M. Veiga, *Mercury Fate and Transport in the Global Atmosphere*. Boston, MA: Springer US, 2009.
[39] W. Dong, Y. Bian, L. Liang, and B. Gu, "Sup. Material: Binding Constants of Mercury and Dissolved Organic Matter Determined by DOM added , mg / L," pp. 2–5, 2011.
[40] J. M. Benoit, R. P. Mason, C. C. Gilmour, and G. R. Aiken, "Constants for mercury binding by organic matter isolates from the Florida Everglades," *Geochim Cosmochim Acta*, vol. 65, no. 24, pp. 4445–4451, 2001.
[41] H. Hintelmann, P. M. Welbourn, and R. D. Evans, "Measurement of Complexation of Methylmercury(II) Compounds by Freshwater Humic Substances Using Equilibrium Dialysis," *Environ Sci Technol*, vol. 31, no. 2, pp. 489–495, 1997.
[42] G. Mierle and R. Ingram, "The role of humic substances in the mobilization of mercury from watersheds," *Water, Air, Soil Pollut*, vol. 56, no. 1, pp. 349–357, 1991.
[43] A. Matilainen, M. Vepsäläinen, and M. Sillanpää, "Natural organic matter removal by coagulation during drinking water treatment: A review," *Adv Colloid Interface Sci*, vol. 159, no. 2, pp. 189–197, Sep. 2010.
[44] A. Nebbioso and A. Piccolo, "Molecular characterization of dissolved organic matter (DOM): A critical review," *Anal Bioanal Chem*, vol. 405, pp. 109–124, 2013.
[45] T. Pagano, M. Bida, and J. Kenny, "Trends in Levels of Allochthonous Dissolved Organic Carbon in Natural Water: A Review of Potential Mechanisms under a Changing Climate," *Water*, vol. 6, no. 10, pp. 2862–2897, 2014.
[46] D. M. Owen, G. L. Amy, Z. K. Chowdhury, R. Paode, G. McCoy, and K. Viscosil, "NOM characterization and treatability," *J / Am Water Work Assoc*, vol. 87, no. 1, pp. 46–63, 1995.
[47] J. K. Edzwald, "Coagulation in drinking water treatment: particules, organics and coagulants," *Water Sci Technol*, vol. 27, no. 11, pp. 21–35, 1993.
[48] J. Edzwald and J. Tobiason, "Enhanced coagulation: US requirements and a broader view," *Water Sci Technol*, vol. 40, no. 9, pp. 63–70, 1999.
[49] A. Matilainen, E. T. Gjessing, T. Lahtinen, L. Hed, A. Bhatnagar, and M. Sillanpää, "An overview of the methods used in the characterisation of natural

organic matter (NOM) in relation to drinking water treatment," *Chemosphere*, vol. 83, no. 11, pp. 1431–1442, 2011.
[50] E. L. Sharp, S. a. Parsons, and B. Jefferson, "Seasonal variations in natural organic matter and its impact on coagulation in water treatment," *Sci Total Environ*, vol. 363, no. 1–3, pp. 183–194, 2006.
[51] J. Weishaar and G. Aiken, "Evaluation of specific ultra-violet absorbance as an indicator of the chemical content of dissolved organic carbon," *Environ Chem*, vol. 41, no. 2, pp. 843–845, 2001.
[52] Y. K. Henneberry, T. E. C. Kraus, J. A. Fleck, D. P. Krabbenhoft, P. M. Bachand, and W. R. Horwath, "Removal of inorganic mercury and methylmercury from surface waters following coagulation of dissolved organic matter with metal-based salts," *Sci Total Environ*, vol. 409, no. 3, pp. 631–637, Jan. 2011.
[53] J. L. Weishaar, G. R. Aiken, B. a. Bergamaschi, M. S. Fram, R. Fujii, and K. Mopper, "Evaluation of specific ultraviolet absorbance as an indicator of the chemical composition and reactivity of dissolved organic carbon," *Environ Sci Technol*, vol. 37, pp. 4702–4708, 2003.
[54] S. E. Cabaniss, "Synchronous Fluorescence Spectra of Metal-Fulvic Acid Complexes," *Environ Sci Technol*, vol. 26, no. 6, pp. 1133–1139, 1992.
[55] P. Chakraborty, K. M. Yao, K. Chennuri, K. Vudamala, and P. V. Raghunadh Babu, "Interactions of mercury with different molecular weight fractions of humic substances in aquatic systems," *Environ Earth Sci*, vol. 72, no. 3, pp. 931–939, 2014.
[56] S. Orsetti, J. L. Marco-Brown, E. M. Andrade, and F. V. Molina, "Pb(II) binding to humic substances: An equilibrium and spectroscopic study," *Environ Sci Technol*, vol. 47, no. 15, pp. 8325–8333, 2013.
[57] W. B. Chen, D. S. Smith, and C. Guéguen, "Influence of water chemistry and dissolved organic matter (DOM) molecular size on copper and mercury binding determined by multiresponse fluorescence quenching," *Chemosphere*, vol. 92, no. 4, pp. 351–359, 2013.
[58] K. Xia, U. L. Skyllberg, W. F. Bleam, P. R. Bloom, E. A. Nater, and P. A. Helmke, "X-ray absorption spectroscopic evidence for the complexation of Hg(II) by reduced sulfur in soil humic substances," *Environ Sci Technol*, vol. 33, no. 2, pp. 257–261, 1999.
[59] S. M. Henrichs, "Organic geochemistry of natural waters (E. M. Thurman [cd.])," *Limnol Oceanogr*, 1987.
[60] L. Boszke, A. Kowalski, G. Glosińska, R. Szarek, and J. Siepak, "Environmental factors affecting speciation of mercury in the bottom sediments; an overview," *Polish J Environ Stud*, vol. 12, no. 1, pp. 5–13, 2003.
[61] M. Haitzer, G. R. Aiken, and J. N. Ryan, "Binding of mercury(II) to aquatic humic substances: Influence of pH and source of humic substances," *Environ Sci Technol*, vol. 37, no. 11, pp. 2436–2441, 2003.
[62] IHSS, "International Humic Substances Society," 2018. [Online]. Available: http://humic-substances.org/.
[63] M. Filella, "Freshwaters: Which NOM matters?," *Environ Chem Lett*, vol. 7, no. 1, pp. 21–35, 2009.
[64] P. A. Lozovik, A. K. Morozov, M. B. Zobkov, T. A. Dukhovicheva, and L. A.

Osipova, “Allochthonous and autochthonous organic matter in surface waters in Karelia,” *Water Resour*, vol. 34, no. 2, pp. 204–216, 2007.
[65] M. Lindqvist, O., Johansson, K., Bringmark, L., Timm, B., Aastrup, M., Andersson, A., ... & Meili, “Mercury in the Swedish environment—recent research on causes, consequences and corrective methods,” *Water Air Soil Pollut*, vol. 55, no. 1–2, p. xi--261, 1991.
[66] J. A. Dittman, J. B. Shanley, C. T. Driscoll, G. R. Aiken, A. T. Chalmers, and J. E. Towse, “Ultraviolet absorbance as a proxy for total dissolved mercury in streams,” *Environ Pollut*, vol. 157, no. 6, pp. 1953–1956, 2009.
[67] J. A. Leenheer and J.-P. Croué, “Characterizing aquatic dissolved organic matter,” *Environ Sci Technol*, vol. 37, no. 1, p. 18A–26A, 2003.
[68] T. Bond, E. H. Goslan, S. A. Parsons, and B. Jefferson, “A critical review of trihalomethane and haloacetic acid formation from natural organic matter surrogates,” *Environ Technol Rev*, vol. 1, no. 1, pp. 93–113, 2012.
[69] L. Leita, A. Margon, A. Pastrello, I. Arčon, M. Contin, and D. Mosetti, “Soil humic acids may favour the persistence of hexavalent chromium in soil,” *Environ Pollut*, vol. 157, no. 6, pp. 1862–1866, 2009.
[70] S. F. R. Sinsabaugh, *Aquatic Ecosystems: Interactivity of Dissolved Organic Matter*, 1st ed. Academic Press, 2003.
[71] a F. Ashery, K. Radwan, and M. I. G. a-a Rashed, “The effect of pH control on turbidity and NOM removal in conventional water treatment,” *Fifteenth Int Water Technol Conf IWTC 15 2010, Alexandria, Egypt*, pp. 1–16, 2010.
[72] R. T. Drexel, M. Haitzer, J. N. Ryan, G. R. Aiken, and K. L. Nagy, “Mercury(II) sorption to two Florida Everglades peats: Evidence for strong and weak binding and competition by dissolved organic matter released from the peat,” *Environ Sci Technol*, vol. 36, no. 19, pp. 4058–4064, 2002.
[73] M. Haitzer, S. Höss, W. Traunspurger, and C. Steinberg, “Effects of dissolved organic matter (DOM) on the bioconcentration of organic chemicals in aquatic organisms — a review —,” *Chemosphere*, vol. 37, no. 7, pp. 1335–1362, Sep. 1998.
[74] W. Dong, Y. Bian, L. Liang, and B. Gu, “Binding Constants of Mercury and Dissolved Organic Matter Determined by a Modified Ion Exchange Technique,” pp. 3576–3583, 2011.
[75] A. Manceau and K. L. Nagy, “Quantitative analysis of sulfur functional groups in natural organic matter by XANES spectroscopy,” *Geochim Cosmochim Acta*, vol. 99, pp. 206–223, 2012.
[76] W. F. Bleam, P. R. Bloom, E. A. Nater, and P. A. Helmke, “X-ray Absorption Spectroscopic Evidence for the Complexation of Hg (II) by Reduced Sulfur in Soil Humic Substances,” vol. 33, no. 3, pp. 257–261, 2004.
[77] K. Xia, F. Weesner, W. F. Bleam, P. a. Helmke, P. R. Bloom, and U. L. Skyllberg, “XANES Studies of Oxidation States of Sulfur in Aquatic and Soil Humic Substances,” *Soil Sci Soc Am J*, vol. 62, no. 5, p. 1240, 1998.
[78] a Vairavamurthy, “Using X-ray absorption to probe sulfur oxidation states in complex molecules,” *Spectrochim Acta Part A Mol Biomol Spectrosc*, vol. 54, no. 12, pp. 2009–2017, 1998.
[79] J. Prietzel, J. Thieme, M. Salomé, and H. Knicker, “Sulfur K-edge XANES

spectroscopy reveals differences in sulfur speciation of bulk soils, humic acid, fulvic acid, and particle size separates," *Soil Biol Biochem*, vol. 39, no. 4, pp. 877–890, 2007.

[80] M. J. Morra, S. E. Fendorf, and P. D. Brown, "Speciation of sulfur in humic and fulvic acids using X-ray absorption near-edge structure (XANES) spectroscopy," *Geochim Cosmochim Acta*, vol. 61, no. 3, pp. 683–688, 1997.

[81] L. S. Hundal, A. M. Carmo, W. L. Bleam, and M. L. Thompson, "Sulfur in biosolids-derived fulvic acid: Characterization by XANES spectroscopy and selective dissolution approaches," *Environ Sci Technol*, vol. 34, no. 24, pp. 5184–5188, 2000.

[82] D. Veiga, M. M., Baker, R. F., Fried, M. B., & Withers, *Protocols for environmental and health assessment of mercury released by artisanal and small-scale gold miners*. United Nations Publications, 2004.

[83] L. D. & P. W. C. de Lacerda, "Mercury From Gold Mining In The Amazon Environment - An Overview.pdf," *Quim Nova*, vol. 15, no. 2, pp. 155–160, 1992.

[84] J. R. Ikingura, M. K. D. Mutakyahwa, and J. M. J. Kahatano, "Mercury and mining in Africa with special reference to Tanzania," *Water Air Soil Pollut*, vol. 97, no. 3–4, pp. 223–232, 1997.

[85] D. Limbong, J. Kumampung, J. Rimper, T. Arai, and N. Miyazaki, "Emissions and environmental implications of mercury from artisanal gold mining in North Sulawesi, Indonesia.," *Sci Total Environ*, vol. 302, no. 1–3, pp. 227–36, Jan. 2003.

[86] M. Jiménez-Moreno, V. Perrot, V. N. Epov, M. Monperrus, and D. Amouroux, "Chemical kinetic isotope fractionation of mercury during abiotic methylation of Hg(II) by methylcobalamin in aqueous chloride media," *Chem Geol*, vol. 336, pp. 26–36, Jan. 2013.

[87] J. M. Parks, A. Johs, M. Podar, R. Bridou, R. a Hurt, S. D. Smith, S. J. Tomanicek, Y. Qian, S. D. Brown, C. C. Brandt, A. V Palumbo, J. C. Smith, J. D. Wall, D. a Elias, and L. Liang, "The genetic basis for bacterial mercury methylation.," *Science*, vol. 339, no. 6125, pp. 1332–5, 2013.

[88] M. E. Hines, E. N. Poitras, S. Covelli, J. Faganeli, A. Emili, S. Žižek, and M. Horvat, "Mercury methylation and demethylation in Hg-contaminated lagoon sediments (Marano and Grado Lagoon, Italy)," *Estuar Coast Shelf Sci*, vol. 113, pp. 85–95, Nov. 2012.

[89] P. Taylor, S. M. Ullrich, T. W. Tanton, and S. A. Abdrashitova, "Critical Reviews in Environmental Science and Technology Mercury in the Aquatic Environment : A Review of Factors Affecting Methylation Mercury in the Aquatic Environment : A Review of Factors Affecting Methylation," *Environ Sci Technol*, vol. 31, no. 3, pp. 241–293, 2001.

[90] P. M. Randall and S. Chattopadhyay, "Mercury contaminated sediment sites-An evaluation of remedial options," *Environ Res*, vol. 125, pp. 131–149, Aug. 2013.

[91] O. Pfeiffer, W. C., Lacerda, L. D., Salomons, W., & Malm, "Environmental fate of mercury from gold mining in the Brazilian Amazon," *Environ Rev*, vol. 1, no. 1, pp. 26–37, 1993.

[92] P. V. & C. A. Andrade, J. D., Bueno, M. I. M. S., Soares, "The fate of mercury released from prospecting areas ('garimpos') near Guarinos e Pilar de Goiás," *An Acad Bras Cienc*, vol. 60, no. 3, pp. 292–303, 1988.

[93] P. D. Maia, L. Maurice, E. Tessier, D. Amouroux, D. Cossa, M. Pérez, P. Moreira-Turcq, and I. Rhéault, "Mercury distribution and exchanges between the Amazon River and connected floodplain lakes," *Sci Total Environ*, vol. 407, no. 23, pp. 6073–84, Nov. 2009.
[94] J. J. Berzas Nevado, R. C. Rodríguez Martín-Doimeadios, F. J. Guzmán Bernardo, M. Jiménez Moreno, a M. Herculano, J. L. M. do Nascimento, and M. E. Crespo-López, "Mercury in the Tapajós River basin, Brazilian Amazon: a review.," *Environ Int*, vol. 36, no. 6, pp. 593–608, Aug. 2010.
[95] Redacción Vivir, "Mercurio en el agua de Ayapel," *El Espectador*, Bogotá, 26-Aug-2013.
[96] J. . Appleton, T. . Williams, N. Breward, A. Apostol, J. Miguel, and C. Miranda, "Mercury contamination associated with artisanal gold mining on the island of Mindanao, the Philippines," *Sci Total Environ*, vol. 228, no. 2–3, pp. 95–109, Apr. 1999.
[97] C. T. Driscoll, V. Blette, C. Yan, C. L. Schofield, R. Munson, and J. Holsapple, "The role of dissolved organic carbon in the chemistry and bioavailability of mercury in remote Adirondack lakes," *Water Air Soil Pollut*, vol. 80, no. 1–4, pp. 499–508, 1995.
[98] J. C. Bonzongo, K. J. Heim, J. J. Warwick, and W. B. Lyons, "Mercury levels in surface waters of the Carson River-Lahontan reservoir system, Nevada: Influence of historic mining activities," *Environ Pollut*, vol. 92, no. 2, pp. 193–201, 1996.
[99] S. E. Rothenberg, R. F. Ambrose, and J. a Jay, "Mercury cycling in surface water, pore water and sediments of Mugu Lagoon, CA, USA.," *Environ Pollut*, vol. 154, no. 1, pp. 32–45, Jul. 2008.
[100] J. A. Davis, R. E. Looker, D. Yee, M. M. Pasquale, J. L. Grenier, C. M. Austin, L. J. Mckee, B. K. Greenfield, R. Brodberg, and J. D. Blum, "Reducing methylmercury accumulation in the food webs of San Francisco Bay and its local watersheds," *Environ Res*, vol. 119, pp. 3–26, 2012.
[101] Burton P, "The Colombian Gold Mining Industry - World Gold Analyst Special Report," *World Gold Analyst*, p. 87, 2011.
[102] E. D. Stein, Y. Cohen, and A. M. Winer, "Environmental distribution and transformation of mercury compounds," *Crit Rev Environ Sci Technol*, vol. 26, no. 1, pp. 1–43, 1996.
[103] EPA, "Treatment Technologies For Mercury in Soil, Waste, and Water," Washington, D.C., 2007.
[104] P. I. Girginova, A. L. Daniel-da-Silva, C. B. Lopes, P. Figueira, M. Otero, V. S. Amaral, E. Pereira, and T. Trindade, "Silica coated magnetite particles for magnetic removal of Hg2+ from water," *J Colloid Interface Sci*, vol. 345, no. 2, pp. 234–240, May 2010.
[105] H. Parham, B. Zargar, and R. Shiralipour, "Fast and efficient removal of mercury from water samples using magnetic iron oxide nanoparticles modified with 2-mercaptobenzothiazole," *J Hazard Mater*, vol. 205–206, pp. 94–100, Feb. 2012.
[106] M. M. Benjamin and D. F. Lawler, *Water quality engineering: Physical/chemical treatment processes*. Wiley, 2013.
[107] K. K. Au, S. M. Alpert, and D. J. Pernitsky, "Particle and Natural Organic Matter Removal in Drinking Water," *Oper Control Coagul Filtr Process - Man Water*

Supply Pract M37 (3rd Ed, pp. 1–16, 2011.
[108] J. Hur and M. A. Schlautman, "Using selected operational descriptors to examine the heterogeneity within a bulk humic substance," *Environ Sci Technol*, vol. 37, no. 5, pp. 880–887, 2003.
[109] J. A. Korak, A. D. Dotson, R. S. Summers, and F. L. Rosario-Ortiz, "Critical analysis of commonly used fluorescence metrics to characterize dissolved organic matter," *Water Res*, vol. 49, pp. 327–338, 2014.
[110] K. Bell-Ajy, M. Abbaszadegan, E. Ibrahim, D. Verges, and M. LeChevallier, "Conventional and optimized coagulation for NOM removal," *J / Am Water Work Assoc*, vol. 92, no. 10, pp. 44–58, 2000.
[111] C. Catrouillet, M. Davranche, A. Dia, M. Bouhnik-Le Coz, M. Pédrot, R. Marsac, and G. Gruau, "Thiol groups controls on arsenite binding by organic matter: New experimental and modeling evidence," *J Colloid Interface Sci*, vol. 460, pp. 310–320, 2015.
[112] J. Kaleta and M. Elektorowicz, "Removal of humic substances from aqueous solutions by the coagulation process," *Environ Technol*, vol. 30, no. 2, pp. 119–127, 2009.
[113] M. S. Twardowski, E. Boss, J. M. Sullivan, and P. L. Donaghay, "Modeling the spectral shape of absorption by chromophoric dissolved organic matter," *Mar Chem*, vol. 89, no. 1–4, pp. 69–88, 2004.
[114] J. R. Helms, A. Stubbins, J. D. Ritchie, E. C. Minor, D. J. Kieber, and K. Mopper, "Absorption spectral slopes and slope ratios as indicators of molecular weight, source, and photobleaching of chromophoric dissolved organic matter," *Limnol Oceanogr*, vol. 53, no. 3, pp. 955–969, 2008.
[115] P. Roccaro, M. Yan, and G. V. Korshin, "Use of log-transformed absorbance spectra for online monitoring of the reactivity of natural organic matter," *Water Res*, vol. 84, pp. 136–143, 2015.
[116] Y. Henneberry, T. E. C. Kraus, D. P. Krabbenhoft, and W. R. Horwath, "Investigating the Temporal Effects of Metal-Based Coagulants to Remove Mercury from Solution in the Presence of Dissolved Organic Matter," *Environ Manage*, no. September, 2015.
[117] M. R. Collins, G. L. Amy, and C. Steelink, "Molecular Weight Distribution, Carboxylic Acidity, and Humic Substances Content of Aquatic Organic Matter: Implications for Removal during Water Treatment," *Environ Sci Technol*, vol. 20, no. 10, pp. 1028–1032, 1986.
[118] G. Crozes, P. White, and M. Marshall, "Enhanced coagulation: Its effect on NOM removal and chemical costs," *J / Am Water Work Assoc*, vol. 87, no. 1, pp. 78–89, 1995.
[119] R. D. Letterman, A. Amirtharajah, and O. C. R, "Chapter 6. Coagulation and Flocculation," in *Water Quality and Treatment*, 5th ed., R. D. Letterman, Ed. McGraw-Hill, 2005.
[120] O. C. R. Hundt T R., "Aluminum-Fulvic Acid Interactions: Mechanisms and Applications," vol. 80, no. 4, pp. 176–186, 1988.
[121] J. Y. Shin and R. F. Spinette, "Stoichiometry of Coagulation Revisited," vol. 42, no. 7, pp. 2582–2589, 2008.
[122] Gerald A. Edwards and A. Amirtharajah, "Removing Colour Caused by Humic

Acid," *J / Am Water Work Assoc*, vol. 77, no. 3, pp. 50–57, 1985.
[123] H. Ødegaard, B. Eikebrokk, and R. Storhaug, "Processes for the removal of humic substances from water - An overview based on Norwegian experiences," *Water Sci Technol*, vol. 40, no. 9, pp. 37–46, 1999.
[124] J. Duan and J. Gregory, "Coagulation by hydrolysing metal salts," vol. 102, pp. 475–502, 2003.
[125] X. Lu, Z. Chen, and X. Yang, "Spectroscopic study of aluminium speciation in removing humic substances by Al coagulation," *Water Res*, vol. 33, no. 15, pp. 3271–3280, 1999.
[126] P. Jin, J. Song, L. Yang, X. Jin, and X. C. Wang, "Selective binding behavior of humic acid removal by aluminum coagulation," *Environ Pollut*, vol. 233, pp. 290–298, 2018.
[127] X. C. Wang, P. K. Jin, and J. Gregory, "Structure of Al-humic flocs and their removal at slightly acidic and neutral pH," in *Water Science and Technology: Water Supply*, 2002, vol. 2, no. 2, pp. 99–106.
[128] V. Pallier, G. Feuillade-Cathalifaud, B. Serpaud, and J. C. Bollinger, "Effect of organic matter on arsenic removal during coagulation/flocculation treatment," *J Colloid Interface Sci*, vol. 342, no. 1, pp. 26–32, 2010.
[129] C. P. McNaughton, "The Influence of Mercury-Dissolved Organic Matter (DOM) Complexation on Toxicity in Natural Waters," 2007.
[130] X. Lu and R. Jaffe, "Interaction between Hg(II) and natural dissolved organic matter: a fluorescence spectroscopy based study," *Water Res*, vol. 35, no. 7, pp. 1793–1803, 2001.
[131] W. Stumm and J. J. Morgan, *Aquatic Chemistry: Chemical equilibria and rates in natural waters*, 3rd ed. New York: Wiley, 1996.
[132] del V. R. Blough N, *Chromophoric DOM in the coastal environment. In: Biogeochemistry of Marine Dissolved Organic Matter*. 2002.
[133] S. S. Marais, E. J. Ncube, T. A. M. Msagati, J. Haarhoff, T. I. Nkambule, and B. B. Mamba, "Characterization and removal of natural organic matter by a water treatment plant in South Africa," 2015.
[134] W. Dong, L. Liang, S. Brooks, G. Southworth, and B. Gu, "Roles of dissolved organic matter in the speciation of mercury and methylmercury in a contaminated ecosystem in Oak Ridge, Tennessee," *Environ Chem*, vol. 7, no. 1, pp. 94–102, 2010.
[135] A. Amirbahman, A. L. Reid, T. A. Haines, J. S. Kajl, and C. Arnold, "Association of methylmercury with dissolved humic acids," *Environ Sci Technol*, vol. 36, no. 4, pp. 690–695, 2002.
[136] R. von Wandruszka, "Humic acids: Their detergent qualities and potential uses in pollution remediation," *Geochem Trans*, vol. 1, no. March, pp. 10–15, 2000.
[137] T. L. Barr, "Advances in the Application of X-Ray Photoelectron Spectroscopy (ESCA) Part I. Foundation and Established Methods," *Crit Rev Anal Chem*, vol. 22, no. 1–2, pp. 567–635, Jan. 1991.
[138] J. Wilcox, E. Sasmaz, A. Kirchofer, and S.-S. Lee, "Heterogeneous Mercury Reaction Chemistry on Activated Carbon," *J Air Waste Manage Assoc*, vol. 61, no. 4, pp. 418–426, 2011.
[139] E. Sasmaz, A. Kirchofer, A. D. Jew, A. Saha, D. Abram, T. F. Jaramillo, and J.

Wilcox, “Mercury chemistry on brominated activated carbon,” *Fuel*, vol. 99, pp. 188–196, 2012.
[140] N. Fairley, C. S. Ltd, and C. S. L. Staff, *CasaXPS Manual 2.3.15: Introduction to XPS and AES*. Casa Software, Limited, 2009.
[141] B. Zacharie, T. P. Connolly, and C. L. Penney, “A Simple One-Step Conversion of Carboxylic Acids to Esters Using EEDQ,” *J Org Chem*, vol. 60, no. 21, pp. 7072–7074, 1995.
[142] T. Yoshino, S. Imori, and H. Togo, “Efficient esterification of carboxylic acids and phosphonic acids with trialkyl orthoacetate in ionic liquid,” *Tetrahedron*, vol. 62, no. 6, pp. 1309–1317, 2006.
[143] J.-L. Burgot, “Conditional Stability Constants,” in *Ionic Equilibria in Analytical Chemistry*, New York, NY: Springer New York, 2012, pp. 485–501.
[144] H. Schäfer (Muñster, “Die Komplexometrische Titration: Gerold Schwarzenbach, Die chemische Analyse, Bd. 45, zweite umgearbeitete und erwiterte Auflage, Verlag Enke, Stuttgart, 1956, 119 Seiten,” *Anal Chim Acta*, vol. 18, p. 184, 1958.
[145] M. Bieroza, A. Baker, and J. Bridgeman, “Relating freshwater organic matter fluorescence to organic carbon removal efficiency in drinking water treatment,” *Sci Total Environ*, vol. 407, no. 5, pp. 1765–1774, 2009.
[146] N. Hudson, A. Baker, and D. Reynolds, “Fluorescence analysis of dissolved organic matter in natural, waste and polluted waters—a review,” *River Res Appl*, vol. 23, no. 6, pp. 631–649, Jul. 2007.
[147] J. C. G. Esteves Da Silva, A. A. S. C. MacHado, C. J. S. Oliveira, and M. S. S. D. S. Pinto, “Fluorescence quenching of anthropogenic fulvic acids by Cu(II), Fe(III) and UO2/2+,” *Talanta*, vol. 45, no. 6, pp. 1155–1165, 1998.
[148] S. C. Myneni, J. T. Brown, G. A. Martinez, and W. Meyer-Ilse, “Imaging of Humic Substance Macromolecular Structures in Water and Soils,” *Science*, vol. 286, no. 5443, pp. 1335–1337, 1999.
[149] N. Hidayati, T. Juhaeti, and F. Syarif, “Mercury and Cyanide Contaminations in Gold Mine Environment and Possible Solution of Cleaning Up by Using Phytoextraction,” *HAYATI J Biosci*, vol. 16, no. 3, pp. 88–94, 2009.
[150] J. D. Gasper, G. R. Aiken, and J. N. Ryan, “A critical review of three methods used for the measurement of mercury (Hg2+)-dissolved organic matter stability constants,” *Appl Geochemistry*, vol. 22, no. 8, pp. 1583–1597, Aug. 2007.
[151] J. Chen, E. J. LeBoeuf, S. Dai, and B. Gu, “Fluorescence spectroscopic studies of natural organic matter fractions,” *Chemosphere*, vol. 50, no. 5, pp. 639–647, 2003.
[152] D. J. Cremin, A. F. Hegarty, and M. J. Begley, “Mechanism of Reaction of 2-Ethoxy-1 -ethoxycarbonyl-I ,2-dihydroquinoline (EEDQ) with Nucleophiles and its Crystal Structure,” *J Chem Soc Perkin Trans 2*, vol. 0, no. 412, pp. 412–420, 1980.
[153] S. Ou, Z. Lin, C. Duan, H. Zhang, and Z. Bai, “A sugar-quinoline fluorescent chemosensor for selective detection of Hg2+ ion in natural water,” *Chem Commun*, no. 42, pp. 4392–4394, 2006.
[154] J. Hu, J. Li, J. Qi, and J. Chen, “Highly selective and effective mercury(II) fluorescent sensors,” *New J Chem*, vol. 39, no. 2, pp. 843–848, 2015.
[155] F. Wu, Y. Cai, D. Evans, and P. Dillon, “Complexation between Hg(II) and dissolved organic matter in stream waters: An application of fluorescence

spectroscopy," *Biogeochemistry*, vol. 71, no. 3, pp. 339–351, 2004.
[156] M. Serrano, "Despite economic growth, Colombia continues to be one of the most unequal countries in the world," *UN Periódico*, 2018. [Online]. Available: http://unperiodico.unal.edu.co/pages/detail/despite-economic-growth-colombia-continues-to-be-one-of-the-most-unequal-countries-in-the-world/. [Accessed: 14-Nov-2018].
[157] O. Malm, "Gold mining as a source of mercury exposure in the Brazilian Amazon.," *Environ Res*, vol. 77, no. 2, pp. 73–8, May 1998.
[158] K. Drace, A. M. Kiefer, M. M. Veiga, M. K. Williams, B. Ascari, K. A. Knapper, K. M. Logan, V. M. Breslin, A. Skidmore, D. A. Bolt, G. Geist, L. Reidy, and J. V. Cizdziel, "Mercury-free, small-scale artisanal gold mining in Mozambique: utilization of magnets to isolate gold at clean tech mine," *J Clean Prod*, vol. 32, pp. 88–95, Sep. 2012.
[159] M. M. Veiga, D. Nunes, B. Klein, J. A. Shandro, P. C. Velasquez, and R. N. Sousa, "Mill leaching: a viable substitute for mercury amalgamation in the artisanal gold mining sector?," *J Clean Prod*, vol. 17, no. 15, pp. 1373–1381, Oct. 2009.
[160] W. C. Pfeiffer and L. D. de Lacerda, "Mercury inputs into the Amazon Region, Brazil," *Environ Technol Lett*, vol. 9, no. 4, pp. 325–330, Apr. 1988.
[161] W. R. Pfeiffer, W. C., Drude de Lacerda, L., Malm, O., Souza, C. M. M., da Silveira, E. G., & Bastos, "Mercury concentrations in inland waters of gold-mining areas in Rondônia, Brazil.," *Sci Total Environ*, vol. 87–88, pp. 233–240, Nov. 1989.
[162] W. C. Malm, O., Castro, M. B., Bastos, W. R., Branches, F. J., Guimarães, J. R., Zuffo, C. E., & Pfeiffer, "An assessment of Hg pollution in different goldmining areas, Amazon Brazil," *Sci Total Environ*, vol. 175, no. 2, pp. 127–140, 1995.
[163] D. B. Bloom, N. S. & Porcella, "Less mercury?," *Nature*, vol. 367, no. 24 Feb 1994, p. 694, 1994.
[164] P. Cordy, M. M. Veiga, I. Salih, S. Al-Saadi, S. Console, O. Garcia, L. A. Mesa, P. C. Velásquez-López, and M. Roeser, "Mercury contamination from artisanal gold mining in Antioquia, Colombia: The world's highest per capita mercury pollution," *Sci Total Environ*, vol. 410–411, pp. 154–160, Dec. 2011.
[165] Thomson Reuters, "GFMS Gold Survey 2018," 2018.
[166] Verité, "The Nexus of Illegal Gold Mining and Human Trafficking in Global Supply Chains," 2016.
[167] Global Initiative against Transnational Organized Crime, "Organized Crime and Illegally Mined Gold in Latin America," Switzerland, 2016.
[168] J. Olivero, B. Johnson, and E. Arguello, "Human exposure to mercury in San Jorge river basin, Colombia (South America)," *Sci Total Environ*, vol. 289, no. 1–3, pp. 41–7, Apr. 2002.
[169] T. M. Palapa and A. A. Maramis, "Heavy Metals in Water of Stream Near an Amalgamation Tailing Ponds in Talawaan – Tatelu Gold Mining, North Sulawesi, Indonesia," *Procedia Chem*, vol. 14, pp. 428–436, Jan. 2015.
[170] J. Marrugo-Negrete, L. N. Benitez, and J. Olivero-Verbel, "Distribution of mercury in several environmental compartments in an aquatic ecosystem impacted by gold mining in northern Colombia," *Arch Environ Contam Toxicol*, vol. 55, no.

2, pp. 305–316, 2008.
[171] R. N. y Economía, “El 80% de la producción de oro colombiano sigue en manos ilegales,” *El Espectador*, 2016.
[172] P. de las N. U. para el M. A. (PNUMA) and M. de A. y D. S. (MADS), “Sinopsis Nacional de la Mineria Aurífera Artesanal y de Pequeña Escala,” Bogotá D.C., 2012.
[173] Oficina de las Naciones Unidas contra la Droga y el Delito (UNODC), “Explotación de oro de aluvión Evidencias a partir de percepción remota,” 2016.
[174] “Unidad de Planeación Minero Energética.” [Online]. Available: http://www1.upme.gov.co/Paginas/default.aspx. [Accessed: 07-Nov-2018].
[175] “Mercurio en los ríos de Colombia - Ciencia - ELTIEMPO.COM.” [Online]. Available: http://www.eltiempo.com/estilo-de-vida/ciencia/mercurio-en-los-rios-de-colombia/16190798. [Accessed: 04-Aug-2015].
[176] “Habitantes de Ayapel estarían condenados a morir por el mercurio | El Heraldo.” [Online]. Available: http://www.elheraldo.co/region/cordoba/habitantes-de-ayapel-estarian-condenados-a-morir-por-el-mercurio-121871. [Accessed: 26-Jun-2015].
[177] Angélica María Cuevas Guarnizo / Periodista de El Espectador - Especial para Vice Colombia, “¡Bañados en mercurio! | ELESPECTADOR.COM,” *El Espectador*, 12-Aug-2015.
[178] “Decomisan 24 dragas por explotación ilegal de oro en Chocó y hallan peces contaminados con mercurio - Archivo - Archivo Digital de Noticias de Colombia y el Mundo desde 1.990.” [Online]. Available: http://www.eltiempo.com/archivo/documento/CMS-5034048. [Accessed: 18-Sep-2013].
[179] U. de Córdoba, UPME, and Ministerio de Minas y Energía, “Estudio de la Cadena del Mercurio con énfasis en la actividad minera aurífera Colombiana,” Bogotá D.C., 2014.
[180] Ministerio de Minas y Energía, Agencia Nacional de Minería, U. Unidad de Planeación Minero Energética, and S. Servicio Geológico Colombiano, “Plan estratégico sectorial para la eliminación el uso del mercurio: La ruta hacia un beneficio sostenible del oro Ministerio de Minas y energía,” Bogotá D.C., 2016.
[181] W. C. Malm, O., Guimaraes, J. R. D., & Pfeiffer, “Accumulation of metallic mercury and natural amalgams findings in Madeira River basin bottom sediments, Amazon,” in *Proceedings Int. Symp. Perspectives for environmental geochemistry in tropical countries*, 1993, pp. 391–393.
[182] M. M. Veiga, J. Hinton, and C. Lilly, “Mercury in the Amazon : A Comprehensive Review with Special Emphasis on Bioaccumulation and Bioindicators,” *Natl Inst Minamata Dis Forum’99*, pp. 19–40, 1999.
[183] S. Moore, J. W., & Ramamoorthy, *Heavy metals in natural waters. Applied monitoring and impact assessment*. Springer-Verlag, 1984.
[184] S. G. Egler, S. Rodrigues-Filho, R. C. Villas-Bôas, and C. Beinhoff, “Evaluation of mercury pollution in cultivated and wild plants from two small communities of the Tapajós gold mining reserve, Pará State, Brazil.,” *Sci Total Environ*, vol. 368, no. 1, pp. 424–33, Sep. 2006.
[185] P. van Straaten, “Mercury contamination associated with small-scale gold mining in Tanzania and Zimbabwe,” *Sci Total Environ*, vol. 259, no. 1–3, pp. 105–13,

Oct. 2000.
[186] E. Oliveira, L. J., Hylander, L. D., & de Castro e Silva, "Mercury behavior in a tropical environment: the case of small-scale gold mining in Poconé, Brazil," *Environ Pract*, vol. 6, no. 2, pp. 121–134, 2004.
[187] J. P. Hurley, D. P. Krabbenhoft, L. B. Cleckner, M. L. Olson, G. R. Aiken, and P. S. R. Jr, "System controls on the aqueous distribution of mercury in the northern Florida Everglades," *Biogeochemistry*, vol. 40, no. 2, pp. 293–310, 1998.
[188] G. Qiu, X. Feng, S. Wang, and L. Shang, "Environmental contamination of mercury from Hg-mining areas in Wuchuan, northeastern Guizhou, China.," *Environ Pollut*, vol. 142, no. 3, pp. 549–58, Aug. 2006.
[189] "Policía Nacional de Colombia." [Online]. Available: https://www.policia.gov.co/. [Accessed: 07-Nov-2018].
[190] "Fuerzas Militares de Colombia." [Online]. Available: http://www.fuerzasmilitares.org/. [Accessed: 07-Nov-2018].
[191] UNODC, "Coca Crops in Colombia at all-time high, UNODC Report finds." [Online]. Available: https://www.unodc.org/unodc/en/frontpage/2018/September/coca-crops-in-colombia-at-all-time-high--unodc-report-finds.html. [Accessed: 07-Nov-2018].
[192] NPR, "Colombia Is Growing Record Amounts Of Coca, The Key Ingredient In Cocaine : NPR." [Online]. Available: https://www.npr.org/2018/10/22/658547337/colombia-is-growing-record-amounts-of-coca-the-key-ingredient-in-cocaine. [Accessed: 07-Nov-2018].
[193] FIP - Fundación Ideas para la Paz, "¿Por qué siguen aumentando los cultivos de coca en Colombia? · Documentos · FIP - Ideas para la Paz." [Online]. Available: http://www.ideaspaz.org/publications/posts/1686. [Accessed: 07-Nov-2018].
[194] United Nations Environment Programme, "Minamata Convention on Mercury - text and annexes," *United Natl Environ Progreamme Geneva, Switz*, 2013.
[195] O. US EPA, "Artisanal and Small-Scale Gold Mining Without Mercury."
[196] "Mercurio, prohibido pero en venta en Ecuador." [Online]. Available: https://www.expreso.ec/actualidad/mercurio-prohibido-pero-en-venta-BY230047. [Accessed: 07-Nov-2018].
[197] "Antioquia aún no logra erradicar el mercurio." [Online]. Available: http://www.elcolombiano.com/antioquia/antioquia-aun-no-logra-erradicar-el-mercurio-YM8943247. [Accessed: 07-Nov-2018].
[198] "Minería ilegal usa mercurio en regla - Investigación - Justicia - ELTIEMPO.COM." [Online]. Available: https://www.eltiempo.com/justicia/investigacion/mineria-ilegal-usa-mercurio-en-regla-76266. [Accessed: 07-Nov-2018].
[199] M. Veiga, "Mercurio en la Minería Artesanal de Oro: Problemas Ambientales y de Salud," in *Lumex Intruments - Webinar*, 2017.
[200] Redacción Nacional, "'Es necesario diferenciar la minería ilegal de la informal' | ELESPECTADOR.COM," *El Espectador*, 2014. [Online]. Available: https://www.elespectador.com/noticias/nacional/necesario-diferenciar-mineria-ilegal-de-informal-articulo-524651. [Accessed: 12-Nov-2018].
[201] Ministerio de Mina y Energía, "Política Minera De Colombia- Bases para la minería del futuro," Bogotá D.C., 2016.

[202] Ministerio de Minas y Energía, “Censo Minero Departamental 2010-2011,” Bogotá D.C. , 2012.
[203] Ministerio de Minas y Energía, “Plan de Acción de Formalización,” Bogotá D.C., 2016.
[204] S. Normandin, “The Minamata Convention on Mercury: A Beginner’s Guide - Artisanal Gold Council,” *Artisanal Gold Council*, 2018. [Online]. Available: http://www.artisanalgold.org/publications/articles/the-minamata-convention-on-mercury-a-beginner-s-guide/. [Accessed: 13-Nov-2018].
[205] O. US EPA, OSWER, “Superfund: CERCLA Overview.” [Online]. Available: https://www.epa.gov/superfund/superfund-cercla-overview. [Accessed: 06-Nov-2018].
[206] “SUPERFUND Trends in Federal Funding and Cleanup of EPA’s Nonfederal National Priorities List Sites Report to Congressional Requesters United States Government Accountability Office,” 2015.
[207] K. N. Probst, “Superfund 2017 Cleanup Accomplishments and the Challenges Ahead.”
[208] C. Ottawa, “Federal Contaminated Sites Cost,” 2014.
[209] EFE, “¿Cuánto le costará el posconflicto a Colombia?” [Online]. Available: https://www.dinero.com/economia/articulo/cuanto-le-costara-el-posconflicto-a-colombia/232147. [Accessed: 06-Nov-2018].
[210] M. de Salud, A. Padilha Ministro de Salud Dra Nila Heredia, M. Santamaría, G. Franco Netto, D. Daniela Buosi Rohlfs, N. Jové, and A. Díaz Dra Andrea Soler Coordinación de Salud Ambiental Dra Marcela Varona, “Cooperación técnica entre Brasil, Bolivia y Colombia: Teoría y Práctica para el Fortalecimiento de la Vigilancia de la Salud de Poblaciones Expuestas a Mercurio,” 2011.
[211] N. Legales, “569076 poder ejecutivo normas legales,” 2015. [Online]. Available: http://www.minam.gob.pe/wp-content/uploads/2015/12/Decreto-Supremo-N°-015-2015-MINAM.pdf. [Accessed: 05-Nov-2018].
[212] “WHO (World Health Organization). Mercury in drinking-water: Background document for development of WHO guidelines for drinking-water quality. 2003. http://www.who.int/water{_}sanitation{_}health/dwq/chemicals/en/mercury.pdf. Accessed December 30 2014.” .
[213] US EPA, “National Recommended Water Quality Criteria,” Washington, D.C., 2014.
[214] Environment Canada Guidelines and Standards Division, “Canadian Water Quality Guidelines for the Protection of Aquatic Life,” Quebec, 2003.
[215] US EPA, “Clean Water Act Section 303(d): Impaired Waters and Total Maximum Daily Loads (TMDLs).” [Online]. Available: https://www.epa.gov/tmdl. [Accessed: 05-Nov-2018].

VITA

Farith Adilson Díaz Arriaga was born to Ibeth Arriaga and Alfonso Díaz in Quibdó (Colombia). In 1998 he received a B.S. degree in Chemical Engineering at the Universidad de Antioquia. In January 2000, he entered the Graduate School at the Universidad de los Andes where he received a M.S. in Civil Engineering in 2002. After his master, Farith worked at different companies such as General Motors Colombia, and Ignacio Gomez IHM S.A., and also as an Assistant Professor and Graduate Program Coordinator at the Universidad Tecnológica del Chocó. In 211, Farith began graduate school at the University of Texas at Austin (UT) in the Environmental and Water Resources Engineering Department. Funded by Fulbright Colombia and Colciencias, Farith began his research on the influence of natural organic matter on the removal of mercury from drinking water treatment under the supervision of Drs. Lynn E. Katz and Desmond F. Lawler. Farith was a General Engineering Teaching Assistant for four years in a row at the University of Texas at Austin for the courses Chemistry 301 and Physics 303K.

Email: fdiaz@utexas.edu

This dissertation was typed by the author